Universidad Autónoma de Madrid

Facultad de Ciencias

Departamento de Biología

ENDOLITHIC LIFE IN THE ATACAMA DESERT: MICROBIAL ECOLOGY AND ADAPTATION STRATEGIES THROUGH A MULTIDISCIPLINARY APPROACH

LA VIDA ENDOLÍTICA EN EL DESIERTO DE ATACAMA: ECOLOGÍA MICROBIANA Y ESTRATEGIAS DE ADAPTACIÓN A TRAVÉS DE UN ENFOQUE MULTIDISCIPLINAR

Doctoral Dissertation

Tesis Doctoral

MARÍA CRISTINA CASERO CHAMORRO

Madrid, 2019

ENDOLITHIC LIFE IN THE ATACAMA DESERT: MICROBIAL ECOLOGY AND ADAPTATION STRATEGIES THROUGH A MULTIDISCIPLINARY APPROACH

LA VIDA ENDOLÍTICA EN EL DESIERTO DE ATACAMA: ECOLOGÍA MICROBIANA Y ESTRATEGIAS DE ADAPTACIÓN A TRAVÉS DE UN ENFOQUE MULTIDISCIPLINAR

Doctoral Dissertation

Tesis Doctoral

MARÍA CRISTINA CASERO CHAMORRO

Madrid, 2019

Memoria presentada para optar al Grado de Doctor en Microbiología

María Cristina Casero Chamorro

Licenciada en Biología

Directores:

Dr. Jacek Wierzchos

Científico Titular

Departamento de Biogeoquímica y Ecología Microbiana

Museo Nacional de Ciencias Naturales, CSIC

Dr. Antonio Quesada del Corral

Profesor Titular

Departamento de Biología

Universidad Autónoma de Madrid

This work has been possible due to the “Ayuda para Contratos Predoctorales para la Formación de Doctores” fellowship (FPI 2014 program) of Ministerio de Economía, Industria y Competitividad (MINECO) /Ministerio de Ciencia, Innovación y Universidades, Gobierno de España (Ref: BES-2014-069106) and the research project: CGL2013-42509-P from MINECO.

A mi familia, Papá, Mamá, Coru, Emilio y Petros

A Marcos

Table of contents

Chapter 4

SUMMARY

The hyper-arid Atacama Desert (North Chile) is one of the most challenging polyextreme environments on Earth due to its hyper-aridity, extreme solar irradiance, both ultraviolet radiation (UVR) and photosynthetic active radiation (PAR), high day/night temperature fluctuations and, in some cases, high salinity. Despite the combination of extreme environmental conditions, microbial life has found a refuge in endolithic (inside rocks) microhabitats, as in other arid deserts, in diverse lithic substrates (gypcrete, granite, calcite, gypsum crust, halite and ignimbrite). Endolithic microhabitats are constituted by a network of pores and fissures connected to the surface within semi-translucent rock known to provide protection from lethal UVR and excess of PAR, as well as enhance moisture availability. Despite the fact that the light regime within rocks seems very scarce, the microbial communities in these microhabitats are photosynthetic-based, so that oxygenic phototrophic primary producers (mainly cyanobacteria) support a diversity of heterotrophic microorganisms. Due to the harsh conditions the cyanobacterial community is usually dominated by members of the *Chroococcidiopsis* genus, characterized by their extremely high resistance to ionizing radiation and desiccation.

The scope of this doctoral thesis is to explore the endolithic life, paying special attention to the phototrophic fraction that supports the microbial community and its adaptations strategies and acclimation capacity, by adopting a multidisciplinary approach. This main goal is addressed in four chapters.

In Chapter 1 the biogeography of microbial communities in three different endolithic microhabitats of gypcrete was investigated through a pioneering approach, on a micro scale. Microhabitat architecture was characterized using Scanning Electron Microscopy in BackScattered Electron mode (SEM-BSE) and Computerized Tomography (CT-Scan) along with the exploration of the

composition and diversity of the endolithic microbial communities by means of high-throughput sequencing. These results demonstrated that microhabitats less exposed to sun radiation showed a lower diversity in the endolithic community, as well as the presence of unique cyanobacteria taxa. Thus, it was suggested that the differences in the habitable architecture of a microhabitat, even within the same piece of lithic substrate, determines microbial community diversity and composition.

Chapter 2 was focused on describing the cyanobacterial community inhabiting the hypersaline endolithic microhabitat of halite in one of the driest locations on Earth, Yungay. The morphology and ultrastructure of the obtained cyanobacterial isolates from *Chroococcidiopsis* genus along with the cyanobacterial aggregates was characterized by means of a combination of microscopy techniques (light, fluorescence and transmission electron microscopy (TEM)). The development of a specific DNA isolation protocol allowed to perform a phylogenetic study and describe the adaptation strategies to osmotic stress through whole genome sequencing of the *Chroococcidiopsis* isolated strain. The comparison of the *Chroococcidiopsis* isolate features with those of the major cyanobacteria observed inhabiting the halite endolithic habitat pointed to *Chroococcidiopsis* as the dominant cyanobacterium in the halite endolithic habitat in Yungay.

In Chapter 3, the response to UVR and PAR of *Chroococcidiopsis* strains isolated from the chasmoendolithic microhabitat of calcite and the cryptoendolithic microhabitat of halite was addressed. Oxidative stress was evaluated by studying Reactive Oxygen Species (ROS) accumulation, through spectrofluorometric measurements and microscopy observations, and the adaptation strategies of the cyanobacterial isolates to oxidative stress were described thanks to whole genome sequencing. In addition, the accumulation of the UV-screening compound scytonemin was evaluated through high performance liquid chromatography (HPLC) along with the metabolic activity and ultrastructural

characterization studied by microscopy techniques (fluorescence microscopy and TEM). The results revealed differences in their acclimation to similar microhabitats exposed to slightly different light conditions. This suggested specific adaptation strategies related to their original microhabitat and a strain-specific environmental pressure selection.

In Chapter 4, the bioactive compounds present in four cyanobacterial strains from the *Chroococcidiopsis* and *Gloeocapsopsis* genera isolated from different endolithic microhabitats and lithic substrates were explored. Bioassays (antibacterial and cytotoxicity), liquid chromatography tandem mass spectrometry (LC-MS/MS) and genomic tools (identification, annotation and analysis of secondary metabolites gene clusters-antiSMASH) were used to determine the actual and potential activity of each strain. The results showed a large number of compounds actually and potentially produced by the studied cyanobacterial strains with weak antibacterial activity and important cytotoxic activity against cancer cells. This suggests that cyanobacterial strains from this polyextreme environment constitute a promising source of natural products of biomedical interest.

The set of results presented in this thesis suggests the importance of a "micro" perspective when analyzing the distribution and composition of microbial communities colonizing such a restrictive microhabitat as the endolithic. The microenvironmental conditions in each microhabitat and substrate and the specific biotic interactions determine the whole selection of genotypes and phenotypes able to colonize efficiently each microhabitat and lithic substrate in a polyextreme environment.

This thesis, which aims to understand the ecology and behavior of endolithic microbial communities in extreme environments, encourages further studies towards understanding the limits of life, offering a new perspective on

environmental selection due to the abiotic and biotic factors that occur in a microhabitat as particular as the endolithic.

RESUMEN

El desierto de Atacama, en el norte de Chile, es uno de los ambientes poliextremos más desafiantes de la Tierra debido a su hiperaridez, radiación solar extrema, tanto radiación ultravioleta (UVR) como radiación fotosintética activa (PAR), grandes fluctuaciones de temperatura entre el día y la noche e incluso, en algunos casos, alta salinidad. A pesar de la combinación de condiciones ambientales extremas, la vida microbiana ha encontrado refugio en los llamados microhábitats endolíticos (dentro de las rocas), como ocurre en otros desiertos, en diversos sustratos líticos (yeso, granito, calcita, halita e ignimbrita). Los microhábitats endolíticos están constituidos por una red de poros y fisuras conectados a la superficie en rocas semitraslúcidas que protegen de los letales efectos del UVR y PAR, a la vez que facilitan la retención de agua. A pesar de que el régimen de luz dentro de las rocas aparenta ser escaso, las comunidades microbianas que habitan estos microhábitats están basados en microorganismos fotosintéticos, donde los productores primarios (principalmente cianobacterias) sostienen una diversidad de microorganismos heterótrofos. Debido a las severas condiciones ambientales, la comunidad de cianobacterias suele estar dominada por miembros del género *Chroococcidiopsis*, que se caracterizan por su extrema resistencia tanto a las radiaciones ionizantes como a la desecación.

El objetivo de esta tesis doctoral es explorar la vida endolítica prestando especial atención a la porción fototrófica que sustenta a la comunidad microbiana y analizar sus estrategias de adaptación y capacidad de aclimatación, mediante el uso de un enfoque multidisciplinar. Este objetivo principal se aborda en cuatro capítulos.

En el Capítulo 1 se realizó un estudio de la biogeografía de las comunidades microbianas en tres microhábitats endolíticos diferentes del yeso mediante una aproximación pionera, a escala micro. La arquitectura de los distintos microhábitats se caracterizó mediante microscopía electrónica de barrido en modo de electrones retrodispersados (SEM-BSE) y el análisis por tomografía computarizada (CT-Scan). Por otro lado, se estudió la estructura, composición y diversidad de las comunidades microbianas endolíticas de los diferentes microhábitats del yeso por medio de secuenciación masiva de ADN. Estos resultados mostraron que los microhábitats menos expuestos a la radiación solar presentaban una comunidad endolítica menos diversa albergando, a su vez, taxones de cianobacterias únicos. Este escenario sugiere que las diferencias en la arquitectura habitable de un microhábitat, incluso dentro de una misma pieza de sustrato lítico, determinan la diversidad y composición de la comunidad microbiana.

El Capítulo 2 se orientó a la descripción de la comunidad de cianobacterias presente en el microhábitat endolítico hipersalino de la halita, específicamente en las halitas que se encuentran en uno de los lugares más secos de la Tierra, Yungay. En primer lugar, se caracterizaron mediante una combinación de técnicas de microscopía (óptica, fluorescencia y microscopía electrónica de transmisión (TEM)) la morfología y ultraestructura de las cianobacterias aisladas de este microhábitat, identificadas como género *Chroococcidiopsis*, y las de los agregados presentes en el sustrato. Por otro lado, se realizó un estudio filogenético y se describieron las estrategias de adaptación al estrés osmótico mediante la secuenciación del genoma completo de la cepa aislada de *Chroococcidiopsis*, para lo que fue necesario el desarrollo y puesta a punto de un protocolo específico de extracción de ADN. Los resultados derivados de comparar las características del cultivo de *Chroococcidiopsis* con los de las cianobacterias mayoritarias observadas en el hábitat endolítico de la halita

indicaron que *Chroococcidiopsis* es el género de cianobacterias dominante en el hábitat endolítico de las halitas de Yungay.

En el Capítulo 3 se abordó la respuesta a la UVR y la PAR de cepas de *Chroococcidiopsis* aisladas del microhábitat casmoendolítico de la calcita y del microhábitat criptoendolítico de la halita. Se evaluó la respuesta al estrés oxidativo mediante el estudio de la acumulación de especies reactivas de oxígeno (ROS) a través de mediciones espectrofluorométricas y microscopía de fluorescencia. También se pudieron describir las estrategias de adaptación al estrés oxidativo de las cepas de estudio gracias a la secuenciación del genoma completo. Se evaluó la acumulación de la scytonemina, un compuesto de protector frente a la UVR, mediante cromatografía líquida de alta resolución (HPLC), estudiándose a su vez la actividad metabólica y los cambios ultraestructurales mediante técnicas de microscopía (fluorescencia y TEM, respectivamente). Los resultados revelaron diferencias significativas entre la capacidad de aclimatación de ambas cepas procedentes de microhábitats endolíticos donde las condiciones lumínicas son ligeramente diferentes. Esto sugirió la existencia de presiones ambientales específicas en sus microhábitats de origen, donde las condiciones lumínicas son ligeramente diferentes, que seleccionarían adaptaciones y capacidades de aclimatación distintas en función de sus condiciones microambientales.

En el Capítulo 4 se investigó acerca de los compuestos bioactivos producidos por cuatro cepas de cianobacterias de los géneros *Chroococcidiopsis* y *Gloeocapsopsis* aislados de diferentes microhábitats endolíticos y sustratos líticos. Para determinar la actividad real y potencial de cada cepa se utilizaron bioensayos (antibacterianos y citotoxicidad), cromatografía líquida espectrometría de masas en tándem (LC-MS/MS) y herramientas genómicas (identificación, anotación y análisis de grupos de genes de metabolitos secundarios - antiSMASH). Los resultados evidenciaron un gran número de compuestos reales y potencialmente producidos por las cepas de cianobacterias estudiadas, cuyos

extractos mostraron una débil actividad antibacteriana pero importante actividad citotóxica contra las células cancerosas. Esto sugiere que las cepas de cianobacterias de este ambiente poliextremo constituyen una fuente prometedora de productos naturales de interés biomédico.

El conjunto de resultados presentados en esta tesis doctoral sugiere la importancia de aplicar una escala "micrométrica" a la hora de analizar la distribución y composición de las comunidades microbianas que colonizan un microhábitat tan restrictivo como el endolítico. De esta manera, las condiciones microambientales de cada microhábitat en cada sustrato lítico y las interacciones bióticas específicas determinan la selección de genotipos y fenotipos capaces de colonizar eficientemente cada microhábitat y sustrato lítico en un ambiente poliextremo.

Esta tesis, que tiene por objeto comprender la ecología y el comportamiento de las comunidades microbianas endolíticas en ambientes extremos, anima a llevar a cabo estudios adicionales para comprender los límites de la vida, ofreciendo una nueva perspectiva sobre la selección ambiental debida a los factores abióticos y bióticos que se dan en un microhábitat tan particular como el endolítico.

Abbreviations / Abreviaturas

AI: Aridity Index

ASA: Ascorbic Acid

a_w: Water Activity

BIC: Bayesian Inference Criterion

BLAST: Basic Local Alignment Search Tool

CAT: Catalase

CDSs: Coding DNA Sequences

CH: Chasmoendolithic

Chl *a*: Chlorophyll a

CLSI: Clinical and Laboratory Standards Institute

CR: Cryptoendolithic

CSLM: Confocal Laser Scanning Microscopy

CTC: 2,3-Ditolyl Tetrazolium Chloride

CT-Scan: Computerized Tomography

DCFH-DA: 2',7'-Dichlorodihydrofluorescein diacetate

DGGE: Denaturing Gradient Gel Electrophoresis

DIC: Differential Interference Contrast Mode

DMSO: Dimethyl Sulfoxide

DNA: Desoxyribonucleic Acid

DW: Dry weight

EDS: Energy Dispersive X-ray spectroscopy

EIP: Enhanced Ion Product

EMC: Endolithic Microbial Community

EPSs: Extracellular Polymeric Substances

EUCAST: European Committee on Antimicrobial Susceptibility Testing

FM: Fluorescence Microscopy

GPX: Glutathione Peroxidase

HE: Hypoendolithic

HPLC: High Performance Liquid Chromatography

IC_{50}: Half Maximal Inhibitory Concentration

IDA: Information Dependent Acquisition

IR: Infrared Radiation

LC-MS/MS: Liquid Chromatography Tandem Mass Spectrometry

LM: Light Microscopy

LT-SEM: Low Temperature Scanning Electron Microscopy

m/z: Mass / charge ratio

MAAs: Mycosporine-Like Aminoacids

MIA: Multichannel Image Acquisition

ML: Maximum Likelihood

MTT: 3-(4,5-dimethylthiazol-2-yl)-2,5-diphenyltetrazolium bromide

NADPH: reduced nicotinamide adenine dinucleotide phosphate

NCBI: National Center for Biotechnology Information

NGS: Next Generation Sequencing

NRPS: Nonribosomal Peptide Synthetases

OTU: Operational Taxonomic Unit

PAR: Photosynthetic Active Radiation

PCR: Polymerase Chain Reaction

PDA: Photodiode Array

PET: Potential Evapotranspiration

PKS: Polyketide Synthases

RAST: Rapid Annotations using Subsystems Technology

RDP: Ribosomal Database Project

RH: Relative Humidity

ROS: Reactive Oxygen Species

rRNA: Ribosomal Ribonucleic Acid

RuBisCo: ribulose-1,5 bisphosphate carboxylase

SD: Standard Deviation

SEM-BSE: Scanning Electron Microscopy in BackScattered Electron mode

SOD: Superoxide Dismutase

SPE: Solid Phase Extraction

TEM: Transmission Electron Microscopy

TIC: Total Ion Current

tRNA: Transfer Ribonucleic Acid

TWRC: Total Water Retention Capacity

UC-OTU: Unclassified Cyanobacterial Operational Taxonomic Unit

UVA: Ultraviolet-A Radiation

UVB: Ultraviolet-B Radiation

UVC: Ultraviolet-C Radiation

UVI: Ultraviolet Index

UVR: Ultraviolet Radiation

WGS: Whole Genome Sequencing

WHO: World Health Organization

XIC: Extracted Ion Chromatogram

XRD: X-ray Powder Diffraction

α-TOC: α-tocopherols

Figure index / Índice de figuras

Table index / Índice de tablas

Supplementary material index / Índice de material suplementario

GENERAL INTRODUCTION

"Everything is everywhere, but, the environment selects"

The statement developed by Professor Lourens Gerhard Marinus Baas-Becking (1934) in the book *Geobiologie of inlerding tot de milieukunde* (Geobiology or introduction to the science of the environment) which established the most referred principle for microbial biogeography remains in discussion regarding the first half of the statement (*everything is everywhere*) (de Wit and Bouvier 2006, O'Malley 2008, Bass and Boenigk 2011, Fontaneto and Hortal 2012, van der Gast 2015). Without going into detail about the literal interpretation of this statement, it can be considered, from a lukewarm position, that the distribution of microorganisms is connected with their high dispersal potential (in comparison to macroorganisms), although, their growth and colonization of each niche is limited by the environmental conditions (both biotic and abiotic) occurring there. Regarding the second half of the statement (*but, the environment selects*) extreme environments are some of the most palpable scenarios. Extreme environments are inhabited only by those microorganisms that, after reaching those emplacements, have been able to thrive in the respective physical or geochemical extreme condition or conditions (for example, temperature, radiation, pressure, desiccation, pH) (Rothschild and Mancinelli 2001).

One of these types of extreme environments are deserts, which are distributed worldwide comprising over 30% of Earth's land and as such represent the most extensive terrestrial biome (e.g. Pointing and Belnap 2012). Deserts can be classified based on their aridity by the aridity index (AI) which relates average annual precipitation (P) to potential evapotranspiration (PET), considering as arid regions those where P/PET is below 1 (Barrow 1992). According to this classification, hyper-arid deserts (AI<0.05) constitute the most extreme deserts, and usually combine a series of stress conditions simultaneously such as water stress, extreme high and low temperatures, scarcity of organic carbon, high solar radiation and osmotic stress (Pointing and Belnap 2012). While these environments can be considered polyextreme, they may be inhabited by

microbiota able to survive in such multiple extreme conditions. Hence, polyextreme environments are excellent microbial ecology models for the study of the biochemical resistance mechanisms of microorganisms.

What sets the Atacama Desert apart

Among others deserts, the Atacama Desert (North Chile) is perhaps the most challenging polyextreme environment on Earth and the most barren region imaginable. Its hyper-arid climate is the result of the confluence of a subtropical high-pressure zone, the cold Humboldt Current on the coast, offshore winds, as well as the Andean rain-shadow effect and the latitudinal position of the region (Houston and Hartley 2003). The Longitudinal Valley of the Atacama Desert is the driest place on Earth (Hartley et al. 2005; Houston and Hartley 2003) with scarce precipitations of 3.27 mm yr^{-1} (McKay et al. 2003; Wierzchos et al. 2012a) and an extremely low mean annual relative humidity (RH) of 17.3%, as reported by (Azúa-Bustos et al. 2015). Further, this desert holds another world record: the highest surface ultraviolet radiation (UV) (UV index above 20 in summer season (Cordero et al. 2018)), photosynthetic active radiation (PAR up to 2700 µmol m^{-2} s^{-1}) and annual mean surface solar radiation (up to 312 Wm^{-2}). Altogether, the hyper-aridity, solar irradiance, high day/night temperature fluctuations (up to 60°C; J. Wierzchos unpublished results) and in some cases high salinity, make the Atacama Desert an exceptional polyextreme environment.

The last refuge for life in the Atacama Desert

In this inhospitable polyextreme desert, microbial life has found a refuge in very specific endolithic (inside rocks) microhabitats, which consist of a network of pores and fissures connected to the surface within semi-translucent rock (rev. by (Wierzchos et al. 2018; Wierzchos et al. 2012b). Three different rock locations of these endolithic habitats have been described within rocks of the Atacama Desert: cryptoendolithic (occupying pore spaces in the rock), chasmoendolithic (living within cracks and fissures in the rock), and hypoendolithic (living inside

the rock but close to the soil interface at the bottom). Endolithic colonization can be viewed as a stress avoidance strategy whereby the overlying mineral substrate provides certain protection from incident lethal UV and PAR radiation, and also offers enhanced moisture availability (Walker and Pace 2007; Wierzchos et al. 2012b). These habitats are as diverse as the interior of gypsum (DiRuggiero et al. 2013; Ziolkowski et al. 2013), gypcrete (Meslier et al. 2018; Vítek et al. 2016; Wierzchos et al. 2015), calcite (Meslier et al. 2018; DiRuggiero et al. 2013), volcanic rocks (ignimbrite and rhyolite) (Meslier et al. 2018; Vítek et al. 2017; Crits-Christoph et al. 2016b; Cámara et al. 2015; Wierzchos et al. 2013; DiRuggiero et al. 2013) and granite (Meslier et al. 2018).

These microbial communities, regardless of the position they occupy in the rock or the type of rock are supported by oxygenic phototrophic primary producers supporting a diversity of heterotrophic microorganisms (rev. in Wierzchos et al. 2018). Molecular and microscopy characterization of these endolithic microbial communities shows that, overall, these communities are dominated by Cyanobacteria, mostly from the *Chroococcidiopsis* genus, and Actinobacteria, Proteobacteria, Chloroflexi, Bacterioidetes and Euryarchaeota phyla (Meslier et al. 2018).

The dominant phylum: Cyanobacteria

Cyanobacteria are photosynthetic prokaryotes that inhabit most types of illuminated environments, constituting one of the most important group of organisms quantitatively on Earth (estimated 10^{15} g wet biomass, García-Pichel et al. 2003) whose record extends back to about 3,500 million years ago (Whitton and Potts, 2012). This phylum is currently divided in 8 orders: Gloeobacteriales, Synechococcales, Spirulinales, Pleurocapsales, Chroococcidiopsidales, Chroococcales, Oscillatoriales and Nostocales (Komárek et al. 2014). The diversity of families comprises unicellular and filamentous members occasionally occurring in colonies with a cellular division in one, two or more planes leading to diverse tridimensional configurations.

The environmental pressures present in the hyper-arid Atacama Desert described above constitute the second half of the Baas-Becking (1934) statement (*but, the environment selects*). Thus, only microorganisms or microbial communities able to deal with the polyextreme environmental conditions can be found inhabiting endolithic communities in this desert. Due to these circumstances the cyanobacterial community in these endolithic microhabitats is usually dominated by members belonging to the extremely resistant to ionizing radiation and desiccation *Chroococcidiopsis* genus (Meslier et al. 2018, Crits-Christoph et al. 2016b, Billi et al. 2000, Cockel et al. 2005). In order to deal with the extreme conditions in the Atacama Desert, especially those affecting their photosynthetic activity, these organisms have been found to count on several strategies (Vítek et al. 2017, Wierzchos et al. 2015, Vítek et al. 2016). Some of these adaptations include changes in carotenoid composition (Vítek et al. 2017), which could have a possible role in mediating a non-photochemical quenching mechanism (Kirlovsky and Kerfeld 2016) or the synthesis of large amounts of the UV-screening pigment, scytonemin (Vítek et al. 2016, Vítek et al. 2014a, Vítek et al. 2012, Vítek et al. 2010) to avoid photoinhibition and photooxidative damage.

Cyanobacteria exhibit a large variety of secondary metabolites (alkaloids, toxins, lactones, amino acids, peptides, lipopeptides, polyketides and lipids) (Mazur-Marzec et al. 2015). It has been suggested that, at least some of them, would constitute an element of the adaptive strategies enabling them to survive in a wide range of physical and chemical conditions (Kultschar and Llewellyn 2018). Thus, considering these substances as a worthy source of new therapeutic lead compounds, cyanobacterial strains from still unexplored and polyextreme habitats as the Atacama Desert could serve as good candidates in this regard.

Understanding the endolithic microhabitat, community and mainstream members

Motivated by the general scenario outlined above, this PhD thesis embarks on a multidisciplinary journey in the endolithic life of the polyextreme Atacama Desert. This cruise has been conducted through the exploration of the micro-scale differences in the microhabitats and their effects on the microbial community, drawing attention to the main inhabitants of those communities and basis of the trophic chain, cyanobacteria, and their responses and adaptations to the extreme environmental conditions, considering their potential applications in the biomedical field.

GOALS AND THESIS STRUCTURE

This thesis is framed in the context of the geomicrobiology and microbial ecology of endolithic communities from the Atacama Desert. The work developed throughout the different chapters aims to explore endolithic life from different perspectives, with special attention to the phototrophic fraction that supports the microbial community, by means of the use of a multidisciplinary approach with molecular, microscopy and analytical techniques. This holistic basis seeks to allow for a more comprehensive understanding of how the endolithic life occurs, behaves and responds to the polyextreme environment of the Atacama Desert.

The structure of the thesis along with the outlook and specific objectives of each chapter is listed below.

Chapter 1: Endolithic communities' composition in gypcrete is determined by the specific microhabitat architecture

This chapter addresses the exploration of the microbial communities inhabiting three different types of endolithic microhabitats (cryptoendolithic, chasmoendolithic and hypoendolithic) in gypcrete from the Monturaqui area.

Specific goals:

- Identification of the impact of the architectural features of each endolithic microhabitat in gypcrete (cryptoendolithic, chasmoendolithic and hypoendolithic) on the availability and access to the resources that drive the communities' composition and diversity.
- Determination of abiotic drivers on the composition of endolithic microbial communities' on gypcrete.

In order to achieve these goals, a combination of microscopy techniques (SEM-BSE, light microscopy, CT-Scan) was used to characterize the microhabitat

architecture, as well as high-throughput sequencing (16S rRNA gene amplicon sequencing) to characterize the endolithic microbial communities' composition and diversity.

Chapter 2: *Chroococcidiopsis*, the hidden cyanobacterium supporting the endolithic community of halite in Yungay.

This chapter addresses the exploration of the cyanobacterial members of the endolithic community inhabiting halite rocks in Yungay, one of the driest locations on Earth, and their specific adaptations to the polyextreme environment.

Specific goals:

- Determination of the discussed identity of the major cyanobacterial component sit on the endolithic microbial community of halite from Yungay.
- Identification of the molecular and ultrastructural tools of this major cyanobacterium to deal with extreme osmotic stress.

These goals were addressed through the morphological and ultrastructural characterization of the cyanobacterial community in halite and of cyanobacterial isolates using microscopy techniques (light and fluorescence microscopy, TEM). The phylogenetic study (16S rRNA gene) was performed by means of the development of a new DNA isolation procedure and the description of the molecular strategies of the cyanobacterial isolate to deal with osmotic stress through the whole genome sequencing

Chapter 3: Dealing with one of the highest solar radiation on Earth: response of *Chroococcidiopsis* strains from the Atacama Desert.

This chapter analyses the different levels of response of two *Chroococcidiopsis* strains against UVR and PAR, isolated from the cryptoendolithic microhabitat of halite in Yungay (studied in Chapter 2) and from the chasmoendolithic microhabitat of Calcite from the Valle de la Luna area.

Specific goals:

- Diagnose the stress response to UVR and PAR of cyanobacterial strains belonging to the major genus *Chroococcidiopsis*.
- Identify the relation between features related to the original microenvironmental conditions of each strain with differences in the stress response of each of them.
- Understand if acclimation strategies developed by these cyanobacterial strains have a protective role against UVR for the whole microbial community.

The specific goals of this chapter are addressed through the analysis of the response to UVR in the short and long term by means of a combination of analyses. The short-term response, oxidative stress, was evaluated by studying ROS accumulation (through spectrofluorometric measurements and microscopy observations) and the description of the molecular strategies of the cyanobacterial isolates to deal with oxidative stress through whole genome sequencing. The long-term response was evaluated by studying the accumulation of the UV-screening compound scytonemin (HPLC), the analysis of metabolic activity (fluorescence microscopy) and ultrastructural characterization (TEM).

Chapter 4: Bioactivity of secondary metabolites produced by cyanobacteria isolated from the Atacama Desert

This chapter addresses the screening for bioactivity of the secondary metabolites of four cyanobacterial strains isolated from endolithic communities from different substrates and microhabitats: three *Chroococcidiopsis* strains isolated from the cryptoendolithic microhabitat of Yungay halite (studied in Chapters 2 and 3), from the chasmoendolithic microhabitat of calcite of Valle de la Luna (studied in Chapter 3), and from the cryptoendolithic microhabitat of ignimbrite of Monturaqui and one strain of *Gloeocapsopsis* strains isolated from the chasmoendolithic microhabitat of gypcrete from Monturaqui.

Specific goals:

- Explore the potential of cyanobacteria from the polyextreme environment of the Atacama Desert in the actual and potential production of novel bioactive compounds

The proposed goal has been addressed by means of a multidisciplinary approach combining bioassays (antibacterial and MTT assay), LC-MS/MS and genomic tools (identification, annotation and analysis of secondary metabolites gene clusters-antiSMASH).

Currently, the manuscripts corresponding to the different chapters are in preparation for their publication. Nevertheless, during the development of my PhD I participated in eight scientific publications tightly related with the content of this thesis:

Crits-Christoph, A., Gelsinger, D.R., Ma, B., Wierzchos, J., Ravel, J., Davila, A., Casero, M.C. and Jocelyne DiRuggiero. (2016) Functional interactions of archaea, bacteria, and viruses in a hypersaline endolithic community. Environmental Microbiology 18(6), 2064-2077

Crits-Christoph, A., Robinson, C.K., Ma, B., Ravel, J., Wierzchos, J., Ascaso, C., Artieda, O., Souza-Egipsy, V., Casero, M.C. and DiRuggiero, J. (2016) Phylogenetic and Functional Substrate Specificity for Endolithic Microbial Communities in Hyper-Arid Environments. Front. Microbiol. 7:301.

Culka, A., Jehlička, J., Ascaso, C., Artieda, O., Casero, M.C. and Wierzchos, J. (2017) Raman microspectrometric study of pigments in melanized fungi from the hyper-arid Atacama Desert gypsum crust. J. Raman Spectrosc., doi: 10.100

Cirés, S., Casero, M.C. and Quesada, A. (2017) Toxicity at the Edge of Life: A review on cyanobacterial toxins from extreme environments. Mar. Drugs, doi: 10.3390/md150702332/jrs.5137.

Vítek, P., Ascaso, C., Artieda, O., Casero, M.C. and Wierzchos, J. (2017) Discovery of carotenoid redshift in endolithic cyanobacteria from the Atacama Desert. Sci. Rep., 7:11116, doi: 10.1038/s41598-017-11581-7

Wierzchos, J., Casero, M.C., Artieda, O. and Ascaso, C. (2018) Endolithic microbial habitats as refuges for life in polyextreme environment of the Atacama Desert. Curr. Op. Microbiol., 43:124-131, doi 10.1016/j.mib.2018.01.003

Meslier, V., Casero, M.C., Dailey, M., Wierzchos, J., Ascaso, C., Artieda, O., McCullogh, P.R. and DiRuggiero, J. (2018) Fundamental drivers for endolithic microbial community assemblies in the hyper-arid Atacama Desert: Desert endolithic microbial communities. Env. Microbiol pp. doi: 10.1111/1462-2920.14106

Casero, M. C., Velázquez, D., Medina-Cobo, M., Quesada A. and Cirés, S. (2019). Unmasking the identity of toxigenic cyanobacteria driving a multi-toxin bloom by high-throughput sequencing of cyanotoxins genes and 16S rRNA metabarcoding. Science of The Total Environment 665: 367-378, doi: 10.1016/j.scitotenv.2019.02.083

CHAPTER 1

ENDOLITHIC COMMUNITIES' COMPOSITION IN GYPCRETE IS DETERMINED BY THE SPECIFIC MICROHABITAT ARCHITECTURE

CHAPTER 1: ENDOLITHIC COMMUNITIES COMPOSITION IN GYPCRETE IS DETERMINED BY THE SPECIFIC MICROHABITAT ARCHITECTURE

1.1. Abstract

Endolithic microhabitats have been described as the last refuge for life in arid and hyper-arid deserts where life has to deal with harsh environmental conditions. A number of rock substrates from the hyper-arid Atacama Desert, colonized by endolithic microbial communities, such as halite, gypcrete, calcite and ignimbrite, have been characterized and compared using different approaches. In this chapter, three different endolithic microhabitats are described, each one with a particular architecture, found within a lithic substrate known as gypcrete. Gypcrete, an evaporitic rock mainly composed of gypsum ($CaSO_4 \cdot 2H_2O$) and collected in the Cordon de Lila area of the desert (Preandean Atacama Desert), was found to harbor cryptoendolithic (pores beneath rock surface), chasmoendolithic (cracks and fissures) and hypoendolithic (microcave-like pores in rock-bottom layer) microhabitats. A combination of microscopy techniques and high-throughput sequencing approaches were used to characterize the endolithic communities at the microscale in different microhabitats within the same piece of lithic substrate. Microscopy techniques revealed differences in the architecture of the endolithic microhabitats and in the distribution of the microorganisms within those microhabitats. Cyanobacteria and Proteobacteria were dominant in the endolithic communities, of which the hypoendolithic community was the least diverse and hosted unique taxa. These results show, for the first time, that the differences in the habitable architecture of a microhabitat, even within the same piece of lithic substrate, might be an essential factor in shaping the diversity and composition of endolithic microbial communities. The microscale dimension and peculiar diversity distribution in this unique environment has led us to coin the new term "microbiogeography".

1.2. Introduction

Desert microbial communities are adapted to extreme environmental conditions and are particularly sensitive to changes in water availability, which may alter their desiccation-tolerance traits (She et al. 2018). In both hot and cold deserts, these communities are subject to high solar ultraviolet radiation (UVR) and photosynthetic active radiation (PAR), water scarcity, intense desiccation, strong temperature fluctuations, and oligotrophic conditions (Wierzchos et al. 2012b; Billi et al. 2017). These environments can be considered as polyextreme environments and could be inhabited by polyextremophilic and/or polyextremotolerant microorganisms (*sensu* McElroy, 1974) surviving under multiple extreme conditions.

Microorganisms from desert communities have been used as model systems to investigate the limits of life (Dassarma 2006; Pikuta et al. 2007), and a number of studies have addressed their metabolic diversity and survival strategies (Dassarma 2006; Pointing and Belnap, 2012; Wierzchos et al. 2018). Additionally, since the most arid and hyper-arid deserts around the world (Atacama, Chile; Dry Valley, Antarctica; Mojave, USA; The Qaidam Basin, China) are analogues for Mars environments, the study of desert extremophiles might help us guide our search for life elsewhere (Fairén et al. 2010; Foing et al. 2011; Smith et al. 2014; Xiao et al. 2017; Bull et al. 2018). More recently, extremophiles have received attention in applied research as potential sources for high-value bioactive compounds or enzymatic activities at high temperatures due to their ability to resist extreme environmental conditions (Finore et al. 2016; Stan-Lotter and Fendrihan 2017; Neifar et al. 2015; Sayed et al. 2019).

In the world's arid and hyper-arid deserts, microorganisms find refuge inside rock substrates as a survival strategy, colonizing what is known as the endolithic habitat (Golubic et al. 1981; Wierzchos et al. 2012b). Apart from the above-mentioned interest in the ability of these microorganisms to survive extreme

environments, the interest of this type of microbial communities also lies in their peculiar isolated structure. Thus, they can be observed as "living fossils" of endolithic microbial communities of the Proterozoic and Archean, since they are known to have already exist in those periods (Mergelov et al. 2018). Nowadays, there are many examples of these endolithic microbial communities (EMCs), which are photosynthetic-based with primary producers supporting the diversity of heterotrophic microorganisms (Friedmann, 1980; Walker and Pace 2007, de los Ríos et al. 2014), and more specifically, in the Atacama Desert (Wierzchos et al. 2006; Wierzchos et al. 2012b; Wierzchos et al. 2018).

Several ecological features of the EMCs, originally proposed by (Friedmann and Ocampo-Friedmann 1984) and later summarized by (Walker and Pace 2007), include the following:

a. EMCs are among the simplest microbial ecosystems.
b. EMCs are characterized by a core group of microorganisms that co-occur within a defined habitat.
c. The extreme endolithic environment is seeded from a relatively small reservoir of microorganisms highly acclimated to this unique environment.
d. The composition of EMCs is influenced by biogeography and environmental factors such as the physical and chemical properties of substrates and climate.

Most studies of EMCs from the Preandean Depression of the Atacama Desert have focused on the determination of (i) the diversity, structure and composition of the communities (who is there?) (Crits-Christoph et al. 2016b; Meslier et al. 2018; DiRuggiero et al. 2013), (ii) the physico-chemical structure of the substrate, also called architecture (Wierzchos et al., 2015), and the spatial organization of the community within that substrate (where are they?) (Wierzchos et al. 2015; Meslier et al. 2018; Cámara et al. 2015), and (iii) the

acclimation strategies at the community and/or cellular levels (how are they able to survive?) (Wierzchos et al. 2015; Vítek et al. 2016; Vítek et al. 2017).

1.2.1. A multidisciplinary approach to describe EMCs structure, composition and spatial arrangement

The first reports on EMCs from hyper-arid deserts involved the use of direct microscopy methods to visualize the microbe-rock interface and the endolithic settings [(Wierzchos and Ascaso 2001) and references here in]. At the time, EMCs were mostly characterized by their phototrophic members (prokaryotic or eukaryotic-based communities), because of the difficulty in identifying heterotrophic members solely based on their morphology (Friedmann et al. 1988; de los Ríos et al. 2014). Early identifications of the heterotrophic component of EMCs were performed using culture-based methods (Hirsch et al. 1988, Siebert and Hirsh 1988) but because of the limitations of these methods, their diversity remained largely unexplored at the time. The emergence of high-throughput sequencing tools has deeply changed our view of microbial diversity across ecosystems, including that of the endolithic habitat (Walker and Pace 2007). Nowadays, characterization of EMCs, including those found in the Preandean area of the Atacama Desert, is done through a multidisciplinary approach that involves vanguard microscopy and molecular tools (Fig. 1.1).

The main contributions of microscopy and microanalytical tools to the study of EMCs have been the visualization and characterization of the microhabitats, including the spatial distribution of the microorganisms within them (Fig. 1.2). Scanning electron microscopy in backscattered electron mode (SEM-BSE) was essential in defining the different endolithic microhabitats and types of colonization. Thus, three different endolithic microhabitats were described (Fig. 1.3): (i) the cryptoendolithic habitat (Golubic et al. 1981), where microorganisms colonized the pore spaces of the lithic substrate, (ii) the chasmoendolithic habitat (Golubic et al. 1981), characterized by colonized cracks and fissures, and

(iii) the hypoendolithic habitat (Wierzchos et al. 2011; 2015), where the colonization is located underneath the lithic substrate.

SEM-BSE has also provided invaluable information on the distribution of the microorganisms within each of these microhabitats (Wierzchos et al. 2011, Wierzchos et al. 2013, Wierzchos et al. 2018, Cámara et al. 2015, Crits-Christoph et al. 2016b, DiRuggiero et al. 2013, Meslier et al. 2018) and, together with computed tomography scanning (CT-Scan), has allowed the description of the substrate's architecture (Wierzchos et al. 2018). Substrate architecture has been defined as the space available for colonization, and includes the pores, fissures, and cracks of the substrate and how they are connected to the surface, as was shown by Wierzchos et al. (2015). The use of SEM at low temperatures (LT-SEM) offered additional information, such as the cytological identification of cells *in situ* and the characterization of their ultrastructural features (Wierzchos and Ascaso 2001). Other microscopy methods, such as bright field microscopy, led to the identification of the major phototrophic members (Wierzchos and Ascaso 2001, Wierzchos et al. 2013, Wierzchos et al. 2015), while fluorescent microscopy and confocal laser scanning microscopy (CSLM) gave us essential information about the metabolic status of the microorganisms inhabiting EMCs. In particular, these methods revealed assemblages of living and intact dead cells (Wierzchos et al. 2011), as well as the spatial organization of cyanobacterial aggregates surrounded by extracellular polymeric substances (EPSs) (Crits-Christoph et al. 2016b, Robinson et al. 2015) and embedded in a matrix of heterotrophic microorganisms (Wierzchos et al. 2011). Microanalytical tools such as Energy Dispersive X-ray spectroscopy (EDS) coupled with SEM-BSE have further shed light on the spatial arrangements of microbial cells around sepiolite nodules in gypcrete rocks (Wierzchos et al 2015, Meslier et al. 2018). This is of great significance because sepiolite is a mineral with a high capacity for water retention. X-ray powder diffraction (XRD) has also revealed the mineral composition of many different lithic substrates such as calcite, ignimbrite, and

gypcrete (Wierzchos et al 2015, Meslier et al. 2018). Raman spectroscopy has been used to characterize the distribution of pigments in the endolithic microhabitat of gypcrete, ignimbrite and halite (Vítek et al. 2010; Vítek et al. 2013; Vítek et al. 2014a; Vítek et al. 2014b; Vítek et al. 2016;Vítek et al. 2017).

Microscopy tools, combined with culture-independent methods such as denaturing gradient gel electrophoresis (DGGE) (Wierzchos et al. 2013; Cámara et al. 2015) and, more recently, Next Generation Sequencing (NGS) (DiRuggiero et al. 2013; Meslier et al. 2018; Crits-Christoph et al. 2016b; Wierzchos et al. 2015), have been used to characterize the phylogenetic diversity of EMCs. Pioneer studies have demonstrated discrepancies in biomass estimates between microscopy and molecular methods. For example, Dong et al. (2007) reported that cyanobacteria in gypsum surface crust endolithic communities represented 95% of the community when using microscopy, whereas the number fell to 40% when molecular methods were used. They suggested that those differences were potentially the result of contamination, of the difficulty in isolating DNA from cyanobacteria, and of the bias introduced by amplification of the DNA by PCR (Dong et al. 2007). Today, molecular tools such as amplicon sequencing of marker genes (i.e. 16S rRNA gene) and whole genome shotgun sequencing (WGS), combined with microscopy methods, have led to a more comprehensive description of the endolithic microbiome. Habitats for these microbiomes include (i) the chasmoendolithic habitat of calcite (DiRuggiero et al. 2013; Meslier et al. 2018; Crits-Christoph et al. 2016b) and granite (Meslier et al. 2018), and (ii) the cryptoendolithic habitat found in gypcrete (Wierzchos et al. 2015; Dong et al. 2007; Meslier et al. 2018) and ignimbrite (Wierzchos et al. 2012b; Cámara et al. 2015; Crits-Christoph et al. 2016b; Meslier et al. 2018) (Table 1.1).

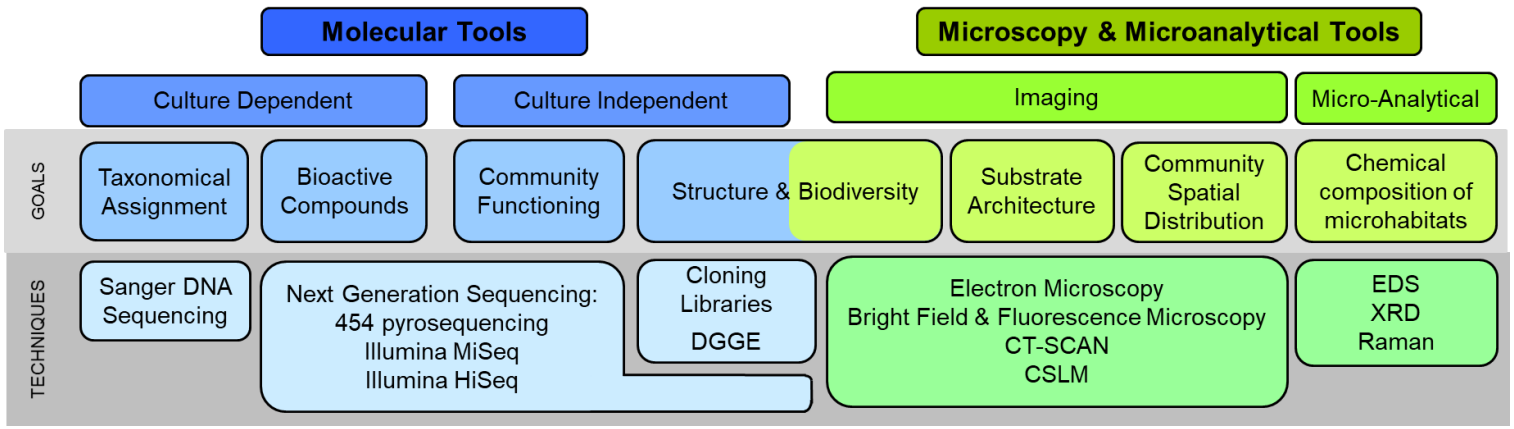

Figure 1.1. Research tools used to study EMCs classified by techniques and specific goals.

Some of the most diverse EMCs found in the Preandean Atacama Desert are those of gypcrete in Cordón de Lila and Tilocalar (Table 1.1). Phototrophs in these communities included *Cyanobacteria* (36-83%) and algae belonging to the *Chlorophyta* class. The algae were only detected at very low abundance, first through microscopy (Wierzchos et al. 2015); their occurrence was later confirmed by cloning of the 18S rRNA gene and by metagenome sequencing (Meslier, pers. com.). Major heterotrophic bacteria of the gypcrete EMCs included *Actinobacteria* (10-25%) and *Proteobacteria* (13-30%), and, at lower relative abundance, *Chloroflexi* (0-11%) and *Gemmatimonadetes* (0-6%) (Table 1.1).

Another highly diverse EMC of the Preandean area of the Atacama Desert is the chasmoendolithic community of calcite from the nearby Valle de la Luna area. In this substrate, primary producers exclusively included *Cyanobacteria* with a relative abundance of 50 to 60%, while the heterotrophs included *Actinobacteria* (10-20%), *Proteobacteria* (3-5%), *Chloroflexi* (0-11%) and *Gemmatimonadetes* (0-15%) (Table 1.1). Using WGS, Crits-Christoph et al. (2016b) identified additional heterotrophic bacteria with significant occurrence, such as *Deinococcus-Thermus* and *Bacteroidetes*.

EMCs from ignimbrite and granite were found to harbor significantly less diverse communities than other EMCs of the Preandean Atacama. In these substrates *Cyanobacteria* were the only primary producers, reaching a relative abundance of 80% and 77% in ignimbrite and granite, respectively, while *Proteobacteria* relative abundances dropped below 5% in the ignimbrite community and below 1% in the granite community (DiRuggiero et al. 2013; Crits-Christoph et al. 2016b; Meslier et al. 2018). The low relative abundance of heterotrophic bacteria in these EMCs might be the result of the phototrophs' low metabolic activity in harsher environments, leading to a reduced amount of fixed inorganic carbon

and limiting, in turn, the abundance and diversity of the heterotrophic component of the community (Wierzchos et al. 2018; Meslier et al. 2018).

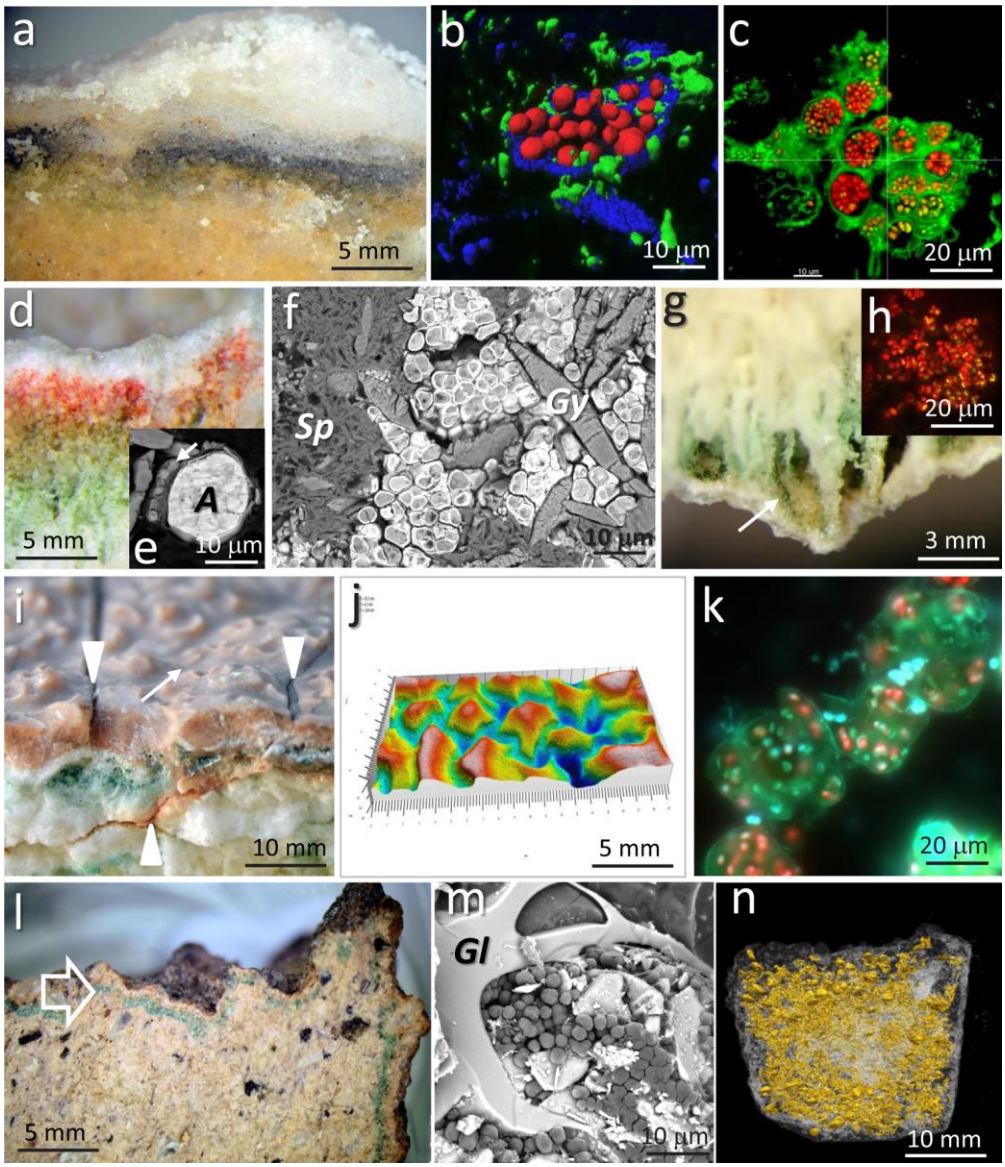

Figure 1.2. Cross-sections of lithic substrates and endolithic microbial communities within these habitats from the hyper-arid core of the Atacama Desert: halite (a–c); gypcrete (d–h); calcite (i–k) and ignimbrite (l–n). **(a)** A cross-section of halite (from the Yungay area) reveals a distinct gray layer representing the zone colonized by cryptoendoliths a few millimeters beneath the surface; the dark color is due to scytonemin, a UVR protective pigment produced by cyanobacteria. **(Cont.)**

Cont. legend Figure 1.2: (b) and **(c)** CLSM images of cryptoendoliths in halites from Yungay and Salar Grande respectively; cyanobacterial aggregates (red autofluorescence signal), associated heterotrophic bacteria and archaea (SYBR Green stained DNA structures – green signal) and scytonemin pigment (blue reflection laser light signal). **d)** SM view of the orange-to-green cryptoendolithic colonization layer comprising algae close to the gypcrete surface. **(e)** SEM-BSE image of alga (A) and detailed view of bacteria (arrow). **(f)** SEM-BSE image of cryptoendolithic cyanobacteria in gypcrete surrounding gypsum crystals (Gy) and attached to sepiolite (Sp). **(g)** SM view of a hypoendolithic habitat in gypcrete colonized by cyanobacteria (arrow) and shown in detail by CLSM in the image in **(h). (i)** SM view of the fissure wall of calcite colonized by chasmoendoliths (green color); other potentially colonized fissures are indicated with arrowheads. White arrow points to the calcite surface exhibiting microrill weathering features. **(j)** HD-CIM view of calcite microrills produced by dewfall at a depth of 1 mm; deep-coded image provides surface metrology details. **(k)** FM image of chasmoendolithic microorganisms within calcite rock showing undisturbed aggregates of viable and damaged cyanobacteria (red and green-blue autofluorescence respectively); extra polymeric substance sheaths surrounding cyanobacterial aggregates are also visible. **(l)** SM view of a cross-section of ignimbrite; arrow points to the distinct green layer of cryptoendolithic colonization beneath the rock surface. **(m)** Cryo-SEM image of cyanobacteria within a bottle-shaped pore with glass (Gl) shard walls. **(n)** CT-Scan 3D reconstruction showing pores (yellow signal) distributed within the ignimbrite rock. Abbreviations: CLSM — confocal laser scanning microscopy; SM — stereoscopic microscopy; SEM-BSE — scanning electron microscopy in backscattered electron detection mode; HD-CIM — high definition confocal and interference microscopy Leica DCM8 3D surface measurement system; FM — fluorescence microscopy; Cryo- SEM — scanning electron microscopy in low temperature mode; CT-Scan — computerized tomography scan; 3D — three dimensional. (From Wierzchos et al. 2018).

Abiotic factors promoting the diversity and composition of EMCs in the Preandean Atacama have been investigated through a number of multidisciplinary approaches (DiRuggiero et al. 2013, Wierzchos et al. 2015, Crits-Christoph et al. 2016b, Meslier et al. 2018). These studies have shown that the rock architecture, i.e. the space available for colonization, defined by the size of the cracks, fissures, and pores and their connection among them and to the surface, tightly linked to substrate water retention capacities, was the main driver of community structure and diversity. In addition, certain properties of the substrates were also found to have beneficial effects on the EMCs; these include sepiolite nodules in gypcrete, which considerably increase the water retention capacity of the substrate, or the high thermal conductivity of calcite,

which assists dewfall formation (DiRuggiero et al. 2013, Wierzchos et al. 2015, Crits-Christoph et al. 2016b, Meslier et al. 2018).

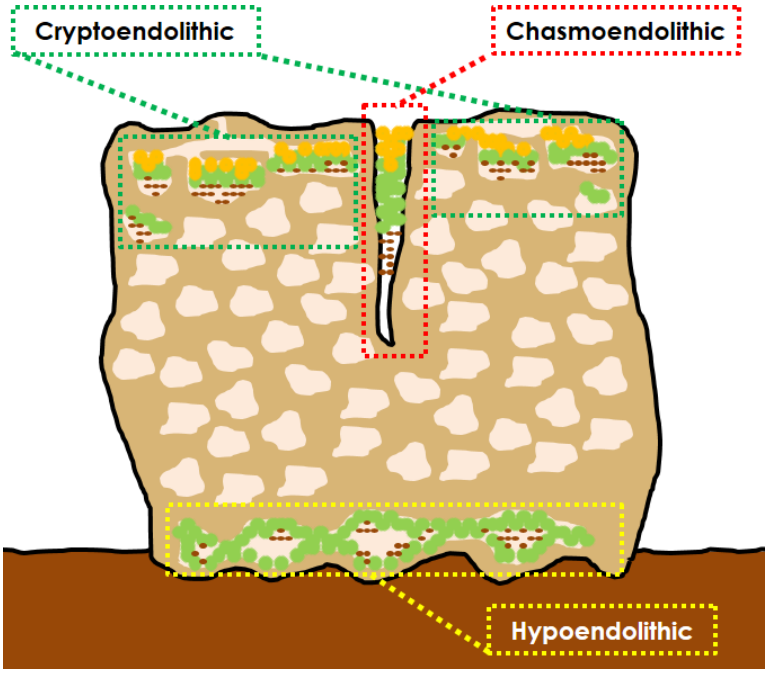

Figure 1.3. Endolithic habitats found within rocks in the hyper-arid core of the Atacama Desert (figure in part adapted from Golubic et al. 1981). Cryptoendoliths inhabit rock pores; chasmoendoliths inhabit cracks and fissures; hypoendoliths inhabit the undermost layer of the rock. Small brown ovals represent heterotrophic members of the endolithic communities. Green circles represent phototrophic members of the endolithic communities. Orange circles represent phototrophic members containing UVR protective compounds

By colonizing rock substrates, EMCs find protection from the extremely intense solar irradiance of hyper-arid deserts (Rondanelli et al. 2015). Additional adaptation strategies, in particular against the damaging effects of UV, include protective cell-layering, an array of screening pigments, and lipid production by phototrophs (see below; Vítek et al. 2013; Wierzchos et al. 2015, Vítek et al. 2016, Vítek et al. 2017, Wierzchos et al. 2018). While UVR can significantly be attenuated by the substrate, the decline in visible light transmission occurs at a much lower rate, allowing for sufficient light for photosynthesis (Hughes and

Lawley 2003; Amaral et al. 2006). Meslier et al. (2018) measured light transmittance in several substrates from the Preandean Atacama and found a direct relationship between the spectral properties of the substrate and the depth of the colonization zone; higher light transmitting substrates (calcite, gypcrete and granite) exhibited EMCs located deeper in the substrate, while EMCs from darker ignimbrite were located closer to the surface (Meslier et al. 2018).

The recent use of metagenomics has provided new insight into the adaptation of EMCs to their unique environment. The functional analysis of calcite and ignimbrite EMCs revealed a broad diversity of stress response pathways, especially in relation to survival under harsh conditions (Crits-Christoph et al. 2016b). These pathways were involved in (i) carbon starvation and low-nutrient stress, (ii) cold shock genes, (iii) oxidative stress genes related to osmotic stress/desiccation tolerance, and (iv) secondary metabolites production (Crits-Christoph et al. 2016b). The large number of gene clusters related to iron acquisition in the ignimbrite community also suggested iron starvation, while the presence of molecular pathways that lead to the production of mycosporine-like aminoacids (MAAs) in the calcite community, but not in the ignimbrite community, indicated possible differences in the UVR radiation exposure of the EMCs (Crits-Christoph et al. 2016b). The differential abundances of secondary metabolites demonstrate the key role played by the substrate in the molecular adaptations of community members. Surprisingly, pathways for nitrogen fixation were not found in the metagenome of any of the Atacama EMCs investigated so far (Crits-Christoph et al. 2016a; Crits-Christoph et al. 2016b, Finstad et al. 2016). It is likely that the long-term accumulation of nitrate in the Atacama Desert, via atmospheric deposition, provides a major source of nitrogen to microbial communities in the form of nitrate and ammonium (Michalski et al. 2004; Crits-Christoph et al. 2016b, Finstad et al. 2016). However, another explanation for the absence of nitrogen fixation genes could be space limitation

in these microhabitats which could restrict sufficient gas exchange. In this scenario, oxygen could reach concentrations too high to allow for nitrogen fixation in cyanobacteria that do not count on a protective structure such as heterocysts.

As demonstrated by the discussion above, only a comprehensive approach to the study of EMCs, through the use a combination of methods and tools, can elucidate the mechanisms that generate and maintain their diversity.

1.2.2. Photoautotrophs as primary producers.

Phototrophs are essential for the survival of EMCs because they are the only primary producers in a system where the import of exogenous organic carbon is negligible. As such, *Cyanobacteria* and microalgae fulfill essential functions in EMCs.

Phototrophic microorganisms perform photosynthesis via two photosystems, PSI and PSII, connected by an electron transfer chain, as is the case with plants (Falkowski and Raven 2013). In oxygenic photosynthesis, photons collected by antenna complexes coupled to photosystems are transferred to chlorophyll molecules located in the photosystem core. This photon energy is then used to break water molecules producing reduced nicotinamide adenine dinucleotide phosphate (NADPH) with oxygen as a by-product. In a subsequent step, NADPH is used to synthesize organic carbon from carbon dioxide via the Calvin cycle. The two main elements required for oxygenic photosynthesis, liquid water and light, are often limiting factors for the chlorophototrophs inhabiting endolithic substrates in hyper-arid deserts. Endolithic phototrophs can only perform photosynthesis during periods of time when liquid water is available and, because of high PAR and UVR, they also need to employ strategies to prevent photo-inhibition and photo-oxidative damage to their photosystems (Vítek et al. 2013; Wierzchos et al. 2015; Vítek et al. 2016; Vítek et al. 2017; Wierzchos et al.

2018). While substrate colonization at greater depths inside the rock might give access to more retained water and increase protection against damaging UVR, it might also reduce essential requirements for photosynthesis such as photosynthetic active radiation and CO_2 availability (Boison et al. 2004; Rothschild et al. 1994). An example of such a strategy is the spatial arrangement of *Cyanobacteria* within Preandean EMCs habitats (Meslier et al. 2018).

Cyanobacteria are found in most types of illuminated environments, and were responsible for the "Great Oxidation Event" 2.4-2.1 billion years ago (Lyons et al. 2014). Their success as primary producers is due to several fundamental features (Whitton and Potts 2000).

a. Their optimum temperature is higher by several degrees than that of most eukaryotic algae (Castenholz and Waterbury 1989), allowing them to colonize warmer environments.

b. Desiccation and water stress tolerance have made them some of the most successful organisms in hypersaline environments (Hu et al. 2012; Oren 2012).

c. They display high tolerance to high levels of UV light radiation (Castenholz and García-Pichel 2012).

d. They can perform efficient photosynthetic CO_2 reduction with low concentrations of inorganic carbon (Pierce and Omata 1988; Raven 2012), by means of carbon concentrating mechanisms.

Table 1.1. Endolithic microbial communities found in lithic substrates from the Preandean area of the Atacama Desert: main members and relative abundances in the community. Abbreviations: ns- not specified, nd- not detected. [1] Meslier et al. 2018, [2] Crits-Christoph et al. 2016b, [3] Cámara et al. 2015 [4] Wierzchos et al. 2015, [5], DiRuggiero et al. 2013, [6] Wierzchos et al. 2012 b[7] Dong et al. 2007.

Substrate	Shannon Index	Main Phyla Relative Abundance (%)					Other phyla detected	Refs
		Cyanobacteria	*Actinobacteria*	*Proteobacteria*	*Chloroflexi*	*Gemmatimonadetes*	*Chlorophyta*	
Gypcrete and gypsum crust	2.2 – 6.1	36 -83	10 - 25	13 - 30	nd - 11	< 5 - 6	ns	[1] [4] [5] [7]
Calcite	3.7 – 6.1	50 - 60	10 - 20	3 - 5	nd – 10.9	< 5 - 15	nd	[1] [2] [5]
Ignimbrite	4.3 – 4.9	ns - 80	5-14	< 5	< 5-11	< 1	nd	[1] [2] [3] [6]
Granite	3.8	77	17	0.3	4	< 1	nd	[1]

Most of the Cyanobacteria in EMCs from the Atacama Desert are members of the *Chroococcidiopsis* (Wierzchos et al. 2011; Vítek et al. 2013; DiRuggiero et al. 2013; Wierzchos et al. 2015; Cámara et al. 2015; Vítek et al. 2016; Crits-Christoph et al. 2016b; Vítek et al. 2017; Meslier et al. 2018; Wierzchos et al. 2018). This cyanobacterial genus of the Chroococcidiopsiales order (Komárek et al. 2014) is the most abundant type of cyanobacteria in hyper-arid environments thanks to their adaptability to extreme conditions, as has widely been demonstrated (Smith et al. 2014). *Chroococcidiopsis* is often accompanied by other cyanobacterial taxa, including members of other unicellular orders such as Chroococales and Synechococcales, and even members of filamentous orders such as Oscillatoriales and Nostocales (Table 1.2). Despite the detection of other cyanobacterial genera, *Chroococcidiopsis* is the only genus that has consistently been detected in all EMCs through microscopy approaches (Table 1.2).

Table 1.2. Cyanobacterial taxa in endolithic microbial communities from the Preandean area of the Atacama Desert and the approaches used for their detection. Gyp: gypcrete; Ca: calcite; Ign: ignimbrite; Gr: granite. [1] Meslier et al. 2018, [2] Crits-Christoph et al. 2016b, [3] Cámara et al. 2015 [4] Wierzchos et al. 2015, [5] DiRuggiero et al. 2013, [6] Wierzchos et al. 2012b [7] Dong et al. 2007

Order	Genus	Tools used for Cyanobacterial Detection		Substrate	Refs.
		Molecular	Microscopy		
Chroococcidiopsiales	*Chroococcidiopsis*	X	X	Gyp Ca Ign Gr	[1]-[7]
Chroococcales	*Gloeocapsa*	X		Ca	[2]
	Halothece	X		Gyp Ca	[1]
Synechococcales	*Acaryochloris*	X		Ca	[2]
	Synechococcus	X		Gyp Ca	[1]
Oscillatoriales	*Aerosakkonema*	X		Gyp Ca Ign Gr	[1]
	Phormidium	X		Ca	[5]
Nostocales	*Anabaena*	X		Gyp Ca	[5]

The discrepancy observed between molecular and microscopy methods with regard to cyanobacterial diversity is the result of a number of factors. First, there is a technical aspect associated with the evolution of research tools over the last decade, from DGGE to clone libraries, and more recently, to high-throughput sequencing platforms (454 pyrosequencing, Illumina-MiSeq, Illumina-HiSeq). Additionally, all these methods present intrinsic limitations regarding DNA isolation, the selection of marker genes and their primers, library preparation, read length and sequencing depth. Each of these steps can introduce significant biases which make it difficult to compare studies (Rastogi and Sani 2011). The analysis of the sequencing data may also lead to significant biases, particularly with regard to the choice of parameters in defining unique taxa and of the type of database (and its version) used for taxonomic annotation. While culture-independent methods have provided a large amount of sequencing information, especially during the last few years with NGS platforms, the increasing number of sequences in databases that belong to "uncultured cyanobacterium clone" seriously impedes the accurate taxonomical assignment of this phylum. On the other hand, taxonomical assignment based on microscopy methods is limited to morphologically different *Cyanobacteria* and their relative abundances in the sample, and requires extensive experience.

Another issue is the fact that the taxonomy and phylogeny of *Cyanobacteria* is an ongoing debate, especially because of their antiquity, the existence of fossil representatives with very similar morphology to present-day species (Schopf 1974; Knoll 2008), and their complex evolutionary history. Several features, in addition to genetic sequences, should be taken into account when defining cyanobacterial taxa, including morphological characteristics, ultrastructural details such as the thylakoid structure, and the types of cell division (Komárek et al. 2014). This is essential for an accurate taxonomy assignment of *Cyanobacteria* but is not always practical, particularly in studies with large numbers of samples.

Several adaptation strategies to water stress have been identified for *Chroococcidiopsis*. Firstly, *Chroococcidiopsis* belongs to the group of anhydrobiotic cyanobacteria. These cyanobacteria cope with the lack of water by entering into an ametabolic state involving structural, physiological and molecular changes (Feofilova 2003). Another adaptation mechanism to water scarcity is the production of EPSs providing a depository for water and stabilizing desiccation-related enzymes and molecules (Wright et al. 2006). Since *Cyanobacteria* are major components of EMCs and are most often located in the upper part of the endolithic microhabitat, the strategies developed by this phylum to deal with extreme environmental conditions brings benefits to the entire community.

This chapter addresses the impact of microhabitat architecture in the diversity and composition of gypcrete EMCs. The study is based on the hypothesis that the differential architecture of endolithic microhabitats involves small-scale differences in the microenvironmental conditions which determine the distribution of organisms in each community. The question is addressed by using a multidisciplinary approach combining microscopy and molecular tools for their characterization.

1.3. Experimental Procedures

1.3.1. Site description and sampling

Colonized rocks were collected in the Atacama Desert in December 2015 from the Monturaqui area (MTQ) (GPS coordinates 23°57'S; 068°10'W; 2868 m.a.s.l.) located in a N-S trending depression of the Cordón de Lila Range. This area exhibits a pronounced rain shadow effect by the western slope of the central Andes from 15° to 23°S (DiRuggiero et al. 2013; Wierzchos et al. 2015). Gypcrete rocks were randomly collected within a 50 m^2 area. All samples were packed in

sterile bags and stored at room temperature, dry and dark environment before further processing.

1.3.2. Microclimate data

Microclimate data (Meslier et al. 2018) were recorded using an Onset HOBO® Microweather Station Data Logger (H21-USB), as previously described by Wierzchos et al. (2015). Air temperature (T), air relative humidity (RH in %) and Photosynthetic Active Radiation (PAR in µmol photons m^{-2} s^{-1}) were recorded from January 2011 to February 2013 (22 months) (Wierzchos et al. 2015). Rainfall data were obtained from DiRuggiero et al. (2013). Thermal measurements of the gypcrete surface were acquired at zenith time at 20 cm distance from the substrate. Thermal images were taken using a thermal infrared camera (FLIR® E6, FLIR Systems, Oregon, USA) whose technical specifications are: ±2°C or ±2% of reading; < 0.06°C pixel sensitivity; 160 × 120 pixels).

1.3.3. Total water retention capacity (TWRC) and porosity

TWRC was determined on rock samples of about 5 cm^3 by total immersion of samples in H_2O at 20°C for 24 h, which corresponds to the estimated time during which water content was constant. Dry samples were weighed prior to the experiment. Volumes of rock were measured by their immersion into water in a graduated cylinder. After 24 h, gravitational water excess was removed, and rocks were weighted again. TWRC was expressed in (%) w/w of retained water per g of rock and porosity of connected pores in (%) v/v (Meslier et al. 2018).

1.3.4. Microscopy analyses

Colonized gypcrete samples were processed for SEM-BSE according to methods described by Wierzchos et al. (Wierzchos and Ascaso 1994; Wierzchos et al. 2011). In brief, several colonized gypcrete fragments were chemically fixed in 2.5% glutaraldehyde (Sigma Chemical Co., St. Louis, MO, USA) in 0.1 M sodium cacodylate buffer pH 7.4 [$Na(CH_3)_2$ AsO_2•$3H_2O$] (CB) for 16 h at 4°C. Once fixed,

the samples were washed in 0.1 M CB (3x30 min) and post-fixed in 1% osmium tetroxide (Electron Microscopy Sciences, Port Washington, PA, USA) in H_2O for 3 h at 4°C. Samples were again washed in 0.1 M CB (3x30 min) and then dehydrated in a 30% graded ethanol series for 3 h, followed by a 50% one for another 3 h. During dehydration with the next ethanol dilution, the samples were contrasted overnight with saturated uranyl acetate in 70% ethanol at 4°C. This was followed by immersion in 96% (2x3 h) and finally 100% (3x3 h) ethanol. Next, the samples were gradually infiltrated with LR-White (The London Resin Co. Ltd, Hampshire, UK) embedding medium, first with a 1:1 mixture of LR-White in 100% ethanol (3 days at 4°C) and finally with pure LR-White resin (3x3 days at 4°C). This step was followed by polymerization in an oxygen-free atmosphere (48 h, 60°C). After this, the polymerized specimen blocks were cut at low speed with a diamond saw and fine polished using grinding papers (from nr. 300 to 1200) and silicon carbide abrasive sheets (Electron Microscopy Sciences, Hatfield, PA, USA) with grain diameters of 15,9 and 3 μm. For final polishing, a liquid diamond polishing compound was used containing diamond particles with a size of 1 and 0.25 μm in an oil-based lubricant fluid (Kemet International Ltd., Maidstone, UK) on a napped cloth. After washing in distilled water and air-drying, the polished block surfaces were coated with evaporated carbon and observed using a scanning electron microscope (FEI Quantum 200) equipped with a solid-state four diodes BSE detector and X-Ray Energy Dispersive Spectroscopy system of INCA (Oxford, London, UK). Light microscopy (LM) in differential interference contrast mode (DIC) was performed on cell aggregates gently isolated from the cryptoendolithic, chasmoendolithic and hypoendolithic microhabitats and on cyanobacterial isolated cultures from those microhabitats. The samples were examined using a microscope (AxioImager M2, Carl Zeiss, Germany) in DIC mode equipped with Apochrome 63x n=1.4 oil immersion objective.

1.3.5. CT-Scan analysis

Micro-CT scans were run on a piece of gypcrete with an X-Ray Computed Tomography system (CT-scan) — HMXST 225 micro-CT system (Nikon Metrology, Tring, UK) to observe volume, bulk density, and variations in internal density. For volume and bulk density measurements a Nikon X-Tek CT-Scan device was used, placed in the MNCN laboratories, with an X-ray peak voltage of 146 kV and current of 65 mA, collecting 1583 sections at 1000 micro-seconds on average from four frames. The system operates with an X-ray tube of W and added filtration (0.875 mm Cu) to reduce the beam hardening. Three dimensional viewing and analyses of the obtained X-ray sections were performed by software VG Studio Max Version 2.2. The auto-threshold feature determined the gray-scale intensity for 3-D surface segmentation and subsequent analysis.

1.3.6. Cyanobacteria isolation and characterization

Scrapped material from endolithic colonization zones of gypcrete was transferred to BG11 1.5%-agar plates. All samples were incubated in growth chamber at 28±2°C with illumination of 20 μmol photons m^{-2} s^{-1} by cool white 40W fluorescent tubes (Philips). After 15 days of incubation, when visible cyanobacterial growth appeared, colonies were isolated by repeated plating on 0.8%-agar with BG11 medium (Rippka et al. 1979), and successfully isolated colonies were transferred to liquid BG11 medium. Culture material from each strain (2 mL) was harvested during exponential growth and centrifuged (10,000 g, 5 min). Genomic DNA was extracted from the cell pellet using the UltraClean DNA isolation kit (MoBio Laboratories, Solana Beach, CA, USA). 16 S rRNA was amplified using primers PA (Edwards et al. 1989) and B23S (Lepère et al. 2000), PCR reaction and sequencing were performed as described in Casero et al. (2014).

1.3.7. DNA extraction procedures from natural samples

Three individual rocks were processed. Colonization zone was scrapped and ground for DNA extraction. This DNA extraction was performed using 0.3 g of samples and the UltraClean DNA isolation kit (MoBio Laboratories, Solana Beach, CA, USA) with minor modifications.

1.3.8. 16S rRNA gene libraries preparation and sequencing

A two-step PCR strategy was used to prepare the sequencing libraries of endolithic microbial communities, as previously described (Robinson et al., 2015). DNA was amplified using primers 338F and 806R (V3-V4 hypervariable region) barcoded for multiplexing; amplicons from 2 PCR reactions were pooled after the first step. Illumina paired-end sequencing (2 x 250bp) was performed using the MiSeq platform at the Johns Hopkins Genetic Resources Core Facility (GRCF). Libraries from 3 samples were used on all sequencing runs to test for batch effect.

1.3.9. Computational analysis

After demultiplexing and barcode removal, sequence reads with phred score<20 and length<100bp were discarded using sickle (Joshi and Fass, 2011), representing only 2% of the initial reads count. The Qiime package (v1.6.0) was used to further process the sequences (Caporaso et al. 2010) and diversity metrics were calculated based on Operational Taxonomic Units (OTUs) at the 0.03% cutoff against the Ribosomal Database Project (RDP) database release 11 (Cole et al. 2014). The resulting OTUs table was filtered of the rare OTUs (total abundance across all samples 1%), representing 40% of the initial count (1511 OTUs).

1.3.10. Phylogenetic analysis

Sequences of 16S rRNA gene from Cyanobacterial OTUs which showed significant differences in their relative abundance between endolithic

microhabitats, together with 16S rRNA sequences from cyanobacterial isolates, were aligned with sequences obtained from the NCBI GenBank using the Clustal W 1.4 software (Thompson et al. 1994). 16S rRNA sequences from GenBank were selected using NCBI MegaBlast tool (http://blast.ncbi.nlm.nih.gov/ Blast.cgi, accessed 28.08.18). The final alignment length was 400 bp. Phylogenetic trees of each of the genes were constructed in MEGA 7.0 using the Maximum Likelihood (ML) method (Kumar et al. 2016). The best-fitting evolutionary model, chosen following the BIC (Bayesian Inference Criterion) in MEGA 7.0, was the Kimura 2-parameter model (Kimura 1980) for 16S rRNA. 1000 bootstrap replicates were performed for all trees.

1.4. Results

We combined microclimate measurements, microscopy analyses and high throughput culture-independent molecular data to identify the effect of micro-biogeography and the factors underlying the structure and composition of microbial assemblages on gypcrete endoliths from the hyper-arid Atacama Desert.

1.4.1. Sampling Site

Eleven samples from 4 different rock substrates were collected from the Monturaqui area (MTQ), located in the Preandean Depression of the Atacama Desert (Fig. 1.4) on December 2015. Climate data were recorded over a period of 22 months (Wierzchos et al. 2015) (Table 1.3). The mean air temperature was about 15°C, with strong amplitude between minima and maxima (from -4.7°C to 49.3°C), while the surface temperature of the gypcrete samples showed a maximum daily temperature of 68°C. The average diurnal PAR was ~ 1000 µmol

photons m^{-2} s^{-1} with a maximum of 2553.7 µmol photons m^{-2} s^{-1}, providing evidence for the extremely intense solar irradiance found in this region (Cordero et al. 2014). This area experiences extremely dry conditions, with an average air RH of about 20% with frequent lows of 1%. Precipitations were extremely scarce with mean annual values of 24.5 mm. Gypcrete surface temperature examined with thermal infrared camera revealed a maximum temperature of 68°C.

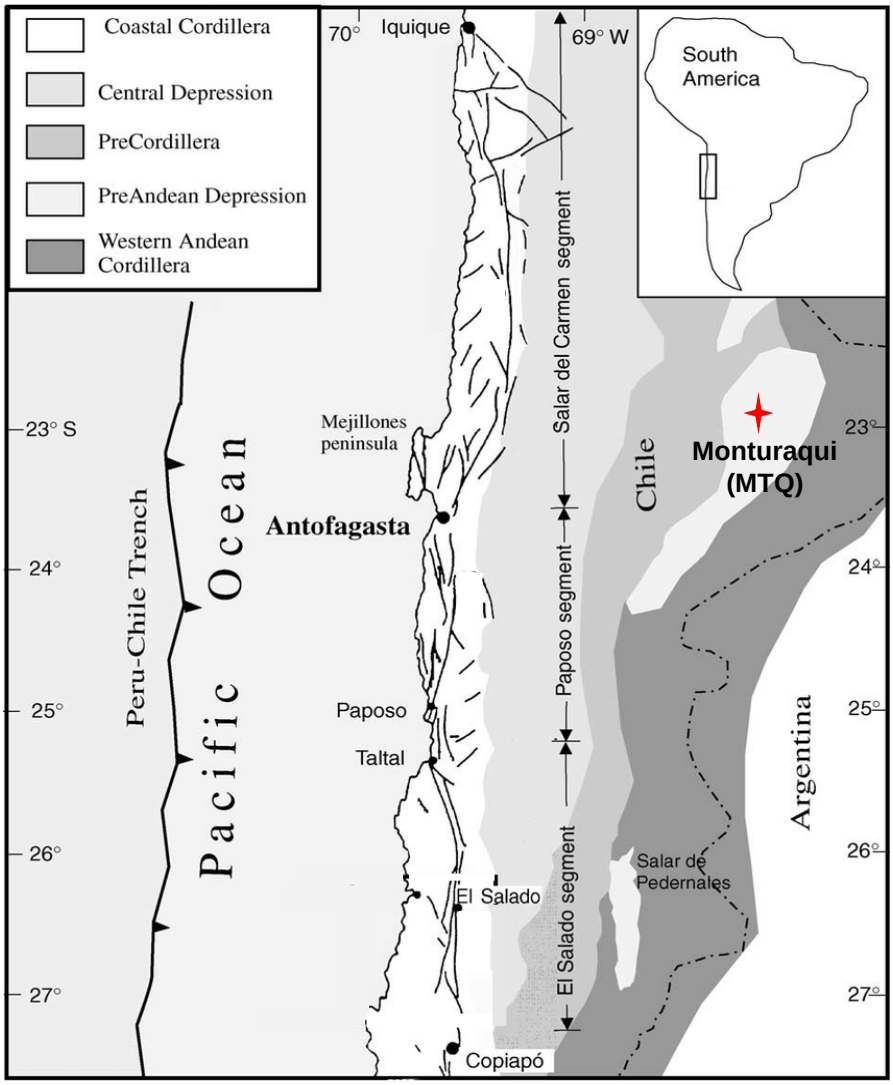

Figure 1.4. Sampling location in the Atacama Desert. Monturaqui area. MTQ, (red diamond). Modified from (Hock et al. 2007)

Table 1.3. Microclimate data from Monturaqui (MTQ)-Data extracted from Wierzchos et al., 2015. Avg =Annual mean of daily average; Max= Annual mean of daily maximum; Min = Annual mean of daily minimum.

Microclimate Data from Monturaqui (MTQ)		
Air Temperature (°C)	Min	-4.7
	Avg	15.0
	Max	49.3
PAR (µmol photons m^{-2} s^{-1})	Avg	1178.5
	Max	2553.7
Air RH (%)	Min	1.0
	Avg	18.3
	Max	100.0
Rainfall (mm/year)		24.5

1.4.2. Total water retention capacity, porosity and pores micromorphology of gypcrete

Total water retention capacity (TWRC) and rock porosity were measured by total immersion of rocks into water. Gypcrete rocks showed a TWRC of 10.7% (w/w) and porosity of 12.15% (v/v). CT-Scan images provided a 3D spatial visualization of pore shapes and their distribution inside the gypcrete rock (Fig. 1.5). The pores revealed capillary-like micromorphology following a vertical orientation as is shown in both top and lateral views**.** Detailed 3D images pointed to the apparent absence of connectivity with the surface of most of the pores (Fig. 1.5). However, the presence of this connectivity cannot be discarded due to the limited resolution of the CT-Scan technique. Moreover, CT-scan images of the gypcrete surface reveal undulated furrows due to the dissolution of gypsum after scarce rains.

1.4.3. Endolithic microhabitats

Cross sections of the gypcrete rocks revealed the presence of three clearly differentiated microhabitats where a significant heterogeneity in the micromorphology and structure was found (Figs. 1.6-1.8). The cryptoendolithic

colonization zone was close to the compact gypcrete surface layer. Within cryptoendolithic microbial communities, two characteristic pigment layers, orange for carotenoids (closer to the gypcrete surface) and green for chlorophylls (beneath the orange layer) were distinguished. The presence of these pigments was indicated by Wierzchos et al. (2015) and Vítek et al. (2016) (Fig. 1.6, A). The chasmoendolithic colonization zone reached a deeper position in the substrate and was directly connected to the surface. (Fig. 1.7, A). Finally, the hypoendolithic colonization zone, as well as the cryptoendolithic microhabitat, were located close to a compact gypcrete crust, shaped like microcaves (Fig. 1.8, A).

Cyanobacteria were found in the cryptoendolithic habitat among lenticular gypcrete crystals, filling up vertically elongated pores, and aggregated around sepiolite nodules (Fig. 1.6, B-C), a clay mineral with high water retention capacity, previously identified in gypcrete by Wierzchos et al. (2015). SEM-BSE also revealed dense arrangements of cyanobacterial cells embedded in concentric sheets of EPSs that were filled by heterotrophic bacteria (Fig. 1.6, C). By contrast, the microbial assemblages inhabiting the chasmoendolithic and hypoendolithic microhabitats were coating the walls of the cracks and caves previously described (Fig. 1.7, B-C). Detailed SEM-BSE (Fig. 1.6, C; Fig. 1.7, C; Fig. 1.8, C) and OM images (Fig. 1.6, D; Fig. 1.7, D; Fig. 1.8, D) of each microhabitat showed mainly Cyanobacteria with different micromorphology (larger cells) accompanied by heterotrophic bacteria.

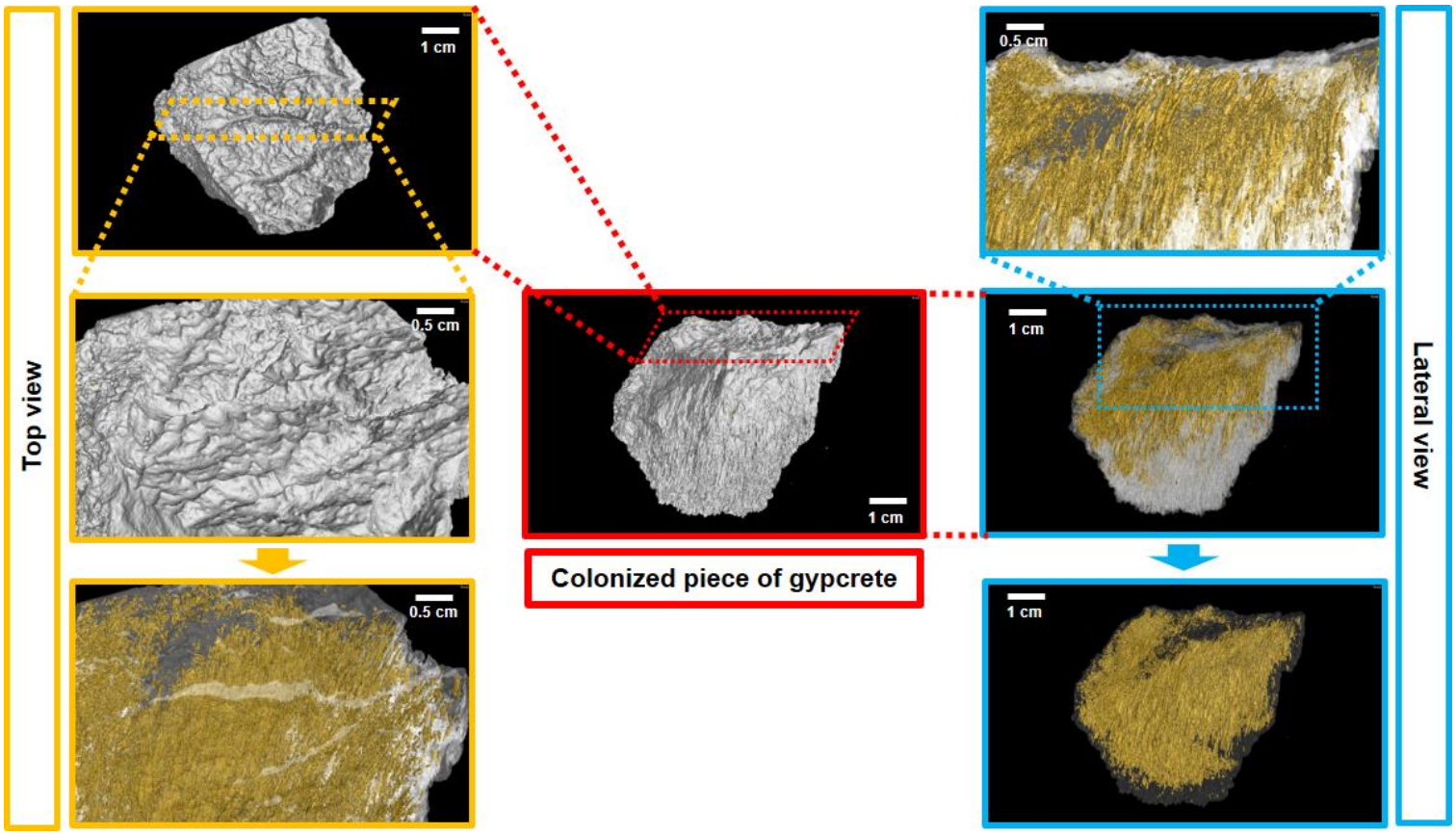

Figure 1.5. CT-Scan images of a colonized piece of gypcrete. 3D spatial distribution of porosity on top (yellow) and lateral (blue) views of gypcrete. Porous micromorphology is capillary-shaped in vertical position due to gravity movement direction of water.

1.4.4. Cyanobacterial isolates from endolithic microhabitats

A total of 12 cyanobacterial strains were isolated from the three different endolithic microhabitats (Table 1.4, Fig. 1.9): cryptoendolithic (3), chasmoendolithic (3) and hypoendolithic (6). The cyanobacterial strains were identified, following Komárek et al. (2014), as *Chroococcidiopsis* sp. (GMTQ2C, GMTQ3, GMTQ5, GCL1A, GCL4C, GCL10A, GCL10B, GCL10C), *Gloeocapsa* sp. (GMTQ6, GMTQ12) and *Gloeocapsopsis* sp. (GCL2, GCL3).

1.4.5. Structure and composition of endolithic communities

High throughput sequencing of 16S rRNA gene amplicons across 11 samples and 3 microhabitats resulted in a total of 385,440 V3-V4 SSU rDNA reads, with an average number of paired-end reads per sample of 35,040 ± 6,288 and an average length of 456 ± 11 bp. Diversity metrics, calculated from OTUs clustered at 97%, revealed no significant differences between microhabitats in terms of alpha-diversity (Table 1.5).

A total of 11 bacterial phyla with a relative abundance >0.1% were found across all microhabitats. Of these only 7 had a relative abundance over 1% of sequences across the different microhabitats (Fig. 1.10). *Cyanobacteria*, *Proteobacteria*, *Actinobacteria* and *Gemmatimonadetes* were the most abundant phyla, representing 82%–83% of the total community (Fig. 1.10, A). *Cyanobacteria* dominated the communities, inhabiting all endolithic microhabitats; in cryptoendolithic and chasmoendolithic communties they did not exceed 40% of the sequences, while in the hypoendolithic community they reached a relative abundance of 60% (Fig. 1.10, A). *Proteobacteria* were the second most abundant phylum, contributing ~30% of the sequences in the cryptoendolithic and chasmoendolithic communities, and less than a half in the hypoendolithic community (13%). The relative abundance of *Actinobacteria* was regular across all microhabitats, never exceeding 10% of the sequences. *Gemmatimonadetes* relative abundance showed differences across microhabitats representing 7-

4.4% and 2.3% of sequences in cryptoendolithic, chasmoendolithic and hypoendolithic communities, respectively (Fig. 1.10, A). *Bacteroidetes* and *Thermi* phyla also exhibited variation between the different endolithic communities, showing the higher abundance in the hypoendolithic (8.2%) and cryptoendolithic (4.9%) microhabitats respectively. *Firmicutes* and *Planctomycetes* were also found in all three microhabitats in very low abundance (0.003% and 0.002%). No archaeal OTUs were detected after the quality filtering of sequences during the samples processing.

The relative abundance provides a different picture when expressed in percentage of OTUs in which the sequences have been clustered (Fig. 1.10, B). The abundance of the four main phyla represented ~ 80% of the OTUs occurring in every microhabitat, but presents a very different distribution in comparison with the % of sequences. The three major phyla, *Cyanobacteria, Proteobacteria* and *Actinobacteria*, compiled their sequences in very similar % of OTUs across all three microhabitats (25%, 32% and 21% respectively). The greatest difference between the distribution of the relative abundance of sequences and that of OTUs is observed for *Cyanobacteria* in the hypoendolithic community.

Compared to other microhabitats this phylum showed the highest relative abundance in terms of sequences (60.4%) but the lowest in terms of OTUs (21.9%), thus revealing the high abundance of a very low number of cyanobacterial OTUs. Adonis and ANOSIM tests, performed with microhabitats categories, confirmed the statistical significance of the grouping (R^2 =0.38, *p*-value=0.014 and R^2=0.48, *p*-value=0.003 for adonis and ANOSIM respectively).

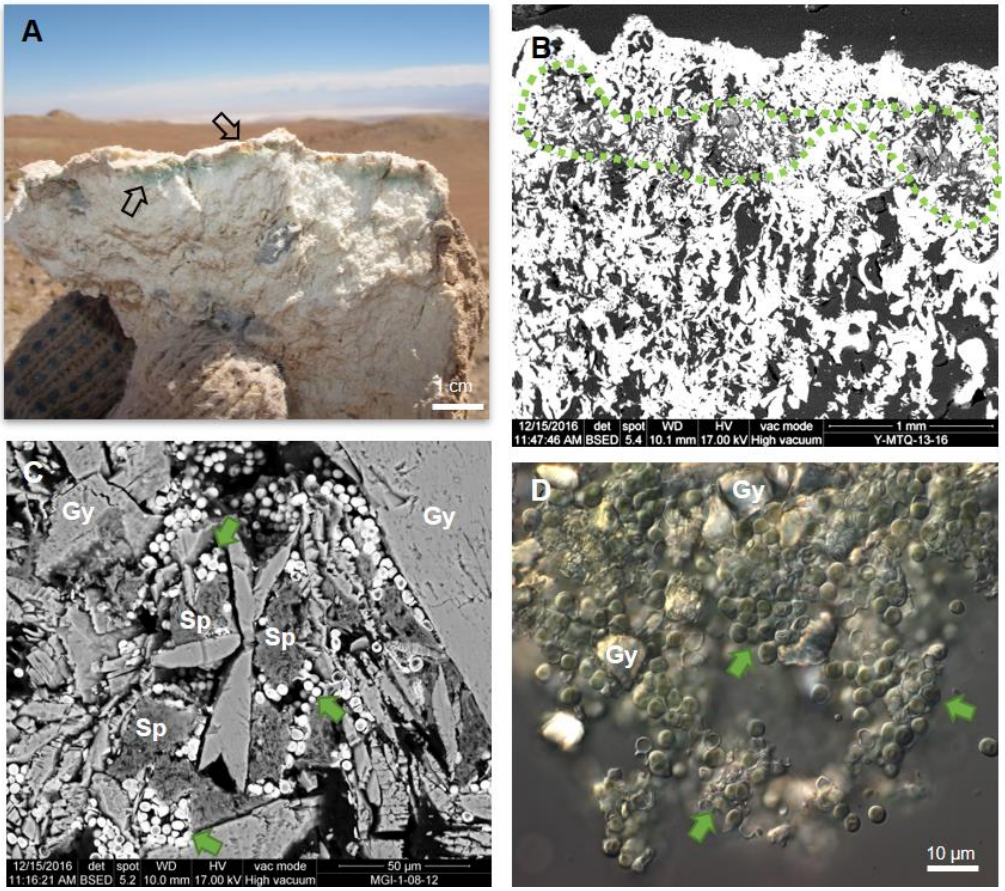

Figure 1.6. Cryptoendolithic colonization zone. Gypcrete cross-sections, SEM-BSE and LM images of cryptoendolithic colonization zone and isolated cyanobacteria from gypcrete. **A.** Cross-section of colonized microhabitat. Black arrows indicate green and orange colored microorganisms within 5mm beneath the surface. **B & C**. SEM-BSE images revealing aggregates of cryptoendolithic community, in light grey surrounded by green dots, inside the pores of gypcrete (white crust). Green arrows indicate aggregates of cyanobacteria among gypcrete (Gy) crystals and surrounding sepiolite (Sp) nodules. **D**. LM image in DIC mode of cyanobacterial aggregates, indicated by green arrows, with gypcrete crystals (Gy)

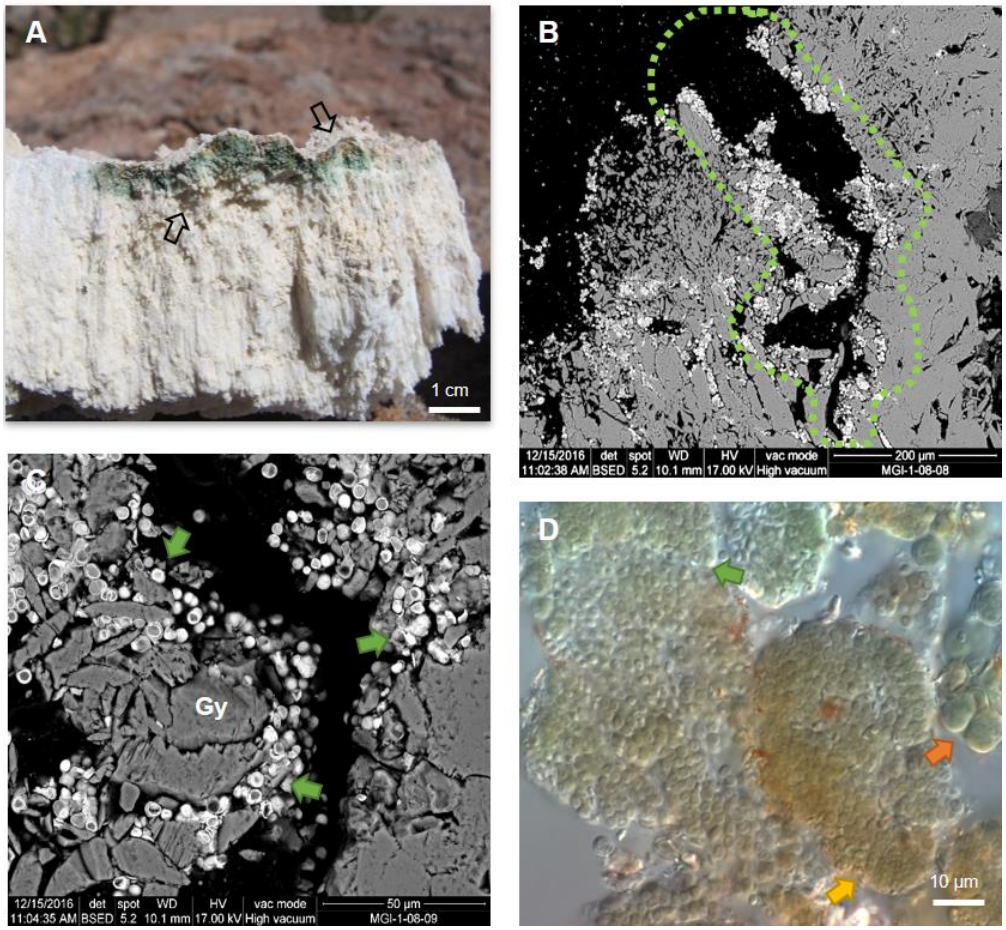

Figure 1.7. Chasmoendolithic colonization zone. Gypcrete cross-section, SEM-BSE and LM images of chasmoendolithic colonization zone and isolated cyanobacteria from gypcrete. **A.** Cross-section of colonized microhabitat. Black arrows indicate green and orange colored microorganisms within 8 mm beneath the surface. **B & C.** SEM-BSE image revealing aggregates of chasmoendolithic community, in bright white surrounded by green dots, inside cracks of gypcrete. Green arrows indicate aggregates of cyanobacteria in the gypcrete (Gy) walls. **D**. LM image in DIC mode of aggregates of different morphotypes of cyanobacteria, indicated by green, yellow and orange arrows.

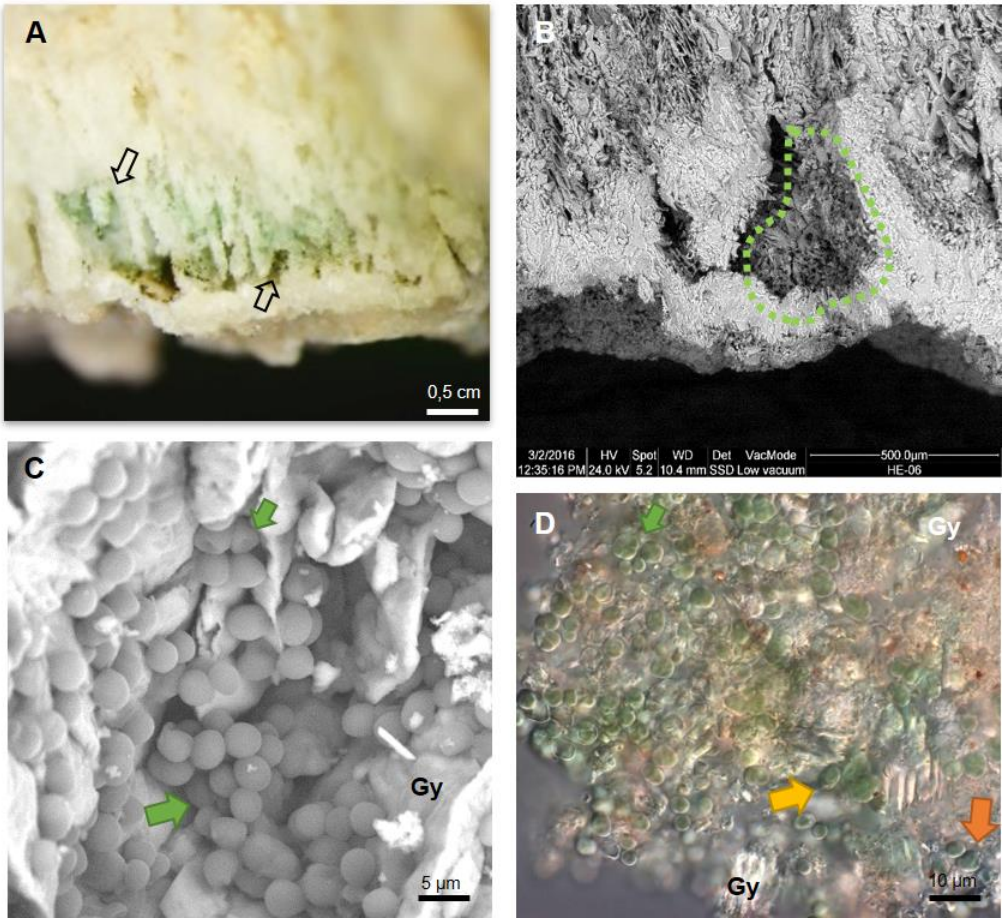

Figure 1.8. Hypoendolithic colonization zone. Gypcrete cross-section, SEM-BSE and LM images of hypoendolithic colonization zone and isolated cyanobacteria from gypcrete. A. Cross-section of colonized microhabitat. Black arrows indicate blue-green and dark green colored microorganisms. **B & C.** SEM-BSE image revealing aggregates of hypoendolithic community, inside micro caves of gypcrete. Green arrows indicate aggregates of cyanobacteria in the gypcrete (Gy) walls. **D.** LM image in DIC mode of aggregates of different morphotypes of cyanobacteria, indicated by green, yellow and orange arrows, with gypcrete crystals (Gy).

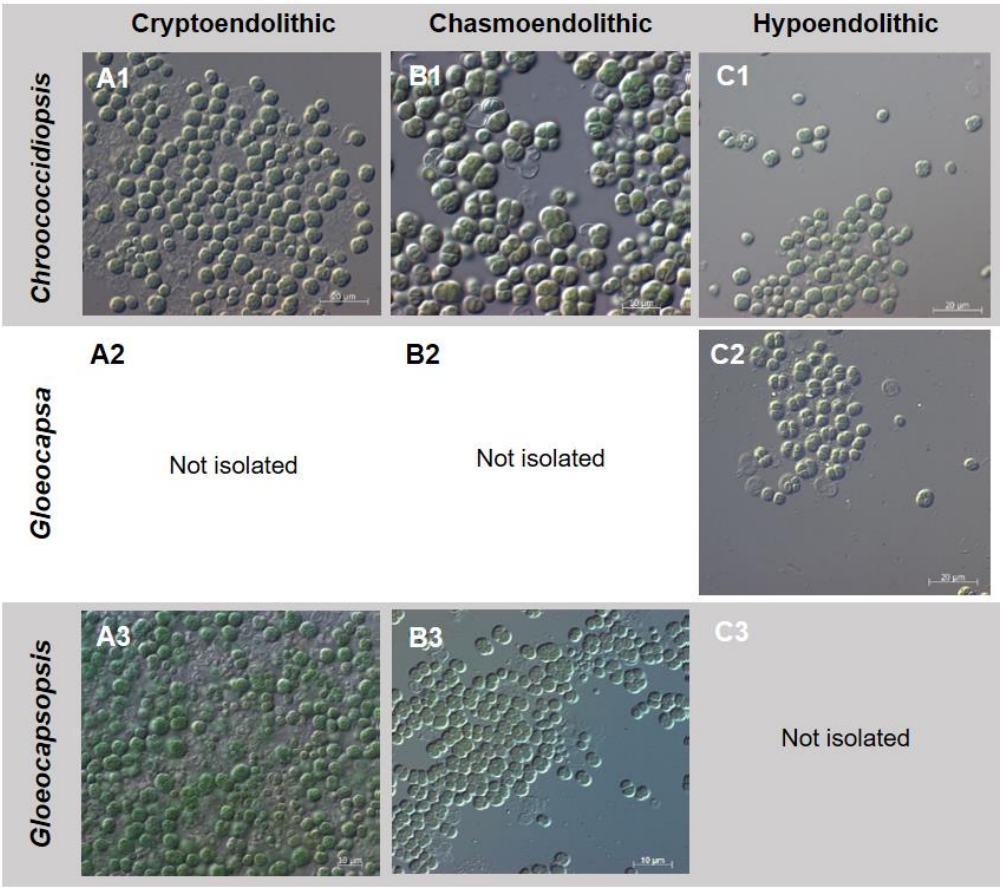

Figure 1.9. Light microscopy images from representative cyanobacteria isolated from endolithic microhabitats of gypcrete belonging to *Chroococcidiopsis* (1), *Gloeocapsa* (2) and *Gloeocapsopsis* (3) genera. Series A: Cryptoendolithic microhabitat. Series B: Chasmoendolithic microhabitat. **Series C**: Hypoendolithic microhabitat.

1.4.6. Cyanobacterial composition

As the major component of the three endolithic communities, OTUs and isolates of the *Cyanobacteria* phylum were studied in detail. A phylogenetic analysis of the 15 major cyanobacterial OTUs (relative abundance > 1%), together with the 12 isolated strains, showed that they were distributed in 6 main clusters supported by high bootstrap values (Fig. 1.11).

Most of these OTUs (9) and isolates (8) were assigned to the *Chroococcidiopsis* genus and were distributed in three clusters (I, III and V) containing representatives of *Chroococcidiopsis* isolates sequences and clone sequences from various deserts. Cluster I was the one that included a higher number of sequences from this study: six of the cyanobacterial strains (GMT3, GCL10B, GMTQ5, GCL10A, GMTQ2C and GCL4C) and four of the cyanobacterial OTUs (OTU1, OTU497, OTU8, OTU112). This cluster was constructed around two reference *Chroococcidiopsis* sp. sequences from soils of the Atacama Desert (Patzelt et al. 2014). Cluster III included only one sequence from isolated strains (GCL1A) and three OTUs sequences (OTU1772, OTU420 and OTU4) accompanied by reference sequences belonging to *Chroococcidiopsis* sp. strains from three different culture collections. The last *Chroococcidiopsis* sp. cluster, number V, had no sequences from isolates and two OTUs sequences (OTU7 and OTU98), together with sequences from cloning libraries from two deserts, Atacama and Jordan (Dong et al. 2007, and one *Chroococcidiopsis* sp. sequence from Mediterranean biocrust (Muñoz-Marín et al. 2019).

Table 1.4. Cyanobacterial strains isolated from cryptoendolithic, chasmoendolithic and hypoendolithic microhabitats of gypcrete from MTQ.

Microhabitat	Strain code	Taxonomical Assignment
Cryptoendolithic	GCL3	*Gloeocapsopsis* sp.
	GCL4C	*Chroococcidiopsis* sp.
	GMTQ3	*Chroococcidiopsis* sp.
Chasmoendolithic	GCL1A	*Chroococcidiopsis* sp.
	GCL2	*Gloeocapsopsis* sp.
	GMTQ2C	*Chroococcidiopsis* sp.
Hypoendolithic	GMTQ5	*Chroococcidiopsis* sp.
	GMTQ6	*Gloeocapsa* sp.
	GMTQ12	*Gloeocapsa* sp.
	GCL10A	*Chroococcidiopsis* sp.
	GCL10B	*Chroococcidiopsis* sp.
	GCL10C	*Chroococcidiopsis* sp.

Cluster II comprised cyanobacterial sequences belonging to the Nostocales order from the *Fischerella* and *Calothrix* genera to which OTU18 and OTU11 were assigned respectively. A total of 6 members of this study were clustered with members of the *Gloeocapsa* and *Gloeocapsopsis* genera (order Chroococcales), four isolated strains (GCL2, GCL3, GMTQ12 and GMTQ6) and two OTUs (OTU9, OTU854), resulting in cluster IV. Two reference sequences of *Synechococcus* together with the OTU5 constitute Cluster VI.

Table 1.5. Diversity estimates of microbial communities in the microhabitats of gypcrete.

Microhabitats		Chao	OTU Richness	Shannon
Cryptoendolithic	Avg	583.8	430	6.3
	SD	43.2	38	0.2
Chasmoendolithic	Avg	574.9	419	6.1
	SD	46.0	29	0.1
Hypoendolithic	Avg	564.9	409	4.6
	SD	31.7	32	1.0

The sequences that were more similar (% identity) to OTU2 (Supp. Mat. 1.1) were chosen to develop its phylogeny (Fig. 1.11). However, due to the low % of identity with its closest relatives in the database (< 95%) and with the sequences obtained from the endolithic isolates (Fig. 1.11), it was not possible to provide an accurate taxonomical assignment for it.

Nine of the cyanobacterial OTUs were found to be differentially abundant among microhabitats (Fig. 1.12). Both OTUs phylogenetically assigned to the Nostocales order (OTU11- *Calothrix* sp., OTU18- *Fischerella* sp.) showed a differential abundance (p-value < 0.01) in the chasmoendolithic community, representing 3.8% and 1.5%, respectively, compared to the cryptoendolithic and hypoendolithic communities (< 0.4% for both OTUs). OTUs clustered with *Gloeocapsa* and *Gloeocapsopsis* (cluster IV), with *Synechococcus* (cluster VI), as well as *Chroococcidiopsis* sp. OTUs from the three different clusters (I, III and V),

showed significantly different abundances (*p*-value < 0.001) in the hypoendolithic community and in the two endolithic communities from the upper side of the substrate (cryptoendolithic and chasmoendolithic). OTU8 (*Chroococcidiopsis* sp.) was the only one displaying a higher abundance in the hypoendolithic community, while OTU9 (*Gloeocapsopsis* sp.), OTU5 (*Synechococcus* sp.), OTU854 (*Gloeocapsa* sp.) and OTU1772, OTU7 (*Chroococcidiopsis* sp.) exhibited a higher abundance in cryptoendolithic and chasmoendolithic communities. The Unassigned Cyanobacterial OTU (OTU2) displayed the highest differential abundance (*p*-value < 0.0001) in the hypoendolithic community, attaining an average relative abundance of more than 39%, while its relative abundance in the other two communities barely reach 0.4%.

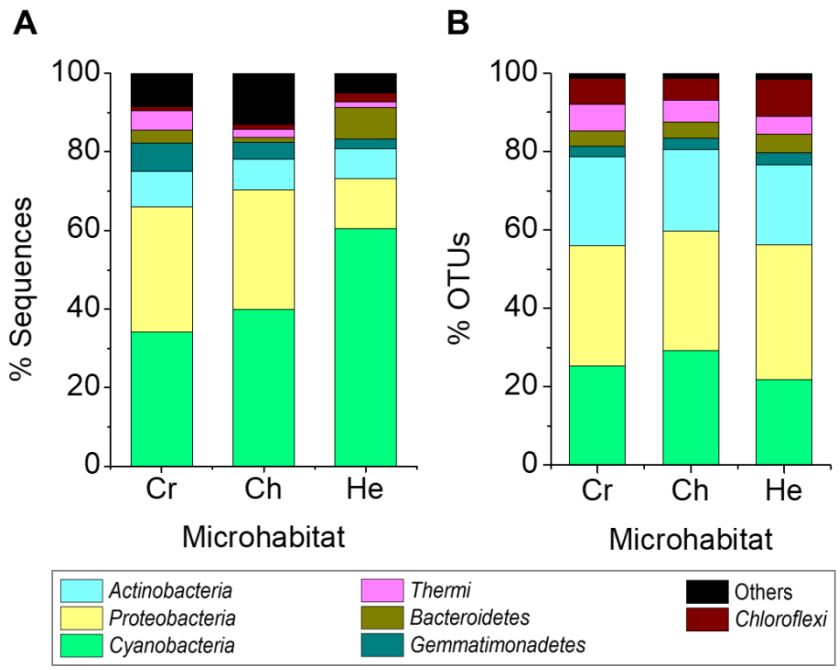

Figure 1.10. Average relative abundance of sequences (A) and OTUs (B) of major bacterial phyla (at least 1% across the samples) on microbial assemblages in the cryptoendolithic (Cr) chasmoendolitic (Ch) and hypoendolithic (He) microhabitats of gypcrete.

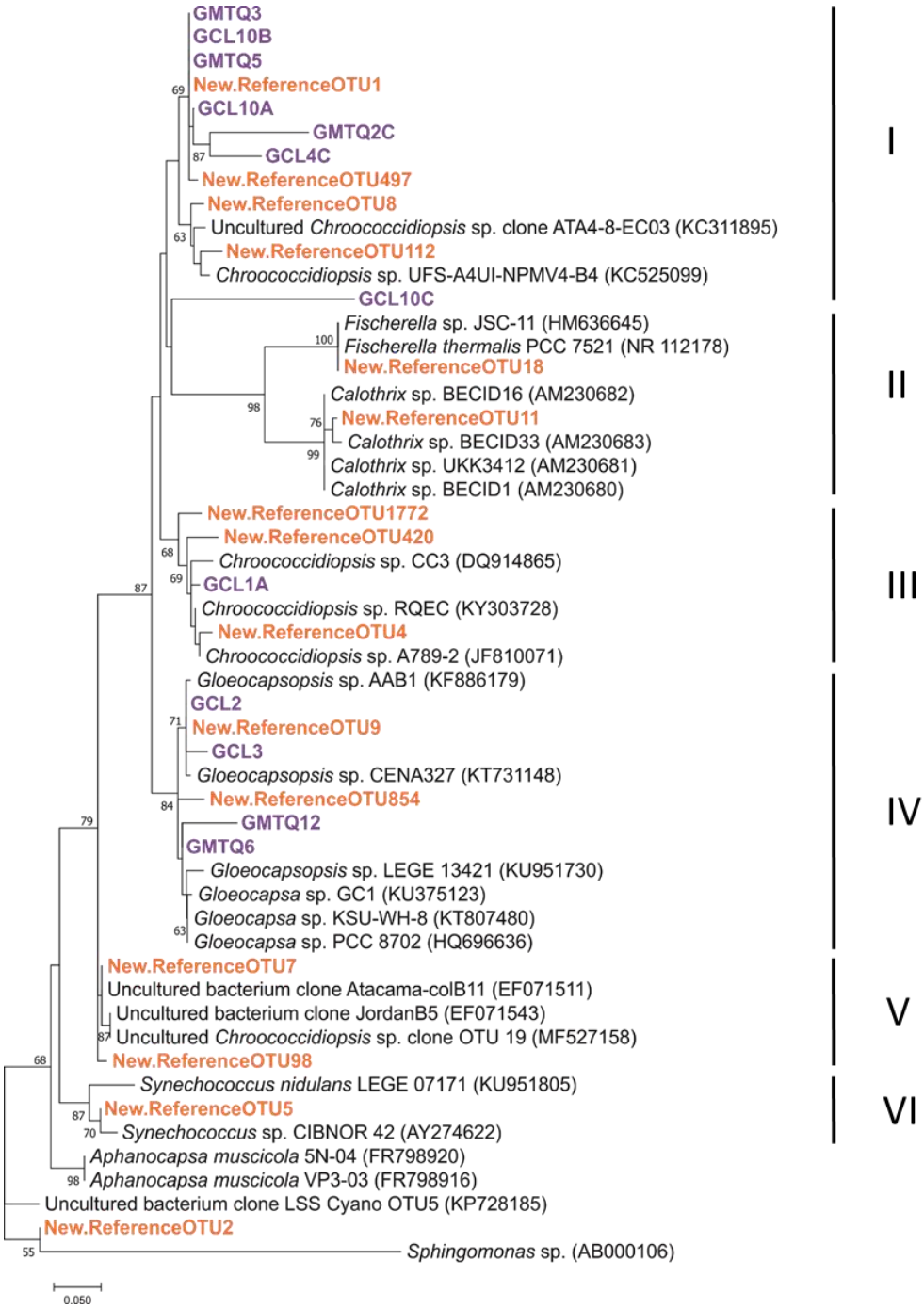

Figure 1.11. Maximum likelihood tree based on partial 16S rRNA sequences of the Cyanobacteria OTUs above 1% relative abundance (orange) **and cyanobacterial strains isolated from the three different microhabitats** (purple). Scale bars indicates 5% sequence divergence

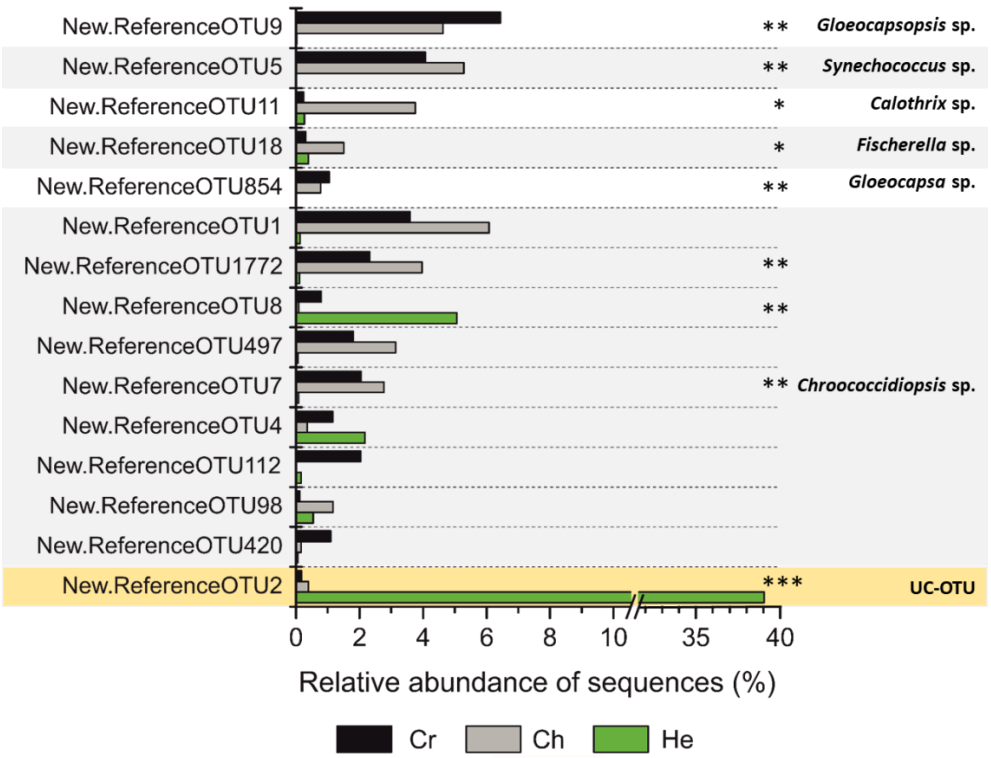

Figure 1.12. Average relative abundance of sequences of cyanobacterial OTUs above 1% relative abundance. Differentially abundant cyanobacterial OTUs across the three different microhabitats are represented by *(Diff-OTUs *p*-value <0.01 Ch / Cr-He), ** (Diff-OTUs *p*-value <0.001 He / Cr-Ch), ***(Diff-OTUs *p*-value <0.0001 He / Cr-Ch). UC-OTU (Unclassified Cyanobacterial OTU).

1.5. Discussion

In this study we addressed the characterization of the microbial communities inhabiting gypcrete collected from the Monturaqui area (Preandean Depression), which is of particular interest due to its location in the hyper-arid Atacama Desert. While endolithic colonization of the gypsum crust and gypcrete in this area has previously been studied (Dong et al. 2007, DiRuggiero et al. 2013, Wierzchos et al. 2015, Meslier et al. 2018), this is the first work in which cryptoendolithic and chasmoendolithic communities have been characterized separately. The novelty of this study lies in the consideration of two different

EMCs inhabiting two different endolithic microhabitats located in the upper part of the substrate, and in the description of the structure and composition of the hypoendolithic community, firstly described by Wierzchos et al. (2011) in the gypsum crust from the Tarapacá region of the Atacama Desert. This work was based on a multidisciplinary approach to elucidate the relationship between microhabitat architecture and community composition of EMCs hosted in three different endolithic microhabitats coexisting within the same piece of rock.

The Monturaqui region, located in the Preandean Depression of the Atacama Desert has been found to harbor two different substrates colonized by microbial communities, namely gypcrete (Wierzchos et al. 2015) and ignimbrite, volcanic rock (Wierzchos et al. 2013). Both substrates showed endolithic colonization and, at the same time, the lack of epilithic colonization (rock surface colonization). The absence of this second type of microbial communities in both substrates may be explained by the microclimate conditions of this area (Wierzchos et al. 2015) related to aridity, relative humidity, air and surface temperature, solar irradiation and precipitation. Monturaqui has been described as a hyper-arid area, showing an aridity index – based on the relation between mean annual precipitation (P) and potential evapotranspiration rate (PET) (P/PET) – of 0.0093, up to one order of magnitude lower than the limit established by Nienow (2009) for the classification of a region as hyper-arid (0.05). Regarding the air temperature observed in this region, it showed one of the lowest values registered in the hyper-arid Atacama Desert (-4.7°C), very similar to previously studied areas, such as Lomas de Tilocalar (-7.4°C) (Wierzchos et al. 2013) and Yungay (-6.2°C) (Wierzchos et al. 2012a). On the other hand, the RH values recorded in Monturaqui revealed the greatest range between the maximum (100% RH) and minimum (1% RH) on the Preandean Depression, while other locations such as Valle de la Luna, in which the minimum RH never dropped below 17% (DiRuggiero et al. 2013). The large amplitude on temperatures and RH in this specific region in comparison to other locations

included in the hyper-arid core reveals the need of the EMCs inhabiting the substrates of this area for high adaptability. Concerning the intense solar irradiance recorded in this region of the Preandean Depression compared to other highly irradiated desert areas, PAR values reached 2500 μmol photons m^{-2} s^{-1} and an annual mean of 1178 μmol photons m^{-2} s^{-1}, twice the PAR values detected in the Arctic (maximum PAR: 1393 μmol photons m^{-2} s^{-1}, annual mean: 196.3 μmol photons m^{-2} s^{-1}) (Omelon et al. 2006). Specific measurements of surface temperature for gypcrete revealed values of almost 70°C on its surface, thus approximating the upper limit temperature for photosynthesis, 74°C, under which thermophilic cyanobacteria in hot springs have been found to live (Castenholz et al., 2001). The sum of these environmental conditions has led to the avoidance of epilithic colonization in pursuit of endolithic colonization.

The porosity of lithic substrates is tightly linked to their potential endolithic habitability since the distribution and size of pores have been found to be related to water retention capacity (Cámara et al. 2015; Herrera et al. 2009; Matthes et al. 2001; Omelon 2008; Pointing et al. 2009). Porosity in gypcrete allows microbial communities to survive in different microhabitats, providing sufficient space for the microbial communities while receiving enough light and available water for their development. This porous network slows down water loss by rapid evaporation and helps its longer retention by capillary forces acting in small capillary-like shape pores. The inner architecture of gypcrete allows the habitability of three different locations inside the substrate. The CT-Scan and SEM-BSE images showed that all three types of microhabitats share a vertical axis morphology where vertical cracks constitute the chasmoendolithic (CH) microhabitat and capillary-like pores constitute the cryptoendolithic (CR) and hypoendolithic (HE) microhabitats. This capillary like pore architecture found in the CR microhabitat could be explained by the progressive substrate dissolution due to scarce rains and by the water retained and condensed within the pores, as it occurs in halite endolithic microhabitats (Wierzchos et al. 2012a). The

observed HE microhabitat architecture consolidates the proposal of Wierzchos et al. (2015), in which the authors described the presence of a dense crust delimiting the bottom part of the HE microhabitat. This structure reveals different dissolving and crystallization processes of the gypsum following the water gravity flow and giving rise to the cave-shaped pores, thus providing this HE microhabitat with a hard permeable bottom gypsum layer.

The larger distance between the HE microhabitat and the top surface, as compared to CR and CH microhabitats, may be thought to be a limiting factor for EMC development in terms of water access. However, at the same time, the location of the HE microhabitat in the rock could reduce water losses related to evaporation processes. Thus, the micro-cave structure observed in the HE microhabitat would retain liquid water for longer times, leading to facilitation of cyanobacterial grow. The inner architecture of the gypcrete HE microhabitat differs substantially from the one described by Wierzchos et al. (2011) in the gypsum crust of the Tarapacá Region. The absence of micro-caves and the availability of liquid water through frequent dew formation (J. Wierzchos pers. com.) in the gypsum crusts leads to an extraordinarily different EMC that is dominated by algae and fungal members. Therefore, the higher ratio of cyanobacteria in the gypcrete HE microhabitat in comparison with CR and/or CH microhabitats could be explained by the architectural features just described: the micro-cave structure with dense gypsum crusts and the high distance from the top surface, both of which allow higher liquid water retention and availability.

The microstructure characteristics of endolithic microhabitats located at the top of the substrate also explain the possible ways of access of the EMCs inhabiting them to water. The microstructural features of the CR microhabitat allow the identification of a combination of water retention systems present in this endolithic microhabitat. Pores connected directly or indirectly to the surface

may act as cavities where condensed water running through the rambling substrate would condense and become available for the microbial communities. Additionally, the presence of sepiolite aggregates improves water retention in those pores. On the other hand, although the CH microhabitat does not supply a similar semi-closed space for water condensation and retention, there is an absence of a lithic barrier between rainfall water and the microbial community, so that the less efficient water retention capacity of this microhabitat would be offset by higher direct accessibility to this resource.

Microbial communities inhabiting all three microhabitats occur in aggregates and are often deeply embedded in an EPSs matrix. Both aspects are closely linked to survival strategies under harsh environmental conditions related to water availability and nutrient reservoir. Since water is the most limiting factor for the development of microbial communities inhabiting endolithic microhabitats of gypcrete, it is the component on which adaptive strategies are primarily focused. This is the case with EPSs production, due to their role in hydration and dehydration processes in lithobiontic communities in Antarctic deserts (de los Ríos et al 2007) and the Atacama Desert (Dong et al. 2007; Wierzchos et al. 2011; Wierzchos et al. 2015; Crits-Christoph et al. 2016b). The aggregates-like structure of these communities composed by cyanobacteria and other heterotrophic bacteria with a different physiological status also helps their survival against drought, since dead cells could provide physical protection against desiccation processes (Postgate 1967; Roszak and Colwell 1987; Billi 2009; de los Rios et al. 2004). In the case of the CR community, a special strategy against dryness was observed: microorganisms were located close to sepiolite, as previously reported with respect to gypcrete endolithic communities (Meslier et al. 2018). EPS and dead cells taking part in the aggregates can also act as a nutrient reservoir in such an oligotrophic environment as the endolithic microhabitats, as demonstrated by the low amounts of water soluble ions detected by Meslier et al. (2018).

Water has been described as the main driver for diversity in the EMCs of the Atacama Desert (Meslier et al. 2018). The absence of significant differences in diversity between the three EMCs of gypcrete corroborates this proposal, in accordance with the diversity values of previously reported EMCs in the Atacama Desert (Table 1.1). All three types of microhabitats in gypcrete are encountered under equal climatic conditions, with the same water input as rainfall and sporadically high RH values (Table 1.3). Despite their different architecture, each microhabitat counts on a different set of characteristics for water retention, as has been described in detail: CR counts on porous condensation and sepiolite, CH has an easier access to water, and HE suffers less water loss. Regarding community composition at a phylum level, three main phyla were dominant, Cyanobacteria, Proteobacteria and Actinobacteria (Fig. 1.10) as in other EMCs (Wierzchos et al. 2015, Meslier et al. 2018, Dong et al. 2007). However, a switch in the Proteobacteria and Actinobacteria relative abundances was found compared to other gypcrete cryptoendolithic communities (Meslier et al. 2018). That switch is presumably associated to the bias resulting from the application of different DNA extraction methods. Despite the absence of significant differences in terms of diversity between all three EMCs, a remarkable difference in composition was observed. These main phyla, Cyanobacteria, Proteobacteria and Actinobacteria, were distributed differentially between microhabitats, exhibiting differences between the CR and CH communities as compared to the HE community, especially regarding cyanobacterial OTUs. This notable difference in the relative abundance of cyanobacteria could be related to the particular resources of the phototrophic community. The differential access to sun radiation could explain the contrast between cyanobacterial proportions on both sides, at the top (CR and CH) and bottom (HE) of the substrate. Thus, an update to the proposal in Wierzchos et al. (2018) is here suggested, in which a causal link is evoked to explain the higher abundances of phototrophs as opposed to heterotrophs in EMCs. According to that study, the scarcity of water

was suggested to cause a lower metabolic activity in phototrophs, thus leading to a lower support of the heterotrophic community. However, in this scenario, light should also be considered a crucial factor in understanding the differences between the composition of top and bottom EMCs, since the HE community has a notably lower access to sun radiation. Thus, for EMCs communities based on phototrophic microorganisms, a limitation to one of those resources essential for photosynthesis would further lead to low rates of CO_2 fixation and, consequently, to a smaller heterotrophic community.

While multiple genera of cyanobacteria were found among the different microhabitats, most of them belonged to the genus *Chroococcidiopsis*. Several strains of this genus have previously been described in EMCs of both hot and cold deserts (Friedman 1980) as a result of their capacity to cope with extreme environmental conditions (Billi et al. 2011; Verseux et al. 2017). Further support for the greater difference between the microbial composition of the HE microhabitat and the two endolithic microhabitats located at the top is found in the discovery of an unexpected unclassified cyanobacterial OTU (UC-OTU, New.ReferenceOTU2) which was remarkably more abundant and almost exclusive of the HE microhabitat, covering nearly 40% of the relative abundance of sequences in that community. Although the low percentage of sequence similarity did not allow an accurate taxonomical assignment, its closest relative sequences (~94% sequence identity) were from habitats where light is the limiting factor for photosynthesis, a pinnacle mat at 10 m depth from a sinkhole (Hamilton et al. 2017) and groundwater sample from a tectonically-formed cavern (Supp. Mat. 1.1). This UC-OTU stresses in parallel the effort required in cyanobacteria isolation, description, taxonomical assignment and phylogeny.

The differential distribution of the key element of these EMCs, their primary producers, between microhabitats in the same lithic substrate and the same piece of rock, reveals an "environmental filtering" process (Kraft et al. 2015).

This concept focuses on the relationship between an organism and the environment, recognizing that not all organisms will be able to establish themselves successfully and persist in all abiotic conditions. Thus, in this scenario, the abiotic conditions linked to the architecture and the placement of the endolithic microhabitat would force the development of community assemblages highly specialized to small scale differences, thereby exhibiting a microbiogeographical behavior in the EMCs composition.

1.6. Concluding Remarks and future perspectives

This is the first study addressing the differences between microbial communities inhabiting three differentiated endolithic microhabitats in the same lithic substrate, even in the same piece of rock.

In this study, water was confirmed to be a driver of diversity since the specific architecture features of each microhabitat facilitate water input and retention, suppressing differences in diversity between microhabitats. Furthermore, light was proposed as a driver for phototrophic composition with a specific distribution of certain cyanobacteria, as highlighted with respect to the hypoendolithic community. Water, light, and CO_2, are indispensable resources for photosynthetic activity. Thus, we propose a cause and effect relationship where the restriction of these factors may affect the proportion of phototrophic and heterotrophic components in the EMC communities.

The *Chroococcidiopsis* genus displayed a variety of strains distributed among all microhabitats, proving its high capacity to colonize effectively endolithic microhabitats under polyextreme conditions. Nevertheless, the presence of a singular cyanobacterial OTU stresses the importance of additional efforts in cyanobacterial characterization in these extreme environments.

The obtained results on community composition in this work reveal the importance of using an appropriate scale for the study of microbial communities. The microstructural and microarchitectural features of the lithic substrate are decisive for the structure of endolithic microbial communities. This is due to the effect of architecture on the availability of vital resources as water and light, especially for those taxa supporting the entire endolithic microbial community. Thus, this study suggests a cautious use of "macroenvironmental" parameters in understanding the differences between endolithic microbial communities from different deserts or substrates. Rather, the results obtained point to the need for a more thorough description and study of the microenvironmental conditions that directly exert an effect on this type of microbial communities: light, water and CO_2. Therefore, once the relationship between factors affecting the absence and/or presence of certain taxa, the actual environmental filtering in these microhabitats could be described in more detail, it will be possible to draw on conclusions on the interactions and specific roles of the different members in the community.

1.7. Supplementary Material

Supplementary Material 1. 1. Taxonomical assignment of cyanobacterial OTUs by BLASTn to sequences belonging to uncultured and cultured material.

CYANOBACTERIAL OTUs								
	Uncultured				Cultured			
	BLASTn	Accession Number	Identity (%)	Environment	BLASTn	Accession Number	Identity (%)	Environment
OTU18	Uncultured cyanobacterium clone 332-12	KT453633	99	Sublacustrine thermal vents Yellowstone Lake	*Chroococcidiopsis* sp. CC4	DQ914866	99	China quartz hypoliths
OTU11	Uncultured cyanobacterium clone FWS-B15	KC437357	100	Hot Spring	*Calothrix* sp. NIES-3974	AP018254	100	
OTU854	Uncultured *Gloeocapsa* sp. clone HL4SH30	LN880050	97	shoots of Haloxylon in high salinity	*Gloeocapsa* sp. PKUAC-GDTS1-13	MG822744	97	
OTU9	Uncultured cyanobacterium clone Alchichica_AQ2_1_1C_10	JN825312	99	microbialites from Alchichica alkaline lake	*Gloeocapsa* sp. Ryu5-15d	LC325265	99	blackened part of a surface of a building

OTU497	Uncultured *Chroococcidiopsis* sp. clone ATA4-8-EC03	KC311895	95	soil Atacama Desert	*Chroococcidiopsis* sp. A789-2	JF810071	94	Antarctica: University Valle
OTU420	Uncultured cyanobacterium clone IGW2-36	KP238411	98	volcanic rock ignimbrite, Atacama Desert, Lomas de Tilocalar	*Chroococcidiopsis* sp. RQEC	KY303728	97	Hypolith quartz Taklimankan desert, Xingjiang
OTU1	Uncultured *Chroococcidiopsis* sp. clone ATA4-8-EC03	KC311895	98	soil Atacama Desert	*Chroococcidiopsis* sp. CC1	DQ914863	96	quartz hypoliths China
OTU4	Uncultured cyanobacterium clone IGD2-37	KP238398	98	volcanic rock ignimbrite, Atacama Desert, Lomas de Tilocalar	*Chroococcidiopsis* sp. A789-2	JF810071	99	Antarctica: University Valle
OTU1772	Uncultured cyanobacterium clone IGW2-36	KP238411	96	volcanic rock ignimbrite, Atacama Desert, Lomas de Tilocalar	*Chroococcidiopsis* sp. RQEC	KY303728	96	Hypolith quartz Taklimankan desert, Xingjiang
OTU98	Uncultured cyanobacterium clone AY6_21	FJ891051	99	quartz, Yungay, Atacama Desert	*Chroococcidiopsis* sp. RQEC	KY303729	95	Hypolith quartz Taklimankan desert, Xingjiang
OTU8	Uncultured cyanobacterium clone AY6_17	FJ891047	99	quartz, Yungay, Atacama Desert	*Chroococcidiopsis* sp. CC1	DQ914863	97	quartz hypoliths China

OTU112	Uncultured bacterium clone BJ201305-46	KX507829	100	rain water	*Chroococcidiopsis* sp. CC1	DQ914863	97	quartz hypoliths China
OTU2	Uncultured bacterium clone LSS_Cyano_OTU5	KP728185	95	sinkhole lake	*Aphanocapsa muscicola* 5N-04	FR798920	94	fountain made of Sierra Elvira Stone, gray semi-dry patina on a water jet Spain:Granada, Generalife, Patio de la Sultana"
OTU5	Uncultured cyanobacterium clone 3GA1-12_K89	JX127189	99	stone of castle wall Germany	*Synechococcus* sp. CIBNOR 42	AY274622	99	cyanobacterial bloom in the Urias estuary (Mazatlan, Sinaloa, Mexico) during a fish mortality event in spring 1999
OTU7	Uncultured bacterium clone Atacama-colB11	EF071511	100	Atacama Desert	*Chroococcidiopsis* sp. A789-2	JF810071	94	Antarctica: University Valley

CHAPTER 2

Chroococcidiopsis, THE HIDDEN CYANOBACTERIUM SUPPORTING THE ENDOLITHIC COMMUNITY OF HALITE IN YUNGAY

CHAPTER 2: *Chroococcidiopsis*: THE HIDDEN CYANOBACTERIUM SUPPORTING THE ENDOLITHIC COMMUNITY OF HALITE IN YUNGAY

2.1. Abstract

Chroococcidiopsis is known as the most widespread cyanobacterial genus on both hot and cold deserts due to its endurance to diverse extreme environmental conditions. Controversy has surrounded the discovery of cyanobacterial endolithic colonization of halite pinnacles in the polyextreme Yungay area, in the hyper-arid Atacama Desert, for the last decade, since the different taxonomic approaches have provided different identification. While microscopy techniques offered images where the major component had *Chroococcidiopsis* morphology and ultrastructure, the sequences obtained by molecular studies showed phylogenies close to the halophile genus *Halothece.* A *Chroococcidiopsis* strain from this halite endolithic habitat has been isolated and characterized combining imaging and molecular approaches such as: light and fluorescent microscopy for morphological characterization, TEM for its ultrastructure and the development of a specific DNA isolation protocol and whole genome sequencing for its molecular characterization. Morphological and ultrastructural features and specific adaptations to the specific environmental conditions compared with those of the major cyanobacteria observed inhabiting the halite endolithic habitat leaded to the determination of indeed *Chroococcidiopsis*, and not *Halothece*, as the dominant cyanobacterium in the halite endolithic habitat in Yungay.

2.2. Introduction

2.2.1. Yungay: one of the driest sites on Earth

The Atacama Desert harbors in its hyper-arid core one of the most polyextreme environments on Earth: the Yungay area (Fig. 2.1, A), a site that was labeled as the dry limit of photosynthetic life on Earth (Warren-Rhodes et al. 2006). However, this statement was soon refuted by Wierzchos et al. (2006), who described the abundant endolithic colonization in halite pinnacles from this region and drew a new label for Yungay as one of the driest places on Earth and the driest site in the Atacama Desert where phototrophic life can be found (Wierzchos et al. 2006, Wierzchos et al. 2012a, Robinson et al. 2015).

The Yungay region's most prominent feature is the halite (NaCl) pinnacles, which form part of the Neogene salt-encrusted playas and have been isolated from any significant source of ground or surface water for the entire Quaternary (Pueyo et al. 2002). The environmental conditions outside this halite pinnacles or nodules are characterized by a strong diary thermal amplitude, up to 60°C, combined with extremely high PAR values (Table 2.1), and a mean annual precipitation below 1 mm (de los Ríos et al. 2010; Wierzchos et al. 2012a). Similar scenarios, harboring halite pinnacles colonized by phototrophic microorganisms, can also be found elsewhere in the Atacama Desert. Such are Salar Grande and Salar Soronal (Tarapacá Region), where *camanchaca* fog and stratocumulus clouds occur during more than a third of the year (Robinson et al. 2015). By contrast, the Yungay region has been shown to be under the influence of clouds less than 50 days per year (Robinson et al. 2015).

Water activity (a_w) is a crucial parameter since it is a quantification of the chemical availability of water. Its values range from 0 (absolutely no water) to 1 (pure water) serving as a thermodynamic measure of salinity (Tosca et al. 2008). Most organisms cannot multiply at $a_w < 0.9$, and few are known to tolerate $a_w <$

0.85 (Brown 1976; Moyano et al. 2013), although the most halophilic and xerophilic organisms from the three domains of life can multiply at lower a_w values (Pitt 1975; Williams and Hallsworth, 2009; Stevenson et al. 2015). The minimum water activity determined for eukaryotic systems reaches 0.640 (theoretical a_w =0.632), whereas for Archaea and Bacteria the lower limit is 0.635 (theoretical a_w=0.611) (Stevenson et al. 2015). Water activity in NaCl saturated brine ranges from 0.765 to 0.745 in temperatures between 2-50°C (Winston and Bates 1960); it is therefore the range of a_w occurring in the halite endolithic microhabitat. Thus, only highly halotolerant or halophilic organisms are expected to be found in this type of habitat.

Table 2.1. Microclimate data from Yungay from three 1 year-periods: June 2006 – June 2007 (Davila et al. 2008); May 2008 - May 2009 (Vítek et al. 2010; de los Ríos et al. 2010) and April 2010 - April 2011 (Robinson et al. 2015). Avg =Annual mean of daily average; Max= Annual mean of daily maximum; Min = Annual mean of daily minimum

Microclimate Data from Yungay		
Air Temperature (°C)	Min	-5.85 (± 2.33)
	Avg	18.16 (± 0.42)
	Max	47.78 (± 3.54)
PAR (µmol photons m^{-2} s^{-1})	Avg	820.51 (± 395)
	Max	2281.5 (± 125)
Air RH (%)	Min	2.02 (± 0.78)
	Avg	35.93 (± 1.92)
	Max	88.83 (± 12.97)

The only phototrophic microorganisms found in the Yungay's halite belong to Cyanobacteria, a phylum mostly dependent on the presence of liquid water. Other phototrophic microorganisms such as microalgae, which can more easily use water vapor for their development (Palmer and Friedmann, 1990), were not identified in this endolithic habitat in Yungay, although they have been found in the same microhabitat in Salar Grande (Robinson et al. 2015; Crits-Christoph et

al. 2016a). The question of liquid water sources for the cyanobacteria inhabiting the endolithic habitats of halite pinnacles, in the light of scarce precipitations, uncommon fog and absence of dew, was addressed by Davila et al. (2008) and Wierzchos et al. (2012a). Wierzchos et al. (2006) and Davila et al. (2008) report deliquescence of NaCl as the main source of liquid water, occurring when the air relative humidity (RH) is above 75%. Moreover, Wierzchos et al. (2012a) showed that the nano-porous structure of halite also allows the condensation of water vapor and the retention of liquid water for prolonged periods when the RH is over 55%. Both processes, deliquescence and capillary condensation, occurs during more than 5 months per year (4000 h y^{-1}) (Wierzchos et al. 2012a).

Cyanobacteria, as the main primary producers supporting the endolithic microbial communities inside the halite nodules of Yungay, furthermore need to deal with the osmotic stress from the always saturated with NaCl hypersaline environment.

2.2.2. Cyanobacteria in hypersaline environments

Cyanobacteria are known to inhabit most of the environments on Earth due to their capacity to adapt to diverse environmental conditions, colonizing different ecosystems on land and water (Whitton 1992). The presence of unicellular and filamentous representatives in a variety of hypersaline environments (salt lakes, hypersaline lagoons, solar salterns) is due to the capacity of many species to adapt to changing salinity [Oren (2000), Oren (2012), Oren (2015) and references therein] and to the fact that most of the halophilic and halotolerant species are able to live in a range of salt concentrations from 5% (one and a half times that of seawater) to 25%.

Cyanobacteria inhabiting hypersaline environments possess acclimation mechanisms against osmotic stress generated by the high salt concentration in the surrounding medium in order to maintain osmotic equilibrium and cell turgor. Extremely halophilic microorganisms have developed the “salt-in” or

"salt-out" strategy, which consists of the massive accumulation of K^+ and Cl^- in the cytoplasm and involves the adaptation of the enzymatic machinery to the high ionic concentrations (Oren 2006). However, in cyanobacteria, although ions such as Na^+, K^+ or Cl^- can transiently enter the cells following sudden increases in the salinity of the medium, there is a maintenance ionic concentration at low levels via the accumulation of organic osmotic solutes, also called compatible solutes. These small, uncharged compounds with high solubility are used to osmotically adjust the cytoplasm to the external medium. While less salt-tolerant species use disaccharides such as sucrose and trehalose, the most salt-tolerant or salt-requiring species use glycine betaine as osmotic solute. However, cyanobacteria found in halite pinnacles always live in 100% salt concentration with a_w of 0,75. According to Oren (2015), this is an exceptional hypersaline microbial ecosystem.

2.2.3. The problem of taxonomic assignment

Before defining the distribution of cyanobacteria along the salinity gradient in different hypersaline environments, it is relevant to introduce the problems derived from the taxonomical assignment. Synonymy and oversimplification are general problems in cyanobacteria identification, but this reaches a greater extent in extreme environments.

One notable example is the classification of the most halotolerant organisms. The problems of identification have been pointed out in different studies indicating the variety of names given to a unicellular halotolerant cyanobacterial species, the *Halothece* cluster: from *Aphanothece halophitica* (Oren 2015) to *Halothece*, *Euhalothece* (García-Pichel et al. 1998), *Cyanothece*, *Synechococcus* (De Philippis et al. 1993; Campbell and Golubic 1985), depending on the morphological and ultrastructural criteria used. Especially Komárek has made a huge effort to re-evaluate the classification of this group of unicellular halotolerant cyanobacteria (Komárek 1976; Komárek and Cepak 1998; Komárek et al. 1999; Komárek et al.

2004; Margheri et al. 2008; Komárek and Johansen 2015) using the "polyphasic approach" to define them through different methodological approaches (paleobotanical research, phenotype approach, ecological investigations, ultrastructure by electron microscopy and molecular approach by DNA/DNA hybridization) in order to merge all types of information in the definition of the different taxa (Komárek 2003).

In any case, under this scenario taxonomical assignment is empeded when any of these sources of information is not available, since the definition of cyanobacterial species requires most of these elements: "Group of populations which belongs to one genotype, is characterized by stabilized phenotypic features and by identical ecological demands. These characters should occur repeatedly in various localities with the same ecological conditions" (Komárek 2003).

2.2.4. Cyanobacterial diversity in hypersaline environments

Both unicellular and filamentous types can be found, depending on the salinity range. Revision of cyanobacteria in hypersaline environments by Oren (2015) showed that only unicellular types from the *Halothece* cluster (*Aphanothece, Halothece, Euhalothece*) have resulted the most halotolerant, inhabiting hypersaline environments with over 22% salt concentration. However, environments with lower salt concentration (15-22%) have also been reported to harbor the picocyanobacterial genus *Synechococcus* together with some filamentous types such as *Oscillatoria, Coleofasciculus, Phormidium, Leptolyngbya, Halospirulina/Spirulina* (*Arthrospira*) and *Plectonema*. A higher cyanobacterial diversity can be found at a lower salt concentration range (5-15%) where, in addition to the genera already mentioned, more unicellular (*Dactilococcopsis, Gloeoccapsa, Pleurocapsa* and *Chroococcidiopsis*) and filamentous types (*Lyngbya, Johannesbaptistia, Halomicronema* and *Nodularia*) have been detected. The list of these typical genera found in hypersaline

environments can be completed with Komárek and Johansen's (2015) data collection: unicellular genera such as *Staineria* and *Synechocystis*, and species of the filamentous type such as *Oxynema*.

2.2.5. Cyanobacteria in hypersaline endolithic habitats in the Atacama Desert

Living in the hyper-arid core of the Atacama Desert is already a major challenge for cyanobacteria, and its combination with the hypersaline halite endolithic habitat becomes a real feat. One of the photosynthesis requirements, water, is the most limiting factors and when it is available, it is in the form of NaCl saturated brine which counts with 36% salt concentration and a_w 0.75. This circumstances would limit primary production to extremely halophilic and the most halotolerant cyanobacteria. However, this scenario in conjuction with other extreme environmental conditions (extreme solar radiation and thermal amplitude) restrict even more the possible cyanobacterial colonizers.

During the last decade, several studies have focused on endolithic microbial colonization supported by phototrophs in halite nodules in the Atacama Desert, mainly at two locations: Salar Grande, in the northern Atacama Desert close to the western coastal range (de los Ríos et al. 2010; Vítek et al. 2010; Stivaletta et al. 2012; Roldán et al. 2014; Robinson et al. 2015; Dávila et al. 2015; Christoph et al. 2016a; Uritskiy et al. 2019) and Yungay (Wierzchos et al. 2006; de los Ríos et al. 2010; Vítek et al. 2010; Wierzchos et al 2012a; Vítek et al. 2012; Roldán et al. 2014; Vítek et al. 2014a; Wierzchos et al. 2015; Robinson et al. 2015), while a couple of them included studies from Salar Llamará, in the Central Depression (de los Ríos et al. 2010; Demergasso et al. 2003) and Salar Soronal (Robinson et al. 2015).

While all these studies point to the presence of cyanobacteria, only a few of them supply information about the relative abundance of this phylum in those communities: 15% in Yungay (Robinson et al. 2015; Wierzchos et al. 2018) and

between 5–15% in Salar Grande (Robinson et al. 2015; Crits-Christoph et al. 2016a; Wierzchos et al. 2018; Uritskiy et al. 2019) and in Salar Soronal (Robinson et al. 2015). This scenario differs notably from the cyanobacterial abundance found in other endolithic microbial communities in this desert (~ 40-80%) (Table 1.1, Chapter 1; Wierzchos et al. 2018).

Two cyanobacterial genera have been found in these halite endolithic communities, *Chroococcidiopsis* and *Halothece*, with differential results depending on the methodological approach used for their taxonomic adscription. In Salar Grande, Stivaletta et al. (2012) detected *Chroococcidiopsis* by using both morphological and molecular approaches in contrast with molecular studies performed by Robinson et al. (2015), Crits-Christoph et al. (2016a) and Uritskiy et al. (2019) in which the only cyanobacterium detected was *Halothece*. While the study of de los Ríos et al. (2010) showed cyanobacterial cells morphologically resembling *Chroococcidiopsis*, the obtained clones exhibit a genetic affiliation similar to *Halothece*.

As yet, the available information about the identity of cyanobacteria inhabiting halite endolithic communities in Yungay is not complete, despite the fact that they were the very first to be discovered by Wierzchos et al. (2006). In that microscopy work, the cyanobacterium found was assigned to the *Chroococcidiopsis* genus following morphological and ultrastructural criteria. Four years later the use of a cloning library allowed a molecular approach accompanied by microscopy performed by de los Ríos et al. (2010) where the authors determined that, as in Salar Grande, the cyanobacterium belonged to the *Halothece* genus, although its morphology and ultrastructure resembled that of the *Chroococcidiopsis* genus.

This chapter is focused on unraveling the identity of the cyanobacteria inhabiting one of the most polyextreme environmental contexts on Earth, Yungay, and the problematics of their description, finding and classification. Further, this chapter

aims to explore their adaptations to cope with the different adverse environmental conditions of this site in the hyper-arid Atacama Desert.

2.3. Experimental Procedures

2.3.1. Site description and sampling

Colonized halite rocks were collected in the Atacama Desert in December 2015 from the Yungay area (GPS coordinates 24°04'059''S; 069°54'24''W). This area is located 60 km from the coast at an altitude of 962 m between two mountain ranges–the coastal mountains to the west (1000–3000 m high) and the Domeyko Mountains to the east (about 4000 m high). The coastal mountains block most of the marine fog and humid air from reaching Yungay, except during very rare episodes. All samples were packed in sterile bags and stored at room temperature, dry and dark environment before further processing. (Fig. 2.1)

2.3.2. Cyanobacteria isolation

Three weeks after the collection of the lithic samples, scrapped material from two endolithic colonization zones of halite, the green zone (Z1) and the black zone (Z2), were transferred to two different sets of plates. The first set contained BG11 1.5% - agar plates (Purified Agar, Condalab, Spain) with 20% NaCl and the second set BG11 1.5% - agar plates without NaCl. All samples were incubated in a growth chamber at 28 ± 2°C with illumination of 20 µmol photons m^{-2} s^{-1} by cool white 40W fluorescent tubes (Philips). After 30 days of incubation, visible cyanobacterial growth appeared only in the second set of plates, with BG11 1.5%-agar without NaCl. Colonies from that set of plates were isolated by repeated plating on 0.8%-agar with BG11 medium (Rippka et al., 1979). The successfully isolated colonies were then transferred to liquid BG11 medium. The

first set of plates (with 20% NaCl) was checked every week during 6 months and no cyanobacterial growth was observed.

2.3.3. Light and fluorescence microscopy

Halite samples from the endolithic colonization zone (3-5 mm below the crust surface) were scrapped and dissolved in 5M NaCl. After brief precipitation of scarce mineral particles, the supernatant was centrifuged at 12,000x *g* for 10 min. Cell aggregates on the pellet were resuspended in 20µL of 5M NaCl. Both cell aggregates from cyanobacterial isolated cultures were observed in DIC mode and with fluorescence microscopy (FM) with Apochrome oil immersion objective x64 n=1.4, using a D1 Zeiss fluorescence microscope (AxioImager M2, Carl Zeiss, Germany). The DAPI (Zeiss Filter Set 49; Ex /Em: 365 / 420–470 nm) filter set was used for the acquisition of single section images of autofluorescence signal potentially proceeding from chlorophyll. AxioVision 4.8 software was used for image acquisition and processing.

2.3.4. Transmission Electron Microscopy (TEM)

Specimens of natural endolithic colonization were prepared by dissolving 0.3g of representative colonized halite in distilled water. Following brief precipitation of the scarce mineral particles, the supernatant was centrifuged at 12,000x *g* for 10 min. The microbial cells precipitated were fixed following the protocol described by de los Ríos et al. (2010). Cyanobacterial cells from the culture were centrifuged at 3,000x *g* and transferred to vials with 3% glutaraldehyde in 0.1M cacodylate buffer and incubated at 5°C for 3 hours. The cells were then washed three times in cacodylate buffer, postfixed in 1% osmium tetroxide for 5 hours before being dehydrated in a graded series of ethanol and embedded in LR White resin. Poststained ultrathin sections were observed in a JEOL JEM-2100 200kV electron microscope (Tokio, Japan) with Gatan Orius CCD camera (Pleasatan, CA, USA).

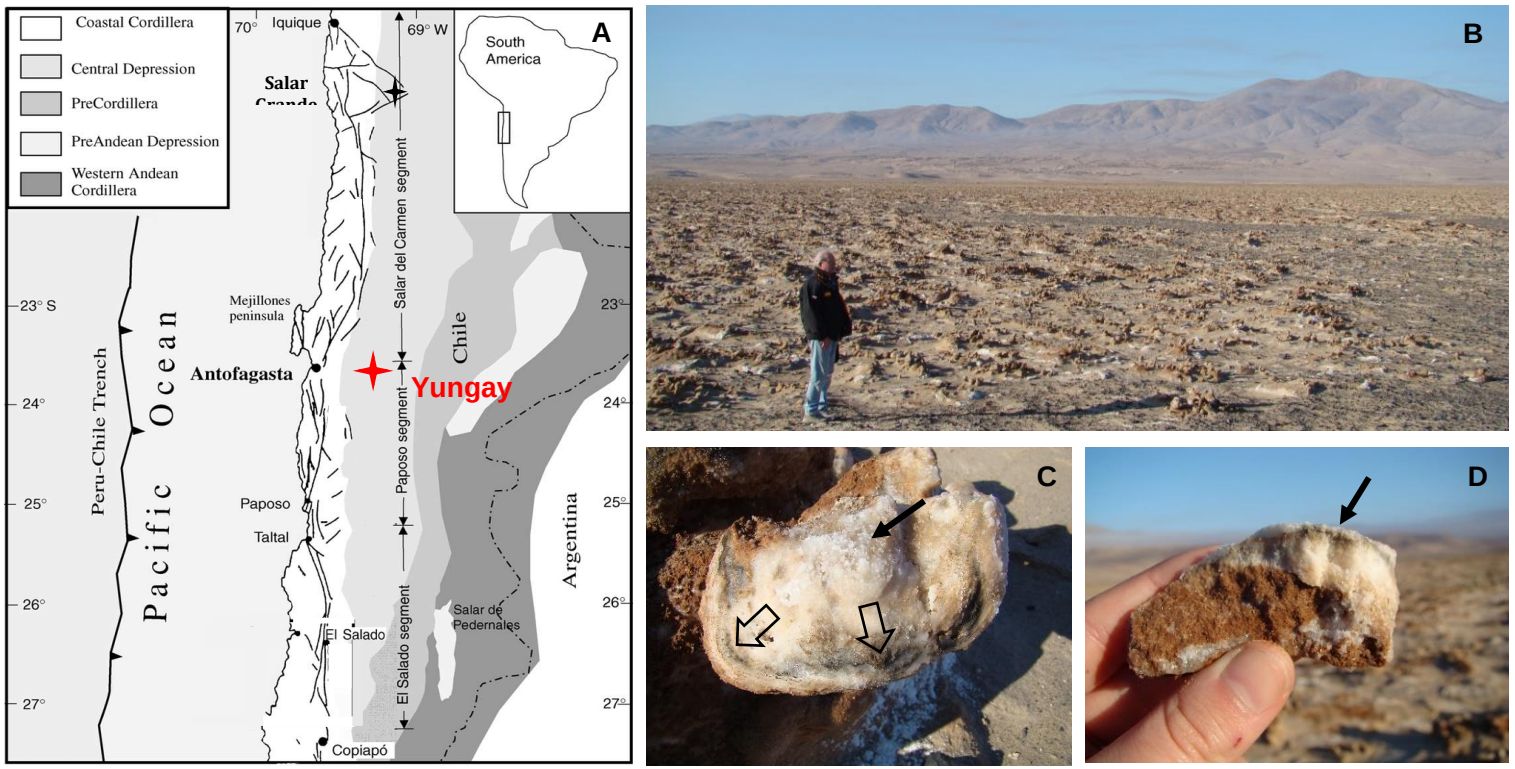

Figure 2.1. Yungay Sampling site. A) Sampling location in the Atacama Desert, Chile. Yungay area (red diamond) and its analog Salar Grande (black diamond). Modified from (Hock et al. 2007) B) Yungay area landscape with halite pinnacles. C) Top view of a halite pinnacle with salt efflorescence crystals (white dots pointed by black arrow) and scytonemin deposits on its surface (black regions pointed by empty arrows). **D)** Fragment of halite pinnacle exhibiting endolithic colonization (black arrows).

2.3.5. Customized DNA extraction procedure

Multiple and unsuccessful attempts to recover DNA were performed using diverse DNA isolation kits known to be successful for other endolithic microbial communities and endolithic cyanobacterial isolates (UltraClean, PowerSoil, PowerBiofilm) with or without modifications. Also, the specific methodology described by Billi et al. (1998) for *Chroococcidiopsis*, which combines enzymatic lysis with the phenol-chloroform protocol, was applied to extract DNA from *Chroococcidiopsis*-like isolates with ineffective results. Thus, a novel DNA isolation method was developed both for the culture material and the cyanobacteria inhabiting the endolithic microbial community in halite from Yungay (Fig. 2.2). Differential procedure for the first lysis step was applied to cyanobacteria from the culture and from the colonization zone. Culture material from each strain (50 mL) was harvested during exponential growth and centrifuged (10,000 x *g*, 5 min). The pellet was washed 3 times with TE Buffer, resuspended in a final volume of 5mL of TE Buffer and passed through French pressure cell press 3 times at 9000 PSI (62,05 MPa). The principle underpinning the high efficiency of French pressure cell press (French and Milner, 1955) consists in subjecting a suspension of microbial cells to high pressure and then abruptly reducing the pressure (Jaschke et al. 2009).

For cyanobacterial material from the endolithic microhabitat in halite, 2g of the colonized zone from the halite were scrapped and dissolved in 5M NaCl. A total of 10 washing steps with decreasing concentrations of NaCl (serial dilutions) were performed in order to avoid an osmotic shock on the cyanobacteria. Finally, cells were resuspended in a final volume of 5mL of TE buffer and passed through French pressure cell press 1 time at 9000 PSI (62.05 MPa) to prevent the damage of DNA from cyanobacteria with weaker membranes. At this point cell lysates from both types of material followed the same protocol. Working with 400µL aliquots, 0.010g of silica beads 20µL of 10% SDS and 250µL of hot phenol

ultrapure (65°C) were added. After 3 steps of vortex and incubation at 65°C, 250µL of chloroform were added, followed by 3 steps of vortex and incubation at 4°C and centrifugation at 13,000x *g* for 15min at 4°C. A second extraction with 1mL of hot ultrapure phenol and vortex and spin down 13,000 rpm for 15min at 4°C, as well as two subsequent extractions with chloroform, were performed. The aqueous phase was transferred and absolute ethanol was added for its incubation for 12h at -20°C. DNA pellets were washed with 70% ethanol and finally resuspended in 20µL of MilliQ water. An estimated 20% efficiency in DNA isolation with customized DNA extraction method was obtained for both cultures (YU-1 and YU-2) and natural samples. This estimation was made by microscopy observation of cellular lysis.

2.3.6. Cyanobacterial isolates molecular characterization.

16S rRNA gene was amplified using primers PA (Edwards et al. 1989) and B23S (Lepère et al. 2000), and PCR conditions from Ballot et al. (2008): 1 cycle of 5 min at 94°C, then 30 cycles of 30 s at 94°C, 30 s at 50°C and 1 min at 70°C, and a final elongation step of 72°C for 3 min. Sequencing was performed as described in Casero et al. (2014).

2.3.7. *Chroococcidiopsis* YU-2 strain whole genome library preparation, sequencing and computing analysis.

The genomic DNA of *Chroococcidiopsis* YU-2 was subjected to paired-end Illumina HiSeq sequencing (Johns Hopkins Genetic Resources Core Facility) after creating a library using KAPA HyperPlus (KAPA Biosystems). Raw reads were quality trimmed with TrmGalore, after quality filtering, library contained over 7.6 Gbp of sequence. Resulting pairs were processed with the MetaWrap pipeline (Uritskiy et al. 2018). A total of 175 high-coverage contigs, encompassing a total of 5,957,924 bases, were selected for further analyses. Among these contigs, the N50 value was 63,683 bases, with an average G+C% of 46.3. CheckM v1.0.7

(Parks et al. 2015) reported a genome completeness of 99.48% and a genome contamination of 1.93%. Finally, gene prediction and annotation of the *Chroococcidiopsis* sp. YU-2 contigs were carried out with the Rapid Annotations using Subsystems Technology (RAST) pipeline (Overbeek et al. 2014). A total of 6,412 coding DNA sequences (CDSs), 36 tRNA genes, and 2 rRNA genes were identified.

2.3.8. Characterization of the cyanobacterial diversity in the halite endolithic community.

The 16S rRNA genes in the extracted DNA from the natural sample were amplified using cyanobacteria-specific oligonucleotide primers CYA359F and CYA781R(a)/CYA781R(b) (Nübel et al. 1997). PCR reaction was performed as described in Casero et al. (2019). Cloning libraries were performed using the StrataClone™ PCR Cloning Kit (Agilent Technologies).

2.3.9. Phylogenetic analysis

Sequences of 16S rRNA gene from cyanobacterial isolates were aligned with sequences obtained from the NCBI GenBank using the Clustal W 1.4 software (Thompson et al. 1994). 16S rRNA sequences from GenBank were selected using NCBI MegaBlast tool (http://blast.ncbi.nlm.nih.gov/ Blast.cgi, accessed 28.08.18). The final alignment length was 400 bp. Phylogenetic trees were constructed in MEGA 7.0 using the Maximum Likelihood (ML) method (Kumar et al. 2016). The best fitting evolutionary model, chosen by following the BIC (Bayesian Inference Criterion) in MEGA 7.0, was the Kimura 2-parameter model (Kimura 1980) for 16S rRNA. 1000 bootstrap replicates were performed for all trees.

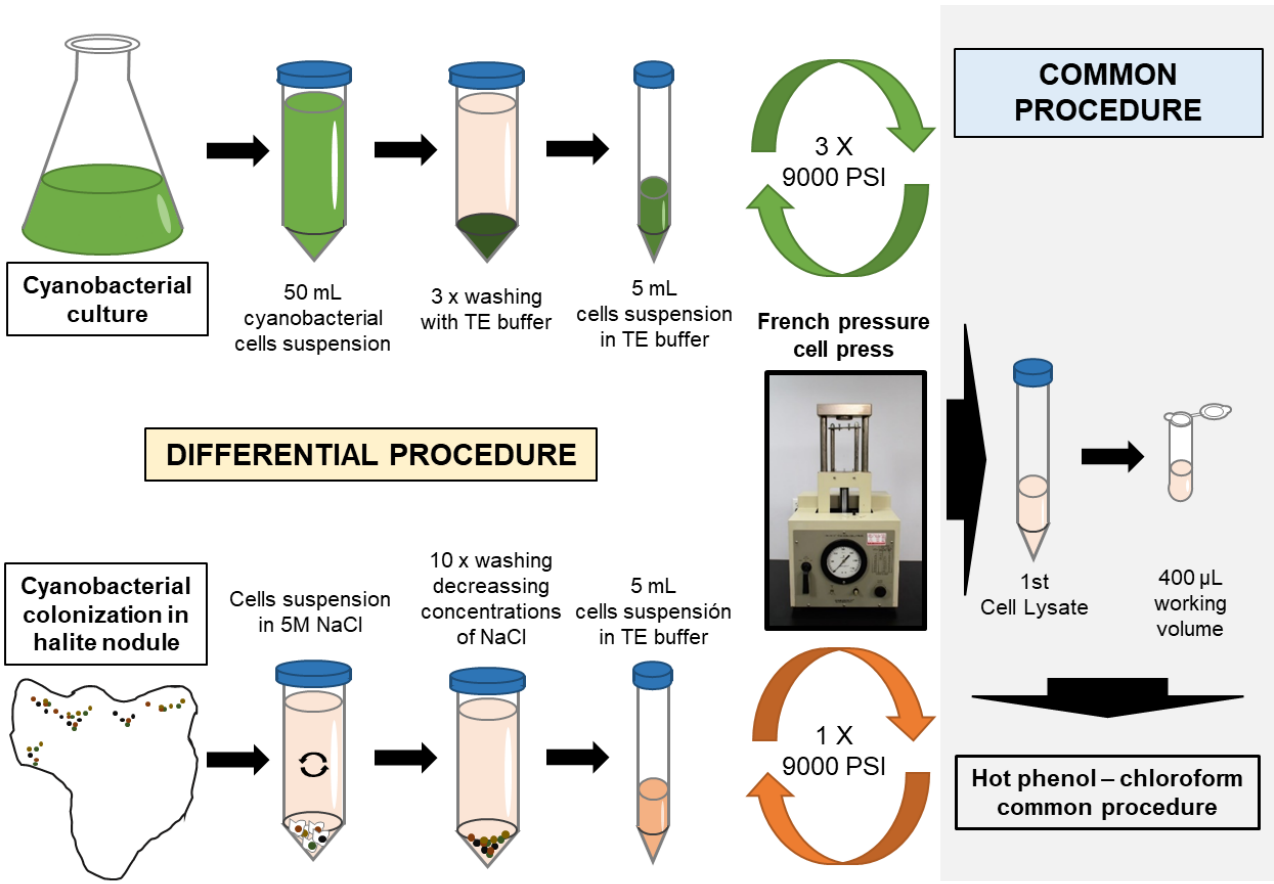

Figure 2.2. Customized DNA isolation lysis step for *Chroococcidiopsis*-like cyanobacterial cultures isolated from halite endolithic community and for endolithic microbial communities inhabiting halite from Yungay. Detailed description in section 2.3.5.

2.4. Results

2.4.1. Cyanobacterial strains isolation

Light microcopy images (DIC) from cyanobacterial aggregates scrapped from two different colonization zones are shown in Fig. 2.3 and Fig. 2.4: Zone 1 (Z1) with green aggregates (Fig. 2.3) and Zone 2 (Z2) with black aggregates (Fig. 2.4). Both preparations showed the presence of cyanobacterial cells with the typical morphology of *Chroococcidiopsis* aggregates according to Komárek and Johansen (2015).

Z1 Green aggregates (Fig. 2.3) exhibited green round shape cells grouped in sacs containing from four to more than ten cells. These aggregates are surrounded by an uncolored thick envelope. By contrast, Z2 brown aggregates (Fig. 2.4) were composed of bigger irregular cells grouped in couples or tetrads surrounded by thick layers from green-orange to intense brown.

During the isolation process, the culture YU-1 obtained from the green endolithic colonization zone Z1 revealed the co-occurrence of two clearly differentiated cyanobacterial morphotypes (Fig. 2.5, B): *Chroococcidiopsis*, solitary or small aggregates of bigger blue-green cells, and *Synechococcus*, lighter green smaller cells organized in spherical aggregates. Again the Cyanobacterial cells were identified according to Komárek and Johansen (2015). *Chroococcidiopsis* aggregates were generated following one or two binary divisions with their planes orthogonal to each other, releasing baeocytes once the sheath envelope was broken. In fact, light microscopy images (DIC) showed the presence of empty sheath envelopes after this release. Concerning the fluorescence microscopy image of this mixed cyanobacterial culture, differences in autofluorescence intensity between *Chroococcidiopsis* and *Synechococcus*-like could easily be observed, detecting a higher intensity in the former. Unfortunately,

Synechococcus- like members were lost during the following steps of the isolation process so that the study based on molecular tools could not be performed.

Culture YU-2 isolated from black colonization zone Z2, in contrast to the previously described YU-1, resulted in an unicyanobacterial culture of *Chroococcidiopsis* (Fig. 2.5, C). Light microscopy images (DIC) showed the co-occurrence of 3 different stages of *Chroococcidiopsis*: a) aggregates where the parental cell was divided in two or four daughter cells after one or two binary divisions respectively, b) some aggregates where these daughter cells started dividing in different planes without intermediate growth and c) baeocytes. Cells exhibiting a lower chlorophyll autofluorescence allowed the observation of a parietal disposal of thylakoids (Fig. 2.5, C).

2.4.2. Ultrastructure characterization and taxonomical assignment

Ultrastructural features of the three samples of the study: the natural sample scrapped from the colonization zone of halite and both YU-1 mixed culture and YU-2 isolate were used for their characterization and taxonomical assignment. A summary of the features found in the TEM micrographs (Fig. 2.6 and Fig. 2.7) and a comparison with the literature description of these genera are shown in Table 2.2.

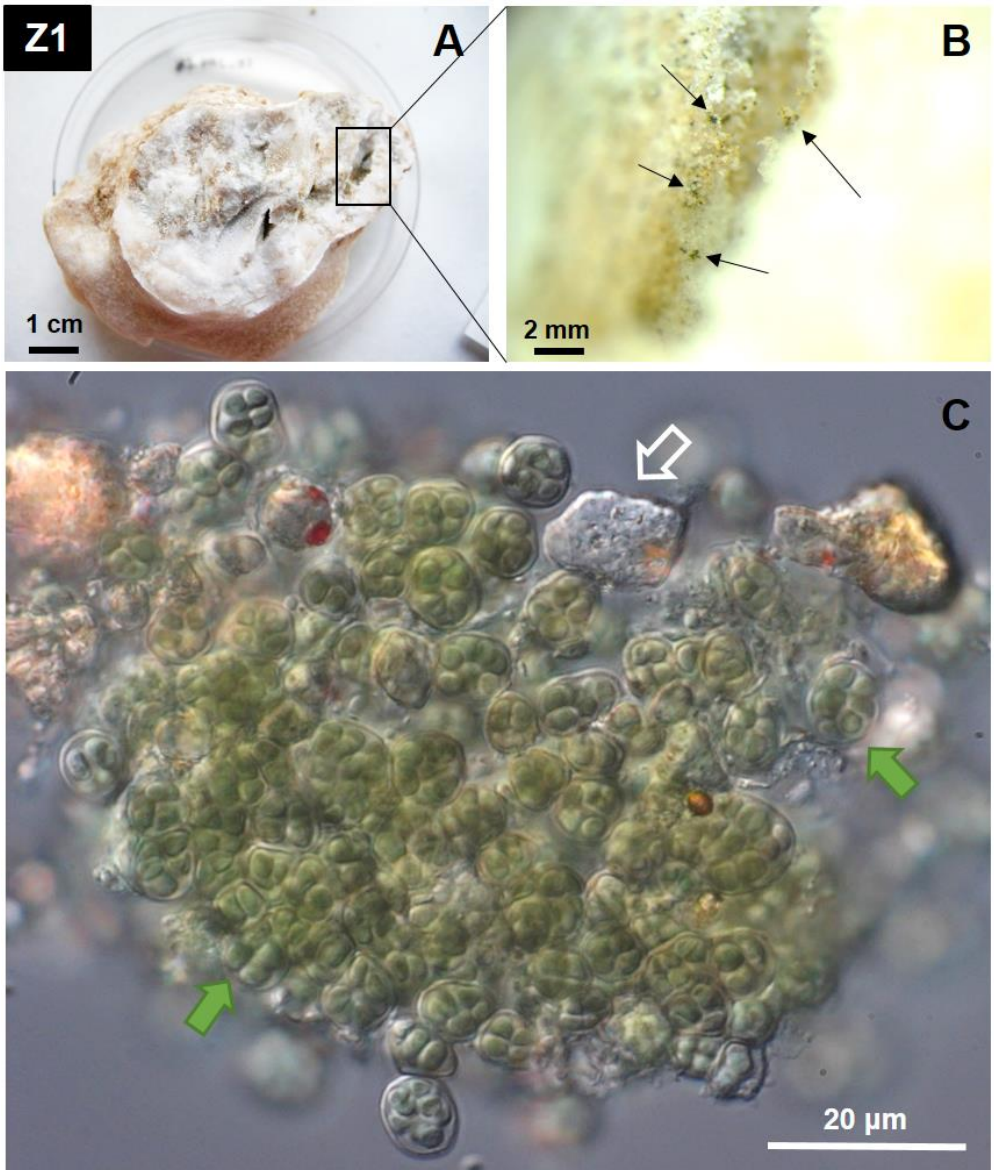

Figure 2.3. **Colonization zone Z1 with green aggregates**. **A)** Halite sample with colonization zone (square). **B)** Detailed colonization zone with green aggregates pointed by arrows). **C)** Scrapped big green cyanobacterial *Chroococcidiopsis*-like aggregate from Z1 colonization zone. Green arrows point at green aggregates containing numerous round shape cells surrounding by a thick envelope. White arrow points NaCl crystal.

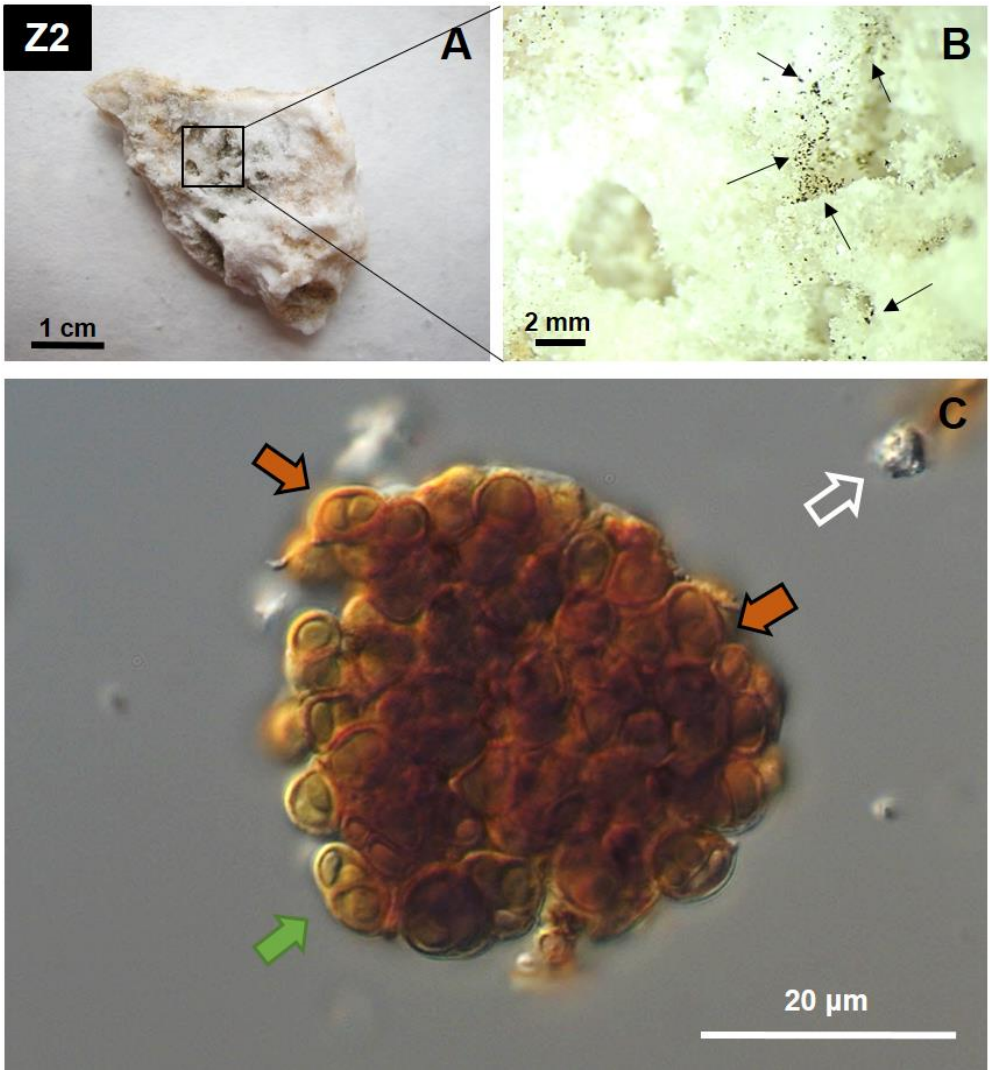

Figure 2.4. Colonization zone Z2 with black aggregates A) Halite sample with colonization zone (square). **B)** Detailed colonization zone with black aggregates (dark dots pointed by arrows). **C)** Scrapped dark brown-orange *Chroococcidiopsis*-like aggregate from Z2 colonization zone. Brown arrows point at brown aggregates where scytonemin is accumulated on the EPS envelope (Chapter 3). Green arrow points at a green aggregate with a thick green-orange envelope where less scytonemin has been accumulated. White arrow points NaCl crystal.

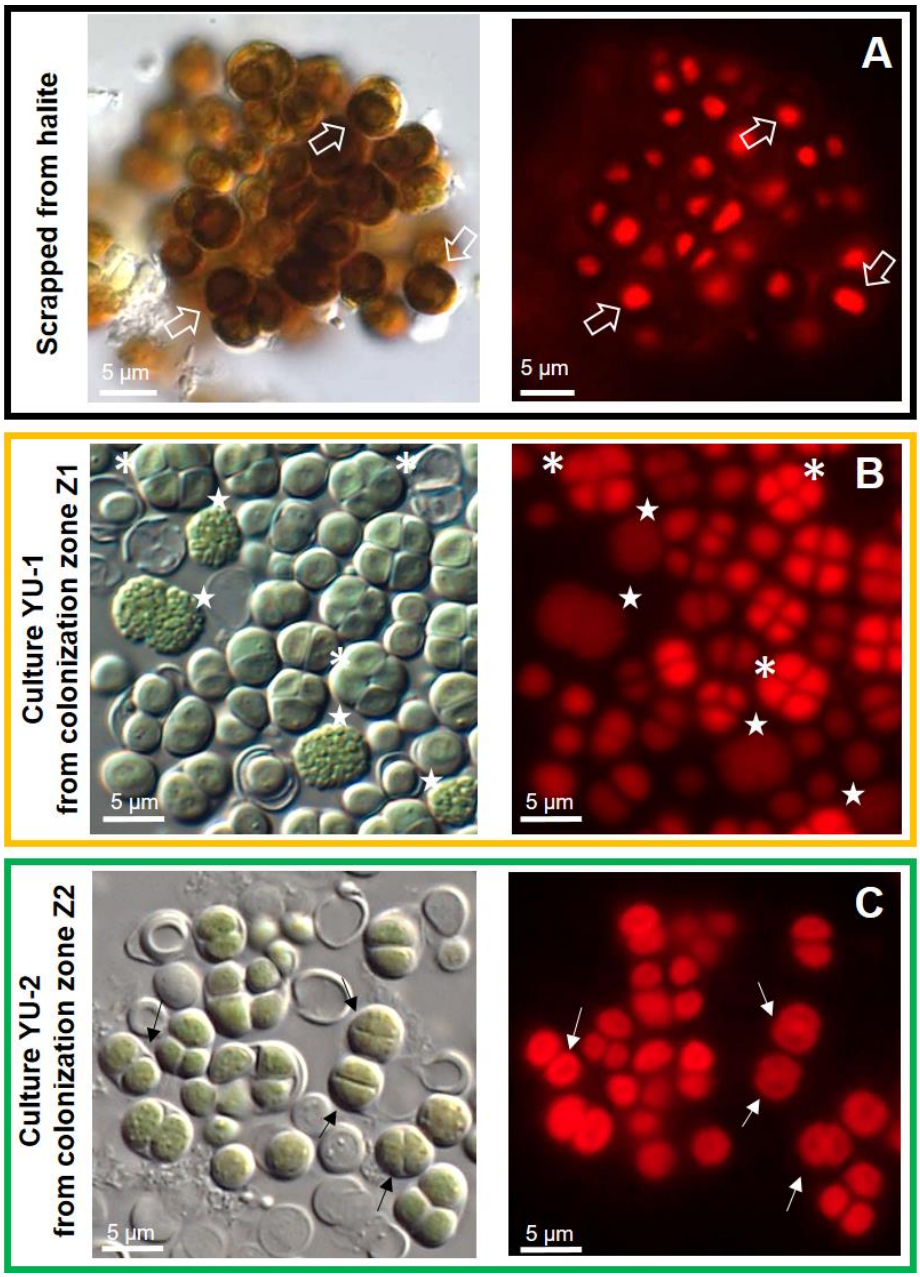

Figure 2.5. **Light and fluorescence microscopy images from cyanobacteria from endolithic microbial community of halite. A)** Cyanobacteria scrapped from natural sample. Empty arrows point at cyanobacterial cells with chlorophyll autofluorescence (red). **B)** Mixed cyanobacterial culture YU-1 isolated from Z1 containing *Chroococcidiopsis* cells with high chlorophyll autofluorescence (asterisks) and Synechococcus like cells with low autofluorescence (stars). **C)** *Chroococcidiopsis* culture YU-2 isolated from Z2**.** Arrows indicate cells exhibiting a parietal disposal of thylakoids.

2.4.2.1. *Chroococcidiopsis* YU-1 and *Chroococcidiopsis* YU-2

Starting with the cyanobacterial cultures, by comparing light microscopy information (Fig. 2.5, B-C) with the ultrastructural features (TEM) found in the bigger cyanobacterial cells from YU-1 (Fig. 2.6, B; Fig. 2.7, B; Table 2.2) and the cyanobacterial isolate YU-2 (Fig. 2.6, C; Fig. 2.7, C; Fig. 2.8, C; Table 2.2), both cyanobacteria were assigned to *Chroococcidiopsis* genus.

Cells from cultures YU-1 (Fig. 2.6, B) and YU-2 (Fig. 2.6, C; Fig. 2.7, C) exhibited the typical morphology of Morphotype II (baeocystous) as described by Rippka et al. (1979). Two main characteristics of this Morphotype II can be observed in the micrographs: the presence of a denser outermost fibrous layer surrounding the aggregates (Fig. 2.6, B-C; Fig. 2.7, C and Fig. 2.8, C) and reproduction through multiple fission in different planes (Fig. 2.7, C).

Although thylakoid structure was not easy to discriminate, regarding the three main patterns of thylakoid arrangement, *Chroococcidiopsis* from YU-1 (Fig. 2.6, B) exhibited a coiled pattern, an irregular distribution in a wavy and dense structure. However, *Chroococcidiopsis* YU-2 exhibited a parietal thylakoid arrangement (Fig. 2.7, C and Fig. 2.8, C) as previously deduced from fluorescence microscopy images (Fig. 2.5, C).

Decisive morphology and ultrastructural features for this taxonomical assignment were cell size, shape of aggregates, binary fission as division pattern and the presence of a dense outermost layer which revealed the identity of both cyanobacteria (Table 2.2). All these factors along with their original habitat, cryptoendolithic, allowed the determination of both cyanobacterial isolates as belonging to the *Chroococcidiopsis* genus.

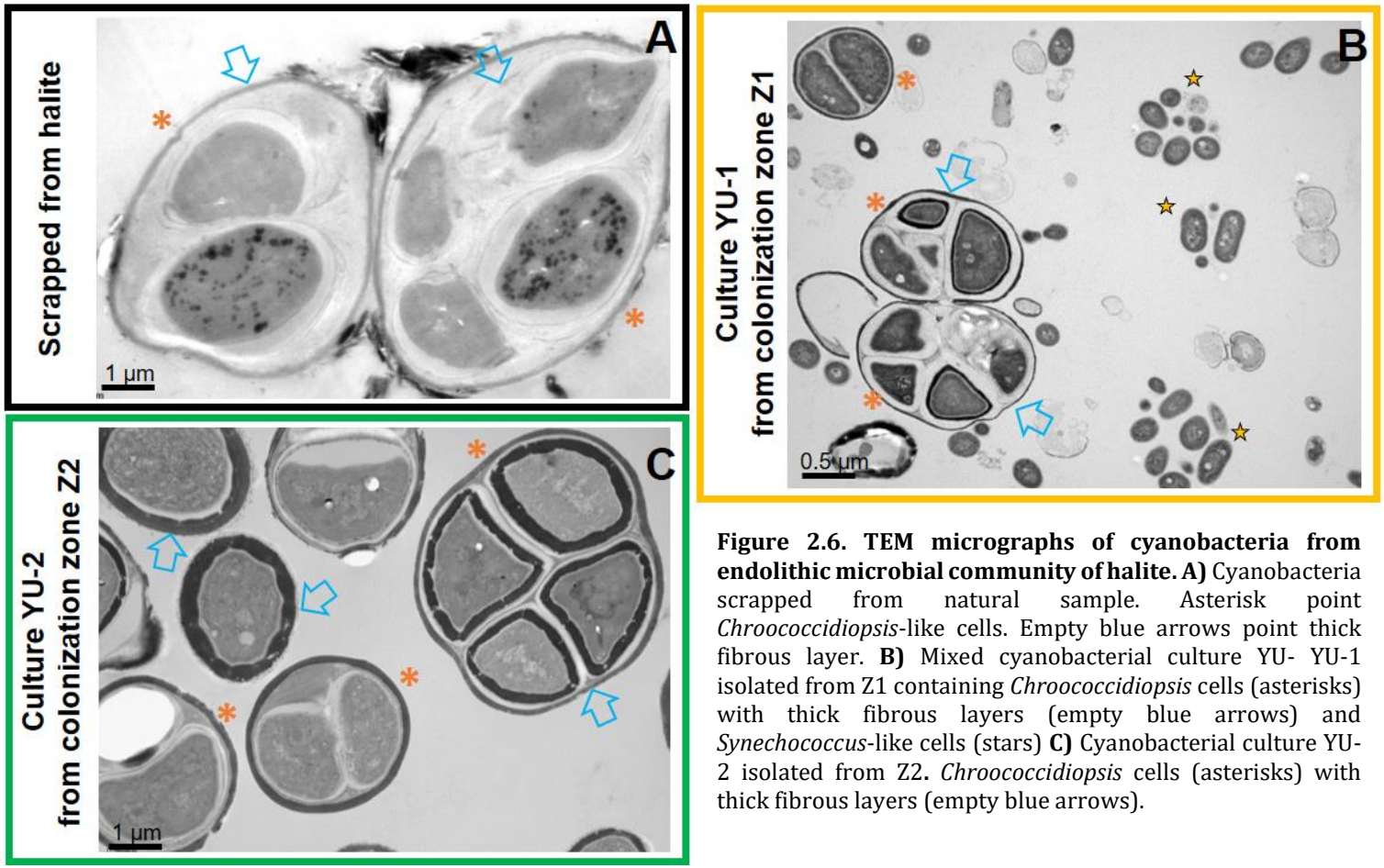

Figure 2.6. TEM micrographs of cyanobacteria from endolithic microbial community of halite. A) Cyanobacteria scrapped from natural sample. Asterisk point *Chroococcidiopsis*-like cells. Empty blue arrows point thick fibrous layer. **B)** Mixed cyanobacterial culture YU- YU-1 isolated from Z1 containing *Chroococcidiopsis* cells (asterisks) with thick fibrous layers (empty blue arrows) and *Synechococcus*-like cells (stars) **C)** Cyanobacterial culture YU-2 isolated from Z2**.** *Chroococcidiopsis* cells (asterisks) with thick fibrous layers (empty blue arrows).

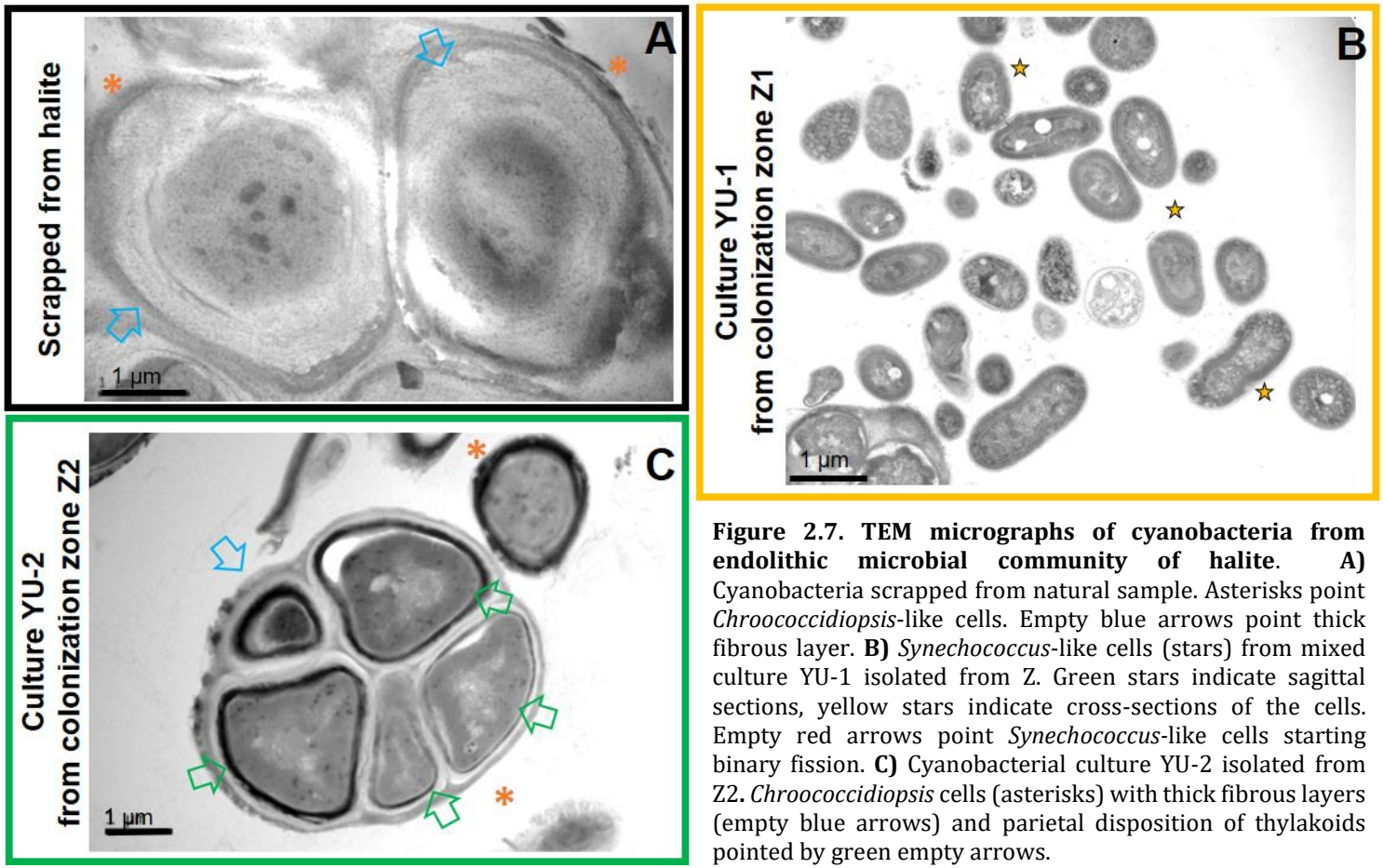

Figure 2.7. TEM micrographs of cyanobacteria from endolithic microbial community of halite. **A)** Cyanobacteria scrapped from natural sample. Asterisks point *Chroococcidiopsis*-like cells. Empty blue arrows point thick fibrous layer. **B)** *Synechococcus*-like cells (stars) from mixed culture YU-1 isolated from Z. Green stars indicate sagittal sections, yellow stars indicate cross-sections of the cells. Empty red arrows point *Synechococcus*-like cells starting binary fission. **C)** Cyanobacterial culture YU-2 isolated from Z2**.** *Chroococcidiopsis* cells (asterisks) with thick fibrous layers (empty blue arrows) and parietal disposition of thylakoids pointed by green empty arrows.

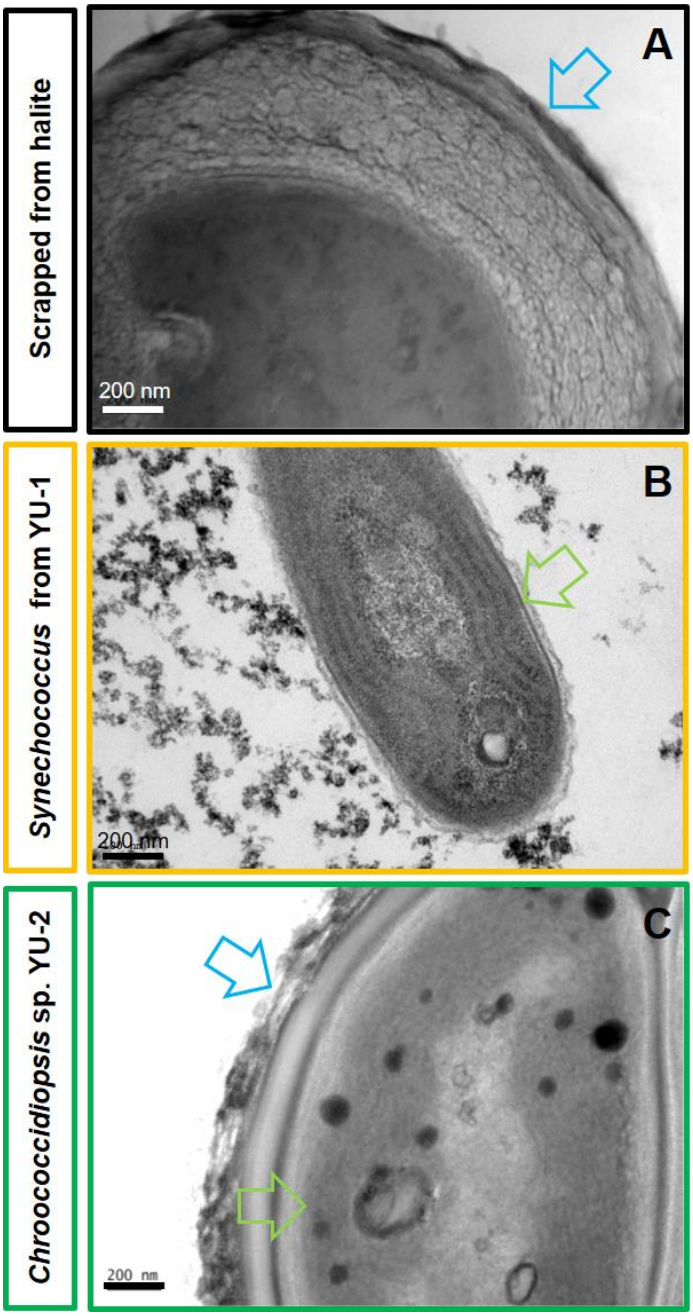

Figure 2.8. **Detailed TEM micrographs of cyanobacteria from endolithic microbial community of halite. A)** *Chroococcidiopsis*-like cell scrapped from natural sample Empty blue arrow points the thick fibrous layer. **B)** *Synechococcus*-like cell exhibiting parietal thylakoid arrangement (green empty arrow). **C)** *Chroococcidiopsis* cell from culture YU-2 isolated from Z2**.** Thick fibrous layer (empty blue arrows) and parietal disposition of thylakoids pointed by green empty arrow.

This taxonomical assignment was complemented by phylogenetic data based on the 16S rRNA gene (Fig. 2.9 and Fig. 2.10) of *Chroococcidiopsis* sp. YU-2. As it is shown in Fig. 2.9, *Chroococcidiopsis* YU-2 was located on the green framed cluster, whose singularity is its closeness to the *Gloeocapsa* and *Gloeocapsopsis* cluster (blue framed), and is clearly different from the *Halothece* cluster (red framed). The phylogenetic tree of cyanobacterial strains isolated from different endolithic microhabitats from separate lithic substrates of the Atacama Desert (Fig. 2.10) grouped this *Chroococcidiopsis* sp. YU-2 strains with most of the cryptoendolithic isolated strains from gypcrete (Chapter 1) and ignimbrite (isolated during this thesis), separating them from the cluster containing chasmoendolithic isolated strains from calcite and gypcrete.

2.4.2.2. *Synechococcus*-like from mixed culture YU-1

Smaller cells and aggregates found in the YU-1 mixed culture follow the typical description of Morphotype I (unicellular) according to Rippka et al. (1979) (Fig. 2.7, B and Fig. 2.8, B): oval single cells reproduced by binary fission, highlighted on Fig. 2.7, B. This second morphotype found in the YU-1 culture was defined as *Synechococcus* based mainly on two features and their differences from the expected *Halothece* as described by Margheri et al. (2008). *Synechococcus* cells exhibited a cell size almost 10-fold smaller than *Halothece* (Table 2.2) and a clear parietal thylakoid arrangement following the oval shape (Fig. 2.8, B).

Table 2.2. Main taxonomic intergeneric features of the natural sample *Chroococcidiopsis*-like, both *Chroococcidiopsis* isolates YU-2 and YU-1, compared to *Chroococcidiopsis* sp. features described by [a] Donner 2013. And *Synechococcus*-like found in the mixed culture YU-1 compared to *Halothece* sp. described by [b] Margheri et al. 2008.

	Halite Cyanobacteria	*Chroococcidiopsis* sp. YU-2 | YU-1	*Chroococcidiopsis* sp. [a]	*Synechococcus* on YU-1	*Halothece* sp. [b]
Cell Dimensions (µm)	1-4	1.5-5	1.25-5.43	1-2 x 0.6-1	2.5-12.6 x 2.6-7.8
Shape	Spherical	Spherical	Spherical, oval to irregular-rounded	Rod shape	Oval
Cell division	Multiple fision	Binary fision	Irregular, successive in numerous baeocytes	Binary fision	Perpendicular binary fission
Thylakoid arrangement	Coiled	Parietal Coiled	Parietal, coiled or stacked thylakoids	Parietal	Irregular position
Other features	Dense outermost layer	Dense outermost layer			
Life form, slime, colony formation	Solitary Two cell aggregates, tetrades and irregular groups	Solitary Two cell aggregates, tetrades and irregular groups	Solitary or aggregated in irregular groups	Solitary cells or aggregates	Solitary cells. No colonies. No mucilage. Facultative short pseudofilaments (2-8 cells long)

2.4.2.3. Natural halite sample visualized *Chroococcidiopsis* cyanobacteria:

Cyanobacterial cells directly scrapped from the colonization zone of halite micrographs (Fig. 2.6, A and Fig. 2.7, A) exhibited the typical morphology of Morphotype II (baeocystous) as described by Rippka et al. (1979). Both features found in the YU-1 and YU-2 *Chroococcidiopsis* cultures were also observed here: a denser outermost fibrous layer surrounding the aggregates (Fig. 2.6, A: Fig. 2.7, A and Fig. 2.8, A), especially developed in *Chroococcidiopsis* from the natural sample, and reproduction through multiple fission in different planes (Fig. 2.7, A). *Chroococcidiopsis* cells on natural sample exhibited the same thylakoid pattern found in the *Chroococcidiopsis* YU-1, i.e. a coiled arrangement.

The morphology of the Cyanobacteria scrapped from halite and their ultrastructural features are similar to those described by Donner (2013) and found in the *Chroococcidiopsis* YU-2 strains (Table 2.2). Spherical shape, cell size (1-4μm), aggregates (Fig. 2.3, Fig. 2.4) binary fission as division pattern, forming two cells groups or tetrades (Fig. 2.6, A) and the presence of a dense outermost layer (Fig. 2.6, A; Fig. 2.7, A and Fig. 2.8, A) revealed their morphological correspondence with *Chroococcidiopsis*. The disparity with *Halothece* (Table 2.2) is indicated by several features exhibited by this halophilic cyanobacterium: a) oval shape, instead of spherical shape, b) the lack of mucilage in contrast with the dense outermost layer, c) their occurrence in solitary cells or pseudofilaments instead of aggregates, d) their irregular distribution of thylakoids. Thus, light microscopy and TEM visualization of this major cyanobacterium inhabiting the endolithic microbial community of halite determined its belonging to the *Chroococcidiopsis* genus. On the other hand, the 16S rRNA sequences of the clones performed on DNA isolated from scrapped material were phylogenetically related to the *Halothece* cluster, as is also the case with the previus clones obtained from this and similar areas in the Atacama Desert (Fig. 2.9)

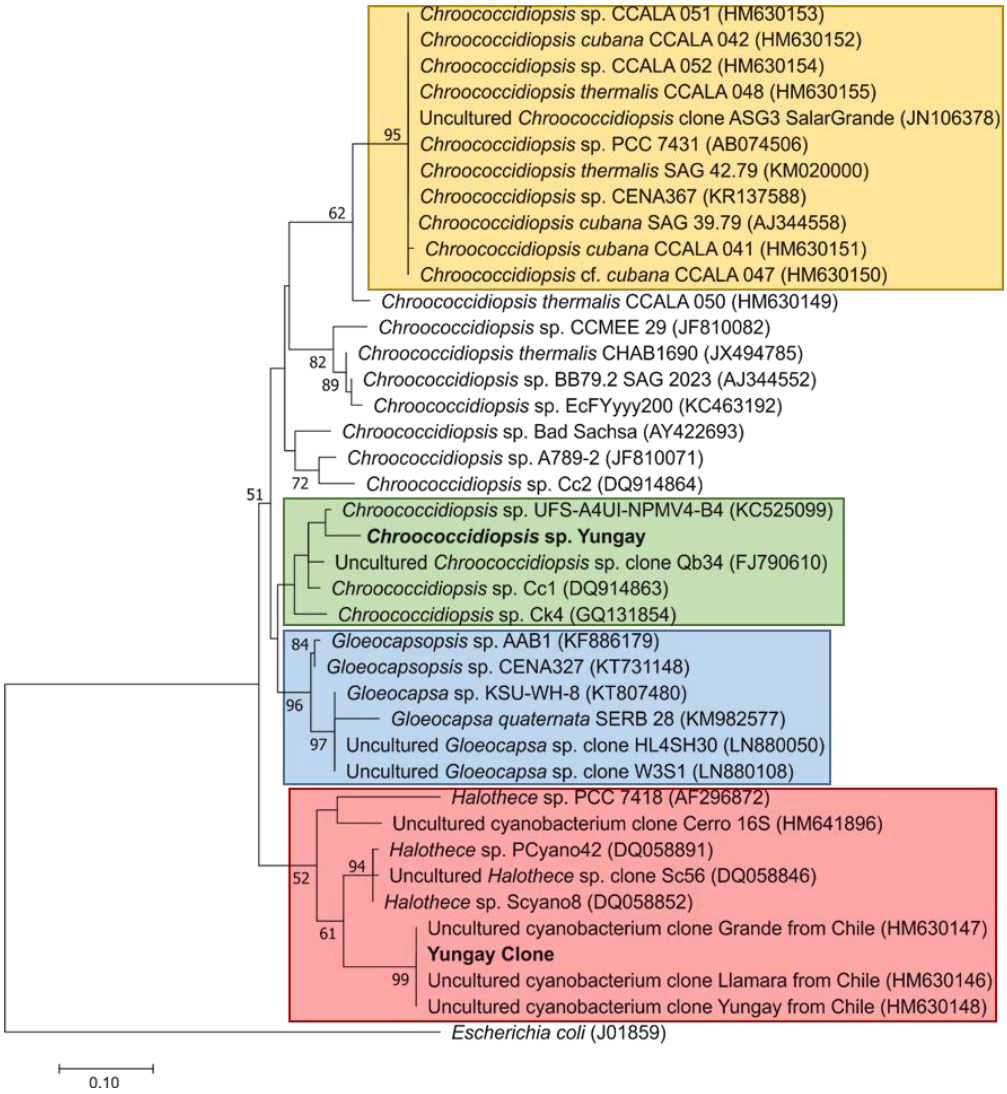

Figure 2.9. **Maximum likelihood tree based on partial 16S rRNA sequences of Cyanobacteria from endolithic and halophilic environments**. Strain of study is marked in bold. Scale bars indicates 10% sequence divergence. Yellow cluster: *Chroococcidiopsis* cluster containing the only *Chroococcidiopsis* sp. sequence from halite endolithic microhabitat (Stivaletta et al. 2012). Green cluster: *Chroococcidiopsis* cluster containing the *Chroococcidiopsis* sp. sequence from halite endolithic microhabitat from Yungay from this study (bold). Blue cluster: *Gloeocapsa* and *Gloeocapsopsis* cluster. Red cluster: *Halothece* cluster containing cyanobacterial sequences from halite endolithic microhabitats in the Atacama Desert (de los Ríos et al. 2010) and Yungay clone sequence from this study (bold).

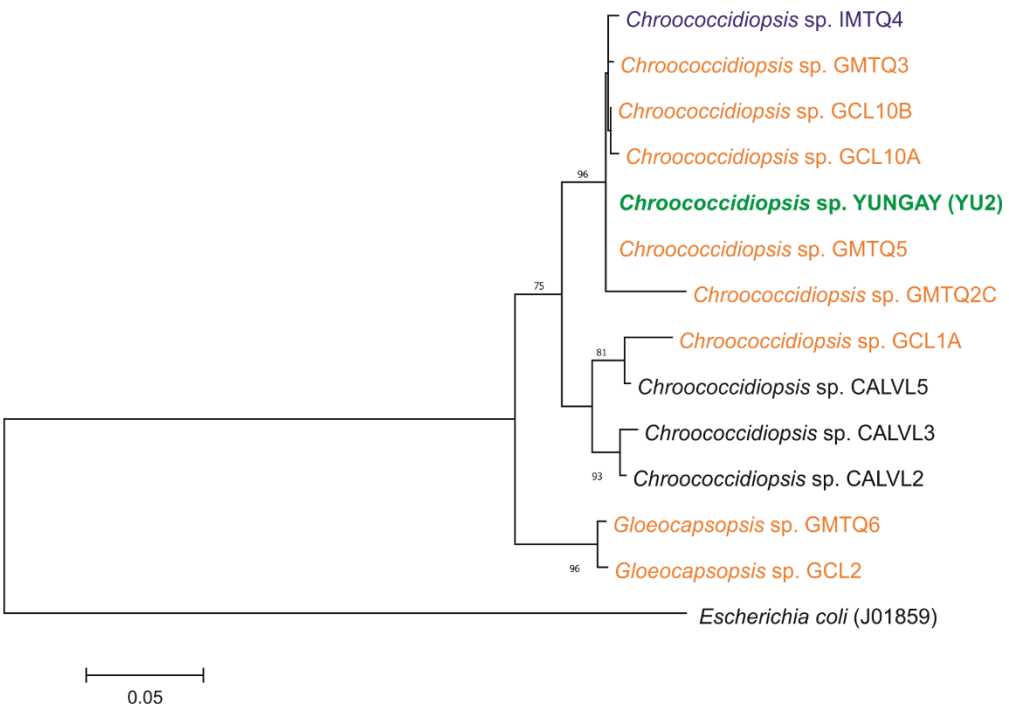

Figure 2.10. **Maximum likelihood tree based on partial 16S rRNA sequences of cyanobacterial isolates from endolithic microhabitats of different lithic substrates of the Atacama Desert.** Strain of study is marked in bold. Scale bars indicates 5% sequence divergence. Color indicates the substrate of origin: purple – ignimbrite, orange – gypsum, green – halite, black – calcite.

2.4.3. Osmotic stress on *Chroococcidiopsis* sp. YU-2 strain

The functional analysis of the genome of *Chroococcidiopsis* sp. YU-2 uncovered a diversity of stress response pathways related to osmotic stress response (Table 2.3). Three SEED subsystems were involved in this kind of stress response: osmoregulation, ectoine biosynthesis and regulation, and choline and betaine uptake and betaine biosynthesis.

Regarding osmoregulation, a gene encoding an aquaporin Z water channel, mediating rapid flux of water across the cellular membrane in response to abrupt changes in osmotic pressure (Calamita 2000), was found. Likewise, a gene was

also found encoding a diaminobutyrate-pyruvate aminotransferase concerning the biosynthesis and regulation of the organic osmolyte ectoine.

Finally, several genes encoding L-proline glycine betaine ABC transport systems and sarcosine oxidase subunits involved in biosynthetic pathway and uptake of the compatible solute betaine were found too (Table 2.3).

Table 2.3. Functional roles of sequence reads assigned to SEED categories (RAST) related to osmotic stress in *Chroococcidiopsis* YU-2 strain genome.

Subsystem	Role
Osmoregulation	Aquaporin Z
Ectoine biosynthesis and regulation	Diaminobutyrate-pyruvate aminotransferase (EC 2.6.1.46)
Choline and Betaine Uptake and Betaine Biosynthesis	L-proline glycine betaine ABC transport system permease protein ProV (TC 3.A.1.12.1) L-proline glycine betaine binding ABC transporter protein ProX (TC 3.A.1.12.1) Sarcosine oxidase alpha subunit (EC 1.5.3.1) Sarcosine oxidase beta subunit (EC 1.5.3.1) Sarcosine oxidase gamma subunit (EC 1.5.3.1) Sarcosine oxidase delta subunit (EC 1.5.3.1)

2.5. Discussion

This study contributes to a more comprehensive knowledge of the identification and characterization of the cyanobacterial component in one of the most polyextreme environments on Earth, the endolithic habitat in the halite pinnacles of Yungay, in the Atacama Desert. Despite the presence of cyanobacteria in this habitat located in the "dry limit for photosynthetic life" (Warren-Rhodes et al. 2006) as was reported for the first time more than 13 years ago (Wierzchos et al. 2006), the question of the identity of this essential

primary producer for the community remained unclear (de los Ríos et al. 2010; Robinson et al. 2015; Gómez-Silva 2018 and Wierzchos et al. 2018).

In this chapter that question is addressed using microscopy and molecular tools after the pioneering isolation and culture of cyanobacteria from this habitat and a taxonomical assignment for the observed cyanobacterial component is advanced, clarifying the possible reasons for the disparities pointed by previous studies and proposing a methodology to approach this type of studies in the future.

The importance of relying on extremophile and extremotolerant cyanobacterial isolates for a proper characterization and taxonomical assignment is constrained by the associated problematics of their collection, specific requirements, low growth rates and the fact that most of them are not cultivable. Thus, the obtaining of cyanobacterial isolates such as *Chroococcidiopsis* YU-2 from such an extreme environment as the halite endolithic habitat in Yungay for the first time, allowed us to explore its identity, *Chroococcidiopsis,* and characterization.

The ultrastructural and morphological features of the small cyanobacteria growing in the mixed culture YU-1, led to its identification as the picocyanobacterium *Synechococcus* instead of the expected *Halothece*, following the criteria of Komárek and Cepák (1998); Komárek et al. (1999); Margheri et al. (2008), Komárek and Johansen (2015). However, the loss of these cells during the purification process did not allow the comparison of these results with molecular data and integrate both approaches.

The presence of thick envelopes surrounding the cells reveals the extreme halotolerance of this *Chroococcidiopsis* YU-2*,* and classifies it as a halotolerant rather than a halophile, since it did not require saline conditions for its isolation and culture. Those mucilaginous envelopes whose complexity increases with age and the high production of polysaccharides have been described to interfere

with DNA extraction by Billi et al. (1998), who already developed a specific DNA isolation protocol for this cyanobacterium with a more aggressive lysis step. The requirement of a specific DNA isolation method in this study for the YU-2 strain exhibits their higher resistance compared to other *Chroococcidiopsis* strains isolated from other endolithic communities in the Atacama Desert (as those isolates reported in Chapter 1). The extremely difficult cell lysis and DNA extraction from *Chroococcidiopsis* from halites in Yungay would explain the absence of its sequences in previous reports (de los Ríos et al. 2010 and Robinson et al. 2015) as well as in the cloning library of this study, while imaging information about its morphology and ultrastructure clearly supported the *Chroococcidiopsis* assignment. In this study, the application of a harder lysis method, using French cell press, but still light to avoid disrupting *Halothece* DNA (just one cycle instead of three as for *Chroococcidiopsis* sp. cultures) resulted in a still inefficient method to isolate the entire cyanobacterial DNA. In the light of the outcome, although molecular techniques, especially NGS, are particularly useful for biological identification and functional biology due to the depth of the results, including information from low abundant taxa not detected by imaging techniques (Casero et al. 2019), the unbalanced DNA extractions represent a clear caveat. On the other hand, the limiting factor of microscopy techniques could contribute to differentiating the dominant organisms, since this less diverse highly abundant community would most be probably revealed by imaging. Therefore, the combination of both approaches, molecular and microscopy, is a crucial requirement to making a closer identification, especially in these extreme environments and unfamiliar microorganisms.

As previously explained, the complicated DNA isolation of *Chroococcidiopsis* and the discrimination of microorganisms in high abundance by microscopy, would justify both the occurrence of *Halothece* sequences and the relative low abundance of the cyanobacterial component in the community in previous reports (de los Ríos et al. 2010 and Robinson et al. 2015) and in our cloning

library. Thus, *Halothece* cells would easily have lysated in spite of occurring in lower abundance, as they have never been detected by imaging techniques in halite samples. The case is strengthened by the detection of scytonemin, a UV-protective pigment produced by cyanobacteria, in the endolithic community (Vítek et al. 2010; Vítek et al. 2012; Vítek et al. 2014a) since *Halothece* has never been reported to produce this pigment in contrast to *Chroococcidiopsis* (Dillon and Castenholz 1999; Dillon et al. 2002; Fleming and Castenholz 2007) and the *Chroococcidiopsis* YU-2 strain in particular (Chapter 3). Following this line of argument, two conclusions could be drawn: a) *Chroococcidiopsis,* not *Halothece,* would be the dominant cyanobacterium supporting the microbial community in the halite endolithic community and b) there was a probable underestimation of cyanobacteria abundance in this endolithic community due to the DNA extraction method bias that would not have lysate *Chroococcidiopsis* cells.

The possible dominance of a halotolerant cyanobacterium as *Chroococcidiopsis* instead of the highly halophilic *Halothece* in an extremely hypersaline environment as the halite could raise questions regarding ecological competitiveness. Accordingly, it would be expected that *Halothece* dominates the cyanobacterial component due to its specific adaptations to high salt concentrations (up to 30-35%) such as the osmolite glycine betaine and an increasing ratio of uncharged to charged lipids with increasing salinity in favor of membrane stability (Oren 2012). However, *Chroococcidiopsis* rely on some of those osmotic stress adaptations as found in its genome: the production, as is already known, by some strains of glycine betaine and the potential production of ectoine, combined with the anhydrobiosis, namely the ability to enter into a dormancy state at the desiccation onset and resume metabolic activities when water becomes scarce (Caiola and Billi 2007), and the scytonemin production.

The above mentioned arguments may explain why the halotolerant *Chroococcidiopsis* can be a more qualified cyanobacterium compared to the

halophile *Halothece* when it comes to cohabiting in the endolithic microhabitat of Yungay, where more than one extreme factors occur simultaneously. Thus, the higher plasticity exhibited by *Chroococcidiopsis* in multiple extreme conditions, and especially its capacity to deal with long drought periods, allow *Chroococcidiopsis* to be more competitive in this context.

2.6. Concluding Remarks and Future projects

A *Chroococcidiopsis* strain arising from the most polyextreme environment in the hyper-arid Atacama Desert, the endolithic habitat of halite nodules in Yungay, has been isolated for the first time, corroborating the first morphological identification of these cyanobacteria by Wierzchos et al. (2006).

This study reflects how a greater effort on cyanobacterial isolation, integrating both microscopy and molecular techniques, enables a suitable approach to the task of taxonomical assignment. Furthermore, the high endurance of *Chroococcidiopsis* strains under extreme environmental pressures has been demonstrated by its ultrastructural characterization and the requirement of a specific DNA isolation method, which explains its nonappearance in previous studies that used traditional protocols. Thus, previous studies of this endolithic environment describing the diversity of this microbial community and the notably low abundance of cyanobacterial members in contrast with other endolithic communities should be revised.

In the future, following the application of an optimized DNA isolation protocol with different lysis conditions, a new NGS analysis should be done to clarify the real abundance of the cyanobacteria phylum in endolithic halite communities including *Chroococcidiopsis* contribution. In parallel, immunological techniques such as CYANOCHIP (Blanco et al. 2015) or Life Detector Chip (LDChip300)

(Parro et al. 2011) could be optimized including more *Chroococcidiopsis* antibodies to explore the diversity of these communities, in case no possible balance of DNA isolation lysis was possible.

This study proves that biodiversity studies of microbial communities, especially from extreme environments, should be performed in the light of a combination of molecular and microscopy techniques. The resistance exhibited by some microorganisms to DNA extraction with conventional protocols, on the one hand, and the appearance in low abundance of some other microorganisms, on the other, are introducing bias in the community composition observed through these methodologies respectively. In fact, specific modifications and the optimization of DNA isolation methods should be performed in order to avoid the loss of information from key members of these communities.

CHAPTER 3

DEALING WITH ONE OF THE HIGHEST SOLAR RADIATION ON EARTH: RESPONSE OF *Chroococcidiopsis* STRAINS FROM THE ATACAMA DESERT

CHAPTER 3: DEALING WITH ONE OF THE HIGHEST SOLAR RADIATION ON EARTH: RESPONSE OF *Chroococcidiopsis* STRAINS FROM THE ATACAMA DESERT

3.1. Abstract

The Atacama Desert is known to be the location on Earth with one of the highest solar radiation, including PAR and UVR, limiting the presence of life to specific niches as endolithic microhabitats. Endolithic microbial communities are supported by photosynthetic primary producers, mainly cyanobacteria, which can be injured by UVR (240-400nm). Therefore, cyanobacteria exposed to high solar radiation and its harmful effects have developed a series of defense mechanisms: avoidance, antioxidant systems or production of photoprotective compounds such as scytonemin among others. Scytonemin is a liposoluble pigment whose absorption maxima (370, 252 nm) are located in UVA and UVC spectrum and highly absorbing in the UVB range.

In order to elucidate the protection capacity of cyanobacteria in endolithic microbial communities, two cyanobacterial strains from *Chroococcidiopsis* genus isolated from different endolithic microhabitats in the Atacama Desert: YU-2 strain, originally from the cryptoendolithic microhabitat of halite (NaCl), and CVL strain from chasmoendolithic microhabitat of calcite ($CaCO_3$). Both were exposed to PAR and UVR+PAR conditions studying their short-term response (oxidative stress) and long-term response (scytonemin production, metabolic activity and ultrastructural damage). The observed response of both strains reveals a high sensitivity to direct light exposure, even to PAR, while differences in their acclimation suggest specific adaptation strategies related to their original microhabitat, unraveling their protective potential and the strain specific environmental pressure selection to inhabit similar microhabitats exposed to slightly different light conditions.

3.2. Introduction

3.2.1. UV radiation effects on Cyanobacteria

It is well known that UVR exerts lethal effects onbiological systems since it is absorbed by the biomolecules (Diffey 1991). Some of the harmful effects of UVR are the alteration of biomolecules (proteins, DNA, lipids), chronic depression of key physiological processes, and acute physiological stress leading to either reduction in growth and cell division, pigment bleaching, N_2 metabolism, energy production, or photoinhibition of photosynthesis (Sinha and Häder 2008) (Fig. 3.1).

3.2.1.1. UV-induced oxidative stress

UVB has the greatest potential for cell damage since it has both direct effects on DNA and proteins regardless of the presence of oxygen (Gao and García-Pichel, 2011) and, like UVA, produces indirect effects through the production of highly active oxidizing agents such as reactive oxygen species (ROS) (Fig. 3.1).

The UVR-induced generation of ROS, such as hydroxyl radical (OH^-), hydrogen peroxide (H_2O_2), singlet oxygen ($^1O_2$) and superoxide anion (O_2^-), has been reported in some cyanobacteria (Rastogi et al. 2010a; Rastogi et al. 2010b; He and Häder 2002a), yet very little is known about the subsequent effects of oxidative stress in cyanobacteria.

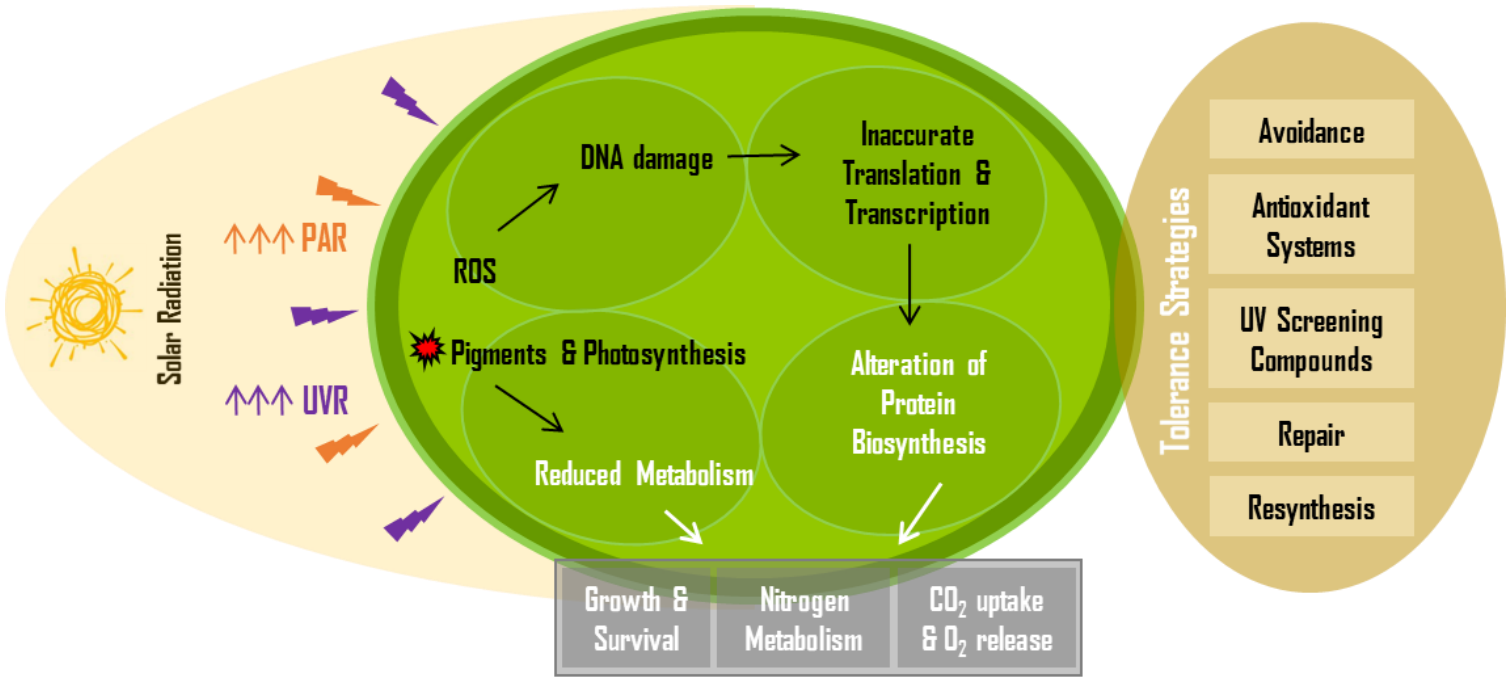

Figure 3.1. Summary of damaging effects, stress responses and tolerance strategies in cyanobacteria against long term exposure to extreme solar radiation. (modified from Rastogi et al. 2014).

3.2.1.2. UV effects on biomolecules

Oxidative stress produced by UVR can induce nucleotides modifications, translocations and DNA-DNA cross-links, and an increase in the susceptibility to proteolysis and fragmentation of the peptide chain and oxidation of specific aminoacids (Rastogi 2015) (Fig. 3.1). In fact, UVR affects genomic function and fidelity, as in the case of *Arthrospira platensis*, where an increase in thymine dimers frequency has been observed after a continued UVR exposure (Gao et al. 2008), in *Synechocystis* PCC 6308, whose DNA degradation due to UVR exposure has been reported by (O'Brien and Houghton 1982), or in *Prochlorococcus marinus* PCC 9511, where UVR induced a delay in chromosomal replication (Kolowrat et al. 2010). Furthermore, a differential lipid peroxidation in response to UVB exposure has been reported in *Nostoc muscorum, Plectonema boryanum* and *Aphanothece* (Zeeshan and Prasad 2009), related to the oxidative degradation of polyunsaturated fatty acids in the cell membranes.

3.2.1.3. UV effects on cyanobacterial physiology

The inactivation of photosynthesis has been shown to occur when cyanobacteria are exposed to intense solar light, above the normal capacity of the photosynthetic electron flow, due to the production of ROS (Rastogi et al. 2015) (Fig. 3.1). Furthermore, different photosynthetic parameters are known to be inhibited when cyanobacteria are exposed to UVR, such as CO_2 uptake, O_2 evolution or ribulose-1,5 bisphosphate carboxylase (RuBisCo) activity (Sinha et al. 1997). Likewise, UVB radiation is known to cause photobleaching of photosynthetic pigments such as chlorophyll *a* (Rastogi et al. 2014) and phycobiliproteins, generating a reduction on its content together with the disassembly of the phycobilisomal complex (Quesada et al. 1995, Sinha et al. 1995, Quesada and Vincent 1997).

3.2.2. UV stress tolerance and mitigation strategies in cyanobacteria

Since cyanobacteria originated in the Precambrian area, when the ozone shield was absent, UVR has presumably acted as an evolutionary pressure leading to the selection of UVR efficient protecting mechanisms (Rahman et al. 2014), although UVR tolerance varies between species. The mitigation strategies against the harmful effects of the exposure to UVR include avoidance, scavenging of ROS by antioxidant systems, the synthesis of UV-screening compounds, repairing systems for UV-induced DNA damage and protein resynthesis (Rastogi et al. 2014) (Fig. 3.1). The three first line of defense will be described below.

3.2.2.1. Avoidance

Cyanobacteria rely on avoidance as a first line of defense against the potential damage caused by their exposure to UVR, preventing its harmful effects through various strategies. Those inhabiting aquatic ecosystems can use migration to escape from high UV to low UV conditions in the water column (Reynolds et al. 1987), while some cyanobacterial species, especially terrestrial species, can form microbial mats in order to minimize the harmful effects of intense solar light and UVR (Quesada and Vincent 1997; Büdel 1999) or colonize endolithic habitats (Wierzchos et al. 2018). On the other hand, it has been shown that some cyanobacterial species, as *Arthrospira platensis*, suffer a morphological transformation to increase self-shading (Wu et al. 2005) and in some other species, the synthesis of EPSs is stimulated by UVR, thus increasing the effective path length for the absorption of radiation (Ehling-Schulz et al. 1997).

3.2.2.2. Antioxidant systems

As a second line of defense, cyanobacteria have developed complex antioxidant enzymatic or non-enzymatic systems to cope with UV-induced oxidative stress (Singh et al. 2013). Enzymatic antioxidants in cyanobacteria comprise superoxide dismutase (SOD), catalase (CAT), glutathione peroxidase (GPX) and the enzymes involved in the ascorbate-glutathione cycle. On the other hand,

carotenoids, α-tocopherols (α-TOC; vitamin E) and ascorbic acid (ASA, vitamin C) are non-enzymatic antioxidants (Rastogi et al. 2014).

SOD protects different cellular proteins against oxidative stress and exists in four different metalloforms: Fe-SOD, Mn-SOD, Cu/Zn-SOD and Ni-SOD. All four SODs have been found in cyanobacteria, exhibiting a pattern: Fe-SOD and Mn-SOD occur in higher orders of cyanobacteria, Ni-SOD is the only one found in primitive cyanobacteria and Cu/Zn-SOD is rarely observed in cyanobacteria (Priya et al. 2007).

3.2.2.3. UV absorbing /screening compounds

The third line of defense against UVR photodamage in cyanobacteria comprises the synthesis of UV-absorbing and/or UV-screening compounds (Cockel and Knowland 1999). Two main UV-absorbing/screening compounds are known in cyanobacteria: mycosporine-like amino acids (MAAs) and scytonemin.

MAAs have an absorption spectrum from 310 to 362 nm. They contribute to photostabilization and resist different physico-chemical stressors such as temperature, strong UVR and pH, becoming successful photoprotectants in diverse habitats (Gröniger and Häder 2000). Several abiotic factors have been reported to affect the biosynthesis of MAAs in cyanobacteria (Quesada and Vincent, 1997), such as PAR and UVR (Rastogi et al. 2014), osmotic stress and desiccation (Rastogi et al. 2010c; Rastogi et al. 2015).

On the other hand, scytonemin is the most widespread sunscreen pigment exclusively produced by cyanobacteria (Rastogi and Incharoensakdi 2014b; Rastogi et al. 2015). It is a yellow-brown lipid-soluble dimeric compound composed of indolic and phenolic subunits (Proteau et al. 1993) and occurs in both oxidized (MW 544 Da) and reduced (MW 546 Da) forms (Fig. 3.2). Its *in vivo* absorption maximum is at 370nm and purified at 386nm, in the UVA region.

Although scytonemin displays an absorption maximum at 252, 278 (UVC) and 370 nm, it shows high absorbance in the entire UVB region.

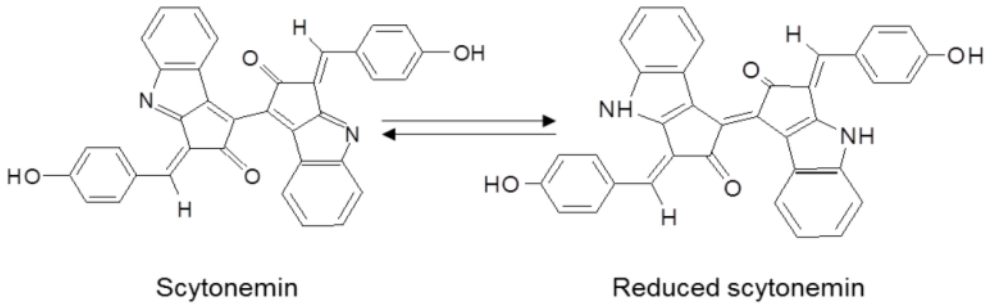

Figure 3.2. Chemical structure of scytonemin found in both oxidized and reduced form (Rastogi et al. 2015).

This pigment is located in the EPS sheath of certain terrestrial cyanobacterial species and is highly stable under different abiotic stresses being able to reduce about 90% of the UVA that reaches the cell (García-Pichel and Castenholz 1991). Its stability allows it to persist very long in terrestrial crusts or in dried mats (Potts 1994,) and performs its function without any further metabolic investment even under prolonged physiological inactivity. It is therefore a successful mechanism against UVR for cyanobacteria in combination with other mechanisms (Jones et al. 2011).

3.2.3. Extreme solar regime in the Atacama Desert and its consequences for life.

The solar spectrum is fractionated in three regions depending on the wavelength: infrared radiation (IR) (750-1000 nm), PAR (400-700nm) and UVR (240-400 nm). The quantity and quality of that solar spectrum in a terrestrial surface depends on seven features: the Sun-Earth distance at that point, the altitude, the solar zenith angle, ground reflectivity or albedo, the ozone and water vapor column, cloudiness and aerosol concentrations (Cordero et al. 2014).

The Atacama Desert has been pointed out as the place where some of the highest surface irradiance is likely to occur based on diverse features: its latitude (close to equator), its high altitude, relatively low ozone column values, prevalent cloudless conditions and low aerosol loading (McKenzie et al. 2015; Cordero et al. 2016) (Fig. 3.3).

UV irradiance is of special interest due to the adverse effects for life on both terrestrial and aquatic ecosystems (Cordero et al. 2014). The World Health Organization uses the international standard measure, the UV index (UVI), to establish different risk levels of harm so that regions where the UVI is greater than 11 would be positioned in the extreme risk of harm category. Following this criterium, the Atacama Desert has been described as the location on the Earth where the highest levels of surface UV irradiance have been measured with UVI reaching values up to 20 (Cordero et al. 2014).

The extreme solar radiation is considered a limitation for life development, and thus not even epilithic (over the rock surfaces) microbial communities can be found in most of the hyper-arid region of the Atacama Desert due to the excessive exposure to the harmful effects of UVR (Cockell et al. 2008).

However, inhabiting endolithic microhabitats constitute an excellent first line of avoidance of the damaging effects of high radiation exposure for microorganisms in the Atacama Desert. The presence of few millimeters of lithic substrate over the endolithic microbial communities provides a certain barrier for UVR damage, as proposed by Cockell et al. (2003), since only a 0.1-2.5% of the total incident solar radiation reaches the endolithic habitat depending on the substrate (Nienow et al. 1988, Wierzchos et al. 2015).

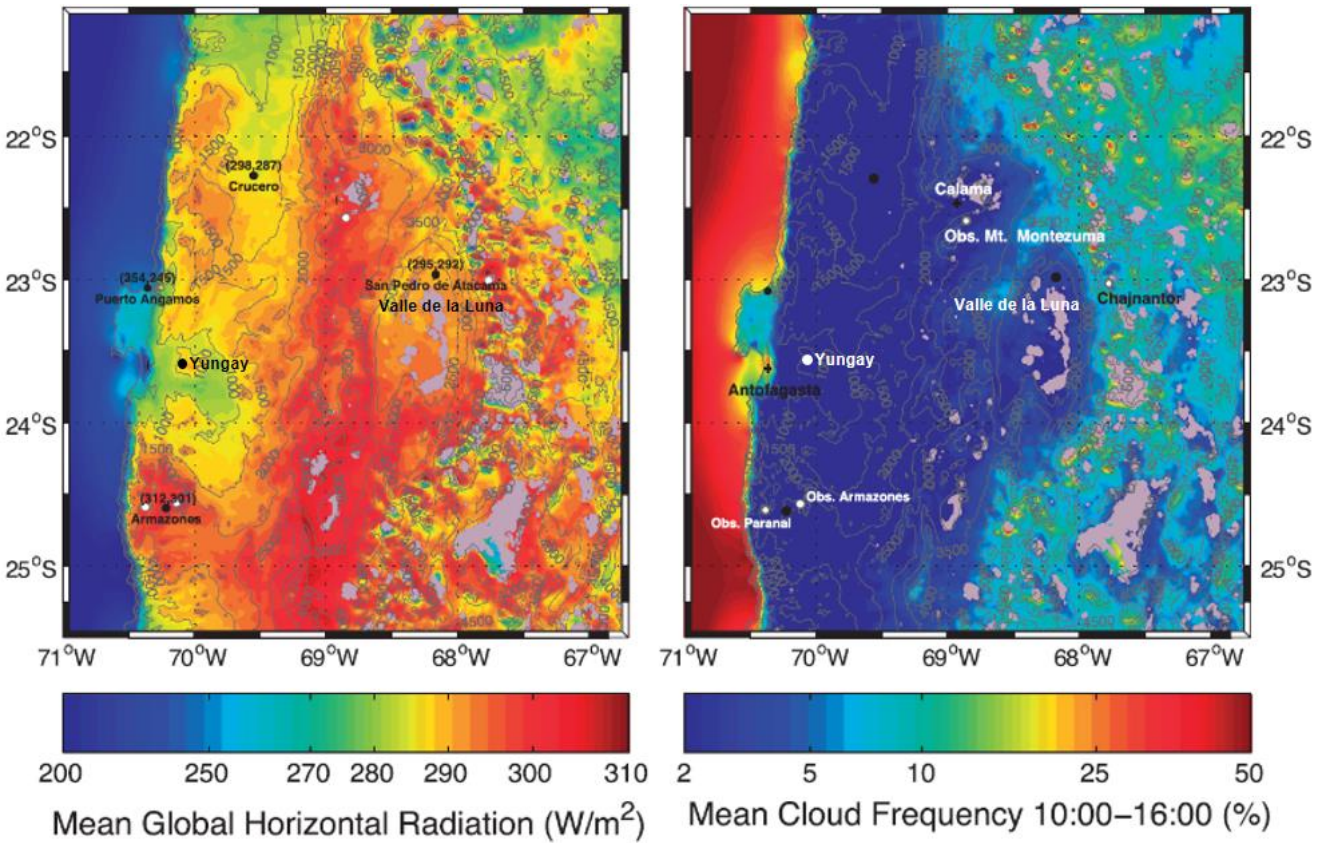

Figure 3.3.(a) The global horizontal surface radiation. The numbers between parentheses correspond to the observed and modeled mean surface radiation in the format (b) Mean cloud fraction between 10:00 and 16:00 local time derived from geostationary satellite data in the visible channel. Both panels correspond to the mean climatological value from 2004 to 2012. Gray areas are regions in which the high albedo of the surface, owing to snow cover or salt pans (Modified from Rondanelli et al. 2015).

Despite the UV-blocking effect provided by the lithic substrate used as an avoidance strategy, cyanobacteria from endolithic microbial communities in the Atacama Desert have been reported to exhibit the second line of defense, namely the production of carotenoids and antioxidant orange-carotenoid protein (Vítek et al. 2017) as well as the third line of defense, the production of a UV-screening compound, such as scytonemin detected *in situ* by Raman spectrometry (Vítek et al. 2016; Wierzchos et al. 2015, Vítek et al. 2014a, Vítek et al. 2017).

3.2.4. *Chroococcidiopsis*: extremotolerant cyanobacteria

Chroococcidiopsis species are considered extremotolerant organisms, occurring in a variety of terrestrial habitats. Members of the *Chroococcidiopsis* genus avoid high light intensities and UVR by living within soil, rocks and caves or in lithobiontic habitats (Wierzchos et al. 2018).

Several strains from *Chroococcidiopsis* have been well characterized in order to identify their UVR tolerance by exposing *Chroococcidiopsis* cells to similar conditions as those occurring on Mars (Cockell et al. 2005, Baqué et al. 2016, Billi et al. 2019). Also the UVR defense mechanism of *Chroococcidiopsis*, the production of scytonemin was analyzed by Fleming and Castenholz (2007), Dillon et al. (2002) and Dillon and Castenholz (1999). Moreover, the special capacity of this genus to deal with UVR has been studied to reveal potential biotechnological applications of its mechanisms (Abed et al. 2011, Gabani and Singh 2013).

The cryptoendolithic habitat in halite has previously been reported to harbor scytonemin produced by *Chroococcidiopsis* (Vítek et al. 2014a). Thus studying the response of the *Chroococcidiopsis* strain (YU-2) isolated from the translucent halite to direct solar simulated radiation gives an approach to its sensibility to this type of abiotic stress among with its capacity to protect the whole community. The second *Chroococcidiopsis* strain, isolated from the chasmoendolithic habitat in calcite (CVL), was chosen since this type of

endolithic habitat is more exposed to direct solar radiation. Hence this chapter aims to describe for the first time the response and potential role in their respective communities of two representatives of the main genus in endolithic communities, *Chroococcidiopsis,* from two highly exposed microhabitats as the cryptoendolithic habitat of halite and the chasmoendolithic habitat of calcite originally from the region with one of the highest solar radiation on Earth.

3.3. Experimental Procedures

3.3.1. Culture organisms and conditions

Two strains of cyanobacteria isolated from endolithic habitats of the Atacama Desert were used in this study: *Chroococcidiopsis* YU-2, from the cryptoendolithic microhabitat in halite from Yungay and *Chroococcidiopsis* CVL, from the chasmoendolithic microhabitat in calcite from Valle de la Luna (DiRuggiero et al. 2013). Both strains are preserved at the Universidad Autónoma de Madrid, Madrid, Spain. *Chroococcidiopsis* YU-2 and CVL were grown as batch cultures in BG11 medium (Rippka et al. 1979) at 28°C under continuous 12 W m^{-2} visible light (~ 60 µmol photons m^{-2} s^{-1}) generated by coolwhite fluorescent lamps.

All described experiments were performed in triplicates following the Fleming and Castenholz (2007) indications. The experimental design remained as follows: cultures were gently homogenized by orbital shaking. Three milliliter aliquots of the homogenized cultures were then filtered onto 25 mm diameter, 0.2 µm pore size Cyclopore Track-Etch Membranes (Whatman), producing a thin layer of cells on the filter. The filtered cells were immediately transferred to 1% agar plates made with BG11 medium. The agar plates with the filtered cells were then kept under the following conditions: continuous 40 W m^{-2} PAR at 25°C, without increasing humidity conditions for 2 days. At the end of the 48 h period, a UV lamp (F20T10/BLB lamp (315-400nm)) was turned on exposing half of the

entire set of filtered cells to continuous 2 W m^{-2} UVA radiation in addition to visible light.

It is assumed that the experimental conditions described above are definitely not exactly the same microenvironmental conditions which can be expected within the cryptoendolithic (halite) or chasmoendolithic (calcite) habitats. However, this experimental design is as close as possible simulating UVA+PAR irradiance within the endolithic habitat in the Atacama Desert.

Visible light (400-700 nm) and UVR (215-400 nm) measurements were made using an ULM-500 universal light meter (Heinz Walz GmbH, Effeltrich, Germany) and Apogee UV Radiation MU-200 meter, respectively. All readings refer to values measured on the surface of the cultures.

3.3.2. *In vivo* detection of oxidative stress

The spectrophotometric detection of the production of ROS after defined time intervals (24, 48 and 72 hours) of exposure to simulated solar radiation was performed by using 2',7'-Dichlorodihydrofluorescein diacetate (DCFH-DA) (Sigma Aldrich- Merck KGaA, Darmstadtm Germany) solubilized in ethanol. Filtered cells were resuspended in 1 mL phosphate buffer where a 5 µM (final concentration) of DCFH-DA was added. Samples were then incubated in a shaker at room temperature in the dark for 1 h DCFH is nonfluorescent but switched to highly fluorescent DCF when oxidized by intracellular ROS or other peroxides having an excitation wavelength of 485 nm and an emission band between 500 and 600 nm. After 1 h incubation, samples were subjected to fluorescence spectrophotometric analysis. The fluorescence of the samples was measured by a spectrofluorophotometer with an excitation wavelength of 485 nm and an emission band between 500 and 600 nm. The fluorescence intensity was corrected against the blank control experiments without cells and then normalized to dry weight. Its comparison with control samples was used to

determine the oxidative stress. All fluorescence measurements were performed in triplicates.

CellROX Green reagent (Invitrogen) was used to detect ROS in both *Chroococcidiopsis* by microscopy following the optimized method described by Cornejo-Corona et al. (2016). Briefly, 2 µL of 5 mM CellROX Green was added to 100 µL of cyanobacterial culture followed by incubation at room temperature and shaking at 120 rpm for 30 min in the dark. The cells were then washed twice for 5 min, each time at room temperature with 1× PBS, 0.1% Triton X-100, and fluorescence was observed using a Zeiss AxioImager M.2 fluorescence microscope (Carl Zeiss, Jena, Germany) and a Apochrome x60, n=1.4 Zeiss oil-immersion objective. Multichannel Image Acquisition (MIA) system was used with a combination of the following filter sets: filter set for eGFP (Zeiss Filter Set 38; Ex/Em: 450-490/500-550 nm) for CellROX Green fluorescence and EPS autofluorescence, and Rhodamine (Zeiss Filter Set 20; Ex/Em: 540-552/567-647 nm) for chlorophyll autofluorescence signal. At least one hundred cells were evaluated for each experimental time and treatment. The samples were observed under white light to locate aggregates for evaluation and then the microscope was switched to fluorescence to identify the number of fluorescent cells.

Every measurement was normalized to dry weight using a XP6 microbalance (Mettler Toledo, Columbus, OH, USA). Although cultures were not axenic, heterotrophic biomass never exceeded 1-2% of the total biovolume based on cell counts according to Schallenberg et al. (1989).

3.3.3. Whole genome library preparation, sequencing and computing analysis.

Genomic DNA from the *Chroococcidiopsis* strains YU-2 and CVL were subjected to paired-end Illumina HiSeq sequencing (Johns Hopkins Genetic Resources Core

Facility) after creating a library using KAPA HyperPlus (KAPA Biosystems). Raw reads were quality trimmed with TrmGalore, and the resulting pairs were processed with the MetaWrap pipeline (Uritskiy et al. 2018). For the *Chroococcidiopsis* YU-2 strain, a total of 175 high-coverage contigs, encompassing a total of 5,957,924 bases, were selected for further analyses. Among these contigs, the N50 value was 63,683 bases, with an average G+C% of 46.3. CheckM v1.0.7 reported a genome completeness of 99.48% and genome contamination of 1.93%. Finally, gene prediction and annotation of the *Chroococcidiopsis* sp. YU-2 contigs were carried out using RAST (Overbeek et al. 2014) pipeline. A total of 6,412 CDSs, 36 tRNA genes, and 8 rRNA genes were identified. For the *Chroococcidiopsis* CVL strain, a total of 324 high-coverage contigs, encompassing a total of 5,884,528 bases, were selected for further analyses. Among these contigs, the N50 value was 32,524 bases, with an average G+C% of 46.3. CheckM v1.0.7 (Parks et al. 2015) reported a genome completeness of 98.88% and genome contamination of 1.55%. Finally, gene prediction and annotation of the *Chroococcidiopsis* sp. CVL contigs were carried out using RAST pipeline (Overbeek et al. 2014). A total of 6,465 CDSs, 37 tRNA genes, and 7 rRNA genes were identified.

A search for SEED categories (RAST) related to oxidative stress in the *Chroococcidiopsis* YU-2 strain and the *Chroococcidiopsis* CVL strain genomes was performed. The obtained results were then contrasted with 376 cyanobacterial genomes available in CyanoBase (Fujisawa et al 2017). (http://genome.microbedb.jp/cyanobase/).

3.3.4. Scytonemin induction experiment

Filtered *Chroococcidiopsis* YU-2 and CVL cells were exposed to PAR or UVR+PAR light in two separate sets for 3, 6, 9, 12 and 15 days. After the respective experimental exposure time cells were scraped out of the filters and suspended in the BG11 medium and then gently homogenized by pumping them multiple

times with a 1000 ml Pipetman (Gilson, Middleton, WI, USA). For the determination of scytonemin content, cells were suspended in 1:1 (v/v) methanol: ethyl acetate by overnight incubation at 4°C in darkness. After centrifugation (10,000x *g* for 5 min) samples were filtered through 0.2 μm pore-sized sterilized syringe-driven filter (Symta, Madrid, Spain) before being subjected to HPLC analyses.

Partially purified scytonemin was analyzed using a HPLC system (Agilent Technologies 1200 Series, Photodiode Array). 20 μL were injected into the HPLC column Phenomenex Peptide 100 A, 3.6 μ x 4.60 mm; XB C18. Elution was at a flow rate of 0.5 mL min^{-1} using the mobile phase of solvent A (5% acetonitrile in milliQ water + 0.1% formic acid) and solvent B (100% acetonitrile + 0.1% formic acid). The 30 min gradient elution program was set with 0–15 min linear increase from 15 % solvent A to 80 % solvent B, and 15–30 min at 100 % solvent B. The detection wavelength was at 384 nm. The PDA scan wavelength ranged from 200 to 700 nm. Oxidized and reduced scytonemin were identified by their characteristic absorption maxima in the solvent corresponding to the appropriate retention time.

At the same time, the absorbance of each extraction was measured at 384 (scytonemin maximum), 490 (pooled carotenoids) and 663 nm (Chl *a*). These absorbance values were partially corrected for residual scatter by subtracting the absorbance at 750 nm. Absorbance measurements were made on a Flame Spectrometer (Ocean Optics, Florida, US.).

Every measurement was normalized to dry weight using a XP6 microbalance (Mettler Toledo, Columbus, OH, USA). Although cultures were not axenic, heterotrophic biomass never exceeded 1-2% of the total biovolume based on cell counts according to Schallenberg et al. (1989).

3.3.5. Metabolic Activity experiment and UVR effect on *Chroococcidiopsis* cellular ultrastructure

The metabolic activity of *Chroococcidiopsis* cells was evaluated at 6 experimental times (0, 3, 6, 9, 12, 15 days) for both experimental conditions, PAR and UVR+PAR. For this purpose, the cell-permeable 5-Cyano-2,3-Ditolyl Tetrazolium Chloride (CTC) redox dye was used. This dye is reduced from a soluble colorless form into its corresponding fluorescent insoluble formazans (CTF) that accumulate intracellularly. The formazan crystals are viewed as intracellular opaque dark-red deposits under transmitted illumination, or as yellow-orange fluorescent spots (excitation and emission maxima at 488 and 630 nm) when using epifluorescence microscopy.

Procedures described by Tashyreva et al. (2013) were followed for CTC staining, increasing incubation times from 2 to 5 hours. A D1 Zeiss fluorescence microscope (AxioImager M2, Carl Zeiss, Germany) was used with Apochrome oil immersion objective x64, n=1.4. The optical system for CTF fluorescence observations included a filter set (Ex/Em: 426-446 / 545-645 nm).

3.3.6. Light microscopy

Light microscopy in DIC mode DIC was performed on cell aggregates of both *Chroococcidiopsis* strains at each experimental time for the scytonemin induction experiment. The samples were examined using a microscope (AxioImager M2, Carl Zeiss, Germany) equipped with Apochrome x64, n=1.4 oil immersion objective.

3.3.7. Transmission Electron Microscopy (TEM)

Cyanobacterial cells from YU-2 and CVL *Chroococcidiopsis* strains were centrifuged at 3,000x *g* and resuspended in 3% glutaraldehyde in 0.1M cacodylate buffer and incubated at 4°C for 3 hours. The cells were then washed three times in cacodylate buffer, postfixed in 1% osmium tetroxide for 5 hours,

before being dehydrated in a graded series of ethanol and embedded in LR White resin. Ultrathin sections were stained with lead citrate and observed with a JEOL JEM-2100 200kV electron microscope (Tokio, Japan) with Gatan Orius CCD camera (Pleasatan, CA, USA).

3.3.8. Statistical analysis

All results are presented as mean values of three replicates. Data from scytonemin induction and oxidative stress were analyzed by one-way analysis of variance. Once a significant difference was detected post-hoc multiple comparisons were made by using the Tukey test. The level of significance was set at 0.05, 0.01 and 0.001 for all tests.

3.4. Results

3.4.1. Oxidative stress in *Chroococcidiopsis*

3.4.1.1. Semi quantitative analysis of intracellular ROS by DCF fluorescence

Oxidative stress on both *Chroococcidiopsis* strains was examined *in vivo* by DCF fluorescence normalized to dry weight at 4 experimental times for a 72 hours' period. The strains were exposed to two different light conditions: to 40 Wm^{-2} PAR (PAR), or under that PAR radiation together with 2 Wm^{-2} UVR (UVR+PAR).

ROS accumulation, represented by DCF fluorescence, in the YU-2 strain increased after 24 hours of exposure, increasing sequentially and reaching maximum fluorescence after 72 hours of exposure (Fig. 3.4). Light treatment revealed a significant effect on ROS accumulation (R^2, 0.979) and punctual significant differences were observed at all three experimental times. Specifically, PAR conditions revealed a higher accumulation of ROS after 24 and 72 hours of

exposure, while UVR+PAR conditions involved significantly greater ROS accumulation after 48 hours of exposure.

Oxidative stress response in the CVL strain shared an increase after 24 hours of exposure for both light treatments where maximum DCF fluorescence values were registered. A significant decrease in DCF fluorescence was observed after 48 and 72 hours. This strain showed a significantly lower accumulation of ROS after 24 hours of PAR in comparison to UVR+PAR conditions. By contrast, significant differences observed at 48 and 72 hours of exposure occurred due to a higher ROS accumulation after PAR exposure (Fig. 3.4).

3.4.1.2. Reactive oxygen species formation

The visualization of ROS produced by *Chroococcidiopsis* under PAR and UVR stress was performed based on the dye CellROX Green at time 0 and after 24 hours of exposure to UVR+PAR on both strains (Fig. 3.5).

Light microscopy images on Fig. 3.5 at time 0 (A1, C1) and 24 hours of exposition to UVR+PAR (B1, D1) already exhibited differences in the color of the cells. The YU-2 strain and CVL strain were light green and blue-green respectively at time 0 turning to brownish green yellow-brown color after 24 hours of exposure to UVR+PAR light conditions.

Over the red chlorophyll autofluorescence of *Chroococcidiopsis* cells (Fig. 3.5), a weak green fluorescence could be observed inside the cells of both YU-2 (A2) and CVL (C2) strains at time 0. After 24 hours of treatment on YU-2 (B2) and CVL (D2), the oxidation of CellROX by ROS and its binding to DNA resulted in most of the cells exhibiting a bright spot-like green fluorescence.

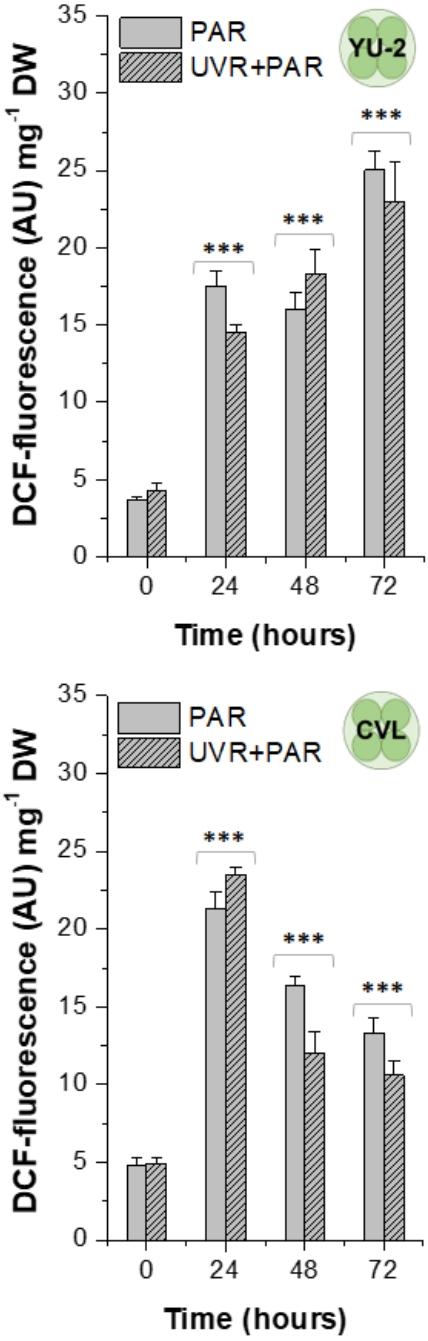

Figure 3.4. DCF fluorescence measurements in *Chroococcidiopsis* strains YU-2 (upper graph) **and CVL** (lower graph) after irradiation with PAR (plain bars) or UVR+PAR (scratched bars) for 72h normalized to dry weight. Significant differences between light conditions at marked by *** (0.001).

Two types of events were also found after the irradiation for 24 hours (Fig. 3.5) by comparing light microscopy (B1, D1) with fluorescence images (B2, D2) in both *Chroococcidiopsis* strains. Arrows on these images point to cells that did not emit red autofluorescence from chlorophyll but a green fluorescence. Arrow heads point to cell-shaped brown covers on light microscopy with no autofluorescence signal.

3.4.2. Oxidative stress systems in YU-2 and CVL *Chroococcidiopsis* strains

The functional analysis of the genome from the *Chroococcidiopsis* strains YU-2 and CVL uncovered a diversity of stress response pathways related to oxidative stress (Table 3.1).

Seven SEED subsystems related to oxidative stress were found in both genomes (Table 3.1). Despite the fact that both *Chroococcidiopsis* genomes shared most of the genes involved in oxidative stress response, they also exhibited some differences. On the one hand, the CVL genome revealed a higher diversity of genes directly related to protection from ROS owing to the iron superoxide dismutase (Fe-SOD) and the cytochrome c551 peroxidase. The former, indeed, was only found in two more cyanobacterial genomes from the *Acaryochloris* and *Tolypothrix* genera (Supp. Mat 3.1). On the other hand, the YU-2 genome showed a higher diversity in genes involved in rubrerythins synthesis, which are peroxide scavengers, and the antioxidant molecule glutathione (redox cycle) with the glutaredoxin 3 and a cell wall endopeptidase from family M23/M37. This cell wall endopeptidase was only found in one more cyanobacterial genome from the *Synechocystis* genus.

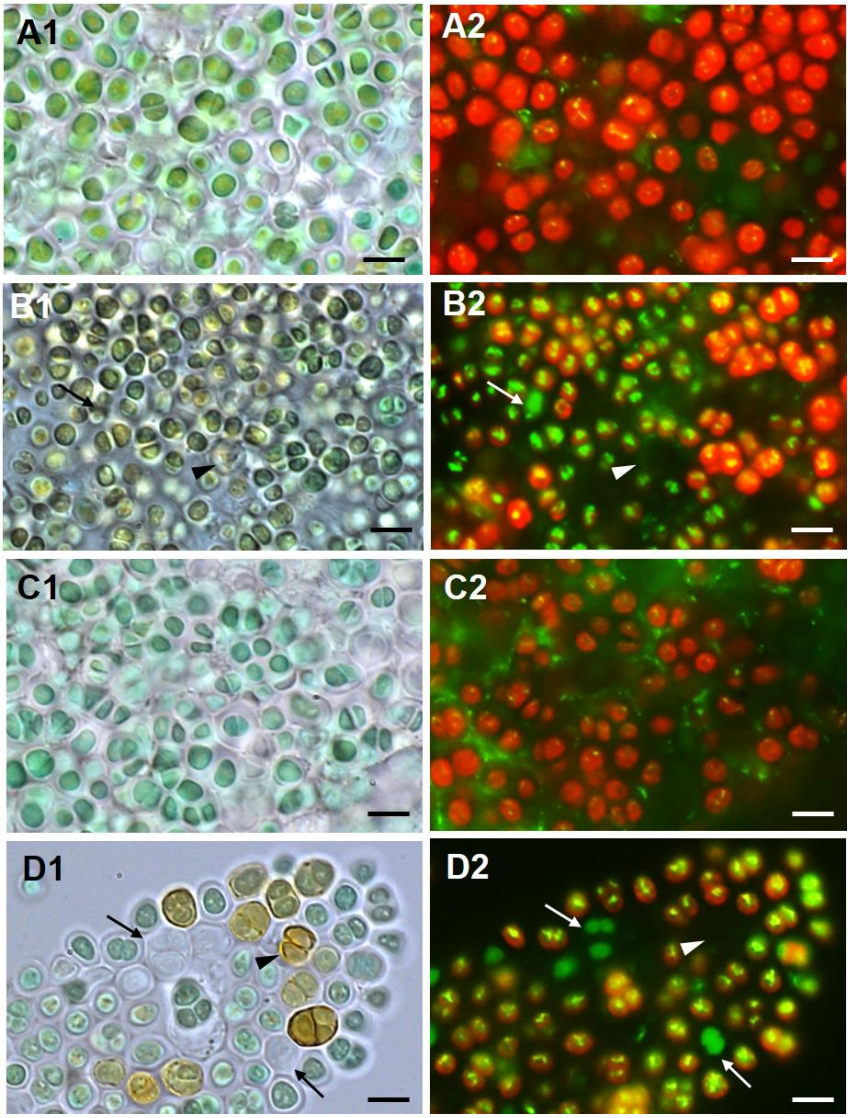

Figure 3.5. **CellRox staining for intracellular detection of ROS in *Chroococcidiopsis* strains YU-2** (Series A and B) **and CVL** (Series C and D). Light microscopy and fluorescence images of Series A and C correspond to exposure time t=0, and from Series B and D after24 hours of exposure to UVR+PAR. Red cells correspond to chlorophyll autofluorescence, higher in non-exposed cells (**A2, C2**) than in UVR+PAR exposed cells (**B2, D2**). Bright yellow/green dots in fluorescence images are due to CellRox fluorescence, the oxidative stress indicator, higher in UVR+PAR exposed cells (**B2, D2**) than in non-exposed cells (**A2, C2**). On images of UVR+PAR treated cells, arrows point at cells revealing apparently structural integrity with green autofluorescence signal (**B1, B2, D1, D2**). In images of UVR+PAR treated cells, arrow heads point at cells revealing apparently structural integrity and brown color, suggesting an increase in scytonemin content, and no autofluorescence signal (**B1, B2, D1, D2**). Scale bar=8 μm.

Both strains showed similar features for the four subsystems left: general oxidative stress, glutathione biosynthesis, glutathione (non-redox rections) and cluster containing glutathione synthetase (Table 3.1). However, two of those shared genes were found almost exclusively in the studied *Chroococcidiopsis* strains compared to the database, since the Cu/Zn-SOD was only found in *Synechococcus* strains and the paraquat-inducible protein B was not found in any of the cyanobacterial genomes available (Supp. Mat. 3.1).

3.4.3. Scytonemin induction in *Chroococcidiopsis*

The total scytonemin content in the *Chroococcidiopsis* strains YU-2 and CVL was evaluated using two different methodologies, HPLC quantification and trichromatic equation based on UV-VIS absorption spectra. No statistical differences in scytonemin values were found between applied the methodologies.

The scytonemin content in YU-2 strain (Fig. 3.6,) increases with time during the first 9 days of experiment in both experimental conditions. When this strain was exposed only to PAR light, the maximum content of 16.4 μg scytonemin mg^{-1} DW was detected after 9 days of exposure. When the strain was exposed to UVR and PAR light, maximum scytonemin content of 20.8 μg scytonemin mg^{-1} DW, was detected also after 9 days of exposure. Significant differences between both experimental conditions were observed after only 6 days of exposure, where the scytonemin content under UVR+PAR conditions was 14.6 μg scytonemin mg^{-1} DW, while it remained as low as 1.9 μg scytonemin mg^{-1} DW under PAR only. Significant differences in scytonemin content between both light treatments were also observed during the last 6 days of experiment. The scytonemin content decreased drastically after 12 days of experiment under PAR light down to the original values at time 0. However, the tendency was significantly different when UVR+PAR light were used, finding non-significant differences in scytonemin content between the last experimental time and the value detected after 9 days.

Table 3.1. Functional roles of sequence reads assigned to SEED categories (RAST) related to oxidative stress in *Chroococcidiopsis* YU-2 strain and *Chroococcidiopsis* CVL strain genomes.

Subsystem	Role	YU-2	CVL
Protection from ROS	Manganese superoxide dismutase (EC 1.15.1.1)	•	•
	Superoxide dismutase [Cu-Zn] precursor (EC 1.15.1.1)	•	•
	Cytochrome c551 peroxidase (EC 1.11.1.5)		•
	Superoxide dismutase [Fe] (EC 1.15.1.1)		•
	Catalase (EC 1.11.1.6)	•	•
Oxidative Stress	Iron-binding ferritin-like antioxidant protein	•	•
	Alkyl hydroperoxide reductase subunit C-like protein	•	•
	Fe2+/Zn2+ uptake regulation proteins	•	•
	Paraquat-inducible protein B	•	•
	Peroxide stress regulator	•	•
	Phytochrome, two-component sensor histidine kinase (EC 2.7.3.-)	•	•
	Non-specific DNA-binding protein Dps	•	•
	Zinc uptake regulation protein ZUR	•	•
	Ferroxidase (EC 1.16.3.1)	•	•
	Ferric uptake regulation protein FUR	•	•
	Metallothionein	•	•
	transcriptional regulator, Crp/Fnr family	•	•
Glutathione: Biosynthesis and gamma-glutamyl cycle	Gamma-glutamyltranspeptidase (EC 2.3.2.2)	•	•
	Glutathione synthetase (EC 6.3.2.3)	•	•
	5-oxoprolinase (EC 3.5.2.9)	•	•
Glutathione: Non-redox reactions	Glutathione S-transferase family protein	•	•
	Glutathione S-transferase (EC 2.5.1.18)	•	•
	Uncharacterized glutathione S-transferase-like protein	•	•
	Lactoylglutathione lyase (EC 4.4.1.5)	•	•
	Hydroxyacylglutathione hydrolase (EC 3.1.2.6)	•	•
	Glutathione S-transferase, unnamed subgroup (EC 2.5.1.18)	•	•
	Glutathione S-transferase, omega (EC 2.5.1.18)	•	•
Rubrerythrin	Rubrerythrin	•	
	Rubredoxin	•	•
	Alkyl hydroperoxide reductase subunit C-like protein	•	•
Glutathione: Redox cycle	Glutathione reductase (EC 1.8.1.7)	•	•
	Glutaredoxin 3	•	•
	Uncharacterized monothiol glutaredoxin ycf64-like	•	•
	Glutaredoxin 3 (Grx1)	•	
	Cell wall endopeptidase, family M23/M37	•	
Cluster containing Glutathione synthetase	Ribosomal RNA small subunit methyltransferase E (EC 2.1.1.-)	•	•
	Putative Holliday junction resolvase YggF	•	•

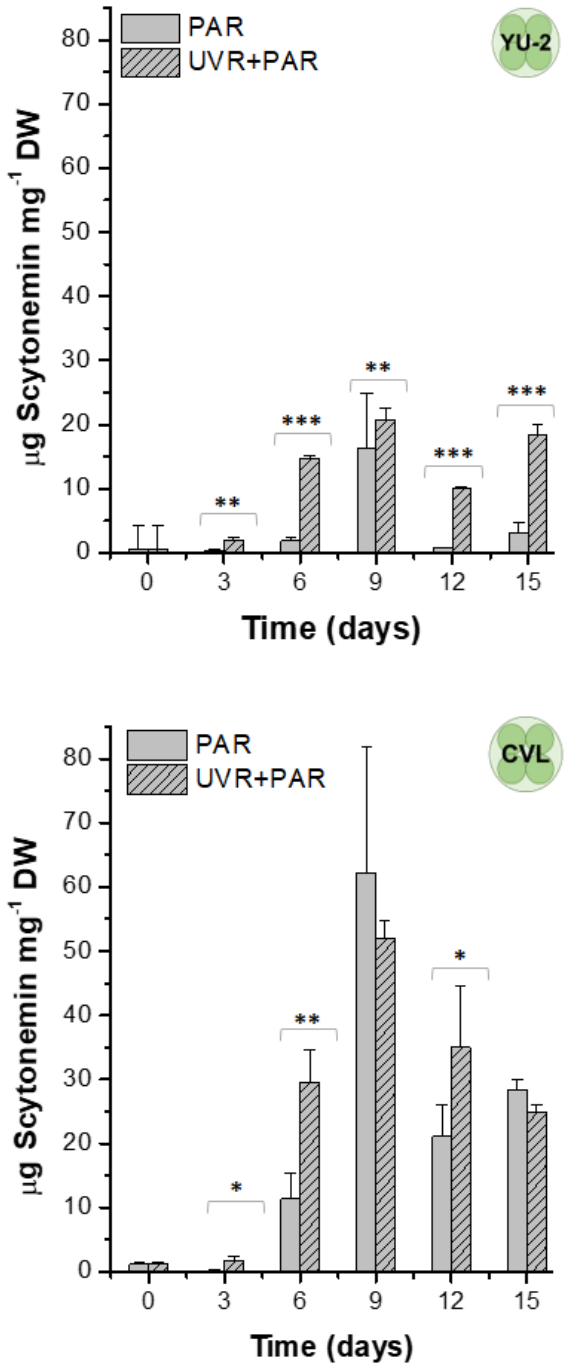

Figure 3.6. **Total scytonemin content on *Chroococcidiopsis* strains YU-2** (upper graph,) **and CVL** (lower graph) after irradiation with PAR (plain bars) or UVR+PARR (scratched bars) for 15 days normalized to dry weight. Significant differences between light conditions are marked by *** (0.001); ** (0.01); * (0.05).

The maximum scytonemin content in the CVL strain (Fig. 3.6) was reached after 9 days of exposure to both experimental conditions, with no significant differences between them. This maximum content was 62.3 μg scytonemin mg^{-1} DW for PAR light conditions and 52 μg scytonemin mg^{-1} DW for UV+PAR light conditions. Relative scytonemin content under both light conditions decreased during the last 6 days of exposure. Significant differences were observed between the experimental conditions at three different times, after 3, 6 and 12 days of exposure. The greater difference between both treatments occurred after 6 days of exposure, exhibiting an almost three times higher scytonemin content after UVR+PAR treatment (29.6 μg scytonemin mg^{-1} DW) in comparison with PAR treatment (11.4 μg scytonemin mg^{-1} DW).

3.4.3.1. Scytonemin characterization

A further analysis was performed to partially characterize scytonemin. The HPLC analysis of the scytonemin showed two prominent peaks in both *Chroococcidiopsis* strains (Fig. 3.7, A-B) at 16.57 min (a) and 17.89 min (b) with a UV absorption maximum at 385 nm identified as reduced scytonemin (a) and oxidized scytonemin (b). The obtained chromatogram revealed the presence of both reduced and oxidized scytonemin on the ethyl acetate: methanol extracts of both *Chroococcidiopsis* strains. However, the proportion of each type of scytonemin occurring in both *Chroococcidiopsis* strains cannot be taken into account due to the absence of a N_2 atmosphere during the extraction procedure.

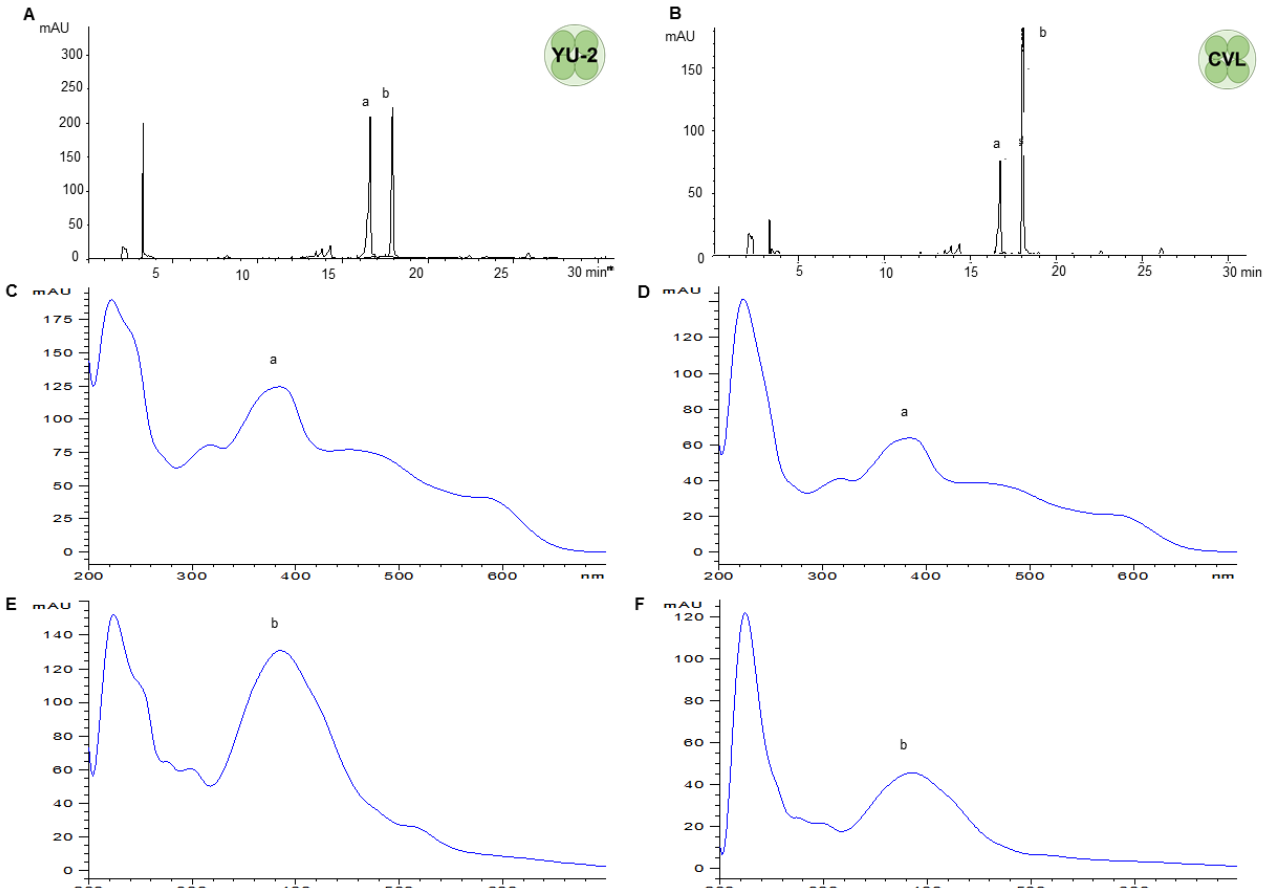

Figure 3.7. **The HPLC chromatogram and absorption spectra of scytonemin extract of *Chroococcidiopsis* strains YU-2** (A, C, E) **and CVL** (B, D, F). A and B: The HPLC chromatogram of the reduced (a) and oxidized (b) scytonemin in YU-2 and CVL. The absorption spectra of the reduced scytonemin of YU-2 **(C)** and CVL **(D**), and the oxidized scytonemin of YU-2 **(E)** and CVL **(F)**

3.4.4. Metabolic activity of *Chroococcidiopsis*

3.4.4.1. *Chroococcidiopsis* cells metabolic activity analysis

The metabolic activity of the *Chroococcidiopsis* cells was evaluated after 15 days of exposure to two different light conditions, PAR and UVR+PAR.

Three categories were stablished for the vital status of the *Chroococcidiopsis* cells depending on their fluorescence emittance after the CTC staining. Those with green autofluorescence (GF+) were defined as *not viable* cells, cells exhibiting only red chlorophyll autofluorescence (CHL+) were defined as *damaged* (not metabolically active); while cells presenting both chlorophyll red autofluorescence and bright orange spots (CTF crystals) (CHL+ / CTC+) were defined as *active* (Fig. 3.8)

Counting results in the YU-2 strain (Fig. 3.9) revealed a growth in active cells during the first 12 days of exposure to PAR (86.9-96.2%). A final decrease in this active cells occurred after 15 days of exposure (90.1%). However, maximum relative abundance of active cells under UVR+PAR light conditions was reached after 9 days of exposure (93.2%), exhibiting a progressive decrease after 12 and 15 days of exposure decaying below the original values (70.5%). In both PAR and UVR+PAR conditions, maximum values of damaged cells (5.9% for PAR, 21.6% for UVR+PAR) were observed after 15 days of exposure, while the relative abundance of not viable cells reached its maximum after 6 days under PAR (4.7%) and after 15 days for UVR+PAR (7.9%).

The CVL strain cells metabolic activity (Fig. 3.9) exhibited a different behavior where the maximum values of active cells for PAR exposure were found after 3 days of exposure (95.2%) maintaining lower relative abundances during the following experimental times (86-90%). That maximum was reached after 15 days under UVR+PAR light conditions (94%) upon a progressive increase during the experiment. This progressive increase was accompanied by a total loss of

damaged cells under UVR+PAR, whereas that loss was disrupted by a recurrence of damaged cells (2.5 %) when they were exposed only to PAR light for 15 days. High presence of death cells was detected during the whole experiment for both light conditions. When exposed to PAR for 9 days the culture experienced its maximum ratio of death cells (15.1%) which fell to 7% after 15 days of experiment. A similar proportion was found when cells were exposed to UVR+PAR, reaching a maximum of death cells after 9 days (15%) and falling to 6% at the end of the experiment.

3.4.4.2. *Chroococcidiopsis* ultrastructure after its exposure to UVR and PAR.

Ultrastructural changes were examined in both YU-2 and CVL *Chroococcidiopsis* strains before UVA irradiation and after 9 days of exposure to UVR+PAR light (Fig. 3.10, Fig. 3.11).

External changes in color were already visible in YU-2 strain cells after UVR+PAR exposure, from light green to brownish (Fig. 3.10, A1-B1). Regarding the thylakoid placement in YU-2 strain cells after UVR+PAR exposure (Fig. 3.10, B2), an increase in the intra-thylakoid space was observed while the thylakoid membranes in cells not exposed to UVR (Fig. 3.10, A2) were positioned touching each other tightly showing a nucleoid area. A more developed electron dense outermost layer was observed in cells after their exposure to UVR+PAR (Fig. 3.10, B2) with a granulose and fibrous appearance (Fig. 3.10, B3) compared to the compact sheath observed in *Chroococcidiopsis* YU-2 cells that did not suffer UVR exposure (Fig. 3.10, A3).

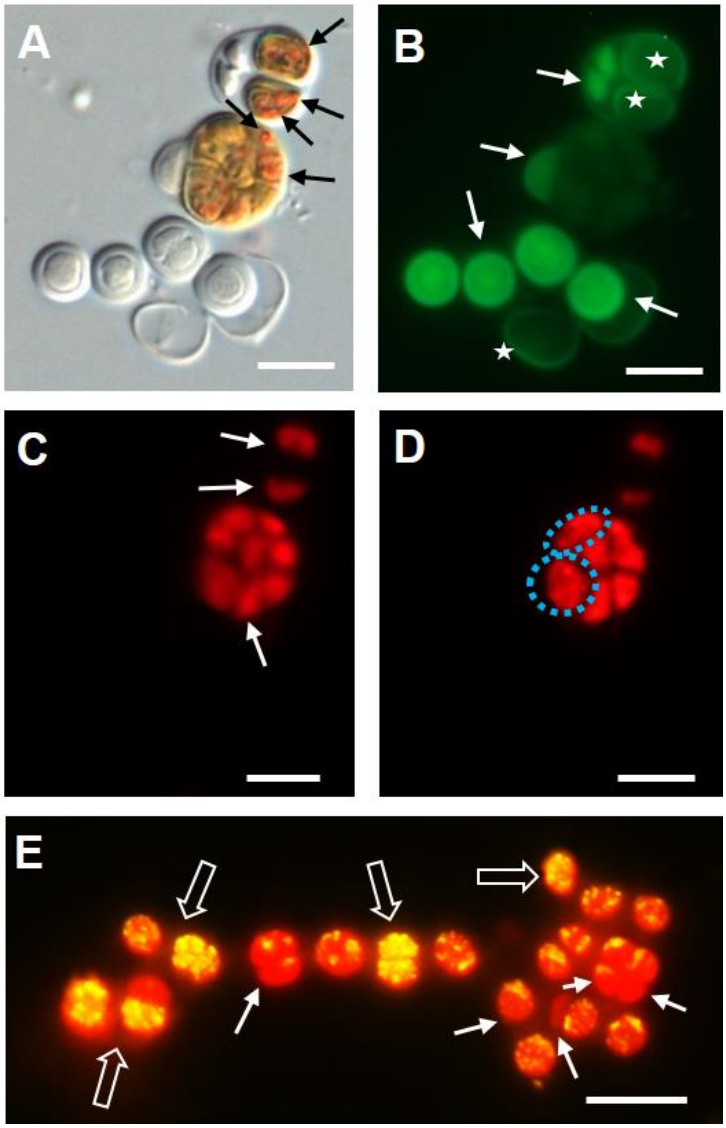

Figure 3.8. **Light (DIC) and fluorescence microscopy images as examples of criteria on metabolic activity assay of *Chroococcidiopsis* sp. CVL cells after 6 days of irradiation with UVR + PAR** (A, B, C, D). **A)** Light microscopy image (DIC) where CTF crystals appear are are already visible in active cells (black arrows). **B)** Fluorescence image with EGFP filter set exhibiting dead cells (GF+) (white arrows). **C)** Fluorescence image with rhodamine filter set exhibiting cells with chlorophyll autofluorescence (white arrows) (CHL+). **D)** Fluorescence image with HE rhodamine filter set exhibiting cells with chlorophyll autofluorescence and CTF fluorescence (granulose red fluorescence) (blue dotted) (CHL+/CTC+). **E)** *Chroococcidiopsis* sp. CVL cells aggregate after 3 days of irradiation with UVR + PAR. The aggregate exhibits cells with chlorophyll autofluorescence and high metabolic activity (CHL+/CTC+) (empty arrows) and damaged cells (white arrows) (CHL+). Scale bar = 10 μm.

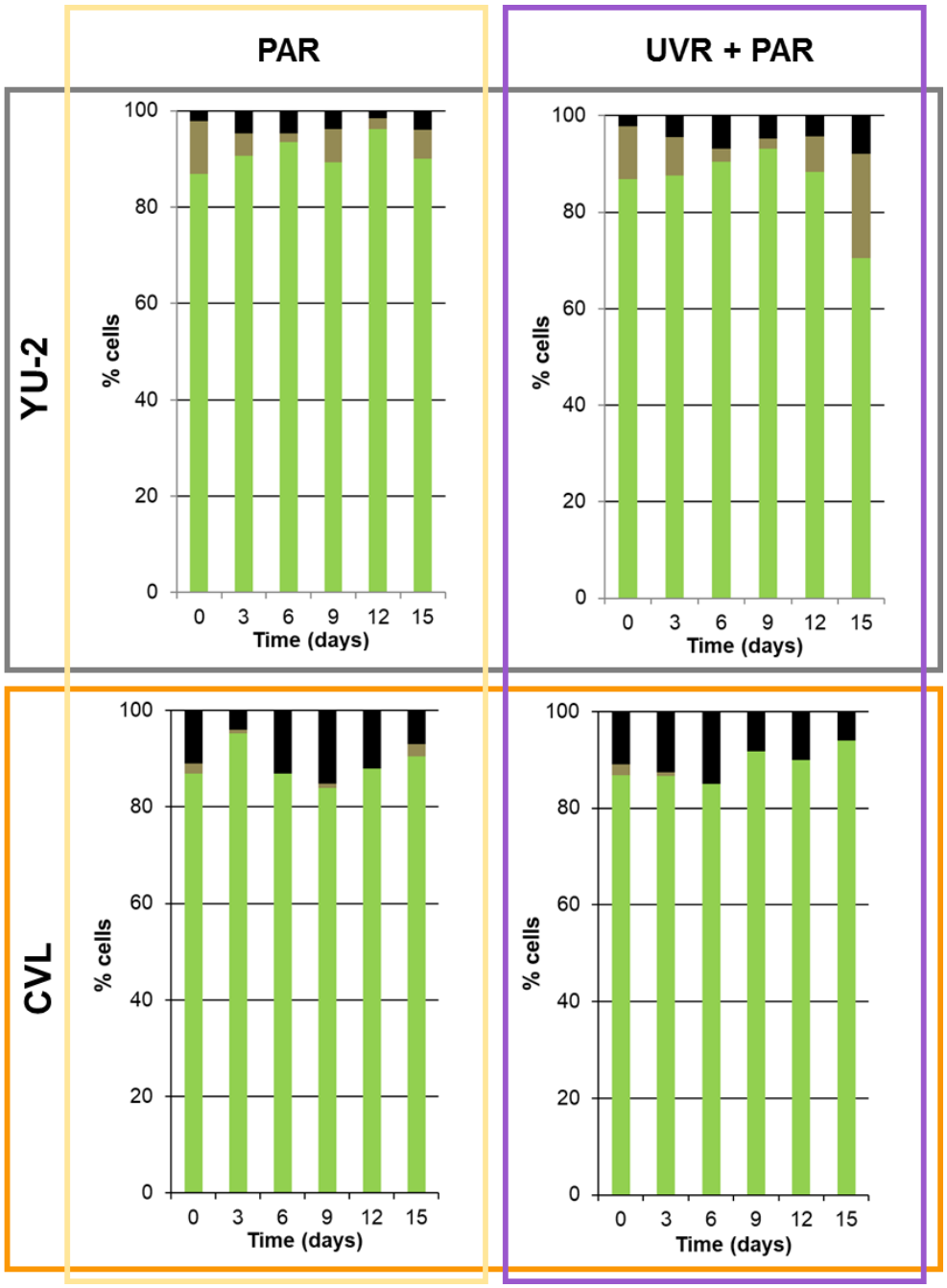

Figure 3.9. Metabolic activity of *Chroococcidiopsis* sp. YU-2 and CVL cells after irradiation with PAR (left graphs) **or UVR + PAR** (right graphs) **for 15 days**. Green: (CTC+/CHL+) active cells. Brown: (CHL+) damaged cells. Black: (GF+) dead cells.

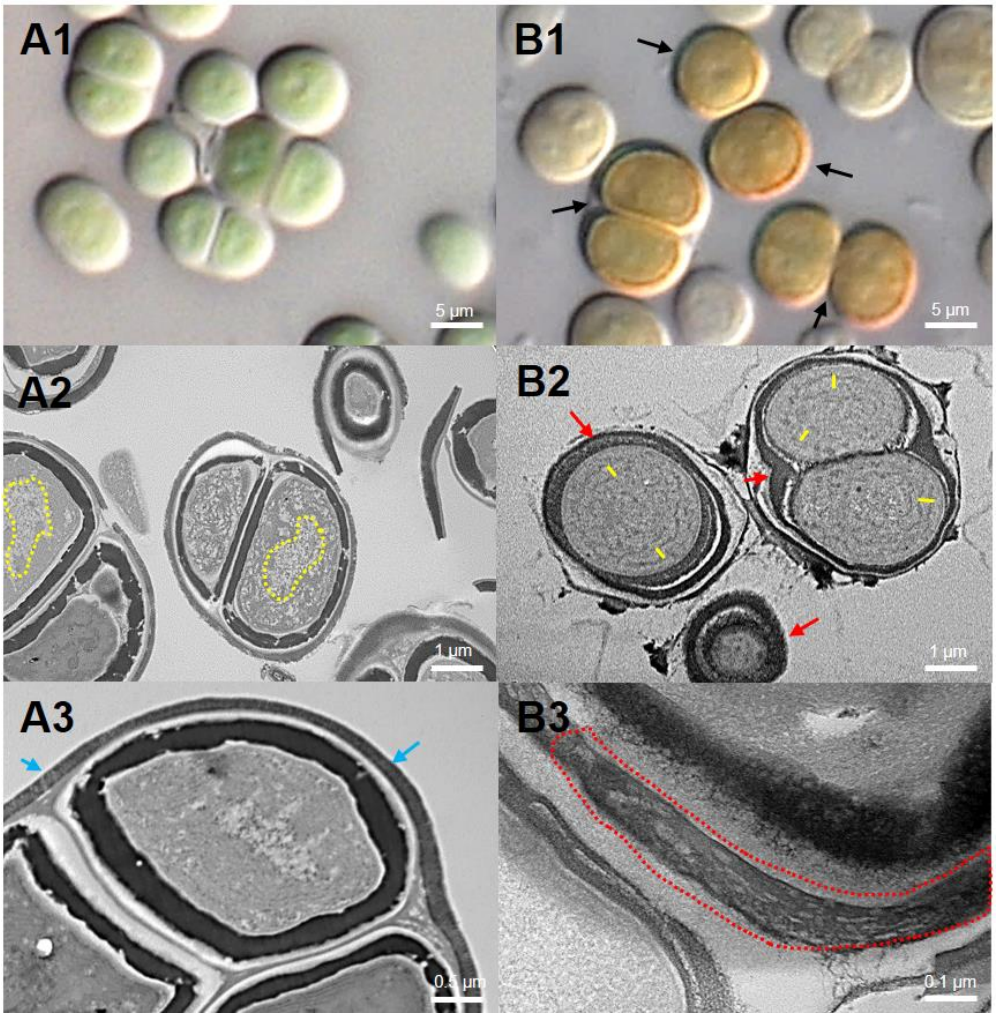

Figure 3.10. Light and transmission electron microscopy images from *Chroococcidiopsis* sp. YU-2 strain. Series A: Cells and aggregates at the beginning of the experiment. **A1)** Green *Chroococcidiopsis* sp. YU-2 cells. **A2)** TEM micrograph with cells exhibiting a visible nucleoid area (yellow dotted line). **A3)** TEM micrograph with an aggregate exhibiting a thin outermost fibrous layer (blue arrows). Series B: Cells and aggregates with maximum scytonemin content after 9 days of irradiation with UVR+PAR. **B1)** Brown *Chroococcidiopsis* sp. YU-2 cells with higher scytonemin content on the edge of cells. **B2)** TEM micrograph with cells exhibiting a higher distance between thylakoids (yellow lines) and the presence of an electron dense outermost fibrous layer (red arrows). **B3)** TEM micrograph of the outer part of the cells from the same aggregate exhibiting a highly fibrous outermost layer (red dotted line).

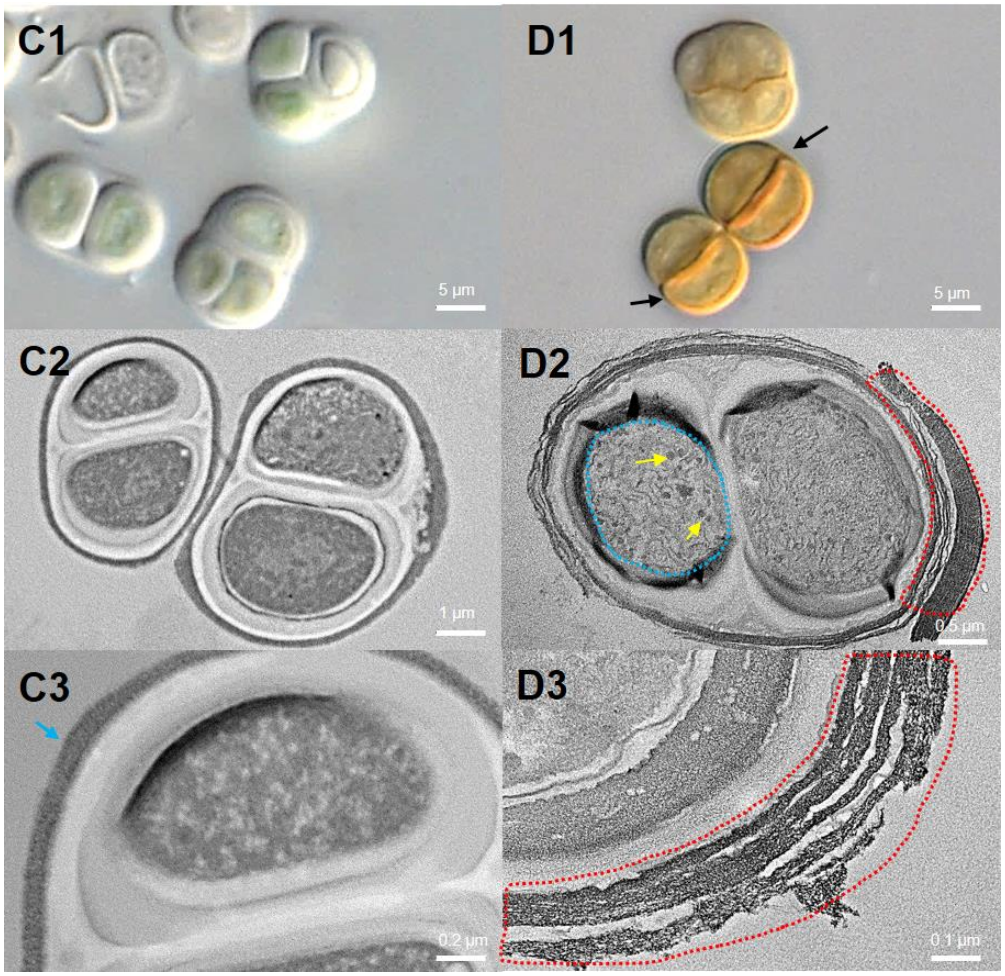

Figure 3.11. Light and transmission electron microscopy images from *Chroococcidiopsis* sp. CVL strain. Series C: Cells and aggregates at the beginning of the experiment. **C1)** Green *Chroococcidiopsis* sp. CVL cells. **C2)** TEM micrograph with cells exhibiting the original thylakoid arrangement. **C3)** TEM micrograph with a *Chroococcidiopsis* sp. CVL cell exhibiting a slightly developed outermost fibrous layer (blue arrow). Series D: Cells and aggregates with maximum scytonemin content after 9 days of irradiation with UVR+PAR. **D1)** Brown *Chroococcidiopsis* sp. CVL cells with higher scytonemin content on the outer part of the cells. **D2)** TEM micrograph with cells exhibiting disaggregation of thylakoid membranes (blue dotted line), glycogen granules (dark spots pointed by yellow arrows) and a highly electron dense outermost fibrous layer (red dotted line). **D3)** TEM micrograph of the outer part of the cell exhibiting a highly fibrous outermost layer (red dotted line).

CVL *Chroococcidiopsis* cells showed evident color differences too, when exposed to UVR+PAR for 9 days (Fig. 3.11, C1-D1). In particular, especially darker brown was observed on the outer part of the cell aggregates. Ultrastructural changes were found in different features as thylakoid arrangement showing the beginning of thylakoid membrane disintegration and glycogen granules along thylakoids (Fig. 3.11, D2). The outermost fibrous layer observed in cells before the treatment (Fig. 3.11, C3) exhibited a more developed denser aspect with an assembly of various fibrous layers, an electron dense matrix within the EPSs, after its exposure to UVR+PAR for 9 days (Fig. 3.11, D3).

3.5. Discussion

This work provides a new insight into the role of cyanobacteria in endolithic communities under extreme solar radiation, as happens in the hyper-arid core of the Atacama Desert, apart from its main function as primary producers. Despite the sole development of lithobiontic microbial communities in endolithic habitats in different lithic substrates in this desert (Wierzchos et al. 2006, Wierzchos et al. 2015, Crits-Christoph et al. 2016a) which act as a first line of defense against the damage provoked by high light exposure, the presence of second and third lines of cyanobacterial defense (Vítek et al. 2014a, Wierzchos et al. 2015, Vítek et al. 2017) points to the existence of specific, not previously characterized, adaptations to the harmful effects of high PAR and UVR, too.

In this chapter, two isolates from the extremotolerant genus *Chroococcidiopsis*, widely distributed in the endolithic communities, were used to unravel the specific responses and adaptations to direct exposure to PAR and UVR. It was shown that both strains reveal specific differences matching their distinct microhabitat origin, cryptoendolithic from halite (YU-2) and chasmoendolithic

from calcite (CVL), and thus the biological implications for the whole microbial community in their original endolithic context.

Both strains shared several features: same genus – *Chroococcidiopsis* -, same type of original habitat –endolithic-, and similar original climatic conditions -those occurring in the hyper-arid Atacama Desert. Despite their similarities, evident differences were found in their response to direct light exposure that will be discussed below.

Accepting the differences found between light treatments, PAR or UVR+PAR, in both *Chroococcidiopsis* strains, a high response to PAR was observed in contrast with other studies when analyzing short-term (ROS accumulation) (Heand Häder 2002) and long-term response (scytonemin content) (Dillon et al. 2002, Fleming and Castenholz 2007, Rajneesh et al. 2019). In fact, both *Chroococcidiopsis* strains exhibited a lower short-term acclimation to PAR, compared to UVR+PAR light treatment. The same pattern was found regarding the long-term response of the CVL strain in both the scytonemin content and the metabolic activity tests. The high sensitivity to PAR light displayed in both cases could be explained by their original habitat, since by living in the endolithic microhabitat the direct and harmful exposure to solar radiation is avoided. This behavior was different in comparison to other studies where no PAR-induced oxidative stress was found in *Anabaena* (He and Häder 2002) or *Nostoc* and *Fischerella* (Rajneesh et al. 2019). The high response observed in the endolithic *Chroococcidiopsis* strains to PAR certainly support the requirement of a second and third line of defense against radiation, despite inhabiting endolithic microhabitats.

Concerning the short-term response exhibited by both *Chroococcidiopsis* strains, it is worth noting the remarkable finding of the very rare Cu/Zn-SOD precursor in both genomes, which reveals the particular evolutionary origin of this extremotolerant genus. The YU-2 strain exhibited a considerably lower

acclimation to both light conditions. The observed subsequent increase of ROS in the YU-2 strain during the 3 days of exposure with no signs of recovery finds its answer in the YU-2 genome where the oxidative stress systems Fe-SOD and cytochrome c551 peroxidase were not found. However, the CVL strain exhibited an acclimation to both light conditions, even better to UVR+PAR, with a similar response pattern to the one reported in *Anabaena* by He and Häder (2002), although CVL acclimation started 24 hours earlier.

Long-term response to direct light should be explored considering three elements: scytonemin production, metabolic activity and ultrastructural changes. Both *Chroococcidiopsis* strains displayed clearly different responses in all three parameters. No severe ultrastructural damages were observed in the YU-2 strain when exposed to 9 days of direct light although a visible increase of cover thickness was detected. This characteristic might be linked to the proportion of dead and damaged cells observed after 15 days of exposure, where both types of physiological status reached their maxima. This fact could explain the low relative content of scytonemin in this strain during the experimental period. The YU-2 strain already showed its low capacity to deal with UVR in short-term exposure, and it seemed to happen again in long-term exposure. The relative scytonemin content reached its maximum after 9 days of exposure. Subsequently, the low abundance of new cells able to produce scytonemin, as exhibited in the metabolic activity test, together with a slight increase in DW due to the thickening of the cellular covers would maintain or slightly decrease the proportion between scytonemin and DW in the culture.

The long-term response of the CVL strain against UVR+PAR could be explained by its ultrastructural changes and metabolic activity. Higher ultrastructural damage could be observed after 9 days of exposure to UV, coinciding with the experimental time where a major dead and damaged cell proportion was observed. The recovery of the physiological status after that point can be

explained by the major capacity of the CVL strain to deal with this type of stress, as demonstrated in the short-term experiment (ROS accumulation). Its capacity to recover and acclimate to the stressful conditions would allow an increase in the population leading to a subsequent decrease in the relative scytonemin content, since, thanks to its high acclimation capacity, growth would occur faster than the scytonemin production.

It was shown that acclimation capacity is strain-dependent, with significantly lower scytonemin content values in both *Chroococcidiopsis* strains from endolithic communities of the Atacama Desert than previously reported *Chroococcidiopsis* from desert crusts of the Vizcaíno Desert (Mexico) (Dillon et al. 2002; Fleming and Castenholz, 2007).

The lower acclimation capacity of the YU-2 strain was observed in both short-term and long-term responses, which could be tightly linked to its original microhabitat. Since the *Chroococcidiopsis* YU-2 strain is originally from a cryptoendolithic microhabitat, it would never be directly exposed to light, being always protected by the halite crust. This could explain its lower acclimation capacity to direct light exposure. On the contrary, the *Chroococcidiopsis* CVL strain comes from a chasmoendolithic microhabitat, thus being more exposed to the effect of direct PAR and UVR. The *Chroococcidiopsis* strains isolated from this microhabitat would therefore be expected to be faster in the acclimation to light exposure.

There could be a linkage between each strain and its original microhabitat explained by a microhabitat specific environmental pressure, as previously suggested in Chapter 1. In this case, the *Chroococcidiopsis* strains inhabiting certain endolithic microhabitats and lithic substrates could be absent from a different endolithic microhabitat and substrate in the same Desert. This differential distribution could be explained by the possession of specific

adaptations and the acclimation capacity of these organisms to the specific abiotic stresses occurring in the endolithic microhabitat they are inhabiting.

The third line of defense displayed by these strains, the production of scytonemin, would have two simultaneous functions: at an individual level and at a community level. The protection provided by scytonemin at an individual level, even against the excess of PAR, as previously discussed, seems expected since these strains have extremely low growth rates in their original microhabitat (Ziolkowski et al. 2013). Thus, each cyanobacterial cell would suffer long exposure times that would lead to scytonemin production and accumulation. Furthermore, the individual protection provided by scytonemin in these microhabitats would influence role of cyanobacteria at an additional community level, apart from the primary production, based on two considerations. On the one hand, the high stability of scytonemin previously reported (Dillon et al. 2002, Fleming and Castenholz 2007, Rastogi et al. 2014, Vítek et al. 2017) that stays in EPS covers even in death cells as observed in this study (Fig. 3.5). On the other, the original microhabitat of these strains where the environmental factors known to promote the induction of scytonemin production occur: high salinity or desiccation (Dillon et al. 2002, Fleming and Castenholz 2007). Hence, the outcome of the combination of both conditions is a UV-screening effect over the whole EMC that could enable its easier development through time, avoiding the harmful effects of extreme solar radiation.

3.6. Concluding Remarks and future projects

This is a pioneer study since it explores the response of cyanobacteria against UVR and PAR in cyanobacterial strains isolated from a place on Earth where one of the highest solar radiation levels have been detected, the hyper-arid core of the Atacama Desert.

The observed response of both *Chroococcidiopsis* strains to radiation suggests a strain specific distribution related to the greater or lesser exposure to abiotic stresses. That distribution would be based on the acclimation capacity and adaptation strategies displayed by different strains, confirming the statement "Everything is everywhere and the environment selects". Everything meaning, the different *Chroococcidiopsis* strains, everywhere, the endolithic microhabitats of the hyper-arid core of the Atacama Desert, and selective environment, the slight differences in direct exposure, in this case to solar radiation, between lithic substrates and the type of endolithic microhabitat.

To continue with the exploration of the response to UVR in organisms inhabiting the most extreme places in terms of solar radiation and answer the strain distribution proposal suggested in this chapter, the metagenomic and metatranscriptomic analysis of the whole endolithic community could be pursued to reveal the global response to the stress. In addition, those analyses could be merged with qPCR at a community level for genes related to oxidative stress and specific fluorescence staining in order to explore the oxidative stress and activity of the different organisms configuring the endolithic community.

3.7. Supplementary Material

Supplementary Material 3.1. Functional roles of sequence reads assigned to SEED categories (RAST) related to oxidative stress in *Chroococcidiopsis* YU-2 strain and *Chroococcidiopsis* CVL strain genomes and hits found in CyanoBase. N.strains: number of strains where gene was found. N. genera: number of genera that those strains belong.

Subsystem	Role	YU-2	CVL	N. strains	N. Genera	Genera
Protection from ROS	Manganese superoxide dismutase (EC 1.15.1.1)	•	•	41	20	*Anabaena, Calothrix,* ***Chroococcidiopsis****, Crocosphaera, Cyanobacterium, Cyanothece, Cylindrospermopsis, Fischerella, Geitlerinema, Gloeocapsa, Halothece, Microcoleus, Microcystis, Nodularia, Nostoc, Oscillatoria, Pseudanabaena, Raphidiopsis, Richelia, Stanieria*
	Superoxide dismutase [Cu-Zn] precursor (EC 1.15.1.1)	•	•	5	1	*Synechococcus*
	Cytochrome c551 peroxidase (EC 1.11.1.5)		•	2	2	*Acaryochloris, Tolypothrix*
	Superoxide dismutase [Fe] (EC 1.15.1.1)		•	15	9	*Acaryochloris, Arthrospira, Coelofasciculus, Cyanobium, Microcystis, Nodularia, Oscillatoria, Synechococcus, Synechocystis*
	Catalase (EC 1.11.1.6)	•	•	82	40	*Acaryochloris, Anabaena, Calothrix, Chamaesiphon,* ***Chroococcidiopsis****, Chrysosporum, Coleofasciculus, Crinalium, Cyanobacterium, Cyanobium, Cyanothece, Cylindrospermum, Fischerella, Geitlerinema, Gloeobacter, Gloeocapsa, Hapalosiphon, Hassallia, Leptolyngbya, Limnoraphis, Lyngbya, Mastigocladus, Mastigocoleus, Microcoleus, Nodularia, Nostoc, Oscillatoria, Phormidesmis, Pleurocapsa Rhodopseudomonas, Richelia, Rivularia, Rubidibacter, Scytonema, Stanieria, Synechococcus, Synechocystis, Tolypothrix, Trichodesmium, Xenococcus*

Oxidative Stress	Iron-binding ferritin-like antioxidant protein	•	•	7	4	*Crocosphaera, Nodularia, Richelia, Synechocystis*
	Alkyl hydroperoxide reductase subunit C-like protein	•	•	40	7	*Crocosphaera, Microcystis, Nodularia, Prochlorococcus, Richelia, Synechocystis, Thermosynechococcus*
	Fe2+/Zn2+ uptake regulation proteins	•	•	6	3	*Crocosphaera, Microcystis, Richelia*
	Paraquat-inducible protein B	•	•	0	0	-
	Peroxide stress regulator	•	•	14	6	*Chrysosporum, Crocosphaera, Microcystis, Nodularia, Prochlorococcus, Richelia*
	Phytochrome, two-component sensor histidine kinase(EC 2.7.3.-)	•	•	9	4	*Crocosphaera, Microcystis, Nodularia, Richelia*
	Non-specific DNA-binding protein Dps	•	•	11	6	*Chrysosporum, Crocosphaera, Microcystis, Nodularia, Richelia, Synechocystis*
	Zinc uptake regulation protein ZUR	•	•	37	6	*Crocosphaera, Microcystis, Nodularia, Prochlorococcus, Richelia, Synechocystis*
	Ferroxidase (EC 1.16.3.1)	•	•	10	7	*Chrysosporum, Crocosphaera, Cyanothece, Halothece, Nodularia, Richelia, Synechocystis*
	Ferric uptake regulation protein FUR	•	•	37	7	*Chrysosporum, Crocosphaera, Microcystis, Nodularia, Prochlorococcus, Richelia, Synechocystis*
	Metallothionein	•	•	69	31	*Anabaena, Arthrospira, Calothrix, Chamaesiphon,* ***Chroococcidiopsis****, Crinalium, Crocosphaera, Cyanobacterium, Cyanobium, Cyanothece, Dactylococcopsis, Fischerella, Geitlerinema, Gloeobacter, Gloeocapsa, Leptolyngbya, Lyngbya, Mastigocoleus, Microcoleus, Microcystis, Nodularia, Nostoc, Oscillatoria, Phormidium, Pleurocapsa, Pseudanabaena, Rivularia, Stanieria, Synechococcus, Thermosynechococcus, Xenococcus*

	transcriptional regulator, Crp/Fnr family	•	•	79	39	*Acaryochloris, Anabaena, Arthrospira, Calothrix, Chlorobium,* ***Chroococcidiopsis****, Chrysosporum, Coleofasciculus, Crinalium, Crocosphaera, Cyanobacterium, Cyanobium, Cyanothece, Cylindrospermopsis, Fischerella, Geitlerinema, Gloeobacter, Gloeocapsa, Halothece, Leptolyngbya, Lyngbya, Microcoleus, Microcystis, Moorea, Nodularia, Nostoc, Oscillatoria, Phormidesmis, Phormidium, Prochlorococcus, Pseudanabaena, Raphidiopsis, Rhodopseudomonas, Richelia, Stanieria, Synechococcus, Synechocystis, Tolypothrix, Trichodesmium*
Glutathione: Biosynthesis and gamma-glutamyl cycle	Gamma-glutamyltranspeptidase (EC 2.3.2.2)	•	•	86	34	*Aphanocapsa, Arthrospira, Calothrix, Chamaesiphon, Coleofasciculus, Crocosphaera, Cyanobium, Cyanothece, Gloeobacter, Hapalosiphon, Hassallia, Leptolyngbya, Limnoraphis, Lyngbya, Mastigocladus, Mastigocoleus, Microcoleus, Microcystis, Neosynechococcus, Nodularia, Nostoc, Oscillatoria, Phormidium, Planktothricoides, Pleurocapsa, Prochlorococcus, Rhodopseudomonas, Richelia, Scytonema, Synechococcus, Synechocystis, Thermosynechococcus, Tolypothrix, Xenococcus*
	Glutathione synthetase (EC 6.3.2.3)	•	•	161	43	*Acaryochloris, Anabaena, Aphanizomenon, Aphanocapsa, Arthrospira, Calothrix, Chamaesiphon, Chrysosporum, Crocosphaera, Cyanobium, Cyanothece, Cylindrospermopsis, Dactylococcopsis, Fischerella, Gloeobacter, Gloeocapsa, Hapalosiphon, Hassallia, Leptolyngbya, Limnoraphis, Lyngbya, Mastigocladus, Matigocoleus, Microcoleus, Microcystis, Neosynechococcus, Nodularia, Nostoc, Oscillatoria, Planktothricoides, Pleurocapsa, Prochlorococcus, Raphidiopsis, Rhodopseudomonas, Richelia, Rivularia, Rubidibacter, Scytonema, Synechococcus, Synechocystis, Thermosynechococcus, Tolypothrix, Xenococcus*
	5-oxoprolinase (EC 3.5.2.9)	•	•	93	42	*Acaryochloris, Anabaena, Aphanizomenon, Aphanocapsa, Arthrospira, Calothrix,* ***Chroococcidiopsis****, Crinalium, Crocosphaera, Cyanobacterium, Cyanobium, Cyanothece, Fischerella, Geitlerinema, Gloeobacter, Gloeocapsa, Halothece, Hapalosiphon, Hassallia, Leptolyngbya, Limnoraphis, Lyngbya, Mastigocladus, Mastigocoleus, Microcoleus, Microcystis, Nodularia, Nostoc, Oscillatoria, Phormidesmis, Phormidium, Planktothricoides, Prochlorococcus, Prochlorothrix, Pseudanabaena, Richelia, Scytonema, Stanieria, Synechococcus, Synechocystis, Tolypothrix, Trichodesmium*

Glutathione: Non-redox reactions	Glutathione S-transferase family protein	•	•	20	14	*Acaryochloris, Calothrix, Chrysosporum, Cylindrospermum, Microcoleus, Microcystis, Nodularia, Oscillatoria, Pleurocapsa, Prochlorococcus, Richelia, Rivularia, Synechococcus, Synechocystis*
	Glutathione S-transferase (EC 2.5.1.18)	•	•	195	58	*Acaryochloris, Anabaena, Aphanizomenon, Aphanocapsa, Arthrospira, Calothrix, Chamaesiphon, Chlorobium,* ***Chroococcidiopsis****, Chrysosporum, Coleofasciculus, Crinalium, Crocosphaera, Cyanobacterium, Cyanobium, Cyanothece, Cylindrospermopsis, Cylindrospermum, Dactylococcopsis, Fischerella, Geitlerinema, Gloeobacter, Gloeocapsa, Halothece, Hapalosiphon, Hassallia, Leptolyngbya, Limnoraphis, Lyngbya, Mastigocladus, Mastigocoleus, Microcoleus, Microcystis, Moorea, Neosynechococcus, Nodularia, Nostoc, Oscillatoria, Phormidesmis, Phormidium, Planktothricoides, Planktothrix, Prochlorococcus, Prochlorothrix, Pseudanabaena, Raphidiopsis, Rhodopseudomonas, Richelia, Rivularia, Rubidibacter, Scytonema, Stanieria, Synechococcus, Synechocystis, Thermosynechococcus, Tolypothrix, Trichodesmium, Xenococcus*
	Uncharacterized glutathione S-transferase-like protein	•	•			
	Lactoylglutathione lyase (EC 4.4.1.5)	•	•	144	43	*Acaryochloris, Anabaena, Arthrospira, Calothrix, Chamaesiphon,* ***Chroococcidiopsis****, Chrysosporum, Coleofasciculus, Crocosphaera, Cyanobacterium, Cyanobium, Cyanothece, Cylindrospermum, Dactylococcopsis, Fischerella, Geitlerinema, Gloeobacter, Gloeocapsa, Leptolyngbya, Lyngbya, Microcoleus, Microcysitis, Moorea, Neosynechococcus, Nodularia, Nostoc, Oscillatoria, Phormidesmis, Phormidium, Pleurocapsa, Prochlorococcus, Prochlorothrix, Pseudanabaena, Rhodopseudomonas, Richelia, Rivularia, Rubidibacter, Stanieria, Synechococcus, Synechocystis, Tolypothrix, Trichodesmium, Xenococcus*
	Hydroxyacylglutathione hydrolase (EC 3.1.2.6)	•	•	172	50	*Acaryochloris, Anabaena, Aphanizomenon, Aphanocapsa, Arthrospira, Calothrix, Chamaesiphon, Chlorobium,* ***Chroococcidiopsis****, Chrysosporum, Crinalium, Crocosphaera, Cyanobacterium, Cyanobium, Cyanothece, Cylindrospermum, Dactylococcopsis, Fischerella, Geitlerinema, Gloeobacter, Gloeocapsa, Halothece, Hapalosiphon, Hassallia, Leptolyngbya, Lyngbya, Mastigocladus, Mastigocoleus, Microcoleus, Microcystis, Nodularia, Nostoc, Oscillatoria, Phormidesmis, Planktothrix, Pleurocapsa, Prochlorococcus, Prochlorothrix, Pseudanabaena, Richelia, Rivularia, Rubidibacter, Scytonema, Stanieria, Synechococcus, Synechocystis, Thermosynechococcus, Tolypothrix, Trichodesmium, Xenococcus*
	Glutathione S-transferase, unnamed subgroup (EC 2.5.1.18)	•	•	2	2	*Nodularia, Richelia*

	Glutathione S-transferase, omega (EC 2.5.1.18)	•	•	10	4	*Crocosphaera, Nodularia, Richelia, Synechocystis*
Rubrerythrin	Rubrerythrin	•		51	23	*Anabaena, Aphanizomenon, Calothrix, Chlorobium, Coleofasciculus, Cyanothece, Cylindrospermopsis, Cylindrospermum, Gloeobacter, Hapalosiphon, Hassallia, Limnoraphis, Lyngbya, Mastigocladus, Mastigocoleus, Nostoc, Oscillatoria, Pleurocapsa, Prochlorococcus, Rivularia, Scytonema, Synechococcus, Tolypothrix*
	Rubredoxin	•	•	194	57	*Acaryochloris, Anabaena, Aphanizomenon, Aphanocapsa, Arthrospira, Calothrix, Chamaesiphon, Chlorobium,* ***Chroococcidiopsis****, Chrysosporum, Coleofasciculus, Crinalium, Crocosphaera, Cyanobacterium, Cyanobium, Cyanothece, Cylindrospermopsis, Cylindrospermum, Dactylococcopsis, Fischerella, Geitlerinema, Gloeobacter, Gloeocapsa, Halothece, Hapalosiphon, Hassallia, Leptolyngbya, Limnoraphis, Lyngbya, Mastigocladus, Mastigocoleus, Microcoleus, Microcystis, Moorea, Neosynechococcus, Nodularia, Nostoc, Oscillatoria, Phormidesmis, Planktothricoides* *Pleurocapsa, Prochlorococcus, Prochlorothrix, Pseudanabaena, Raphidiopsis, Rhodopseudomonas, Richelia, Rivularia, Rubidibacter, Scytonema, Stanieria, Synechococcus, Synechocystis, Thermosynechococcus, Tolypothrix, Trichodesmium, Xenococcus*
	Alkyl hydroperoxide reductase subunit C-like protein	•	•	40	6	*Crocosphaera, Microcystis, Nodularia, Prochlorococcus, Richelia, Synechocystis*

Glutathione: Redox cycle	Glutathione reductase (EC 1.8.1.7)	•	•	176	52	*Acaryochloris, Anabaena, Aphanizomenon, Aphanocapsa, Arthrospira, Calothrix, Chamaesiphon, **Chroococcidiopsis**, Chrysosporum, Coleofasciculus, Crinalium, Crocosphaera, Cyanobium, Cyanothece, Cylindrospermopsis, Cylindrospermum, Dactylococcopsis, Fischerella, Geitlerinema, Gloeocapsa, Halothece, Hapalosiphon, Hassallia, Leptolyngbya, Limnoraphis, Lyngbya, Mastigocladus, Mastigocoleus, Microcoleus, Microcystis, Moorea, Neosynechococcus, Nodularia, Nostoc, Oscillatoria, Phormidesmis, Phormidium, Pleurocapsa, Prochlorococcus, Pseudanabaena, Raphidiopsis, Rhodopseudomonas, Richelia, Rivularia, Rubidibacter, Scytonema, Stanieria, Synechococcus, Thermosynechococcus, Tolypothrix, Trichodesmium, Xenococcus*
	Glutaredoxin 3	•	•	179	53	*Acaryochloris, Anabaena, Aphanizomenon, Aphanocapsa, Arthrospira, Calothrix, Chamaesiphon, **Chroococcidiopsis**, Chrysosporum, Coleofasciculus, Crinalium, Crocosphaera, Cyanobacterium, Cyanobium, Cyanothece, Cylindrospermopsis, Cylindrospermum, Dactylococcopsis, Fischerella, Geitlerinema, Gloeobacter, Gloeocapsa, Halothece, Hapalosiphon, Hassallia, Leptolyngbya, Lyngbya Mastigocoleus, Microcoleus, Microcystis, Moorea, Neosynechococcus, Nodularia, Nostoc, Oscillatoria, Phormidesmis, Planktothricoides, Planktothrix, Pleurocapsa, Prochlorococcus, Pseudanabaena, Raphidiopsis brookii, Richelia, Rivularia, Rubidibacter, Scytonema, Stanieria, Synechococcus, Synechocystis, Thermosynechococcus, Tolypothrix, Trichodesmium, Xenococcus*
	Uncharacterized monothiol glutaredoxin ycf64-like	•	•	9	3	*Crocosphaera, Microcystis, Richelia*
	Glutaredoxin 3 (Grx1)	•		36	6	*Chrysosporum, Crocosphaera, Microcystis, Nodularia, Prochlorococcus, Richelia*
	Cell wall endopeptidase, family M23/M37	•		1	1	*Synechocystis*

Cluster containing Glutathione synthetase	Ribosomal RNA small subunit methyltransferase E (EC 2.1.1.-)	•	•	109	36	*Acaryochloris, Anabaena, Arthrospira, Calothrix, Chamaesiphon, Chrysosporum, Coleofasciculus, Crinalium, Crocosphaera, Cyanobacterium, Cyanobium, Cylindrospermum, Dactylococcopsis, Fischerella, Gloeocapsa, Leptolyngbya, Lyngbya, Mastigocoleus, Microcoleus, Microcystis, Moorea, Nodularia, Nostoc, Oscillatoria, Phormidesmis, Phormidium, Planktothrix, Pleurocapsa, Prochlorococcus, Pseudanabaena, Richelia, Rivularia, Stanieria, Synechocystis, Tolypothrix, Xenococcus*
	Putative Holliday junction resolvase YggF	•	•	3	2	*Microcystis, Synechocystis*

CHAPTER 4

BIOACTIVITY OF SECONDARY METABOLITES PRODUCED BY CYANOBACTERIA ISOLATED FROM THE ATACAMA DESERT

CHAPTER 4: BIOACTIVITY OF SECONDARY METABOLITES PRODUCED BY CYANOBACTERIA ISOLATED FROM THE ATACAMA DESERT

4.1. Abstract

Microorganisms inhabiting extreme environments constitute a promising source for natural products with biotechnological applications. Cyanobacteria, dominant in extreme environments, are already known as producers of diverse secondary metabolites with biotechnological potential. So far, cyanobacteria from extreme environments have not been studied in depth with this purpose due to the difficulties in their isolation and biomass culture. In this chapter, crude extracts from four cyanobacterial strains from *Chroococcidiopsis* and *Gloeocapsopsis* genera isolated from endolithic habitats of the Atacama Desert were obtained. Genomic screening for secondary metabolites and bioassays were conducted in order to test their potential protease inhibitory activity, antibacterial activity against multidrug resistant bacterial strains and cytotoxic effect on the T47D breast cancer cell line. Although no inhibition was observed on the tested proteases by any crude extract, fractions from all four strains revealed a significant inhibition of *Enterococcus durans* 66 cells. The most apolar fractions of *Chroococcidiopsis* strains revealed a significant decrease in the viability of breast adenocarcinoma cells. Active fractions were screened with LC-MS/MS optimized for the detection of peptides, for preliminary characterization of bioactive compounds determining ions possibly linked with effects observed in conducted tests. This work shows for the first time the existing potential of cyanobacterial strains isolated from the polyextreme environment of the Atacama Desert as a source of antibacterial and cytotoxic agents.

4.2. Introduction

The discoveries of new bioactive compounds from microorganisms have been of great interest during the last decades due to their potential biotechnological applications in different fields such as cosmetics, agriculture, pharmacology or biomedicine. Most research has been focused in the discovery of new antibiotics, especially after the publication in 2014 of the first report on the surveillance of antimicrobial resistance by the World Health Organization (WHO) (WHO 2014). An increase in the global resistance to existing antibiotics has been detected linked to the prevalence of multidrug-resistant pathogens which has become a public health problem (Roca et al. 2015).

4.2.1. Extreme environments as a source of bioactive compounds

Microorganisms inhabiting extreme environments, both extremophile and extremotolerant strains, have become a promising source of new bioactive compounds of interest (Neifar et al. 2015). The high expectations placed on these microorganisms are due to the atypical survival strategies they display in order to deal with harsh environmental conditions and to achieve competitive advantages, particularly necessary in those extreme environments where essential resources such as water or nutrients are also scarce or difficult to uptake (Nuñez-Montero and Barrientos 2018). Thus, the genetic adaptation of microorganisms inhabiting extreme conditions could be expected to allow the synthesis of novel metabolites with unique structures and specific biological activity (Okoro et al. 2009), helping in their colonization while establishing antagonistic relationships (Bratchkova and Ivanova, 2011).

Despite the difficulties regarding their sampling and culture, in comparison to mesophiles, the isolation and cultivation of microorganisms from extreme habitats is still productive (Axenov-Gribanov et al. 2016). Recently, an increasing research interest has been observed to discover novel bioactive compounds with

diverse biomedical properties such as antibacterial, antifungal antitumor, anti-inflamatory or antiviral in underexplored habitats (desert soils, permafrost soils, deep-sea sediments, acidic, saline and thermal habitats) (Gulder and Moore, 2009; Undabarrena et al. 2016; Mehetre et al. 2018; Yogabaanu et al. 2017, Sayed et al. 2019). This exploration of natural products has mainly been focused on actinobacteria, cyanobacteria and fungi (Sayed et al. 2019).

Regarding desert environments, decades of studies in Antarctica have allowed the description of dozens of bacterial species exhibiting antagonist activities against microorganisms of biomedical interest such as *Bacillus subtilis, Listeria monocytogenes, Staphylococcus aureus* and *Candida albicans* (Nuñez-Montero and Barrientos 2018). A large variety of microorganisms belonging to the Actinobacteria, Cyanobacteria, Firmicutes and Bacteroidetes phyla where these activities were found, were isolated from diverse habitats as freshwater, sea water, soils, benthic microbial mats, epilithic habitats, and marine sediments, exhibiting the high potential of this cold desert for the discovery of novel compounds.

Apart from the potential of novel natural products from the hyper-arid Atacama Desert for medical purposes (Sayed et al. 2019, Cortés-Albayay et al. 2019), there is a high interest in biotechnological applications in biomining (Azua-Bustos and González-Silva, 2014), biofuel production (Arias-Forero et al. 2013), anti-biofouling (Leyton et al. 2017) or bioremediation (Martínez et al. 2018).

4.2.1.1. Bioactive compounds with biomedical interest in the Atacama Desert

The screening of bioactive compounds with biomedical interest from microorganisms in the Atacama Desert has particularly focused on strains from the Actinobacteria phylum. However, within the last five years, few works have

explored the potential of and fungal members (Gonçalves et al. 2016) isolated from this extreme desert.

The different studies of bioactive compounds from the Atacama actinobacterial strains led to the discovery of secondary metabolites from diverse chemical classes such as alkaloids, peptides, polyketides, macrolides and terpenes (Rateb et al. 2018). Most of these actinobacterial strains belonged to the *Streptomyces* genus exhibiting both antibiotic and antitumor activities deriving from bioactive compounds (Cortés-Albayay et al. 2019, Rateb et al. 2011, Nachtigall et al. 2011, Leirós et al. 2013, Schulz et al. 2011, Abdelkader et al. 2018). Genomic studies of some of those isolates revealed the potential synthesis of many novel specialized metabolites and the presence of stress-related genes that provided an insight into how these organisms deal with extreme environmental conditions on their habitats (Busarakam et al. 2016; Carro et al. 2019).

Concerning the bioactive potential of cyanobacterial members inhabiting the Atacama Desert, the main interest has focused on the UV-screening compound scytonemin (Vítek et al. 2014a; Chapter 3). The biotechnological interest in this compound lies in its anti-inflammatory effects (D'Orazio et al. 2012).

4.2.2. Cyanobacteria as a source of bioactive compounds

Cyanobacteria are characterized by an active secondary metabolism being a source of more than 600 peptidic metabolites (Welker and von Döhren 2006) although the function of many of them remains unknown. Cyanotoxins have received most of the attention so far due to their presence in water bodies with recreational and drinking uses which become a threat for human health (Metcalf and Codd 2012). Furthermore, cyanotoxins have even been found in different extreme environments (Cirés et al. 2017) as hot and cold deserts (Metcalf et al. 2012, Kaasalainen et al. 2012), alkaline lakes (Ballot et al.2004, Nonga et al.

2016), hypersaline environments (Oren 2012; Vishwakarma and Rai 2014), and hot springs (Krienitz et al. 2005, Mohamed 2008).

In addition, cyanobacteria are known to provide a wide range of bioactive compounds possessing antibacterial, antifungal, antialgal and antiviral activities (Dahms et al. 2006, Yadav et al. 2017), most of them produced by members from the orders Nostocales, Stigonematales and Oscillatoriales (Singh et al. 2005). This variety of compounds include alkaloids, lactones, amino acids, peptides, lipopeptides, polyketides and lipids (Mazur-Marzec et al. 2015) produced through nonribosomal peptide synthetases (NRPS) or polyketide synthases (PKS) (Hoffmann et al. 2003). It has been suggested that some of these compounds would constitute an adaptive strategy enabling them to survive in a variety of environmental conditions as they can be involved in interactions with co-occurring organisms (Sønstebø and Rohlrlack, 2011, Sedmak et al. 2008). This phylum has gained attention, since besides its environmental significance, they also display a potential application in biotechnology especially due to their exclusive properties such as low-cost growth requirement, short generation time and ease of genetic manipulation (Yadav et al. 2017) and the unique biological activity of these products.

Most of the studies screening for bioactive compounds have focused on freshwater strains (Mejean and Ploux 2013, Micallef et al. 2014) or marine strains (Szubert et al. 2017, Mazur-Marzec et al. 2015, Chang et al. 2004) while terrestrial strains have hardly been studied with this purpose (Liaimer et al. 2015). Moreover, the synthesis of bioactive compounds by cyanobacteria from extreme environments remains unexplored.

Despite the increasing research efforts on the screening of microorganisms inhabiting extreme environments and cyanobacteria as sources of novel bioactive compounds, a very limited number of studies can be found regarding

this topic. Few Antarctic strains from *Pseudophormidium, Phormidium, Leptolyngbya* and *Nostoc* genera have been described to display some bioactivity (Asthana et al. 2009, Biondi et al. 2008).

This chapter aims to explore the potential of cyanobacteria from the polyextreme environment of the Atacama Desert in the actual and potential production of novel bioactive compounds with a biomedical interest. The screening and characterization of the activity of secondary metabolites extracted from cyanobacterial strains isolated from endolithic habitats has been conducted for the first time. For that purpose, a multidisciplinary approach has been applied using a series of bioassays, liquid chromatography tandem mass spectrometry (LC-MS/MS) and genomic tools following the steps involved in the culture-dependent discovery of natural products: (i) the selection of environmental samples, (ii) a selective isolation and generation of microbial strain libraries. (iii) the screening of the biosynthetic potential of strains (iv) the preparation of extracts of selected isolates and (v) the structural determination of drug leads and biological testing of purified compounds (Sayed et al. 2019).

4.3. Experimental Procedures

4.3.1. Culture organisms and conditions

Four cyanobacterial strains isolated from different lithic substrates and endolithic microhabitats in the Atacama Desert were tested in this study (Table 4.1). Three *Chroococcidiopsis* strains: YU-2, CVL, and IGM; and one *Gloeocapsopsis* strain: GCL. All four strains were grown in 500 mL Erlenmeyer flasks with 300 mL BG11-medium (Rippka et al. 1979) at 28°C and under continuous white light illumination of 35 µmol photons m^{-2} s^{-1} continuously shaken at 135 rpm.

Table 4.1. Features of strains used in this study.

Strain	Genus	Endolithic Microhabitat	Substrate	Sampling site
YU-2	*Chroococcidiopsis*	Cryptoendolithic	Halite	Yungay
CVL	*Chroococcidiopsis*	Chasmoendolithic	Calcite	Valle de la Luna
IGM	*Chroococcidiopsis*	Cryptoendolithic	Ignimbrite	Monturaqui
GCL	*Gloeocapsopsis*	Chasmoendolithic	Gypcrete	Monturaqui

4.3.2. Extraction and fractionation of cyanobacterial strains

Cyanobacterial biomass from the four cyanobacterial strains was harvested after from the culture 4 weeks during 5 months, in the mid exponential growth phase, in order to reach freeze-dried biomass between 1.5-2 g. The lyophilized biomass was then extracted with 75% methanol (20 mL) by vortexing for 10 min, followed by 10 min bath sonication. Then, the extract was centrifuged (10,000 x *g*) for 10 min. The obtained supernatant was dissolved in water, so that the methanol content did not exceed 15%. The sample was loaded onto the 10-[g] SPE cartridge (Sep-Pak; C18 cartridge, Waters, Milford, USA). The cartridge was first washed with MilliQ water and then the sorbed substances were eluted with aqueous solutions of methanol, gradually increasing the strength of the eluent from 0% to 100%, at 10% step. The collected fractions were evaporated to dry residue.

4.3.3. Screening for enzyme inhibitors

Compounds able to deregulate activity of proteases can find application in the treatment of several metabolic disorders, such as urticaria, contact dermatitis, asthma, inflammatory bowel disease, blood clogging, neurological disorders or cancer (Patel 2017; Sapio and Fricker 2014). Thus, crude extracts from the four cyanobacterial strains were screened for enzyme inhibitors against four serine proteases (chymotrypsin, trypsin, elastase, and thrombin) since they are found ubiquitously in both eukaryotes and prokaryotes. For each extract serial dilutions (1:1, 1:10, 1:100, 1: 1,000 and 1: 10,000) and the solutions of inhibitors

were prepared in MilliQ water. The assays were conducted in 96-well microplates; absorbance was measured using microplate reader: Varioskan Flash (Thermo Scientific).

4.3.3.1. Trypsin inhibition assay

Trypsin from porcine pancreas (T0303), the inhibitor aprotinin (A6103) and the substrate (Nα-benzoyl-L-arginine 4-nitroanilide hydrochloride BAPNA, B4875) were purchased from Sigma-Aldrich (St. Louis, USA). Trypsin (0.2 mg mL^{-1}) was dissolved in buffer solution (50 mM Tris-HCl, 100 mM NaCl, 1 mM CaCl2, pH 7.5) and BAPNA in 100% DMSO (2 mM). Solutions of inhibitor within the range between 2.5 – 100 μg mL^{-1} were prepared. The mixtures containing MilliQ water (negative control) or the sample (10 μL) or inhibitor (10 μL), enzyme (10 μL) and buffer (100 μL) were preincubated for 5 min at 36°C. Then, the substrate solution (100 μL) was added. The absorbance was measured at 405 nm after 10 and 20 min.

4.3.3.2. Chymotrypsin inhibition assay

Chymotrypsin (C4129), the inhibitor aprotinin (A6103) and the substrate Suc-Gly-Gly-p-nitroanilide (S1899) were purchased from Sigma-Aldrich (St. Louis, USA). Chymotrypsin (0,2 mg mL^{-1}) was dissolved in buffer solution (50 mM Tris-HCl, 100 mM NaCl, 1 mM $CaCl_2$, pH 8), the substrate in 100% DMSO (2 mM). Solutions of inhibitor within the range between 1.5 – 100 μg mL^{-1} were prepared. The mixtures containing MilliQ water (negative control) or the sample (10 μL) or inhibitor (10 μL), enzyme (10 μL) and buffer (100 μL) were preincubated for 5 min at 36°C. Then, the substrate solution (100 μL) was added. The absorbance was measured at 405 nm after 10 and 20 min.

4.3.3.3. Thrombin inhibition assay

Thrombin from bovine plasma (T4648), the inhibitor 4-(2-aminoethyl) benzenesulfonyl fluoride hydrochloride-AEBSF (A8456) and the substrate, N-p-

tosyl-Gly-Pro-Lys-p-nitroanilide acetate salt (T6140) were purchased from Sigma-Aldrich. Thrombin (0.5 mg mL^{-1}) was dissolved in the buffer (Tris-HCL 0.2 M, pH 8), and the substrate was dissolved in 100% DMSO (2mM). Solutions of inhibitor within the range between 60 – 2400 μg mL^{-1} were prepared. To each microplate well MilliQ water (negative control) or the sample (10 μL) or inhibitor (10 μL, 24–600 μg mL^{-1}), thrombin (10 μL) and buffer (170 μL) were added and preincubated at 36°C for 10 min after which the substrate solution (20 μL) was added. The absorbance was measured at 405 nm after 3 and 10 min.

4.3.3.4. Elastase inhibition assay

Elastase from porcine pancreas (E0258), the inhibitor elastatinal (E0881) and the substrate N-succinyl-AlaAla-Ala-p-nitroanilide (S4760) were purchased from Sigma Aldrich. Elastase (0,75 mg mL^{-1}) was dissolved in the buffer (Tris-HCL 0.2 M, pH 8), and the substrate was dissolved in MilliQ water (0.5 mg mL^{-1}). Solutions of inhibitor within the range between 5 – 200 μg mL^{-1} were prepared. To each microplate well MilliQ water (negative control) or solutions of the cyanobacterial extract (10 μL) or inhibitor (10 μL), enzyme (10 μL) and buffer (150 μL) were added and preincubated at 36°C for 20 min. Then, 30 μL of substrate solution was added to start the reaction. After 5 and 10 min, absorbance was measured at 405 nm.

4.3.4. Antibacterial activity

4.3.4.1. Agar diffusion assay

Crude extracts from the four cyanobacterial strains were used in the agar diffusion assay to test antibacterial activity. Bacterial strains carrying antibiotic-resistance genes (see Table 4.4) are preserved in the Culture Collection of Northern Poland in 50% glycerol (- 80 °C). From freeze cultures bacteria were recovered by streaking on Mueller Hinton Agar (Sigma Aldrich). After 24 h of incubation at 37 °C (STL B50 incubator, POL-EKO) bacteria were transferred to liquid Mueller Hinton Medium (Sigma-Aldrich). After incubation for the next

24h (37°C, 200rpm), bacteria were again transferred to fresh Mueller Hinton Broth. In the test, bacterial cultures were prepared in such a way that the turbidity of cell suspensions was adjusted to an equivalent 0.5 McFarland standard as measured by absorbance (0.08–0.1 at 625 nm). The absorbance was measured using microplate reader (Versa Max Microplate Reader, Molecular Devices). Agar disc diffusion assay was done in accordance with the EUCAST standard, version 5.0 (European Committee on Antimicrobial Susceptibility Testing). Briefly, Sterilized Whatman® filter paper discs (6 mm diameter) (Sigma-Aldrich, St. Louis, Missouri, USA) were saturated with the cyanobacterial extract (50 µg/disc) and placed on Mueller Hinton II Agar (Becton Dickinson, Loveton Circle, Maryland, USA) plates seeded with a lawn of the tested microorganism. Positive controls (streptomycin, trimethoprim, chloramphenicol, methicillin, amphotericin B at 5 mg mL^{-1}) and negative control (water) were run simultaneously. After 24 h incubation at 37°C, the diameter of the inhibition zone was measured.

4.3.4.2. Broth microdilution procedure

Combinations of fractions with the same compounds were used for the broth microdilution assay in order to test their antibacterial activity. Antibacterial assays were performed following the guidelines of the Clinical and Laboratory Standards Institute (CLSI) (2012) and European Committee on Antimicrobial Susceptibility Testing (EUCAST) (http://www.eucast.org). The bacterial strains were precultured in Mueller Hinton II Broth (Becton Dickinson) at 37°C for 16–20 h at 100 rpm. At the beginning of the experiment the density of the culture was 5×10^5 CFU mL^{-1}. Bacterial cultures were incubated in the presence of cyanobacterial SPE fractions at concentrations of 0.1 mg mL^{-1} for 24 h (n=3). Assay plates were incubated for 24 h at 37°C, then optical density was measured at 620 nm. For all microbial strains used in the broth microdilution assay, growth stimulation effects were considered to be significant if the absorbance of the

treated culture was at least 50% higher than in the control (untreated) culture (Mazur-Marzec et al. 2015). Growth inhibition effect was considered significant if absorbance of the treated culture was at least 30% lower than that of the control. Otherwise, effects were considered to be non-significant (Mazur-Marzec et al. 2015).

4.3.5. Cytotoxic activity

Human breast adenocarcinoma cell line was obtained from CLS Cell Lines Service GmbH (Eppelheim, Germany). Monolayer cultures of T47D cells were maintained in RPMI 1640 medium supplemented with 10% (v/v) fetal bovine serum and 1% antibiotics mixture (penicillin and streptomycin). Cells were incubated at 37°C in CO_2 (5%) incubator (New Brunswick Galaxy 170s, Eppendorf, Germany). Cell viability was determined by MTT method as described by Felczykowska et al. (2015). For this purpose, T47D cells were seeded at a density of 4 x 10^3 (for 24 hours) and 2x10^3 (for 72 hours) per well of 96-well plate and allowed to attach overnight. Next, the medium was replaced with a fresh portion of medium containing cyanobacterial extracts at the following concentrations 25, 50, 100 and 200 µg mL^{-1}. Then, 100 µl of MTT solution (4 mg mL^{-1}) were added to each well. After 2h of incubation, the medium was removed and formazan was dissolved in 100 µL of added DMSO. The absorbance of the reaction mixtures was measured at 570 nm (with reference wavelength 660 nm) with a microplate reader. Data from three independent experiments were collected. In MTT assay, cell viability drop below 50% of control was considered as significant.

4.3.6. Mass spectrometry analysis

LC-MS/MS analyses were performed on an Agilent 1200 (Agilent Technologies, Waldboronn, Germany) coupled with a triple-quadrupole mass spectrometer (5500 QTRAP, AB Sciex, Concord, ON, Canada). Sample compounds were separated on a Zorbax Eclipse XDB-C18 column (4.6 mm × 150 mm; 5 µm)

(Agilent Technologies, Santa Clara, CA, USA) with a mobile phase composed of 5% acetonitrile in MilliQ water (A) and acetonitrile (B), both containing 0.1% formic acid. The flow rate was 0.6 Ml min^{-1}, and the injection volume was 5 µL. The column temperature was 35°C. The conditions of gradient elution are shown in Table 2. Mass spectrometer was operated in positive mode, with turbo ion spray (550°C) voltage 5.5 kV and declustering potential of 80 V. Two types of MS/MS experiments were performed. In the first step, the information dependent acquisition method (IDA) was used and fragmentation spectra of all ions with m/z (mass to charge) in a range 500–1250 and signal above the threshold of 500,000 cps were collected. The rough estimation of the relative amount of peptides in the extract was performed based on the intensity of the signal in extracted ion chromatogram. For selected ions, enhanced ion product mode (EIP) was used at a collision energy (CE 60 V) optimized in order to get the richest ion fragmentation spectrum. Data acquisition and processing were accomplished using Analyst QS® 1.5.1 software.

4.3.7. antiSMASH analysis of the genome

Genomic DNA from all four cyanobacterial strains was subjected to paired-end Illumina HiSeq sequencing (Johns Hopkins Genetic Resources Core Facility) after creating a library using KAPA HyperPlus (KAPA Biosystems). Raw reads were quality trimmed with TrmGalore, after quality filtering, library contained over 7.6 Gbp of sequences. Resulting pairs were processed with the MetaWrap pipeline (Uritskiy et al. 2018). The detailed features of the four cyanobacterial genomes are presented in Table 4.2.

To analyze the putative secondary metabolite gene clusters in all four genomes, the Antibiotics and Secondary Metabolite Analysis Shell antiSMASH 4.0 (Blin et al. 2017) software was used with its default parameters.

Table 4.2. Genomic features of four cyanobacterial strains in the study. N50: median contig size the genomic assembly. CDSs: coding sequences

Genome Feature	Cyanobacterial Strain			
	***Chroococcidiopsis* YU-2**	***Chroococcidiopsis* CVL**	***Chroococcidiopsis* IGM**	***Gloeocapsopsis* GCL**
Contigs	175	324	166	356
Total bases	5,957,924	5,884,528	5,741,744	5,738,043
N50	63,683	32,524	60,020	26,980
G+C% average	46.3	46.3	46.3	42,5
Completeness / Contamination (%)	99.48 / 1.93	98.88 / 1.55	99.25 / 2.07	98.66 / 1.3
CDSs	6,412	6,465	6,179	5,802
tRNA genes	36	37	36	35
rRNA genes	8	7	8	7

4.4. Results

4.4.1. Activity of crude extracts

4.4.1.1. Inhibition of enzyme activity

No inhibitory activity of SPE fractions against proteases was found using trypsin, chymotrypsin, thrombin and elastase at the tested concentrations for any of the cyanobacterial crude extracts (Table 4.3).

Table 4.3. Inhibition of serine proteases by crude extracts from cyanobacterial strains from the Atacama Desert. Results are mean of tests done in triplicate; "-" no effect observed. Table summarizes results obtained in serial dilutions (1:1, 1:10, 1:100, 1:1,000 and 1:10,000)

Cyanobacterial strain	Activity			
	Trypsin	Chymotrypsin	Thrombin	Elastase
Chroococcidiopsis YU-2	-	-	-	-
Chroococcidiopsis CVL	-	-	-	-
Chroococcidiopsis IGM	-	-	-	-
Gloeocapsopsis GCL	-	-	-	-

4.4.1.2. Antibacterial activity

Crude extracts showed no antibacterial activity for the gram negative drug resistants Proteobacteria *Klebsiella oxytoca* WW-D 55, *Enterobacter cloacae* PP-VR 3073, *Citrobacter freundii* MW-D 2210 B and *Escherichia coli* ESBL MW-W 727 at tested concentrations (Table 4.4). However, weak antibacterial activity (inhibition zones ranged 2-4mm) was observed for the gram negative drug resistant *Enterococcus durans* 66 and the gram positive *Enterobacter* sp. MW-W 814 by the highest concentrations of CVL, IGM and GCL crude extracts (Table 4.4). Weak activity was found for the gram positive Proteobacteria *Vibrio cholerae* 01 MW D 2329 by YU-2 crude extract, too.

Table 4.4. Antibacterial activity of crude extracts from cyanobacterial strains from the Atacama Desert; "+" weak bacterial growth inhibition; "-" no effect.

Bacterial strain	Cyanobacterial strain / extract concentration (mg mL^{-1})							
	Chroococcidiopsis YU-2		*Chroococcidiopsis* CVL		*Chroococcidiopsis* IGM		*Gloeocapsopsis* GCL	
	1	0.1	1	0.1	1	0.1	1	0.1
Enterococus durans 66	-	-	+	-	+	-	+	-
Vibrio cholerae 01 MW-D 2329	+	-	-	-	-	-	-	-
Klebsiella oxytoca WW-D 55	-	-	-	-	-	-	-	-
Enterobacter sp. MW-W 814	-	-	+	-	+	-	+	-
Enterobacter cloacae PP-VR 3073	-	-	-	-	-	-	-	-
Citrobacter freundii MW-D 2210 B	-	-	-	-	-	-	-	-
Escherichia coli ESBL MW-W 727	-	-	-	-	-	-	-	-

Microdilution assays performed for Escherichia *coli* ESBL MW-W 727 (Supp. Mat. 4.1) using crude extracts in a range of concentrations between 0.002 and 1.25 mg mL^{-1} revealed a very weak activity when maximum concentration was applied (80% relative viability). On the other hand, the microdilution assays performed for *Pseudomonas aeruginosa* exhibited no antibacterial activity (Supp. Mat. 4.1).

4.4.2. LC-MS/MS analysis of SPE fractions

The content of the active fractions was analyzed with LC-MS/MS system optimized for the detection of peptides. The m/z values, retention time and a peak area of the detected ions were determined for each cyanobacterial strain (Tables 4.5, 4.6, 4.7, 4.8). For the most intensive peaks the product ion spectra were collected (Supp. Mat. 4.2) and putative compounds were assigned for m/z values when possible (Supp. Mat. 4.3).

No ions were detected in fractions 50, 70 and 100 from the YU-2 extract (Table 4.5). Besides that, a total of 18 ions were detected and those found in highest concentration were eluted in fraction 0 characterized by m/z at 457 and 527, found also in the same fraction of IGM extract. Other highly present ions were those characterized by m/z at 673 (in fractions 0 and 10),1057 (in fraction 90) and 506 (in fraction 80); last two were only detected in the YU-2 extract.

Table 4.6 exhibits ions detected in SPE fractions of the CVL extract where the lowest number of ions was detected, a total of 10 among all SPE fractions. In fractions 10, 20, 30, 60 and 100 no ions were detected. As it happened in the YU-2 extract, ions in highest concentrations were found in fraction 0, characterized by m/z at 834 and 674, both ions only detected in the CVL extract. Other ions found in high concentrations were those characterized by m/z 527 (in fraction 70), also found in the IGM extract, 689 (in fraction 0), found also in the same

fraction in the IGM extract, and 558 (in fraction 80) which was only detected in the CVL extract.

Table 4.5. Characteristics of ions detected by LC-MS/MS in *Chroococcidiopsis* YU-2 strain SPE fractions.

Fraction	Retention time (min)	m/z	Peak area of extracted ion
0	2.7	457	2.01×10^{10}
	2.7	527	2.01×10^{10}
	3	673	1.41×10^{10}
	3.06	837	5.32×10^{8}
	3.1	997	6.65×10^{8}
	3.1	1013	5.86×10^{8}
10	2.7	673	5.35×10^{9}
	11.8	786	6.37×10^{7}
20	3	478	7.95×10^{9}
30	3.09	677	7.17×10^{8}
	10	1063	5.32×10^{7}
	10.8	1042	3.20×10^{7}
40	3.06	1002	6.27×10^{8}
60	3.09	1067	4.94×10^{8}
	3.1	1128	4.49×10^{8}
	10.8	1106	1.85×10^{8}
80	2.6	506	5.02×10^{9}
90	2.76	1057	8.50×10^{9}

In contrast with the CVL ion content, the highest number of ions of the studied strains was detected in IGM SPE fractions, a total of 31 ions (Table 4.7). Also, the IGM extract was the only one where ions could be detected in every SPE fraction. Twelve ions distributed in four main SPE fractions were detected in high concentrations in the IGM extract (Table 4.7). Notably, the ion characterized by m/z at 420, only detected in the IGM extract, eluted in fractions 60, 70, 80, 90 and 100 in high concentrations. Other ions were found eluted in more than one SPE fractions: m/z 527 (in fractions 60 and 70), found as well in fraction 70 from

the CVL extract; 673 (in fraction 0 and 10) also detected in fractions 0 and 10 from the YU-2 and GCL extracts; 1041 (in fractions 20 and 30) found in fraction 30 of the YU-2 extract as well, and 786 (fractions 40 and 50) found in the same SPE fractions of the CVL extract. In the SPE fractions of IGM, a double-charged ion was detected in high concentration characterized by a m/z at 339/677 (fraction 60), also detected in fraction 50 of the GCL extract.

Table 4.6. Characteristics of ions detected by LC-MS/MS in *Chroococcidiopsis* CVL strain SPE fractions.

Fraction	Retention time (min)	m/z	Peak area of extracted ion
0	2.6	834	9.38×10^{9}
	2.9	674	9.38×10^{9}
	3	689	1.40×10^{9}
40	11.8	786	6.66×10^{7}
50	11.2	1106	1.62×10^{8}
	12.3	786	4.53×10^{8}
70	2.7	527	9.27×10^{9}
80	2.7	558	5.11×10^{9}
90	10.6	1041	5.89×10^{8}
	11.2	1106	1.86×10^{8}

During the LC-MC/MS analysis of the SPE fractions of the GCL extract 25 ions were detected (Table 4.8), although fractions 40, 70 and 100 exhibited no ions. The GCL extract contained 3 different doubly charged ions found in high concentrations characterized by m/z at 511/349 and 457/365 in fraction 0, only detected in the GCL extract, in addition to the previously mentioned doubly charged ion found also in the IGM extract at 339/677 in fraction 50. There was one more ion found in high concentration and only present in GCL extract, characterized by m/z 422 in fraction 30.

Table 4.7. Characteristics of ions detected by LC-MS/MS in *Chroococcidiopsis* IGM strain SPE fractions

Fraction	Retention time (min)	m/z	Peak area of extracted ion
0	1.6	573	3.79×10^{9}
	1.7	937	3.79×10^{9}
	2.2	725	3.84×10^{9}
	2.7	457	1.97×10^{10}
	2.7	527	1.97×10^{10}
	2.9	673	1.97×10^{10}
	3	689	1.53×10^{10}
	3.1	835	1.53×10^{10}
10	2.7	673	5.87×10^{9}
20	10.4	1041	3.89×10^{7}
30	10.6	1041	1.57×10^{7}
40	12	786	2.00×10^{7}
50	1.7	839	3.30×10^{9}
	2.4	871	1.10×10^{8}
	11.7	786	1.18×10^{7}
60	2.69	420	1.98×10^{10}
	2.7	527	1.98×10^{10}
	3	339/677	1.98×10^{10}
70	2.65	420	5.88×10^{9}
	3	527	1.07×10^{10}
80	2.6	420	1.72×10^{10}
	2.8	515	1.72×10^{10}
	3.3	1113	1.72×10^{10}
90	2.6	420	8.35×10^{9}
	2.7	499	8.35×10^{9}
	2.9	407	9.29×10^{9}
	2.9	472	9.29×10^{9}
100	2.7	420	1.54×10^{10}
	2.8	438	1.54×10^{10}
	3	1149	1.54×10^{10}
	10.7	454	9.17×10^{7}

Table 4.8. Characteristics of ions detected by LC-MS/MS in *Gloeocapsopsis* GCL strain SPE fractions

Fraction	Retention time (min)	m/z	Peak area of extracted i-on
0	2.7	511/349	1.21×10^{10}
	2.7	457/365	1.21×10^{10}
	3	673	1.15×10^{10}
	3	837	1.15×10^{10}
10	2.5	871	6.77×10^{9}
	2.7	511	6.77×10^{9}
	2.7	673	6.77×10^{9}
	2.9	402	6.00×10^{9}
	3	835	6.00×10^{9}
	3	997	6.00×10^{9}
	11.3	786	6.09×10^{7}
20	1.7	1074	2.40×10^{9}
	2.3	1099	7.04×10^{7}
	2.7	483	7.13×10^{9}
	2.9	402	6.88×10^{9}
	3	403	6.88×10^{9}
	10.9	1099	1.31×10^{7}
	11	1100	2.71×10^{7}
	11.2	1094	3.97×10^{7}
30	3.1	422	1.09×10^{10}
	10.3	1042	5.79×10^{7}
50	3	339/677	7.39×10^{9}
60	2.7	622	4.41×10^{9}
80	1.75	839	3.22×10^{9}
	3.1	538	2.90×10^{8}

A Venn diagram was created revealing the number of unique and shared ions between the different cyanobacterial strains extracts (Fig. 4.1). Out of the 51 different detected ions among the SPE fractions, only 1 was shared by all cyanobacterial strains, characterized by m/z 786 (Supp. Mat. 4.4). This shared ion was found in SPE fraction 10 from *Chroococcidiopsis* YU-2 sp. (Table 4.5) and

Gloeocapsopsis sp. GCL (Table 4.8), whereas it was found in SPE fractions 40 and 50 from *Chroococcidiopsis* sp. CVL (Table 4.6) and IGM (Table 4.7).

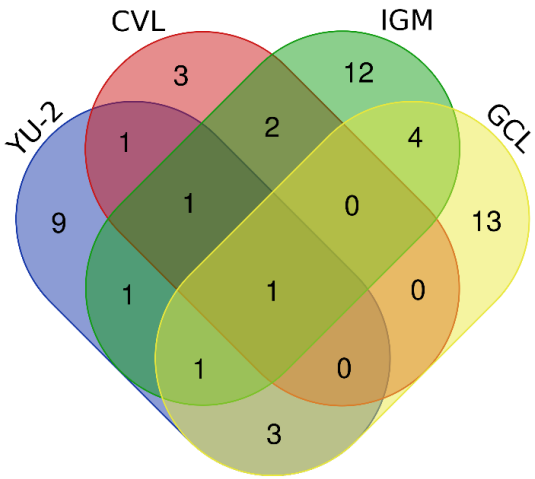

Figure 4.1. Venn diagram of shared and unique detected ions among *Chroococcidiopsis* strains YU-2, CVL, IGM and *Gloeocapsopsis* GCL strains.

The distribution of these shared ions was studied regarding different features (Table 4.1): cyanobacterial genus (*Chroococcidiopsis* or *Gloeocapsopsis*), type of endolithic microhabitat of origin (cryptoendolithic or chasmoendolithic), and original sampling site (Monturaqui IGM and GCL). A first look at each strain on the Venn diagram (Fig.4.1) reveals a remarkable lower number of compounds in the CVL strain (*Chroococcidiopsis* from chasmoendolithic microhabitat), which owned only 3 unique ions characterized by m/z 558, 834 and 647 (Supp. Mat. 4.4), the former one putatively assigned to aeruginosamide C (Supp. Mat. 4.3). In contrast, strains originally from the Monturaqui region, IGM and GCL, exhibited the highest number of compounds along with the highest number of unique ions (12 and 13 respectively). Regarding the genera distribution, the *Chroococcidiopsis* sp. strains shared only one more ion apart from the previously mentioned with m/z 786 (Fig. 4.1). This one is characterized by m/z 527 (Supp. Mat. 4.4) and occurs in high abundance in all of these *Chroococcidiopsis* extracts

(Table 4.5, Table 4.6, Table 4.7). However, no possible *Gloeocapsopsis* assignment could be done due to the absence of several strains from this genus. Concerning the endolithic microhabitat, no shared ions were detected in the chasmoendolithic strains (CVL and GCL), with exception of the one shared with the YU-2 and IGM strains (Fig. 4.1), whereas cryptoendolithic strains (YU-2 and IGM) shared one more highly abundant ion characterized by m/z 457 in SPE fraction 0 (Table 4.5, Table 4.7). The cyanobacterial strains isolated from substrates located in the same sampling site, IGM and GCL, shared the highest number of ions (Fig. 4.1). Four ions were found exclusively in both strains: the double charged ion characterized by m/z 339/677 and ions characterized by m/z 835, 839 and 871 (Supp. Mat. 4.4).

At this point, in order to obtain enough mass to perform the following analyses in triplicates, SPE fractions from each cyanobacterial crude extract were combined as follows: YU-2 (0-10, 20-40, 50-60, 70-100), CVL (0-10, 20-30, 40-50, 60-70, 80-100), IGM (0-10, 20-50, 60-70, 80-100) and GCL (0-10, 20-30, 40-60, 70-100).

4.4.3. Activity of combined SPE fractions

4.4.3.1. Antibacterial activity

During the agar disk diffusion assay with cyanobacterial crude extracts, three antibiotic resistant bacterial strains showed weak inhibition (Table 4.4). Thus, these three strains were further studied in broth microdilution assay against the combined SPE fractions from cyanobacterial extracts.

No activity was detected against *Vibrio cholerae* 01 MW-D 2329 and *Enterobacter* sp. MW-W 814 strains (Fig. 4.3 and Fig. 4.4). These results obtained for every SPE fraction were supported by their high replicability.

In contrast with the previous results observed for the two bacterial strains, weak activity could be observed by some SPE fractions from every cyanobacterial strains for the antibiotic resistant *Enterococcus durans* 66 (Fig. 4.2). The activity shown by several combined SPE fractions among all cyanobacterial strains extracts exhibited large SD. Therefore, the absence of replicability of those results does not allow their consideration. That is the case of fraction 0-10 from the YU-2 extract, 20-50 and 80-100 fractions from the IGM extract and 40-60 and 70-100 fractions from the GCL extract, where SD exceeded 20.

YU-2 fractions, except for 0-10, showed antibacterial activity (Fig. 4.2), especially observed for fraction 20-40 which promoted a mean relative viability of *Enterococcus durans* 66 cells of 28%. In general, CVL fractions revealed the greatest antibacterial activity, where fractions 20-30, 40-50, 60-70 and 80-100 inhibited viability in *Enterococcus durans* 66 cells up to 29-36%. IGM fractions exhibited similar mean antibacterial activity through 0-10 and 60-70 SPE fractions, ~56%, lower than the observed in the most active CVL and YU-2 fractions. Finally, 20-30 SPE fraction from the GCL extract exhibited a strong antibacterial activity, similar to that observed in the strongest CVL and YU-2 fractions, causing a 34% relative viability in *Enterococcus durans* 66 cells. Very weak antibacterial activity was also observed in fraction 0-10 of the GCL extract, 58%, similar to the one previously described for the IGM fractions and the 0-10 CVL fraction.

4.4.3.2. Cytotoxicity against human breast cancer cells

MTT viability test was used to evaluate the cytotoxic activity of combined SPE fractions from cyanobacterial extras toward the T47D human breast cancer cell line. A range of different cytotoxic effects from weak to strong was observed in all SPE fractions from every cyanobacterial extract (Fig. 4.5 and Fig. 4.6) exhibiting a consistent concentration-dependent effect except for the 70-100 fraction from the GCL extract (Fig. 4.6).

The 70-100 combined fraction from the YU-2 extract showed the highest activity in decreasing T47D cells viability, with IC_{50} value 50 μg mL^{-1} (Fig. 4.5). The cytotoxic activity of the CVL extract was shown by the combined fraction 80-100 with IC_{50} value of 50 μg mL^{-1}, exhibiting a concentration-dependent effect (Fig. 4.5). The IGM 80-100 combined fraction exhibited the highest cytotoxic activity against T47D cells, decreasing their viability to 8% at 200 μg mL^{-1} (Fig. 4.6). By contrast, weak cytotoxic activity, not reaching a decrease of 50% in cells viability, was observed in every combined fraction of the GCL extract (Fig. 4.6).

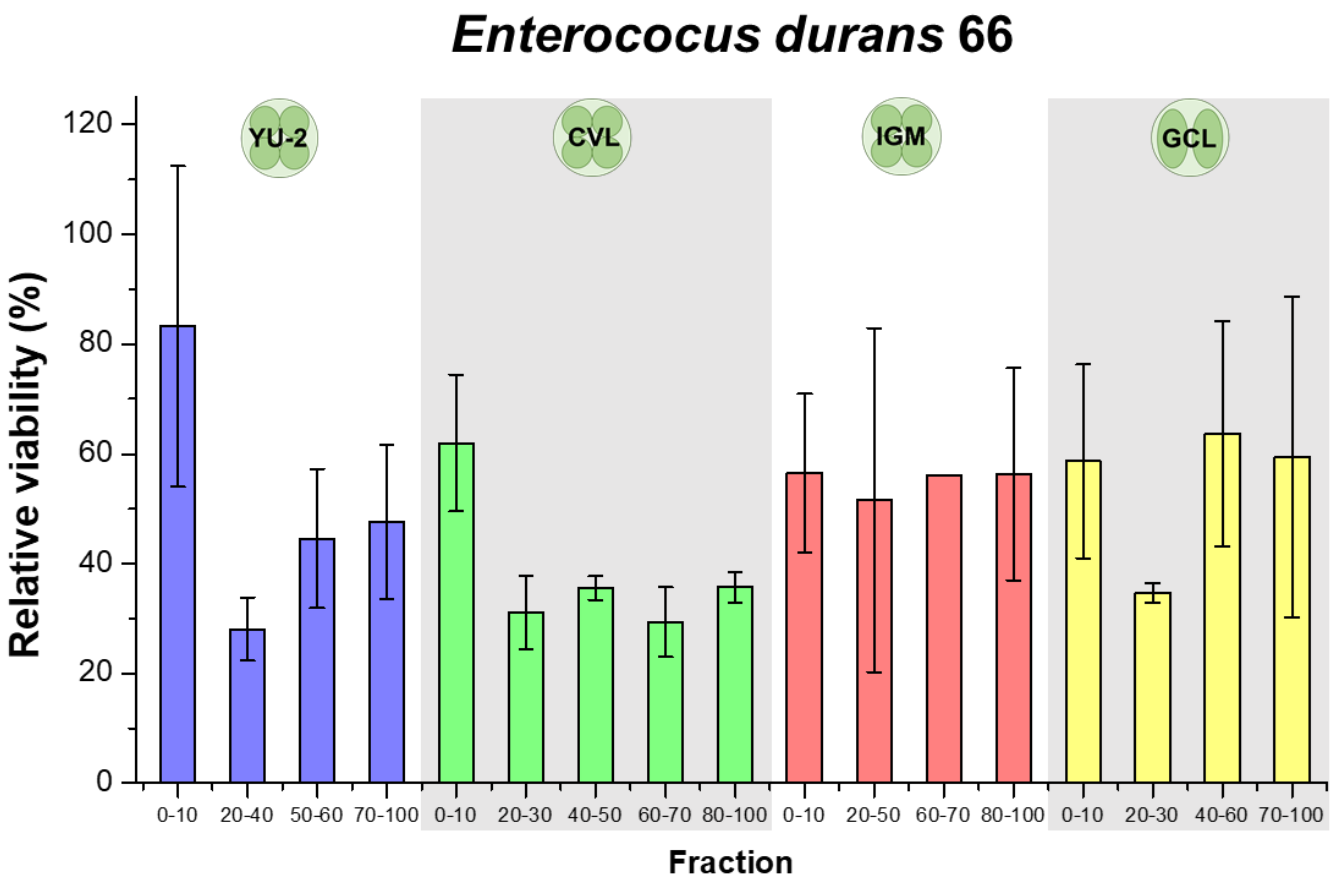

Figure 4.2. The effects of available SPE fractions from cyanobacterial strains extracts on the viability of *Enterococcus durans* 66 antibiotic resistant strain cells. Blue, green, red and yellow bars represent YU-2, CVL, IGM and GCL SPE fractions respectively. Each bar represents a mean (±SD) of two experiments performed in triplicate

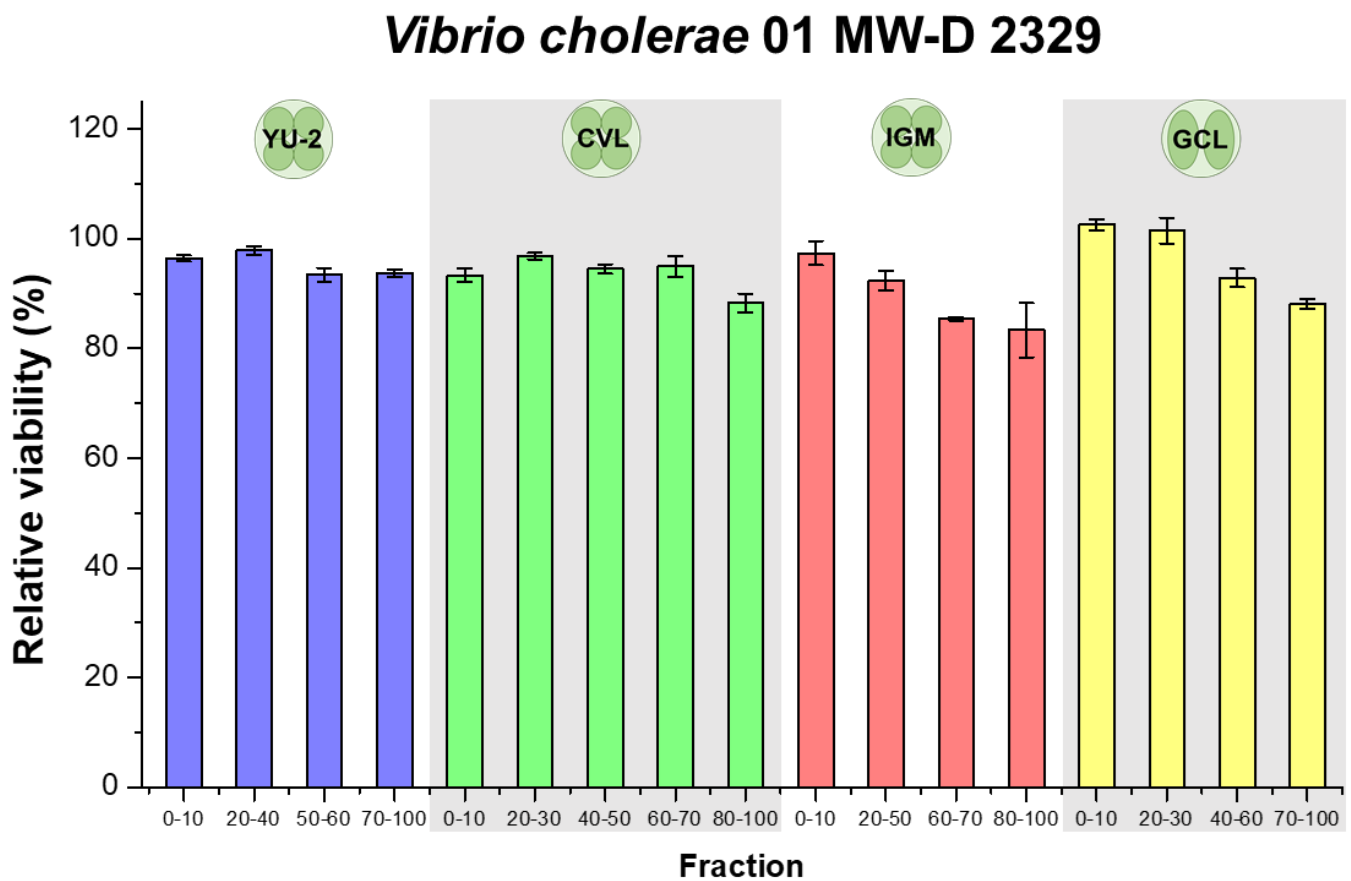

Figure 4.3. **The effects of available SPE fractions from cyanobacterial strains extracts on the viability of *Vibrio cholerae* 01 MW-D 2329 antibiotic resistant strain cells.** Blue, green, red and yellow bars represent YU-2, CVL, IGM and GCL SPE fractions respectively. Each bar represents a mean (±SD) of experiments performed in triplicate.

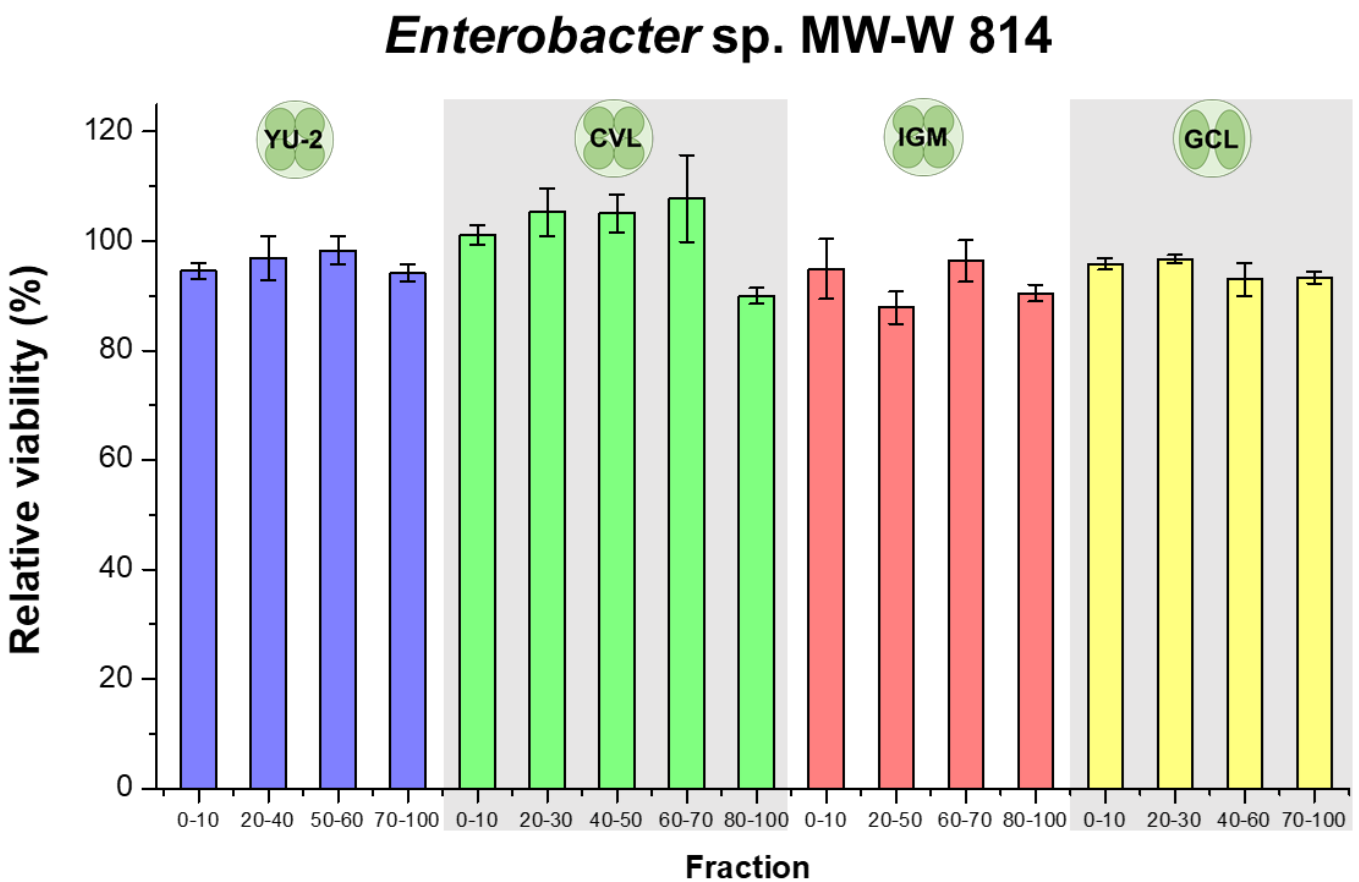

Figure 4.4. The effects of available SPE fractions from cyanobacterial strains extracts on the viability of *Enterobacter* sp. MW-W 814 antibiotic resistant strain cells. Blue, green, red and yellow bars represent YU-2, CVL, IGM and GCL SPE fractions respectively. Each bar represents a mean (±SD) of experiments performed in triplicate.

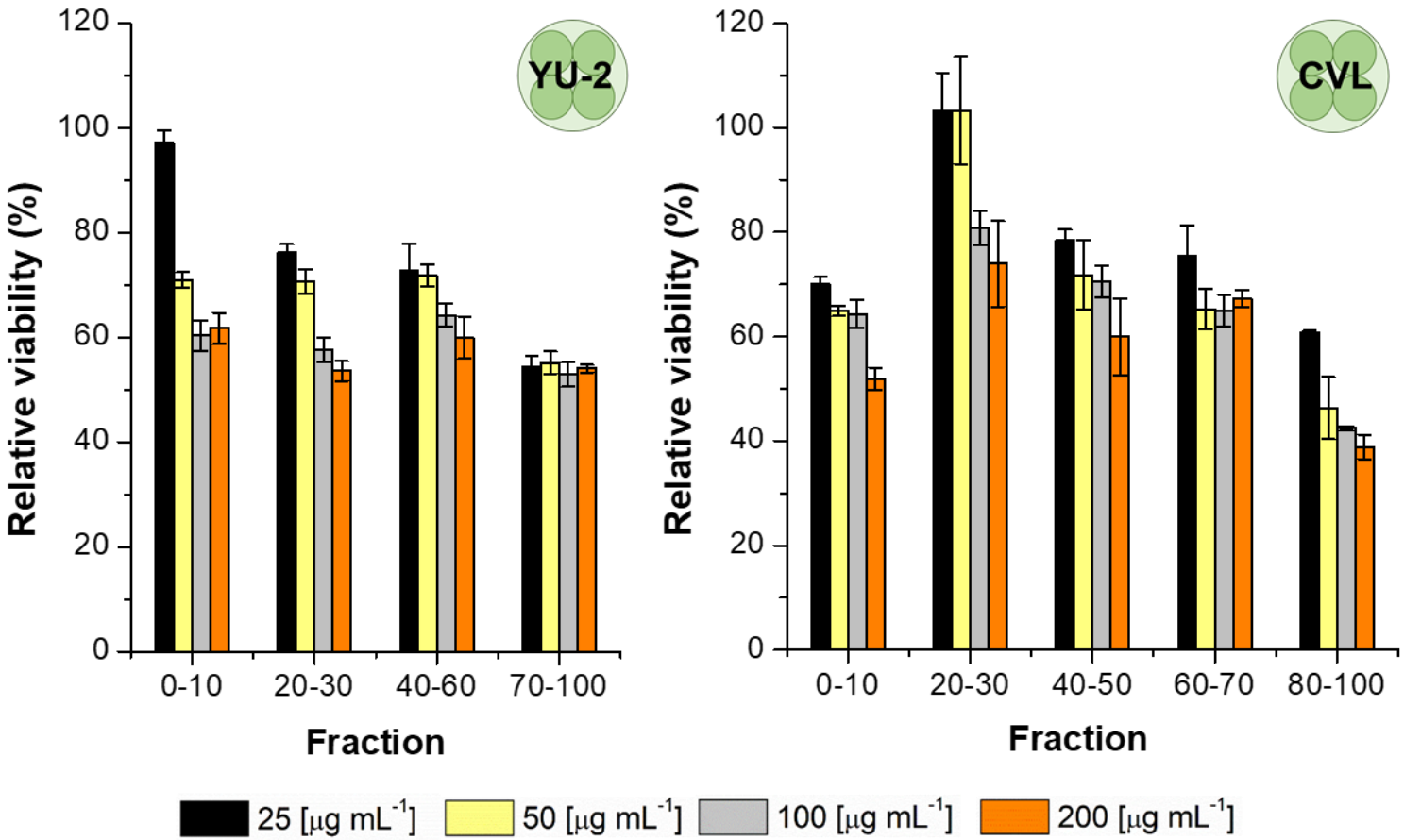

Figure 4.5. The effects of available SPE fractions from *Chroococcidiopsis* strains YU-2 and CVL extracts on the viability of T47D human breast cancer cells. Each bar represents a mean (±SD) of three experiments performed in triplicate.

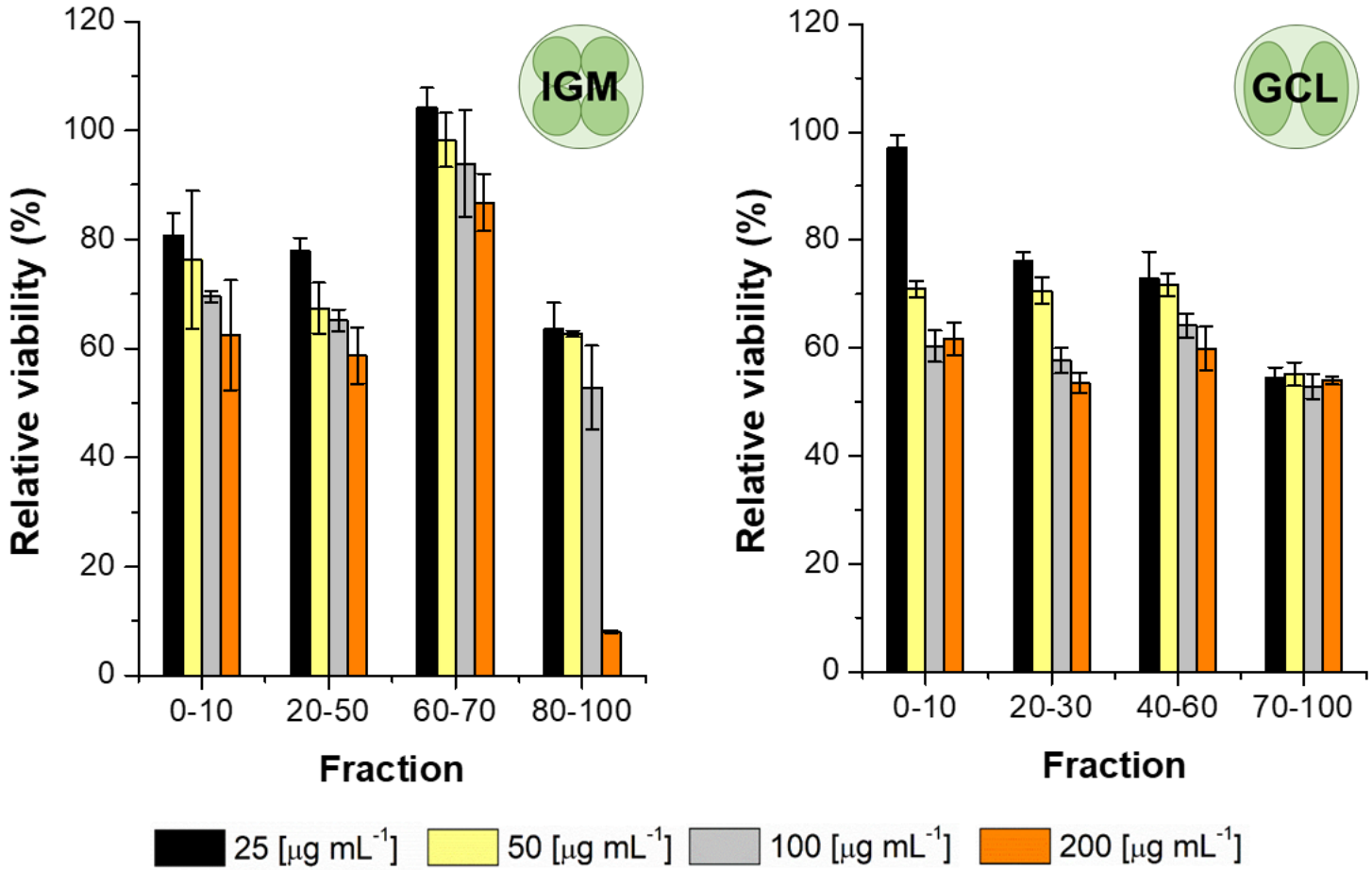

Figure 4.6. The effects of available SPE fractions from *Chroococcidiopsis* IGM strain and *Gloeocapsopsis* GCL strain extracts on the viability of T47D human breast cancer cells. Each bar represents a mean (±SD) of three experiments performed in triplicate.

4.4.4. Prediction of potential bioactive compounds with antiSMASH

To predict gene clusters that encode the biosynthetic pathways for secondary metabolites potentially produced by the *Chroococcidiopsis* strains YU-2, CVL and IGM and the *Gloeocapsopsis* strain GCL, their genomes where analyzed with antiSMASH ver 4.0 (Table 4.9).

The results indicated that the YU-2, CVL and GCL strains harbored 12 gene clusters encoding biosynthetic pathways of secondary metabolites while IGM harbored a lower number of gene clusters, 9 (Table 4.9). At least 4 bioactive metabolites were found to be potentially produced by all four cyanobacterial strains: nostophycin, anabaenopeptin. terpene and bacteriocin. All the *Chroococcidiopsis* strains contained clusters for the production of puwainaphycins, while the *Gloeocapsopsis* GCL strain contained clusters to produce micacocidin and aminoglycoside, and two clusters for merocyclophane C and D.

As shown in Table 4.9, the YU-2 strain was found to be the only studied strain that potentially produces vioprolide and lassopeptide, sharing the theonellamide cluster with the CVL strain and the hapalosin cluster with the *Gloeocapsopsis* GCL strain. The *Chroococcidiopsis* CVL strain was the only studied strain where a cyanopeptolin cluster was found, and together with the *Gloeocapsopsis* GCL strain, that could potentially produce nostopeptolide and micropeptin.

The products of three of the biosynthetic pathways detected by antiSMASH 4.0 could also be assigned as putative compounds based on the ions m/z detected by LC-MS/MS (Supp. Mat. 4.3). On the one hand, despite the fact that cyanopeptolin biosynthetic pathway was only detected in the *Chroococcidiopsis* CVL genome, it was detected as a putative product in extracts from the YU-2 and IGM *Chroococcidiopsis* strains too. In addition, micropeptin was assigned as a putative compound in YU-2 and CVL strains, although its biosynthetic pathway was

detected in CVL and GCL strains. Lastly, two anabaenopeptin variants were assigned based on LC-MS/MS results for YU-2 and GCL strains, while all four strains exhibited biosynthetic pathways for this peptide.

Finally, Tables 4.10-4.13 show the summary of the results for each cyanobacterial strain. These tables (Table 4.10-4.13) exhibit the major ions found in each SPE fraction assigned to a putative compound when possible, together with the activities displayed by each fraction and the biosynthetic pathways found in each genome.

Table 4.9. The information of secondary metabolite biosynthetic gene clusters in *Chroococcidiopsis* strains YU-2, CVL, IGM and *Gloeocapsopsis* strain GCL predicted by antiSMASH ver. 4. Intensity of green means % similarity of genes

			% similar genes					
Cluster type	**Most similar known cluster**	**MIBiG BCG ID**	**YU-2**	**CVL**	**IGM**	**GCL**	**Bioactivity**	**Reference**
NRPS	Nostophycin	BGC0001029	**54 27**	**18**	**54 27**	**27**	Cytotoxic	Fewer et al. 2011
	Cyanopeptolin	BGC0000332		**28**			Protease inhibitor	Tooming-Klunderud et al. 2007
	Anabaenopeptin NZ 857 / nostamide A	BGC0001479	**100**	**100**	**100**		Protease inhibitor	Rouhiainen et al. 2010
	Vioprolide	BGC0001822	**41**				Cytotoxicity	Yan et al. 2018
	Anabaenopaeptin	BGC0000302				**57**	Protease inhibitor	Harms et al. 2016
	Nostopeptolide	BGC0001028		**50**		**50**	Antitoxins	Liaimer et al. 2015
NRPS-T1PKS	Puwainaphycins	BGC0001125	**30**	**20**	**50 30**		Cytotoxic	Mareš et al. 2014
	Hapalosin	BGC0001467	**40**			**60**	MDR- reversing activity	Stratmann et al. 1994b
	Theonellamide	BGC0001800	**21**	**21**				
	Micropeptin	BGC0001018		**50**		**25**	Protease inhibitor	Nishizawa et al. 2011
	Micacocidin	BGC0001014				**20**	Antibacterial	Kobayashi et al. 1998
Polyketide	Merocyclophane C/ D	BGC0001663				**55 55**	Cytotoxic	May et al. 2017
Other	Heterocyst glycolipid	BGC0000869	**57**	**71**	**57**			
Lassopeptide		NA	**X**				Antimicrobial	Hegemann et al. 2015
Terpene		NA	**X**	**X**	**X**	**X**	Antimicrobial /Citotoxicity	Paduch et al. 2016
Bacteriocin		NA	**X**	**X**	**X**	**X**	Antimicrobial	Yang et al. 2014
Aminoglycoside /aminocyclitol		NA				**X**	Antibiotic	Flat and Mahmud 2007
Ladderane		NA			**X**			

Table 4.10. Summary of activities from *Chroococcidiopsis* YU-2 strain in this study. -: no activity, +: very weak activity, ++: weak activity, +++: significant activity, ++++: strong activity. Blue: shared by all cyanobacterial strains. Green: shared exclusively by *Chroococcidiopsis* strains. Red: shared by two Chroococcidiopsis strains. Orange: shared between one *Chroococcidiopsis* and *Gloeocapsopsis* strain. Refs: [1] (Fastner et al. 1999). na: not assigned compound.

YU-2					
SPE fraction	**Major ions (m/z)**	**Putative compound**	**Activity**		**antiSMASH Clusters**
			***Enterococcus durans* 66**	**T47D**	
0-10	457 527 673	na na na	**-**	**+**	Nostophycin Anabaenopeptin NZ 857/nostamide A Terpene Bacteriocin Puwainaphycins Heterocyst glycolipid Theonellamide Hapalosin Vioprolide Lassopeptide
20-40	478 677	na na	**+ +**	**+**	
50-60	1067 1128	MC-WR [1] na	**+ +**	**+**	
70-100	506 1057	na na	**+ +**	**+ +**	

Table 4.11. Summary of activities from *Chroococcidiopsis* CVL strain in this study. -: no activity, +: very weak activity, ++: weak activity, +++: significant activity, ++++: strong activity. Blue: shared by all cyanobacterial strains. Green: shared exclusively by *Chroococcidiopsis* strains. Red: shared by two *Chroococcidiopsis* strains. Orange: shared between one *Chroococcidiopsis* and *Gloeocapsopsis* strain. Refs: [2] (Leikoski et al. 2013). na: not assigned compound.

CVL					
SPE fraction	**Major ions (m/z)**	**Putative compound**	**Activity**		**antiSMASH Clusters**
			***Enterococcus durans* 66**	**T47D**	
0-10	834 674 689	na Aeruginosamide C [2] na	**+**	**+**	Nostophycin Anabaenopeptin NZ 857/nostamide A Terpene Bacteriocin Puwainaphycins Heterocyst glycolipid Theonellamide Micropeptin Cyanopeptolin Nostopeptolide
20-30	-	-	**+ +**	**-**	
40-50	786	na	**+ +**	**+**	
60-70	527	na	**+ +**	**+**	
80-100	558	na	**+ +**	**+ +**	

Table 4.12. Summary of activities from *Chroococcidiopsis* IGM strain in this study. -: no activity, +: very weak activity, ++: weak activity, +++: significant activity, ++++: strong activity. Blue: shared by all cyanobacterial strains. Green: shared exclusively by *Chroococcidiopsis* strains. Red: shared by two *Chroococcidiopsis* strains. Orange: shared between one *Chroococcidiopsis* and *Gloeocapsopsis* strain. Refs: [3] (Beversdorf et al. 2017) [4] (Sandonato et al. 2017) [5] (Harada et al. 1993). na: not assigned compound.

IGM					
SPE fraction	**Major ions (m/z)**	**Putative compound**	**Activity**		**antiSMASH Clusters**
			***Enterococcus durans* 66**	**T47D**	
0-10	457 527 673 689 835	na na na na na	**+**	**+**	Nostophycin Anabaenopeptin NZ 857/ nostamide A Terpene Bacteriocin Puwainaphycins Heterocyst glycolipid Ladderane
20-50	1041 786 839	Cyanopeptolin [3] na Nodularin-R [4]	**-**	**+**	
60-70	420 527 339/677	na na na	**+**	**-**	
80-100	420 515 1113 438 1149	na na na na Aeruginopeptin 95B [5]	**-**	**+ + + +**	

Table 4.13. Summary of activities from *Gloeocapsopsis* GCL strain in this study. -: no activity, +: very weak activity, ++: weak activity, +++: significant activity, ++++: strong activity. Blue: shared by all cyanobacterial strains. Green: shared exclusively by *Chroococcidiopsis* strains. Red: shared by two *Chroococcidiopsis* strains. Orange: shared between one *Chroococcidiopsis* and *Gloeocapsopsis* strain. Refs: [4] (Sandonato et al. 2017), [6] (Erhard et al. 1999). na: not assigned compound.

GCL					
SPE fraction	**Major ions (m/z)**	**Putative compound**	**Activity**		**antiSMASH Clusters**
			***Enterococcus durans* 66**	**T47D**	
0-10	511/349 457/365 673 837	na na na Anabaenopeptin B [6]	**+**	**+**	Nostophycin Anabaenopaeptin Terpene Bacteriocin Hapalosin Micropeptin Micacocidin Merocyclophane C/ D Nostopeptolide Aminoglycoside /aminocyclitol
20-30	422 483 402 403	na na na na	**+ +**	**+**	
40-60	339/677 622	na na	**-**	**+**	
70-100	839	Nodularin-R [4]	**-**	**+**	

4.5. Discussion

Secondary metabolites constitute essential tools for organisms in the ecosystem providing competitive advantages. In the endolithic microhabitat of the polyextreme Atacama Desert, several resources can be limited (space, water, sun radiation). Thus, microorganisms inhabiting such an extreme and competitive habitat are expected to produce a high variety of novel compounds in order to deal with these biotic and abiotic factors.

This chapter constitutes a pioneering research in the potential of endolithic cyanobacteria from the hyper-arid Atacama Desert, whose interest lies in the absence of previous studies of this kind regarding these organisms from this polyextreme environment. The screening of the antibacterial and antitumor activity of extracts and SPE fractions via bioassays is crucial for the future finding of natural products with bioactivities of interest.

Cyanobacterial strains isolated from such a polyextreme environment as the Atacama Desert could be promising in producing metabolites to inhibit bacterial growth. The ecological justification for this expectation is based on the benefits provided by minimizing the growth of other microorganisms in their vicinity as a possible competition strategy for limiting resources as space or water.

One of the possible ways to inhibit microbial growth would be the inhibition of diverse enzymatic activities. A common bioassay is the analysis of the effect of metabolites on the proteolytic activity of proteases. These enzymes prove essential for the functioning of live structures occurring in all living organisms (Patel, 2017). In this study, the wide range of concentrations of peptidic compounds present in the crude extract from all four cyanobacterial strains tested against the enzymes trypsin, chymotrypsin, thrombin and elastase reveals the rare occurrence of enzymatic inhibitors among the metabolites produced by these microorganisms. However, these strains exhibited a high potential in

protease inhibitors as anabaenopeptins, cyanopeptolines and micropeptins (Table 4.9, Supp. Mat. 4.3) that could be active at other concentrations or against other not tested proteases. Taking into account the original microhabitat and environmental conditions of the studied strains, it could be thought that the protease inhibitors found could have specific targets from organisms coexisting in the original extreme environment.

To this date, significant activity has mainly been found among the representatives of the Nostocales, Oscillatoriales and Chroococales although in the work by Silva-Stenico et al. (2011) most of the metabolites with antimicrobial activity were produced by cyanobacteria from the Chroococcales, being more frequently active against bacteria than against other microorganisms as fungi (Silva-Stenico et al. 2011, Mazur-Marzec et al. 2015). Since genomic data from cyanobacterial strains from the Chroococcidiopsidales, YU-2, CVL and IGM, and the Chroococcocales, GCL exhibited possible antibacterial metabolites such as bacteriocins, terpenes, lasso peptide and micacodin, it would be of great interest to test their antibacterial activity in clinically important pathogens that have developed multiresistance to the currently used antibiotics. Despite the fact that crude extracts revealed antibacterial activity against *Vibrio cholerae* 01 MW D 2329, by YU-2 strains, and *Enterobacter* sp. MW-W814 and *Enterococcus durans* 66 by CVL, IGM and GCL strains, an inconsistency was observed after the evaluation of SPE fractions via microdilution assay. The absence of *Vibrio cholerae* 01 MW D 2329 inhibition by the YU-2 strain SPE fractions and *Enterobacter* sp. MW-W814 inhibition by the CVL, IGM and GCL strains SPE fractions could be explained through two scenarios. In the first one, some compounds present in YU-2, CVL, IGM and GCL crude extracts could have been lost or separated into several different fractions during the SPE procedure and, as a consequence, their concentration could have been too low to exert any effect on the growth of *Vibrio cholerae* and *Enterobacter* sp. MW-W814. On the other hand, the unexpected inhibition of *Enterococcus durans* 66 exerted by 20-40, 50-

60 and 70-100 SPE fractions of the YU-2 strain, despite the absence of effect by the crude extract, could be explained by the 0-10 fraction, where the highest concentration of ions could be observed. A possible antagonistic effect of ion peaks m/z 457 or 527 found in high concentration in the 0-10 fraction in the crude extract could have masked the effect of the other SPE fractions. Concerning active fractions, the exerted effect observed in different fractions on the IGM, CVL and GCL extracts could be linked to the shared presence of major peaks in the TIC at m/z 527, in fractions 0-10 and 60-70 of the IGM extract and 60-70 of the CVL extract, and m/z 673, in fractions 0-10 of the IGM and GCL extracts. The TIC of the highly active fractions 60-70 and 80-100 of the IGM extract also showed the presence of a major peak at m/z 420 which could be responsible for the observed inhibition, as would also happen for the major peak at m/z 422 found in the TIC of fraction 20-30 in GCL extract. By contrast, it is not possible to establish any relationship between ion presence and the high activity exerted by fraction 20-30 of CVL since they could not be detected possibly due to an extremely low concentration of these compounds.

An additional point of interest in the discovery of natural products is their potential anticancer properties. Cytotoxic activity against cancer cells has been observed in diverse cyanobacterial strains although active agents were not identified in most of those studies (Szubert et al. 2018, Singh et al. 2011, Rastogi and Sinha, 2009) and some of their mechanisms have not been elucidated yet (Humisto et al. 2016). The T47D cell line derives from a 54-year-old woman, one of the most widely used cell lines in breast cancer studies and previously used to prove cytotoxic activity from cyanobacterial extracts (Szubert et al. 2018, Hassouani et al. 2017, Costa et al. 2014). All cyanobacterial strains tested in this study exhibited a potential cytotoxic effect related to the potential production of nostophycin, terpenes, vioprolide, puwainaphycins and merocyclophane (Table 4.9). Additionally, MTT tests proved that the most polar SPE fractions from *Chroococcidiopsis* sp. YU-2, CVL and IGM strains contain cytotoxic metabolites

against human breast cancer cells line T47D. Mass spectrometry analysis revealed major peaks in the TIC of fractions 70-100 of YU-2 and 80-100 of CVL, probably linked with the observed cytotoxic activity against T47D cells. These ions detected in IDA mode are characterized by m/z 506 and 1057 in fraction 70-100 of the YU-2 strain, and by m/z 558 in fraction 80-100 in of the CVL strain. The exceptional cytotoxic activity exerted by fraction 80-100 in IGM could be linked to the major peak observed in the TIC of all 80, 90 and 100 SPE fractions characterized by m/z 420.

The studied strains displayed an interesting actual and potential production of bioactive compounds (Tables 4.10-4.13) as expected due to their original environmental conditions and microhabitat. In fact, the obtained results concerning their cytotoxic activity against eukaryotic cells finds their analogy in their original EMCs (Table 4.1) since these communities exhibit no eukaryotic members or their very rare presence (Yungay halite - Robinson et al. 2015; Valle de la Luna calcite – DiRuggiero et al. 2013, Meslier et al. 2018; Monturaqui ignimbrite – Crits-Christoph et al. 2016b, Meslier et al. 2018; and Monturaqui gypcrete – Meslier et al. 2018, Chapter 1). This absence is particularly remarkable in the case of fungal members, since algae where found in similar environments to those of the EMCs of halite from Salar Grande (Robinson et al. 2015) and of gypcrete from Cordón de Lila (J. Wierzchos pers. com.); however, there is no coexistence of cyanobacteria and fungi among all of these EMCs. Although the expected antifungal potential of these and other cyanobacterial strains from these communities remains unknown, the chemical diversity presented in this study looks promising.

4.6. Conclusions

The bioactivity of metabolites produced by cyanobacterial strains from the Atacama Desert has never been reported before. This study illustrates the variety of compounds actually and potentially produced by these extremotolerant cyanobacterial strains. The tested extracts not only have antibacterial activity against the multidrug resistant *Enterococcus durans* and cytotoxic activity against T47D cancer cells, but also seem to work selectively, as they do not have any inhibitory effect against the tested enzymes. Despite the fact that the compounds responsible for the observed antibacterial and cytotoxic activities in the conducted bioassays were not characterized and unequivocally identified, some characteristic features of their polarity were exposed together with their putative assignment when available. The tests showed for the first time the existing potential of the desert *Chroococcidiopsis* and *Gloeocapsopsis* strains to be used as a source of important cytotoxic agents. In view of these promising results, further studies are worth to be continued.

4.7. Supplementary Material

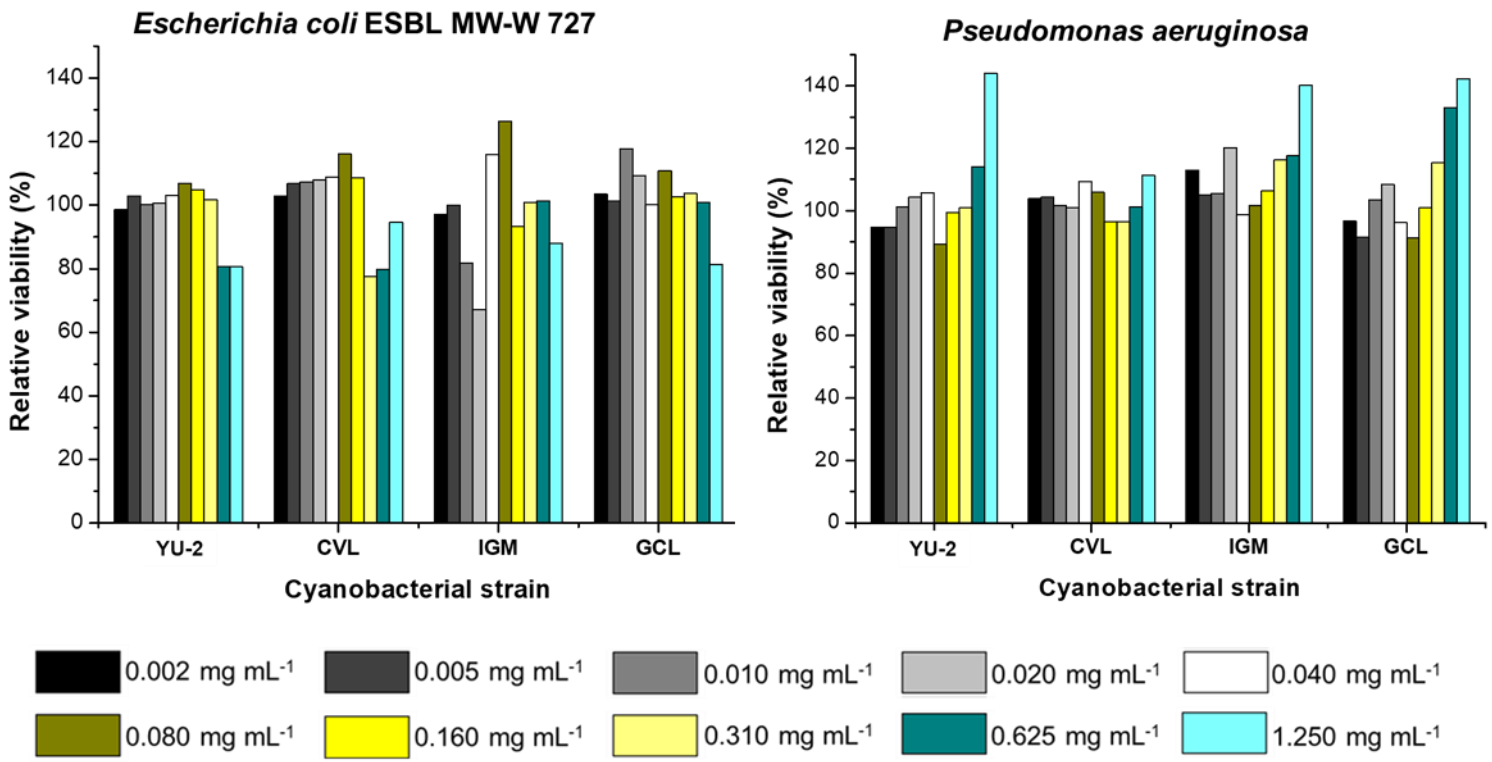

Supplementary Material 4.1. The effects of different concentrations of crude extracts from cyanobacterial strains on the viability of *Escherichia coli* ESBL MW-W 727 and *Pseudomonas aeruginosa* antibiotic resistant strains cells.

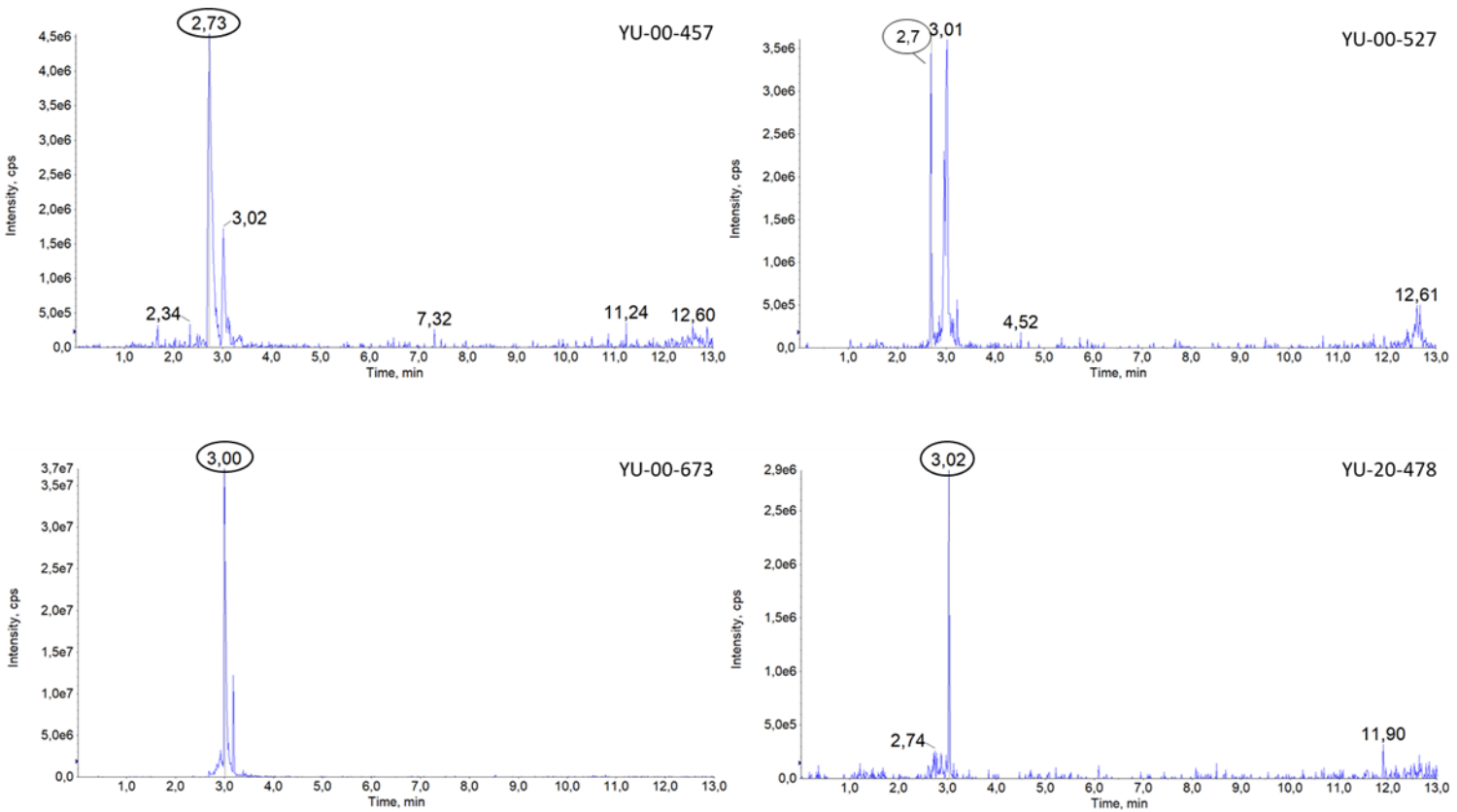

Supplementary Material 4.2. The extracted ion chromatogram (XIC) of highly abundant ions. Code for each figure results from the combination of 3 types of information: STRAIN – FRACTION – m/z. Retention times of described ions are marked with round frames.

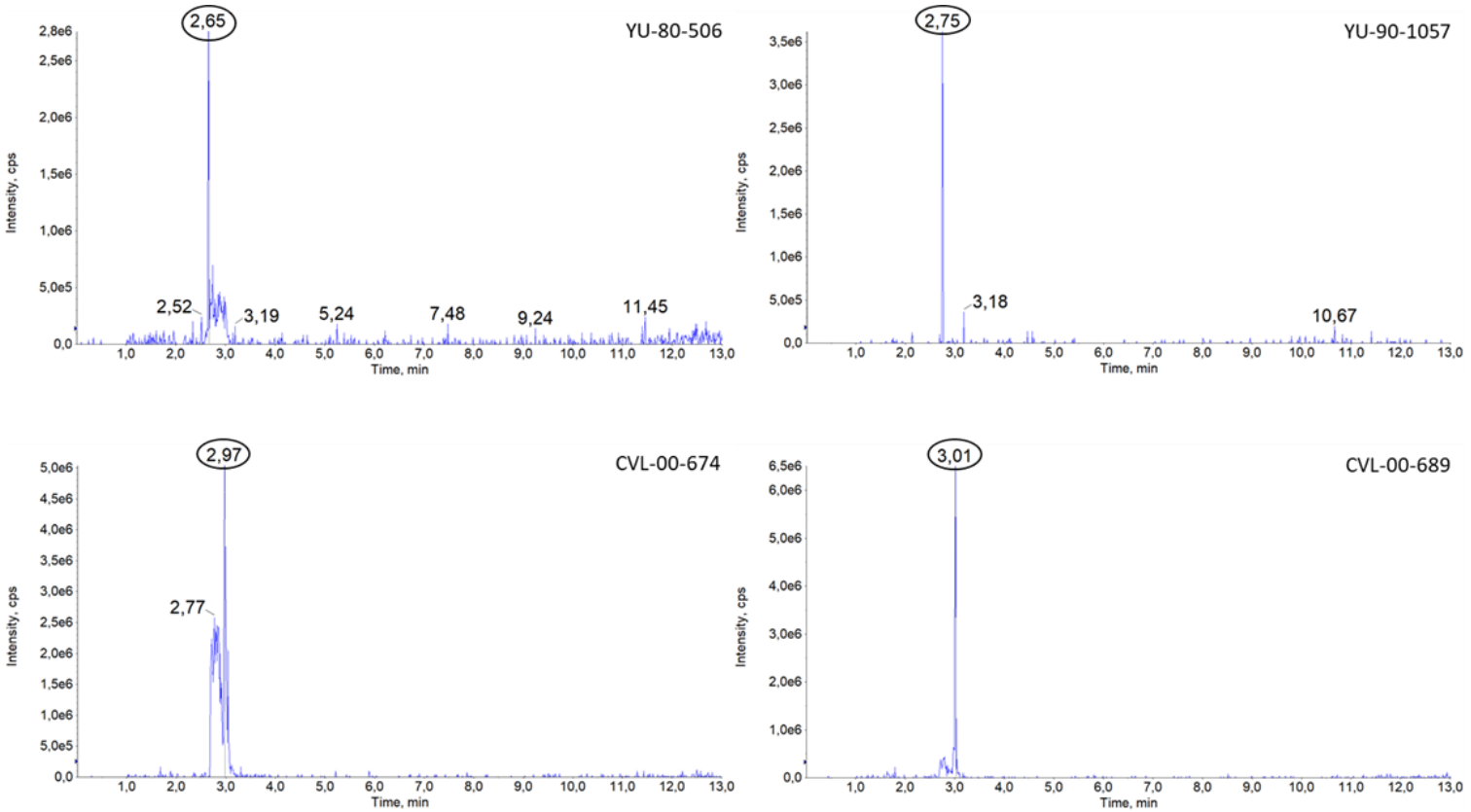

Supplementary Material 4.2. The extracted ion chromatogram (XIC) of highly abundant ions. Code for each figure results from the combination of 3 types of information: STRAIN – FRACTION – m/z. Retention times of described ions are marked with round frames.

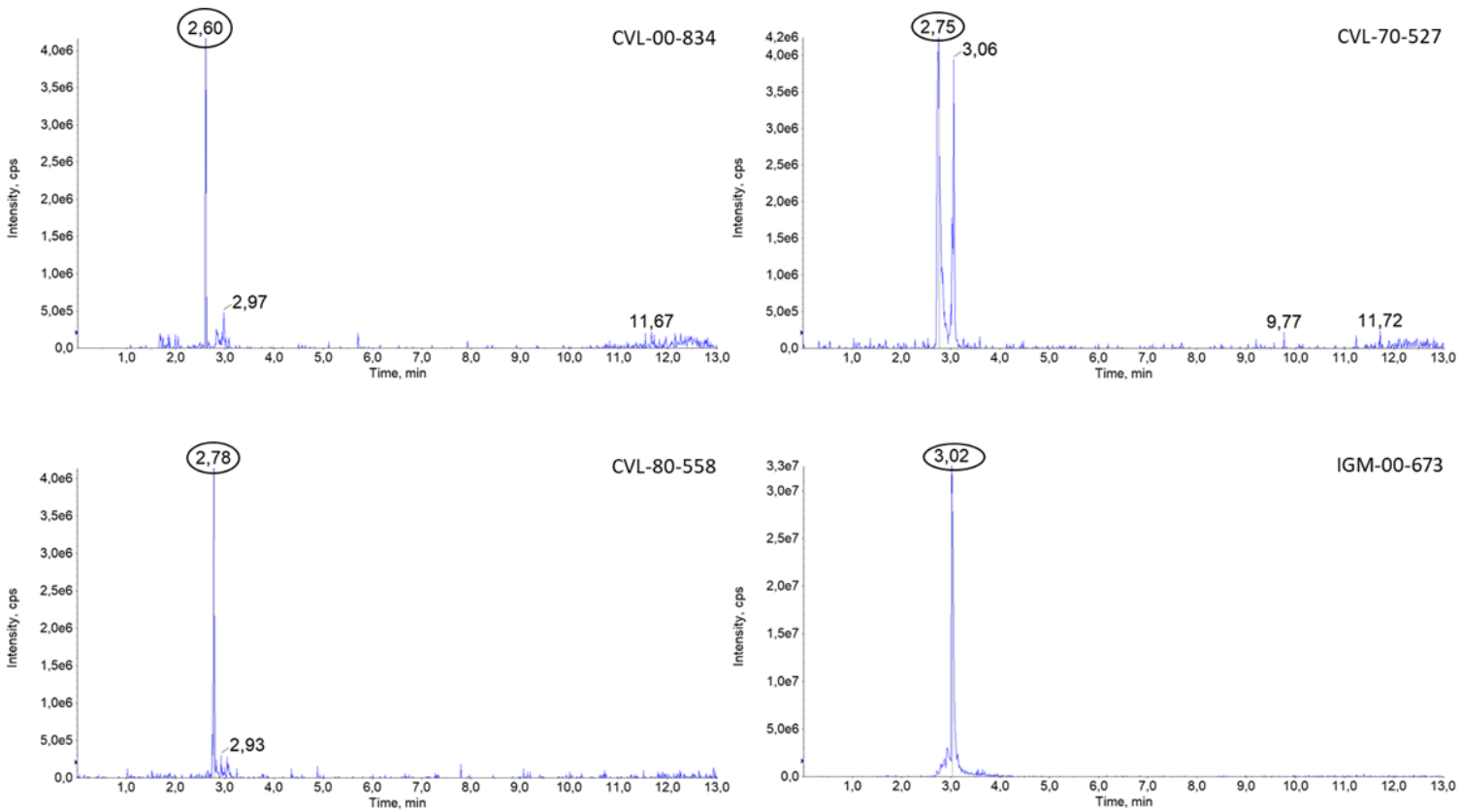

Supplementary Material 4.2. The extracted ion chromatogram (XIC) of highly abundant ions. Code for each figure results from the combination of 3 types of information: STRAIN – FRACTION – m/z. Retention times of described ions are marked with round frames.

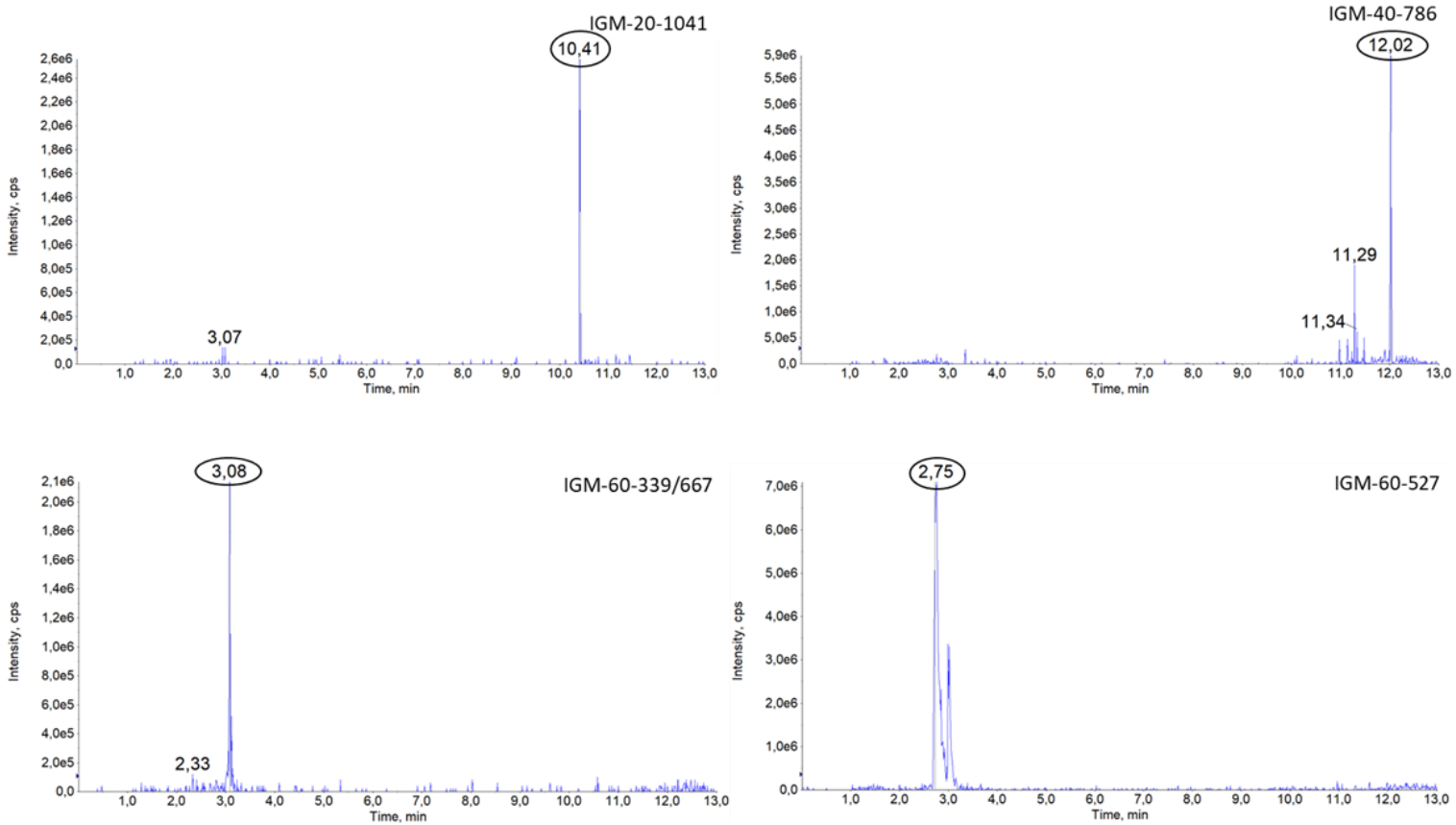

Supplementary Material 4.2. The extracted ion chromatogram (XIC) of highly abundant ions. Code for each figure results from the combination of 3 types of information: STRAIN – FRACTION – m/z. Retention times of described ions are marked with round frames.

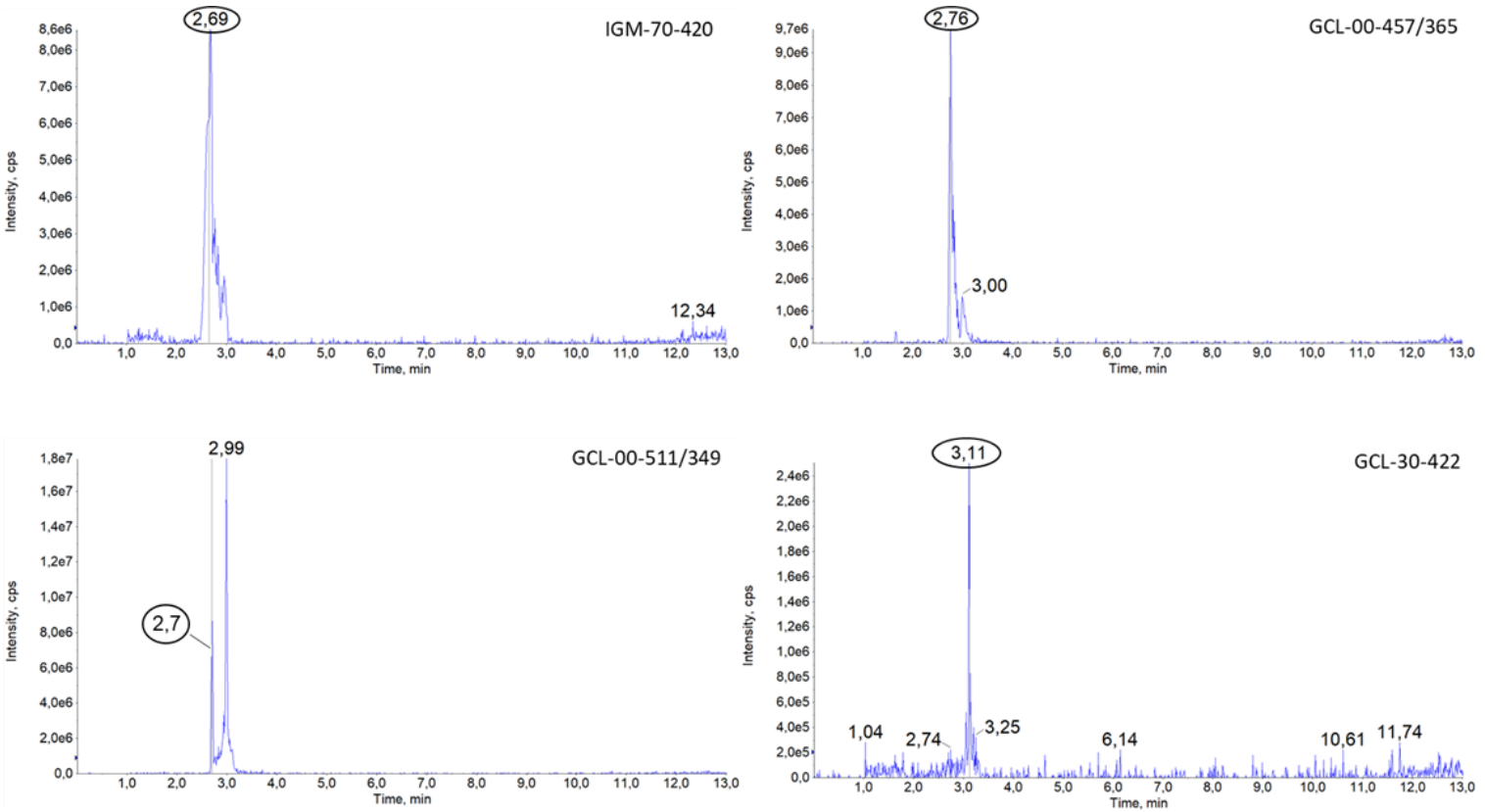

Supplementary Material 4.2. The extracted ion chromatogram (XIC) of highly abundant ions. Code for each figure results from the combination of 3 types of information: STRAIN – FRACTION – m/z. Retention times of described ions are marked with round frames.

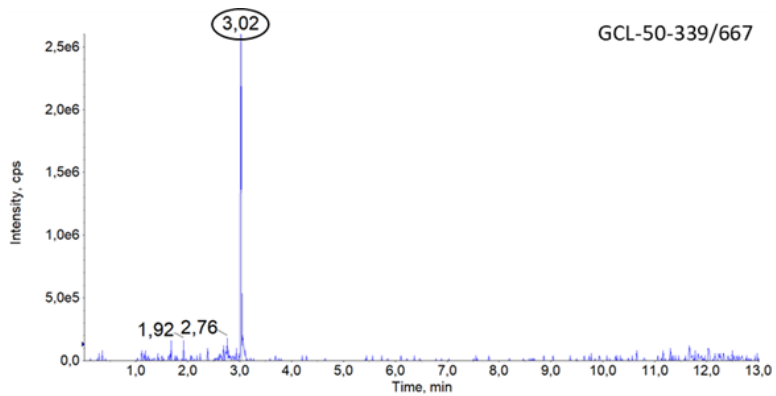

Supplementary Material 4.2. The extracted ion chromatogram (XIC) of highly abundant ions. Code for each figure results from the combination of 3 types of information: STRAIN – FRACTION – m/z. Retention times of described ions are marked with round frames.

Supplementary Material 4.3. Putative compounds detected in *Chroococcidiopsis* strains YU-2, CVL and IGM, and *Gloeocapsopsis* GCL strain from endolithic microhabitats in the Atacama Desert.

m/z	Putative Compound	Reference	Observed in cyanobacterial strains	Bioactivity
674	Aeruginosamide C	Leikoski et al. 2013	CVL	Protein phosphatase inhibitor
725	Aeruginosin 724	Silva-Stenico et al. 2011	IGM	Protein phosphatase inhibitor
837	Anabaenopeptin B	Erhard et al. 1999	YU-2 / GCL	Protein phosphatase inhibitor
839	Nodularin-R	Sandonato et al. 2017	IGM / GCL	PP1 inhibitor, PP2A inhibitor
871	Viridamide A	Esquenazi et al. 2008	IGM / GCL	Cytotoxic
937	Cyanopeptolin	Silva-Stenico et al. 2011	IGM	Serine protease inhibitor
1002	MC-LY	Ballot et al. 2014	YU-2	PP1C and PP2A inhibitor
1013	Cl- Cyanopeptolin W	Welker et al. 2004	YU-2	Serine protease inhibitor
1041	Cyanopeptolin	Beversdorf et al. 2017	CVL / IGM	Serine protease inhibitor
1063	Micropeptin 88-E	Ishida et al. 1998	YU-2	Protein phosphatase inhibitor
1067	MC-WR	Fastner et al. 1999	YU-2	PP1C and PP2A inhibitor
1074	Microcystilide-A	Tsukamoto et al. 1993	GCL	Protein phosphatase inhibitor
1106	Micropeptin 1106	Isaacs et al. 2014	YU-2 / CVL	Protein phosphatase inhibitor
1149	Aeruginopeptin 95B	Harada et al. 1993	GCL	Protein phosphatase inhibitor

Supplementary Material 4.4. Shared and unique ions by the cyanobacterial strains used in this study

Strains	Shared ions	m/z												
CVL/GCL/IGM/YU-2	1	786												
CVL/IGM/YU-2	1	527												
GCL/IGM/YU-2	1	673												
CVL/YU-2	1	1106												
IGM/YU-2	1	457												
GCL/YU-2	3	837	997	1042										
CVL/IGM	2	689	1041											
GCL/IGM	4	339/677	839	835	871									
YU-2	9	478	506	677	1002	1013	1057	1063	1067	1128				
CVL	3	558	674	834										
IGM	12	407	420	438	454	472	499	515	573	725	937	1113	1149	
GCL	13	402	403	422	457/365	483	511	511/349	538	622	1074	1094	1099	1100

GENERAL DISCUSSION

A new insight into the microbial ecology and biogeography of endolithic communities

This Dissertation dwells on two central questions regarding endolithic microbial communities: the relevance of the biogeographic scale to their ecological traits and the strategies developed by their primary producers and major component, cyanobacteria, to survive in the polyextreme environment of the hyper-arid Atacama Desert.

Chapter 1 addresses the impact of microhabitat architecture in microbial communities inhabiting three different endolithic microhabitats in gypcrete. On the other hand, Chapter 2 is devoted to the exploration of the cyanobacterial community colonizing the halite endolithic microhabitat of one of the driest locations on Earth. In Chapter 3 the response of cyanobacterial isolates from endolithic communities to UVR and PAR was studied. Finally, in Chapter 4 the bioactivity of secondary metabolites from cyanobacterial isolates was analyzed by means of bioassays, analytical chemistry and genomic tools.

This General Discussion aims to synthetize and integrate the main findings and proposals suggested along the four chapters in the context of the microbial ecology principles.

…, THE ENVIRONMENT SELECTS (Baas-Becking 1934)

The environment selects…, but, what does "environment" mean when referring to microbial communities?

The spatial distribution of microorganisms has often been understood in terms of the Baas-Becking (1934) statement: "everything is everywhere, but the environment selects", whose second half (*the environment selects*) would constitute the environmental filtering metaphor (Kraft et al. 2015). In hyper-arid deserts, the polyextreme environment represents the first environmental

filtering since the set of extreme environmental factors already prevents the establishment or persistence of organisms that are not previously adapted to or able to tolerate the polyextreme environment. When investigating endolithic communities, the search for the next level of abiotic filter has attracted attention mainly in two directions: (i) microbial biogeography on a macro scale, where the hypothesis is that EMCs from the same type of lithic substrate show differences in diversity and/or composition due to the different (macro)environmental conditions accross different deserts (Qu et al. 2019, Dong et al. 2007; Omelon et al. 2008) and (ii) the physico-chemical properties of the lithic substrate, where it can be hypothesized that different substrates harbor different communities in terms of diversity and/or composition based on their physicochemical characteristics (Meslier et al. 2018; Crits-Christoph et al. 2016b).

At this stage, it is essential to make a brief discussion on the meaning of the term "microbiogeography". Biogeography is a science that attempts to describe and explain spatial patterns of biological diversity and how these patterns change over the time (Ganderton and Coker 2005, Lomolino et al. 2006). The study of these patterns (in space, in time and along environmental gradients) can be used to understand why organisms live where they do, how many taxa can coexist in a place and how they will respond to environmental changes (Green et al. 2008). When studying this field with regard to microorganisms, the term microbiogeography has been used as a synonym for microbial biogeography (Tofalo et al. 2013). However, this study (Chapter 1) proposes to understand the term "microbiogeography" as a "micro" perspective of biogeography similar to the concept used by Stacy et al. (2016). Thus, the "micro" prefix refers not only to the size of the organisms (microorganisms), but also to the size of the patterns that determine why they live where they do, how many different taxa can coexist and how they respond to (micro)environmental changes.

Despite the microscale of the habitat and processes of these communities, few studies considered scale when comparing their composition (Meslier et al. 2018), and no studies have focused on differences on a microscale within the same lithic substrate. However, this aspect has previously been addressed with regard to soil microbial communities, and to the way in which the structure of soil and pore space results in a complex distribution of oxygen, water films and gradients of solutes determining radically different local conditions on very fine scales (Ruamps et al. 2011; Vos et al. 2013; Tecon and Or, 2017; Rabot et al. 2018). The three different endolithic microhabitats within gypcrete have been shown to harbor different microbial communities in terms of composition, particularly observed in the photosynthetic fraction of the community composed by cyanobacteria (Chapter 1). The observed impact of different microhabitat architectures in the microenvironmental conditions occurring in them even when they are found in the same piece of lithic substrate, sheds light to the factors determining the microbiogeography of this type of communities, i.e. those essential for photosynthesis, especially light and liquid water. The lower availability of both these resources appear to shape microbial community composition, decreasing the proportion of the phototrophic fraction, cyanobacteria, in relation to the heterotrophic fraction, since the former would not fix enough CO_2 to support a more developed heterotrophic community.

The environment selects… for specific adaptations and acclimation capacities

The greater the number of extreme conditions concurrent in a specific location, the more restrictive it becomes, and therefore only those organisms tolerant or previously adapted to such conditions will be able to proliferate successfully. Thus, polyextreme environments harbor unique communities constituted by both extremotolerant and extremophile organisms.

Throughout this dissertation, the differences in microenvironmental conditions linked to the features of the lithic substrate and the type of endolithic microhabitat have been found to be a potential selective pressure not only for community composition and structure (Chapter 1) but also for specific adaptation strategies (Chapter 1, Chapter 2, Chapter 3) and acclimation capacities (Chapter 2, Chapter 3). Regarding the adaptation strategies associated with the features of the lithic substrate, the *Chroococcidiopsis* YU-2 strain exhibited in its genome specific adaptations to the osmotic stress caused by the hypersaline environment of halite: the production of osmolites such as glycine betaine and ectoine (Chapter 2), while the thick EPS's envelopes exhibited by this strain seem to be an acclimation response to that hypersalinity and to long drought periods. In addition, Chapter 3 showed in both genomes of the studied *Chroococcidiopsis* strains (YU-2 and CVL) the occurrence of the very rare Cu/Zn SOD precursor, related to the oxidative stress response, which suggests a particular evolutionary origin of this lithobiontic genus, along with their capacity to produce the UV-screening compound scytonemin under stressful light conditions (Chapter 3). Moreover, the environmental filtering caused by the substrate in the distribution of certain previously adapted strains (Chapter 2) could also be observed in the cyanobacterial distribution at microhabitat level (Chapter 1), since the light-limited hypoendolithic microhabitat of gypcrete harbor a highly abundant unclassified OTU (UC-OTU) (40%), whose closest relative sequences belongs to habitats where light is a limiting factor. This suggests the presence of specific adaptation mechanisms for low-light conditions in this highly abundant UC-OTU such as more densely packed photosynthetic membrane systems previously reported in cyanobacteria from light-deprived cave environments belonging to *Chroococcidiopsis, Cyanosarcina, Leptolyngbya, Phormidium, Pseudocapsa* (Asencio and Aboal, 2004), *Chroococcus* (Cox 1977) and *Gloeocapsa* (Cox et al. 1981) genera.

Besides the lithic substrate properties, the microhabitat features also seem to exert an impact on the distribution and selection of acclimation capacities as demonstrated in Chapter 3. Thus, different *Chroococcidiopsis* strains (YU-2 and CVL) owe their different acclimation capacities to the environmental pressure exerted by their original microhabitats. The lower acclimation capability exhibited by the YU-2 strain could be due to its original scattered light-exposed cryptoendolithic microhabitat in comparison to the direct light-exposed chasmoendolithic microhabitat to which the CVL strain belonged, which would explain its higher acclimation capacity. Thus, the "micro" scale becomes essential again when exploring the pressures exerted by the extreme environmental conditions on the selection and distribution of organisms and their adaptations or acclimation capacities.

The occurrence of several extreme environmental conditions as it happens in the Atacama Desert could lead to a tradeoff between adaptation strategies and acclimation capacities, that is, between the *philia* and the tolerance to extreme environmental conditions, as proposed in Chapter 2. The halite endolithic microhabitat constitutes the most polyextreme environment studied in this desert, since it is hypersaline in addition to the common extreme Atacama Desert conditions. The cyanobacterial community inhabiting this microhabitat illustrates the differential colonization efficiency between the extremophile (i.e. *Halothece* (Oren 2012)) and extremotolerant (i.e. *Chroococcidiopsis* (Caiola and Billi, 2007)) members when more than one extreme condition occurs simultaneously and thus, it also illustrates the differential efficiency between adaptation and acclimation capacity. Here it is proposed that polyextreme environments select, to a larger extent, organisms with higher acclimation capacity than highly adapted organisms, namely, extremotolerant organisms rather than extremophiles.

Biotic competition: the significance of traveling companions

Apart from the role of environmental conditions, biotic competition creates an evolutionary pressure on microbial communities that in some cases could have a greater impact on the evolution of strains that overlap in resource use (Bauer et al. 2018). Competition strategies can be classified according to the passive or active harm exerted on the other competitors: (i) it is considered passive competition if one strain harm another through resource consumption, i.e. restricting the competitor's access to nutrients or gaining enhanced access to a given space; (ii) active competition occurs when the strains that are competing damage each other through direct and active interference commonly through chemical warfare in order to eliminate the competitor (Ghoul and Mitri 2016).

The endolithic microhabitat in the hyper-arid Atacama Desert can be considered a highly competitive environment since the limitation of essential resources as water and space allows endolithic microbial communities to meet the criteria that promote competition: (i) a high overlap between coexisting strains in their metabolic and/or spatial niche along with the requirement for similar resources, (ii) a relatively high cell density rate compared to the available resources and (iii) the intermixture of populations increasing the possibility of interaction, shared nutrients and joint secretions (Bauer et al. 2018).

Concerning the phototrophic fraction of the microbial community in endolithic environments of the Atacama Desert, the co-existence of both prokaryotic (cyanobacteria) and eukaryotic (algae) members is highly uncommon (Robinson et al. 2015, Wierzchos et al. 2015). The recurrent absence of eukaryotic phototrophs in endolithic microhabitats where cyanobacteria dominate (Robinson et al. 2015; DiRuggiero et al. 2013, Meslier et al. 2018; Crits-Christoph et al. 2016b, Meslier et al. 2018; Wierzchos et al. 2006, de los Ríos et al. 2010,

Wierzchos et al. 2013, Chapter 1) suggests a competition for essential photosynthetic resources (light, water) that has led to two of the three possible ecologically stable long-term consequences proposed by Ghoul and Mitri (2016): (i) the establishment of a metabolic niche and (ii) the assignment of territorial niches or patches. Thus, as proposed in Chapter 1, cyanobacteria inhabit microhabitats where liquid water is available (Yungay halite – Wierzchos et al. 2012a, Robinson et al. 2015; Valle de la Luna calcite – DiRuggiero et al. 2013, Meslier et al. 2018; Monturaqui ignimbrite – Wierzchos et al. 2013, Crits-Christoph et al. 2016b, Meslier et al. 2018; and Monturaqui gypcrete – Meslier et al. 2018, Chapter 1) while algae inhabit those where high RH values prevail (Salar Grande halite -Robinson et al. 2015 and Tarapacá region gypsum crust - Wierzchos et al. 2011).

The cyanobacterial community studied in this Thesis exhibited diverse competitive strategies. In the frame of passive competition, the observed production of EPSs (Chapter 1, Chapter 2, Chapter 3), besides their function as water retaining structures (de los Ríos et al. 2007; Dong et al. 2007, Wierzchos et al. 2015) and their role in retaining and exchanging nutrients (Meslier et al. 2018), are useful to colonize and gain better access to the limited space available in the endolithic microhabitat. The active competition strategies displayed by some of the cyanobacterial inhabitants of these limiting and competitive environments are shown in Chapter 4. The studied cyanobacterial strains isolated from four different lithic substrates and endolithic microhabitats exhibited a potential production of antibacterial metabolites (bacteriocins, terpenes, lasso peptide, micacodin), protease inhibitors (anabaenopeptins, cyanopeptolines and micropeptins) and cytotoxic activity against eukaryotic cells. This information suggests the evolutionary selection of these pathways and compounds in order to effectively compete for the limited resources both intraspecifically (other cyanobacterial strains from the same genus) and interspecifically (other prokaryotic members and eukaryotic members). The

active competition against eukaryotic cells is of particular interest not only with respect to the previously mentioned competition against other phototrophs (algae) but also to fungal members, since cyanobacteria and fungi have not yet been reported to co-inhabit endolithic microhabitats in the Atacama Desert.

The result of active interference or competition in microorganisms is of special interest in case they can be used for biotechnological and biomedical purposes in the current circumstances where the multiresistant pathogenic bacterial strains become a public health problem (Gottlieb and Nimmo 2011) and alternative cancer therapies are necessary (Demain and Vaishnav 2011). Thus, the results obtained through the diverse bioassays performed to cyanobacterial extracts, especially those exhibiting cytotoxic activity against cancer cells (fraction 80-100 in *Chroococcidiopsis* IGM strain extract), are very promising for further research and the development of new natural anticancer products.

The need for a multidisciplinary analysis

The benefits of using diverse techniques and managing several types of information (molecular, imaging, chemical) have already been highlighted in Chapter 1. In fact, the Dissertation, throughout all four chapters, each one with its own goals, illustrates the urgency of using a multidisciplinary approach when addressing microbial ecology studies, especially from unique and polyextreme environments. The use of different types of information is the only way to understand as much as possible the ecology of these communities, being aware of the technical limitations in each case.

This General Discussion integrates the diversity of evidence and proposals collected throughout the four chapters by means of a multidisciplinary analysis to elucidate the behavior and distribution of microorganisms inhabiting the endolithic microhabitats in the hyper-arid Atacama, with particular focus on the main primary producers, cyanobacteria. Despite the many open-ended

questions that remain after this work and its approach proposal, all these findings point towards the uniqueness of microenvironmental conditions in each microhabitat and substrate and thus, how those conditions along with the specific biotic interactions selected to inhabit such a restrictive environment, determine the whole selection of genotypes and phenotypes able to efficiently colonize each microhabitat and lithic substrate. This proposal, focused on the "micro" perspective when analyzing the ecology and behavior on that scale, stimulates further experimentation and the achievement of both descriptive and applied studies in order to understand the limits of life.

CONCLUSIONS / *CONCLUSIONES*

1. The analysis of the structure and composition of microbial communities inhabiting three different microhabitats of gypcrete reveals the importance of using an appropriate space scale for the study of microbial communities in these environments. The microstructural and microarchitectural features of the lithic substrate are decisive for the structure of endolithic microbial communities due to their impact on vital resources as water and light.

   El análisis de la estructura y la composición de las comunidades microbianas que habitan los tres microhábitats endolíticos del yeso revela la importancia del uso de una escala apropiada para el estudio de las comunidades microbianas. Las características microestructurales y microarquitectónicas del sustrato lítico resultan decisivas para la estructura de las comunidades microbianas endolíticas debido al impacto de estas características en recursos esenciales como son el agua y la luz.

2. The high capacity to colonize effectively endolithic microhabitats under polyextreme conditions by the *Chroococcidiopsis* genus has been proved. Nevertheless, the higher abundance of a singular cyanobacterial OTU without proximity to any known cyanobacteria in the hypoendolithic microhabitat in gypcrete stresses the importance of additional efforts in the characterization of cyanobacteria and other microorganisms in extreme environments.

   Se ha probado alta capacidad del género Chroococcidiopsis *de colonizar de manera efectiva microhábitats endolíticos que se encuentran en ambientes poliextremos. Sin embargo, la abundancia de una OTU singular del filo Cyanobacteria en el microhábitat hipoendolítico del yeso subraya la necesidad de aplicar esfuerzos adicionales en la caracterización de cianobacterias y otros microrganismos en ambientes extremos.*

3. The presence of *Chroococcidiopsis* in the hypersaline endolithic microhabitat in halite from the Yungay region has been proved, corroborating the first morphological identification of cyanobacteria present in the endolithic microbial community in halite at this specific location in the Atacama Desert.

   Se ha probado la presencia de Chroococcidiopsis *en el microhábitat endolítico de halitas en la región de Yungay, corroborando así la primera identificación morfológica de las cianobacterias presentes en la comunidad endolítica de halitas de esta ubicación del Desierto de Atacama.*

4. The high endurance of *Chroococcidiopsis* strains under extreme environmental pressures, as those occurring in the endolithic microhabitat in halite, has been demonstrated by its ultrastructural characterization and the requirement of a specific DNA isolation method, which explains its apparent absence in previous studies of halite endolithic communities that used traditional protocols.

   Se ha demostrado la gran resistencia de las cepas de Chroococcidiopsis *bajo presiones ambientales extremas, como se da en el microhabitat endolítico de halitas, gracias a la caracterización de su ultraestructura y debido a la necesidad de emplear un método específico para la extracción de su ADN. Esto explica la aparente ausencia de este género en estudios previos acerca de la comunidad endolítica de halitas que usan métodos tradicionales de extracción de ADN.*

5. It has been proved that biodiversity studies of microbial communities, especially from extreme environments, should be performed in the light of a combination of molecular and microscopy techniques due to the detection limits of both types of approaches: the endurance exhibited by some microorganisms to DNA extraction with conventional protocols, and the appearance in low abundance of some other microorganisms.

   Se ha demostrado que los estudios de biodiversidad de comunidades microbianas, especialmente de aquellas que habitan ambientes extremos, deben llevarse a cabo mediante la combinación de técnicas tanto moleculares como de microscopía para compensar las limitaciones de ambas técnicas: la resistencia que algunos microorganismos ejercen frente a la extracción de ADN con métodos convencionales y la presencia de algunos taxones en muy baja abundancia.

6. The *Chroococcidiopsis* strains isolated from chasmoendolithic (CVL) and cryptoendolithic (YU-2) microhabitats from calcite and halite, respectively, show a significantly different response to UVR and PAR, with CVL exhibiting a higher acclimation capacity than YU-2. The differential behavior reveals the impact of the greater (chasmoendolithic) and lesser (cryptoendolithic) exposure to light in their original microhabitat.

   Las cepas de Chroococcidiopsis *aisladas de los microhábitats casmoendolítico (CVL) y criptoendolítico (YU-2) de calcita y halita, respectivamente, muestran diferencias significativas en su respuesta frente a UVR y PAR, mostrando la cepa CVL una mayor capacidad de aclimatación que la cepa YU-2. Las diferencias de comportamiento de ambas cepas revelan el efecto de una mayor (casmoendolítico) y una menor (criptoendolítico) exposición a la luz en el microhábitat del que fueron aisladas.*

7. The *Chroococcidiopsis* strains YU-2, CVL and IGM, and *Gloeocapsopsis* strain GCL exhibit a large variety of bioactive compounds actually and potentially produced. The presence of SPE fractions from the extracts obtained from these strains with antibacterial and cytotoxic activity suggests the highly competitive environment they inhabit and their potential as sources of cytotoxic agents.

   Las cepas de Chroococcidiopsis *YU-2, CVL e IGM y la cepa GCL de* Gloeocapsopsis *muestran la producción real y potencial de una amplia variedad de compuestos bioactivos. La actividad antibacteriana y citotóxica observada por parte de las fracciones de los extractos de estas cepas sugiere la alta competitividad existente en el microhábitat en el que se encuentran, a la vez que revela su potencial como fuentes de agentes citotóxicos.*

References

Abdelkader MS, Philippon T, Asenjo JA, Bull AT, Goodfellow M, Ebel R, Jaspars M, Rateb ME (2018) Asenjonamides A–C, antibacterial metabolites isolated from Streptomyces asenjonii strain KNN 42. f from an extreme-hyper arid Atacama Desert soil. The Journal of antibiotics 71 (4):425-431

Abed R, Dobrestov S, Al-Kharusi S, Schramm A, Jupp B, Golubic S (2011) Cyanobacterial diversity and bioactivity of inland hypersaline microbial mats from a desert stream in the Sultanate of Oman. Fottea 11 (1):215-224

Amaral G, Martinez-Frias J, Vazquez L (2006) Astrobiological significance of minerals on Mars surface environment: UV-shielding properties of Fe (jarosite) vs. Ca (gypsum) sulphates, Reviews in Environmental Science and Biotechnology 5(2-3): 219-231

Arias-Forero D, Hayashida G, Aranda M, Araya S, Portilla T, García A, Díaz-Palma P (2013) Protocol for maximizing the triglycerides-enriched lipids production from *Dunaliella salina* SA32007 biomass, isolated from the Salar de Atacama (Northern Chile). Advances in Bioscience and Biotechnology 4 (08):830-839

Asencio AD, Aboal M (2004) Cell inclusions in the chasmoendolithic Cyanophytes from cave-like environments in Murcia (SE Spain). Algological Studies 113 (1):117-127

Asthana RK, Tripathi MK, Srivastava A, Singh AP, Singh SP, Nath G, Srivastava R, Srivastava BS (2009) Isolation and identification of a new antibacterial entity from the Antarctic cyanobacterium *Nostoc* CCC 537. Journal of applied phycology 21 (1):81-88

Axenov-Gribanov D, Rebets Y, Tokovenko B, Voytsekhovskaya I, Timofeyev M, Luzhetskyy A (2016) The isolation and characterization of actinobacteria from dominant benthic macroinvertebrates endemic to Lake Baikal. Folia Microbiologica 61 (2):159-168.

Azua-Bustos A, González-Silva C (2014) Biotechnological Applications Derived from Microorganisms of the Atacama Desert. BioMed Research International vol. 2014. 1-7

Azua-Bustos A, Caro-Lara L, Vicuña R (2015) Discovery and microbial content of the driest site of the hyperarid A tacama Desert, C hile. Environmental microbiology reports 7 (3):388-394

Baas-Becking LGM (1934) Geobiologie; of inleiding tot de milieukunde. The Hague, the Netherlands, WP Van Stockum & Zoon NV.

Ballot A, Dadheech PK, Haande S, Krienitz L (2008) Morphological and phylogenetic analysis of *Anabaenopsis abijatae* and *Anabaenopsis elenkinii* (Nostocales, Cyanobacteria) from tropical inland water bodies. Microbial Ecology 55 (4):608-618

Ballot A, Krienitz L, Kotut K, Wiegand C, Metcalf JS, Codd GA, Pflugmacher S (2004) Cyanobacteria and cyanobacterial toxins in three alkaline Rift Valley lakes of Kenya—Lakes Bogoria, Nakuru and Elmenteita. Journal of Plankton Research 26 (8):925-935

Baqué M, Verseux C, Böttger U, Rabbow E, de Vera J-PP, Billi D (2016) Preservation of biomarkers from cyanobacteria mixed with Marslike regolith under simulated Martian atmosphere and UV flux. Origins of Life and Evolution of Biospheres 46 (2-3):289-310

Barrow C (1992) World atlas of desertification (United nations environment programme), edited by N. Middleton and DSG Thomas. Edward Arnold, London, 1992.

Bass D, Boenigk J (2011) Everything is everywhere: a twenty-first century de-/reconstruction with respect to protists. In D. Fontaneto (Ed,), Biogeography of microscopic organisms: Is everything small everywhere? (Systematics Association Special Volume Series, pp. 88-110

Bauer MA, Kainz K, Carmona-Gutierrez D, Madeo F (2018) Microbial wars: Competition in ecological niches and within the microbiome. Microbial Cell 5 (5):215-219

Beversdorf L, Weirich C, Bartlett S, Miller T (2017) Variable cyanobacterial toxin and metabolite profiles across six eutrophic lakes of differing physiochemical characteristics. Toxins 9 (2):62-83

Billi D (2009) Subcellular integrities in *Chroococcidiopsis* sp. CCMEE 029 survivors after prolonged desiccation revealed by molecular probes and genome stability assays. Extremophiles 13 (1):49-57.

Billi D, Baqué M, Verseux C, Rothschild L, de Vera JP (2017) Desert cyanobacteria: Potential for space and earth applications. In: Adaption of Microbial Life to Environmental Extremes: Novel Research Results and Application, Second Edition. pp 133-146.

Billi D, Friedmann EI, Hofer KG, Caiola MG, Ocampo-Friedmann R (2000) Ionizing-radiation resistance in the desiccation-tolerant cyanobacterium *Chroococcidiopsis*. Applied and Environmental Microbiology 66 (4):1489-1492.

Billi D, Grilli Caiola M, Paolozzi L, Ghelardini P (1998) A Method for DNA Extraction from the Desert Cyanobacterium *Chroococcidiopsis* and Its Application to Identification of ftsZ. Applied and environmental microbiology 64:4053-4056

Billi D, Staibano C, Verseux C, Fagliarone C, Mosca C, Baqué M, Rabbow E, Rettberg P (2019) Dried Biofilms of Desert Strains of *Chroococcidiopsis* Survived Prolonged Exposure to Space and Mars-like Conditions in Low Earth Orbit. Astrobiology 19(8):1008-1017

Billi D, Viaggiu E, Cockell CS, Rabbow E, Horneck G, Onofri S (2011) Damage escape and repair in dried *Chroococcidiopsis* spp. from hot and cold deserts exposed to simulated space and martian conditions. Astrobiology 11 (1):65-73.

Biondi N, Tredici MR, Taton A, Wilmotte A, Hodgson DA, Losi D, Marinelli F (2008) Cyanobacteria from benthic mats of Antarctic lakes as a source of new bioactivities. J Appl Microbiol 105 (1):105-115.

Blanco Y, Quesada A, Gallardo I, Aguirre J, Parro Garcia V (2015) CYANOCHIP: An Antibody Microarray for High-Taxonomical-Resolution Cyanobacterial Monitoring. Environmental science & technology 49(3):1611-1620

Blin K, Wolf T, Chevrette MG, Lu X, Schwalen CJ, Kautsar SA, Suarez Duran HG, de Los Santos EL, Kim HU, Nave M (2017) antiSMASH 4.0—improvements in chemistry prediction and gene cluster boundary identification. Nucleic acids research 45 (1):36-41

Boison G, Mergel A, Jolkver H, Bothe H (2004) Bacterial life and dinitrogen fixation at a gypsum rock. Applied and environmental microbiology 70 (12):7070-7077.

Bratchkova A, Ivanova V (2011) Bioactive metabolites produced by microorganisms collected in Antarctica and the Arctic. Biotechnology & Biotechnological Equipment 25 (sup1):1-7

Brown AD (1976) Microbial water stress. Bacteriol Rev 40 (4):803-846

Büdel B (1999) Ecology and diversity of rock-inhabiting cyanobacteria in tropical regions. European Journal of Phycology 34 (4):361-370

Bull AT, Andrews BA, Dorador C, Goodfellow M (2018) Introducing the Atacama Desert. Antonie van Leeuwenhoek, International Journal of General and Molecular Microbiology 111 (8):1269-1272.

Busarakam K, Bull AT, Trujillo ME, Riesco R, Sangal V, van Wezel GP, Goodfellow M (2016) *Modestobacter caceresii* sp. nov., novel actinobacteria with an insight into their adaptive mechanisms for survival in extreme hyper-arid Atacama Desert soils. Systematic and Applied Microbiology 39 (4):243-251.

Caiola MG, Billi D (2007) *Chroococcidiopsis* from Desert to Mars. In: Seckbach J (ed) Algae and Cyanobacteria in Extreme Environments. Springer Science & Business Media. Netherlands, Dordrecht, pp 553-568.

Calamita G (2000) The *Escherichia coli* aquaporin-Z water channel: MicroReview. Molecular microbiology 37 (2):254-262

Cámara B, Suzuki S, Nealson KH, Wierzchos J, Ascaso C, Artieda O, de los Ríos A (2015) Ignimbrite textural properties as determinants of endolithic colonization patterns from hyper-arid Atacama Desert. International Microbiology 17 (4):235-247.

Campbell SE (1985) Benthic cyanophytes (cyanobacteria) of Solar Lake (Sinai). Algological Studies/Archiv für Hydrobiologie, Supplement Volumes:311-329

Caporaso JG, Kuczynski J, Stombaugh J, Bittinger K, Bushman FD, Costello EK, Fierer N, Peña AG, Goodrich JK, Gordon JI, Huttley GA, Kelley ST, Knights D, Koenig JE, Ley RE, Lozupone CA, McDonald D, Muegge BD, Pirrung M, Reeder J, Sevinsky JR, Turnbaugh PJ, Walters WA, Widmann J, Yatsunenko T, Zaneveld J, Knight R (2010) QIIME allows analysis of high-throughput community sequencing data. Nature Methods 7 (5):335-336.

Carro L, Castro JF, Razmilic V, Nouioui I, Pan C, Igual JM, Jaspars M, Goodfellow M, Bull AT, Asenjo JA (2019) Uncovering the potential of novel micromonosporae isolated from an extreme hyper-arid Atacama Desert soil. Scientific reports 9 (4678): 1-16

Casero MC, Ballot A, Agha R, Quesada A, Cirés S (2014) Characterization of saxitoxin production and release and phylogeny of sxt genes in paralytic shellfish poisoning toxin-producing *Aphanizomenon gracile*. Harmful Algae 37:28-37

Casero MC, Velázquez D, Medina-Cobo M, Quesada A, Cirés S (2019) Unmasking the identity of toxigenic cyanobacteria driving a multi-toxin bloom by high-throughput sequencing of cyanotoxins genes and 16*S* rRNA metabarcoding. Science of The Total Environment 665:367-378.

Castenholz RW, Garcia-Pichel F (2012) Cyanobacterial Responses to UV Radiation. In: Whitton BA (ed) Ecology of Cyanobacteria II: Their Diversity in Space and Time. Springer Science & Business Media. Netherlands, Dordrecht, pp 481-499.

Castenholz RW, Waterbury, J. B. (1989) Cyanobacteria. In: J. T. Staley MPB, N. Pfennig and J. G. Holt, eds, Williams & Wilkins, Baltimore (ed) Bergey's Manual of Systematic Bacteriology, vol Volume 3. pp 1710-1727

Castenholz RW, Wilmotte A, Herdman M, Rippka R, Waterbury JB, Iteman I, Hoffmann L (2001) Phylum BX. Cyanobacteria. In: Boone DR, Castenholz RW, Garrity GM (eds) Bergey's Manual® of Systematic Bacteriology: Volume One : The Archaea and the Deeply Branching and Phototrophic Bacteria. Springer Science & Business Media. New York, New York, NY, pp 473-599.

Chang Z, Sitachitta N, Rossi JV, Roberts MA, Flatt PM, Jia J, Sherman DH, Gerwick WH (2004) Biosynthetic Pathway and Gene Cluster Analysis of Curacin A, an Antitubulin Natural Product from the Tropical Marine Cyanobacterium *Lyngbya majuscula*. Journal of natural products 67 (8):1356-1367

Cirés S, Casero MC, Quesada A (2017) Toxicity at the edge of life: A review on cyanobacterial toxins from extreme environments. Marine Drugs 15 (7):233-251

Cockell C, Rettberg P, Horneck G, Scherer K, Stokes MD (2003) Measurements of microbial protection from ultraviolet radiation in polar terrestrial microhabitats. Polar Biology 26 (1):62-69

Cockell CS, Knowland J (1999) Ultraviolet radiation screening compounds. Biological Reviews 74 (3):311-345

Cockell CS, McKay CP, Warren-Rhodes K, Horneck G (2008) Ultraviolet radiation-induced limitation to epilithic microbial growth in arid deserts - Dosimetric experiments in the hyperarid core of the Atacama Desert. Journal of Photochemistry and Photobiology B: Biology 90 (2):79-87.

Cockell CS, Schuerger AC, Billi D, Friedmann EI, Panitz C (2005) Effects of a simulated Martian UV flux on the cyanobacterium, *Chroococcidiopsis* sp. 029. Astrobiology 5 (2):127-140.

Cole JR, Wang Q, Fish JA, Chai B, McGarrell DM, Sun Y, Brown CT, Porras-Alfaro A, Kuske CR, Tiedje JM (2014) Ribosomal Database Project: data and tools for high throughput rRNA analysis. Nucleic Acids Research 42 (1): 633-642.

Cordero R, Damiani A, Seckmeyer G, Jorquera J, Caballero M, Rowe P, Ferrer J, Mubarak R, Carrasco J, Rondanelli R (2016) The solar spectrum in the Atacama Desert. Scientific reports 6 (22457): 1-15

Cordero RR, Damiani A, Jorquera J, Sepúlveda E, Caballero M, Fernandez S, Feron S, Llanillo PJ, Carrasco J, Laroze D, Labbe F (2018) Ultraviolet radiation in the Atacama Desert. Antonie van Leeuwenhoek, International Journal of General and Molecular Microbiology 111 (8):1301-1313.

Cordero RR, Seckmeyer G, Damiani A, Riechelmann S, Rayas J, Labbe F, Laroze D (2014) The world's highest levels of surface UV. Photochemical & photobiological sciences : Official journal of the European Photochemistry Association and the European Society for Photobiology 13 (1):70-81.

Cornejo-Corona I, Thapa HR, Browne DR, Devarenne TP, Lozoya-Gloria E (2016) Stress responses of the oil-producing green microalga *Botryococcus braunii* Race B. PeerJ 4:e2748-2775

Cortés-Albayay C, Silber J, Imhoff JF, Asenjo JA, Andrews B, Nouioui I, Dorador C (2019) The polyextreme ecosystem, salar de Huasco at the Chilean Altiplano of the Atacama Desert houses diverse streptomyces spp. with promising pharmaceutical potentials. Diversity 11 (5):69-81

Costa M, Garcia M, Costa-Rodrigues J, Costa MS, Ribeiro MJ, Fernandes MH, Barros P, Barreiro A, Vasconcelos V, Martins R (2014) Exploring bioactive properties

of marine cyanobacteria isolated from the Portuguese coast: high potential as a source of anticancer compounds. Marine drugs 12 (1):98-114

Cox G. (1977) Photosynthesis in the deep twilight zone: microorganisms with extreme structural adaptations to low light. In: Ford T.D. (Ed.), Proceedings of the 7th International congress of speleology. University of Leicester, Sheffield, pp. 131-133.

Cox G, Benson D, Dwarte D (1981) Ultrastructure of a cave-wall cyanophyte-*Gloeocapsa* NS4. Archives of Microbiology 130 (2):165-174

Crits-Christoph A, Gelsinger DR, Ma B, Wierzchos J, Ravel J, Davila A, Casero MC, DiRuggiero J (2016a) Functional interactions of archaea, bacteria and viruses in a hypersaline endolithic community. Environmental microbiology 18 (6):2064-2077

Crits-Christoph A, Robinson CK, Ma B, Ravel J, Wierzchos J, Ascaso C, Artieda O, Souza-Egipsy V, Casero MC, DiRuggiero J (2016b) Phylogenetic and functional substrate specificity for endolithic microbial communities in hyper-arid environments. Frontiers in Microbiology 7 (301): 1-15.

D'Orazio N, Gammone MA, Gemello E, De Girolamo M, Cusenza S, Riccioni G (2012) Marine bioactives: Pharmacological properties and potential applications against inflammatory diseases. Marine drugs 10 (4):812-833

Dahms H-U, Ying X, Pfeiffer C (2006) Antifouling potential of cyanobacteria: a mini-review. Biofouling 22 (5):317-327

Dassarma S (2006) Extreme Halophiles Are Models for Astrobiology, Microbe. 1(3):120-126

Davila AF, Gómez-Silva B, de los Rios A, Ascaso C, Olivares H, McKay CP, Wierzchos J (2008) Facilitation of endolithic microbial survival in the hyperarid core of the Atacam Desert by mineral deliquescence. Journal of Geophysical Research: Biogeosciences 113 (1):1-9

Davila AF, Hawes I, Araya JG, Gelsinger DR, DiRuggiero J, Ascaso C, Osano A, Wierzchos J (2015) In situ metabolism in halite endolithic microbial communities of the hyperarid Atacama Desert. Frontiers in Microbiology 6 (1035):1-7

de los Ríos A, Grube M, Sancho LG, Ascaso C (2007) Ultrastructural and genetic characteristics of endolithic cyanobacterial biofilms colonizing Antarctic granite rocks. FEMS Microbiology Ecology 59 (2):386-395.

de los Ríos A, Valea S, Ascaso C, Davila A, Kastovsky J, McKay CP, Gómez-Silva B, Wierzchos J (2010) Comparative analysis of the microbial communities inhabiting halite evaporates of the Atacama Desert. International Microbiology 13 (2):79-89.

de los Ríos A, Wierzchos J, Ascaso C (2014) The lithic microbial ecosystems of Antarctica's McMurdo Dry Valleys. Antarctic Science 25 (4).

de los Ríos A, Wierzchos J, Sancho LG, Ascaso C (2004) Exploring the physiological state of continental Antarctic endolithic microorganisms by microscopy. FEMS Microbiology Ecology 50 (3):143-152.

De Philippis R, Margheri MC, Pelosi E, Ventura S (1993) Exopolysaccharide production by a unicellular cyanobacterium isolated from a hypersaline habitat. Journal of Applied Phycology 5 (4):387-394.

De Wit R, Bouvier T (2006) 'Everything is everywhere, but, the environment selects'; what did Baas Becking and Beijerinck really say? Environmental microbiology 8 (4):755-758

Demain AL, Vaishnav P (2011) Natural products for cancer chemotherapy. Microbial biotechnology 4 (6):687-699

Demergasso C, Chong G, Galleguillos P, Escudero L, Martínez-Alonso M, Esteve I (2003) Microbial mats from the Llamará salt flat, northern Chile. Revista Chilena de Historia Natural 76 (3):485-499

Diffey B (1991) Solar ultraviolet radiation effects on biological systems. Physics in medicine & biology 36 (3):299-328

Dillon JG, Castenholz RW (1999) Scytonemin, a cyanobacterial sheath pigment, protects against UVC radiation: implications for early photosynthetic life. Journal of Phycology 35 (4):673-681

Dillon JG, Tatsumi CM, Tandingan PG, Castenholz RW (2002) Effect of environmental factors on the synthesis of scytonemin, a UV-screening pigment, in a cyanobacterium (*Chroococcidiopsis* sp.). Archives of microbiology 177 (4):322-331

DiRuggiero J, Wierzchos J, Robinson CK, Souterre T, Ravel J, Artieda O, Souza-Egipsy V, Ascaso C (2013) Microbial colonisation of chasmoendolithic habitats in the hyper-arid zone of the Atacama Desert. Biogeosciences 10 (4):2439-2450.

Dong H, Rech JA, Jiang H, Sun H, Buck BJ (2007) Endolithnic cyanobacteria in soil gypsum: Occurences in Atacama (Chile), Mojave (United States), and Al-Jafr Basin (Jordan) Deserts. Journal of Geophysical Research: Biogeosciences 112 (2)1-11

Donner A (2013) The case of *Chroococcidiopsis*: New phylogenetic and morphological insights into ecological important Cyanobacteria. Doctoral dissertation.

Edwards U, Rogall T, Blöcker H, Emde M, Böttger EC (1989) Isolation and direct complete nucleotide determination of entire genes. Characterization of a gene coding for 16S ribosomal RNA. Nucleic acids research 17 (19):7843-7853

Ehling-Schulz M, Bilger W, Scherer S (1997) UV-B-induced synthesis of photoprotective pigments and extracellular polysaccharides in the terrestrial cyanobacterium *Nostoc commune*. Journal of Bacteriology 179 (6):1940-1945

Erhard M, von Döhren H, Jungblut PR (1999) Rapid identification of the new anabaenopeptin G from *Planktothrix agardhii* HUB 011 using matrix-assisted laser desorption/ionization time-of-flight mass spectrometry. Rapid Communications in Mass Spectrometry 13 (5):337-343

Esquenazi E, Coates C, Simmons L, Gonzalez D, Gerwick WH, Dorrestein PC (2008) Visualizing the spatial distribution of secondary metabolites produced by marine cyanobacteria and sponges via MALDI-TOF imaging. Molecular BioSystems 4 (6):562-570

Fairén AG, Davila AF, Lim D, Bramall N, Bonaccorsi R, Zavaleta J, Uceda ER, Stoker C, Wierzchos J, Dohm JM, Amils R, Andersen D, McKay CP (2010) Astrobiology through the ages of Mars: The study of terrestrial analogues to understand the habitability of Mars. Astrobiology 10 (8):821-843.

Falkowski PG, Raven JA (2013) Aquatic photosynthesis. Princeton University Press.

Fastner J, Erhard M, Carmichael W, Sun F, Rinehart K, Ronicke H, Chorus I (1999) Characterization and diversity of microcystins in natural blooms and strains of the genera *Microcystis* and *Planktothrix* from German freshwaters. Archiv fü r Hydrobiologie 145 (2): 147-163

Felczykowska A, Pawlik A, Mazur-Marzec H, Toruńska-Sitarz A, Narajczyk M, Richert M, Węgrzyn G, Herman-Antosiewicz A (2015) Selective inhibition of cancer cells' proliferation by compounds included in extracts from Baltic Sea cyanobacteria. Toxicon 108:1-10

Fewer DP, Österholm J, Rouhiainen L, Jokela J, Wahlsten M, Sivonen K (2011) Nostophycin biosynthesis is directed by a hybrid polyketide synthase-nonribosomal peptide synthetase in the toxic cyanobacterium *Nostoc* sp. strain 152. Appl Environ Microbiol 77 (22):8034-8040

Feofilova EP (2003) Deceleration of Vital Activity as a Universal Biochemical Mechanism Ensuring Adaptation of Microorganisms to Stress Factors: A Review, Applied Biochemistry and Microbiology 39 (1): 1-18

Finore I, Lama L, Poli A, Di Donato P, Nicolaus B (2016) Biotechnology implications of extremophiles as life pioneers and wellspring of valuable biomolecules. In: Microbial Factories: Biodiversity, Biopolymers, Bioactive Molecules: Volume 2. pp 193-216.

Finstad K, Pfeiffer M, McNicol G, Barnes J, Demergasso C, Chong G, Amundson R (2016) Rates and geochemical processes of soil and salt crust formation in Salars of the Atacama Desert, Chile. Geoderma 284:57-72.

Flatt PM, Mahmud T (2007) Biosynthesis of aminocyclitol-aminoglycoside antibiotics and related compounds. Natural product reports 24 (2):358-392

Fleming ED, Castenholz RW (2007) Effects of periodic desiccation on the synthesis of the UV-screening compound, scytonemin, in cyanobacteria. Environmental microbiology 9 (6):1448-1455.

Foing BH, Stoker C, Ehrenfreund P (2011) Astrobiology field research in Moon/Mars analogue environments. International Journal of Astrobiology 10 (3):137-139.

Fontaneto D, Hortal J (2012) Microbial biogeography: is everything small everywhere. Microbial Ecological Theory: Current Perspectives Caister Academic Press, Norfolk:87-98

French CS, Milner HW (1955) Disintegration of bacteria and small particles by high-pressure extrusion. In: Methods in Enzymology, vol 1. Academic Press, pp 64-67.

Friedmann EI (1980) Endolithic microbial life in hot and cold deserts. Origins of Life 10 (3):223-235.

Friedmann EI, Hua M, Ocampo-Friedmann R (1988) Cryptoendolithic lichen and cyanobacterial communities of the Ross Desert, Antarctica. Polarforschung 58 (2-3):251-259

Friedmann EI, Ocampo-Friedmann R (1984) Endolithic microorganisms in extreme dry environments: analysis of a lithobiontic microbial habitat. In: Klug MJ, Reddy CA (ed) Current perspectives in microbial ecology. American Society for Microbiology, Washington, DC, pp 177–185

Fujisawa T, Narikawa R, Maeda SI, Watanabe S, Kanesaki Y, Kobayashi K, Nomata J, Hanaoka M, Watanabe M, Ehira S, Suzuki E, Awai K, Nakamura Y (2017) CyanoBase: a large-scale update on its 20th anniversary. Nucleic Acids Res 45 (1):551-554.

Gabani P, Singh OV (2013) Radiation-resistant extremophiles and their potential in biotechnology and therapeutics. Applied microbiology and biotechnology 97 (3):993-1004

Ganderton PS, Ganderton P, Coker P (2005) Environmental biogeography. Pearson Education,

Gao K, Li P, Watanabe T, Walter Helbling E (2008) Combined effects of ultraviolet radiation and temperature on morphology, photosynthesis, and dna of *Arthrospira* (*Spirulina*) *platensis* (cyanophyta) 1. Journal of Phycology 44 (3):777-786

Gao Q, Garcia-Pichel F (2011) Microbial ultraviolet sunscreens. Nature Reviews Microbiology 9 (11):791-802

Garcia-Pichel F, Belnap J, Neuer S, Schanz F (2003) Estimates of global cyanobacterial biomass and its distribution. Algological Studies 109 (1):213-227

Garcia-Pichel F, Nubel U, Muyzer G (1998) The phylogeny of unicellular, extremely halotolerant cyanobacteria. Arch Microbiol 169 (6):469-482.

Garcia-Pichel F, Castenholz RW (1991) Characterization and biological implications of scytonemin, a cyanobacterial sheath pigment. Journal of Phycology 27 (3):395-409

Ghoul M, Mitri S (2016) The ecology and evolution of microbial competition. Trends in microbiology 24 (10):833-845

Golubic S, Friedmann I, Schneider J (1981) The lithobiontic ecological niche, with special reference to microorganisms. Journal of Sedimentary Petrology 51 (2):475-478

Gómez-Silva B (2018) Lithobiontic life: "Atacama rocks are well and alive". Antonie van Leeuwenhoek, International Journal of General and Molecular Microbiology 111 (8):1333-1343

Gonçalves VN, Cantrell CL, Wedge DE, Ferreira MC, Soares MA, Jacob MR, Oliveira FS, Galante D, Rodrigues F, Alves TMA, Zani CL, Junior PAS, Murta S, Romanha AJ, Barbosa EC, Kroon EG, Oliveira JG, Gomez-Silva B, Galetovic A, Rosa CA, Rosa LH (2016) Fungi associated with rocks of the Atacama Desert: Taxonomy, distribution, diversity, ecology and bioprospection for bioactive compounds. Environmental Microbiology 18 (1):232-245.

Gottlieb T, Nimmo GR (2011) Antibiotic resistance is an emerging threat to public health: an urgent call to action at the Antimicrobial Resistance Summit 2011. Med J Aust 194 (6):281-283

Green JL, Bohannan BJ, Whitaker RJ (2008) Microbial biogeography: from taxonomy to traits. science 320 (5879):1039-1043

Gröniger A, Häder D-P (2000) Stability of mycosporine-like amino acids. Recent research developments in photochemistry and photobiology.4:247-252

Gulder TA, Moore BS (2009) Chasing the treasures of the sea—bacterial marine natural products. Current opinion in microbiology 12 (3):252-260

Hamilton T, Welander P, Albrecht H, Fulton J, Schaperdoth I, Bird L, Summons R, Freeman K, Macalady J (2017) Microbial communities and organic biomarkers in a Proterozoic-analog sinkhole. Geobiology 15:784-797.

Harada K-i, Mayumi T, Shimada T, Suzuki M, Kondo F, Watanabe MF (1993) Occurrence of four depsipeptides, aeruginopeptins, together with microcystins from toxic cyanobacteria. Tetrahedron letters 34 (38):6091-6094

Harms H, Kurita KL, Pan L, Wahome PG, He H, Kinghorn AD, Carter GT, Linington RG (2016) Discovery of anabaenopeptin 679 from freshwater algal bloom material: Insights into the structure–activity relationship of anabaenopeptin protease inhibitors. Bioorganic & medicinal chemistry letters 26 (20):4960-4965

Hartley AJ, Chong G, Houston J, Mather AE (2005) 150 million years of climatic stability: evidence from the Atacama Desert, northern Chile. Journal of the Geological Society 162 (3):421-424

Hassouani M, Sabour B, Belattmania Z, El Atouani S, Reani A, Ribeiro T, Castelo-Branco R, Ramos V, Preto M, Costa P (2017) In vitro anticancer, antioxidant and antimicrobial potential of *Lyngbya aestuarii* (Cyanobacteria) from the Atlantic coast of Morocco. J Mater Environ Sci 8:4923-4933

He Y-Y, Häder D-P (2002) Reactive oxygen species and UV-B: effect on cyanobacteria. Photochemical & Photobiological Sciences 1 (10):729-736

Hegemann JD, Zimmermann M, Xie X, Marahiel MA (2015) Lasso peptides: an intriguing class of bacterial natural products. Accounts of chemical research 48 (7):1909-1919

Herrera A, Cockell CS, Self S, Blaxter M, Reitner J, Thorsteinsson T, Arp G, Dröse W, Tindle AG (2009) A cryptoendolithic community in volcanic glass. Astrobiology 9 (4):369-381.

Hirsch P, Hoffmann B, Gallikowski CC, Mevs U, Siebert J, Sittig M (1988) 3.7 Diversity and Identification of Heterotrophs from Antarctic Rocks of the McMurdo Dry Valleys (Ross Desert). *Polarforschung*, *58*(2/3), 261-269.

Hock AN, Cabrol N, Dohm J, Piatek J, Warren-Rhodes K, Weinstein S, Wettergreen D, Grin E, Moersch J, Cockell C, Coppin P, Ernst L, Fisher G, Hardgrove C, Marinangeli L, Minkley E, Ori G-G, Waggoner A, Wyatt M, Glasgow J (2007) Life in the Atacama: A scoring system for habitability and the robotic exploration for life, vol 112 G04S08 .

Hoffmann D, Hevel JM, Moore RE, Moore BS (2003) Sequence analysis and biochemical characterization of the nostopeptolide A biosynthetic gene cluster from *Nostoc* sp. GSV224. Gene 311:171-180

Houston J, Hartley AJ (2003) The central Andean west-slope rainshadow and its potential contribution to the origin of hyper-aridity in the Atacama Desert. International Journal of Climatology: A Journal of the Royal Meteorological Society 23 (12):1453-1464

Hu C, Gao K, Whitton BA (2012) Semi-arid regions and deserts. In: Ecology of Cyanobacteria II: Their Diversity in Space and Time (Eds. Whitton A) Springer Science & Business Media., pp 345-369.

Hughes KA, Lawley B (2003) A novel Antarctic microbial endolithic community within gypsum crusts. Environmental Microbiology 5 (7):555-565.

Humisto A, Herfindal L, Jokela J, Karkman A, Bjørnstad R, R Choudhury R, Sivonen K (2016) Cyanobacteria as a source for novel anti-leukemic compounds. Current pharmaceutical biotechnology 17 (1):78-91

Isaacs JD, Strangman WK, Barbera AE, Mallin MA, McIver MR, Wright JL (2014) Microcystins and two new micropeptin cyanopeptides produced by unprecedented *Microcystis aeruginosa* blooms in North Carolina's Cape Fear River. Harmful Algae 31:82-86

Ishida K, Matsuda H, Murakami M (1998) Micropeptins 88-A to 88-F, chymotrypsin inhibitors from the cyanobacterium *Microcystis aeruginosa* (NIES-88). Tetrahedron 54 (21):5545-5556

Jaschke PR, Drake I, Beatty JT (2009) Modification of a French pressure cell to improve microbial cell disruption. Photosynthesis research 102 (1):95-97

Jones CS, Esquenazi E, Dorrestein PC, Gerwick WH (2011) Probing the in vivo biosynthesis of scytonemin, a cyanobacterial ultraviolet radiation sunscreen, through small scale stable isotope incubation studies and MALDI-TOF mass spectrometry. Bioorganic & medicinal chemistry 19 (22):6620-6627

Joshi NA, Fass JN (2011) Sickle: a sliding-window, adaptive, quality-based trimming tool for FastQ files (Version 1.33) [Software]. Available at https://github.com/najoshi/sickle.

Kaasalainen U, Fewer DP, Jokela J, Wahlsten M, Sivonen K, Rikkinen J (2012) Cyanobacteria produce a high variety of hepatotoxic peptides in lichen symbiosis. Proc Natl Acad Sci U S A 109 (15):5886-5891

Kimura M (1980) A simple method for estimating evolutionary rates of base substitutions through comparative studies of nucleotide sequences. Journal of molecular evolution 16 (2):111-120

Kirilovsky D, Kerfeld CA (2016) Cyanobacterial photoprotection by the orange carotenoid protein. Nature Plants 2 (12):16180-12187

Knoll A (2008) Cyanobacteria and Earth History. The Cyanobacteria: Molecular Biology, Genomics, and Evolution, 484:1-19

Kobayashi S, Nakai H, Ikenishi Y, Sun W-Y, Ozaki M, Hayase Y, Takeda R (1998) Micacocidin A, B and C, Novel Antimycoplasma Agents from *Pseudomonas* sp. II. Structure Elucidation. The Journal of Antibiotics

Kolowrat C, Partensky F, Mella-Flores D, Le Corguillé G, Boutte C, Blot N, Ratin M, Ferréol M, Lecomte X, Gourvil P (2010) Ultraviolet stress delays chromosome

replication in light/dark synchronized cells of the marine cyanobacterium *Prochlorococcus marinus* PCC9511. BMC microbiology 10 (1):204-228

Komárek J (1976) Taxonomic review of the genera *Synechocystis* SAUV. 1892, *Synechococcus* NÄG.1849, and *Cyanothece* gen. nov. (Cyanophyceae). – Arch. Protistenk. 118: 119–179

Komárek J (2003) Problem of the taxonomic category. Algological Studies 109 (1):281-297

Komárek J, Cepák V (1998) Cytomorphological characters supporting the taxonomic validity of *Cyanothece* (Cyanoprokaryota). Plant systematics and evolution 210 (1-2):25-39

Komárek J, Cepák V, Kaštovský J, Sulek J (2004) What are the cyanobacterial genera *Cyanothece* and *Cyanobacterium*? Contribution to the combined molecular and phenotype taxonomic evaluation of cyanobacterial diversity. Algological Studies 113:1-36.

Komárek J, Johansen J (2015) Coccoid Cyanobacteria. Freshwater Algae of North America: Ecology and Classification:75-133.

Komarek J, Kaštovský J, Mares J, Johansen J (2014) Taxonomic classification of cyanoprokaryotes (cyanobacterial genera) 2014, using a polyphasic approach. Preslia -Praha- 86:295-335

Komárek J, Kopecký J, Cepák V (1999) Generic characters of the simplest cyanoprokaryotes *Cyanobium*, *Cyanobacterium* and *Synechococcus*. Cryptogamie Algologie 20 (3):209-222

Kraft NJ, Adler PB, Godoy O, James EC, Fuller S, Levine JM (2015) Community assembly, coexistence and the environmental filtering metaphor. Functional ecology 29 (5):592-599

Krienitz L, Ballot A, Casper P, Kotut K, Wiegand C, Pflugmacher S (2005) Cyanobacteria in hot springs of East Africa and their potential toxicity. Algological Studies 117 (1):297-306

Kultschar B, Llewellyn C (2018) Secondary Metabolites in Cyanobacteria. Secondary Metabolites: Sources and Applications:23-36

Kumar S, Stecher G, Tamura K (2016) MEGA7: Molecular Evolutionary Genetics Analysis Version 7.0 for Bigger Datasets. Molecular biology and evolution 33 (7):1870-1874.

Leikoski N, Liu L, Jokela J, Wahlsten M, Gugger M, Calteau A, Permi P, Kerfeld CA, Sivonen K, Fewer DP (2013) Genome mining expands the chemical diversity of the cyanobactin family to include highly modified linear peptides. Chemistry & biology 20 (8):1033-1043

Leirós M, Alonso E, Sanchez JA, Rateb ME, Ebel R, Houssen WE, Jaspars M, Alfonso A, Botana LM (2013) Mitigation of ROS insults by *Streptomyces* secondary metabolites in primary cortical neurons. ACS chemical neuroscience 5 (1):71-80

Lepère C, Wilmotte A, Meyer B (2000) Molecular diversity of *Microcystis* strains (Cyanophyceae, Chroococcales) based on 16S rDNA sequences. Systematics and Geography of Plants:275-283

Leyton YE, Letelier AS, Mata MT, Riquelme CE (2017) Marine *Bacillus pumilus* inhibitors of the fixation of microalgae to artificial substrates. Informacion Tecnologica 28 (2):181-190.

Liaimer A, Helfrich EJ, Hinrichs K, Guljamow A, Ishida K, Hertweck C, Dittmann E (2015) Nostopeptolide plays a governing role during cellular differentiation of the symbiotic cyanobacterium *Nostoc punctiforme*. Proceedings of the National Academy of Sciences 112 (6):1862-1867

Lomolino MV, Riddle BR, Brown JH, Brown JH (2006) Biogeography. vol QH84 L65 2006. Sinauer Associates Sunderland, MA,

Lyons TW, Reinhard CT, Planavsky NJ (2014) The rise of oxygen in Earth's early ocean and atmosphere. Nature 506 (7488):307-315.

Mareš J, Hájek J, Urajová P, Kopecký J, Hrouzek P (2014) A hybrid non-ribosomal peptide/polyketide synthetase containing fatty-acyl ligase (FAAL) synthesizes the β-amino fatty acid lipopeptides puwainaphycins in the Cyanobacterium *Cylindrospermum alatosporum*. PLoS One 9 (11):e111904

Margueri M.C, Ventura S, Kaštovský J, Komárek J (2008) The taxonomic validation of the cyanobacterial genus *Halothece*. Phycologia 47:477-486.

Martínez M, Leyton Y, Cisternas LA, Riquelme C (2018) Metal removal from acid waters by an endemic microalga from the Atacama Desert for water recovery. Minerals 8 (9):378-392.

Matthes U, Turner SJ, Larson DW (2001) Light attenuation by limestone rock and its constraint on the depth distribution of endolithic algae and cyanobacteria. International Journal of Plant Sciences 162 (2):263-270

May DS, Chen W-L, Lantvit DD, Zhang X, Krunic A, Burdette JE, Eustaquio A, Orjala J (2017) Merocyclophanes C and D from the cultured freshwater cyanobacterium *Nostoc* sp.(UIC 10110). Journal of natural products 80 (4):1073-1080

Mazur-Marzec H, Błaszczyk A, Felczykowska A, Hohlfeld N, Kobos J, Toruńska-Sitarz A, Devi P, Montalvao S, D'souza L, Tammela P (2015) Baltic cyanobacteria–a source of biologically active compounds. European journal of phycology 50 (3):343-360

McElroy R (1974) Some comments on the evolution of extremophiles. Biosystems 6 (1):74-75.

McKay CP, Friedmann EI, Gómez-Silva B, Cáceres-Villanueva L, Andersen DT, Landheim R (2003) Temperature and moisture conditions for life in the extreme arid region of the Atacama Desert: Four years of observations including the El Niño of 1997-1998. Astrobiology 3 (2):393-406

McKenzie RL, Bernhard G, Madronich S, Zaratti F (2015) Comment on "Record solar UV irradiance in the tropical Andes, by Cabrol et al.". Frontiers in Environmental Science 3 (26): 1-3

Mehetre G, Shah M, Dastager SG, Dharne MS (2018) Untapped bacterial diversity and metabolic potential within Unkeshwar hot springs, India. Archives of microbiology 200 (5):753-770

Méjean A, Ploux O (2013) A genomic view of secondary metabolite production in cyanobacteria. In: Advances in botanical research, vol 65. Elsevier, pp 189-234

Mergelov N, Mueller CW, Prater I, Shorkunov I, Dolgikh A, Zazovskaya E, Shishkov V, Krupskaya V, Abrosimov K, Cherkinsky A, Goryachkin S (2018) Alteration of rocks by endolithic organisms is one of the pathways for the beginning of soils on Earth. Scientific Reports 8 (1): 1-15

Meslier V, Casero MC, Dailey M, Wierzchos J, Ascaso C, Artieda O, McCullough PR, DiRuggiero J (2018) Fundamental drivers for endolithic microbial community assemblies in the hyperarid Atacama Desert. Environmental Microbiology 20 (5):1765-1781.

Metcalf JS, Codd GA (2012) Cyanotoxins. In: Ecology of Cyanobacteria II. Springer Science & Business Media, pp 651-675

Metcalf JS, Richer R, Cox PA, Codd GA (2012) Cyanotoxins in desert environments may present a risk to human health. Science of the Total Environment 421-422:118-123.

Micallef ML, D'Agostino PM, Sharma D, Viswanathan R, Moffitt MC (2015) Genome mining for natural product biosynthetic gene clusters in the Subsection V cyanobacteria. BMC genomics 16 (1):669, 1-20

Michalski G, Böhlke JK, Thiemens M (2004) Long term atmospheric deposition as the source of nitrate and other salts in the Atacama Desert, Chile: New evidence from mass-independent oxygen isotopic compositions. Geochimica et Cosmochimica Acta 68 (20):4023-4038.

Mohamed ZA (2008) Toxic cyanobacteria and cyanotoxins in public hot springs in Saudi Arabia. Toxicon 51 (1):17-27

Moyano FE, Manzoni S, Chenu C (2013) Responses of soil heterotrophic respiration to moisture availability: An exploration of processes and models. Soil Biology and Biochemistry 59:72-85

Muñoz-Martín MA, Becerra-Absalon I, Perona E, Fernandez-Valbuena L, Garcia-Pichel F, Mateo P (2019) Cyanobacterial biocrust diversity in Mediterranean ecosystems along a latitudinal and climatic gradient. The New phytologist 221 (1):123-141.

Nachtigall J, Kulik A, Helaly S, Bull AT, Goodfellow M, Asenjo JA, Maier A, Wiese J, Imhoff JF, Süssmuth RD (2011) Atacamycins A–C, 22-membered antitumor macrolactones produced by *Streptomyces* sp. C38. The Journal of antibiotics 64 (12):775780

Neifar M, Maktouf S, Ghorbel RE, Jaouani A, Cherif A (2015) Extremophiles as source of novel bioactive compounds with industrial potential. In: Biotechnology of Bioactive Compounds: Sources and Applications (Eds. Kumar V, Tuohy MG) John Wiley & Sons. pp 245-267.

Nienow JA (2009) Extremophiles: Dry Environments (including Cryptoendoliths). In: Schaechter M (ed) Encyclopedia of Microbiology (Third Edition). Academic Press, Oxford, pp 159-173.

Nienow JA, McKay CP, Friedmann EI (1988) The cryptoendolithic microbial environment in the Ross Desert of Antarctica: Mathematical models of the thermal regime. Microbial Ecology 16 (3):253-270

Nishizawa T, Ueda A, Nakano T, Nishizawa A, Miura T, Asayama M, Fujii K, Harada K-i, Shirai M (2011) Characterization of the locus of genes encoding enzymes producing heptadepsipeptide micropeptin in the unicellular cyanobacterium *Microcystis*. The Journal of Biochemistry 149 (4):475-485

Nonga H, Mdegela R, Sandvik M, Lie E, Miles C, Skaare J (2016) Cyanobacteria and cyanobacterial toxins in the alkaline-saline Lakes Natron and Momela, Tanzania 34 (1): 108-116

Nübel U, Garcia-Pichel F, Muyzer G (1997) PCR primers to amplify 16S rRNA genes from cyanobacteria. Appl Environ Microbiol 63 (8):3327-3332

Nuñez-Montero K, Barrientos L (2018) Advances in Antarctic Research for Antimicrobial Discovery: A Comprehensive Narrative Review of Bacteria from Antarctic Environments as Potential Sources of Novel Antibiotic Compounds Against Human Pathogens and Microorganisms of Industrial Importance. Antibiotics 7 (4):90-113

O'Brien PA, Houghton JA (1982) UV-induced DNA degradation in the cyanobacterium *Synechocystis* PCC 6308. Photochemistry and Photobiology 36 (4):417-422

O'Malley MA (2008) 'Everything is everywhere: but the environment selects': ubiquitous distribution and ecological determinism in microbial biogeography. Studies in History and Philosophy of Science Part C: Studies in History and Philosophy of Biological and Biomedical Sciences 39 (3):314-325

Okoro CK, Brown R, Jones AL, Andrews BA, Asenjo JA, Goodfellow M, Bull AT (2009) Diversity of culturable actinomycetes in hyper-arid soils of the Atacama Desert, Chile. Antonie van Leeuwenhoek 95 (2):121-133

Omelon CR (2008) Endolithic Microbial Communities in Polar Desert Habitats. Geomicrobiology Journal 25 (7-8):404-414

Omelon CR, Pollard WH, Ferris FG (2006) Chemical and ultrastructural characterization of high arctic cryptoendolithic habitats. Geomicrobiology Journal 23 (3-4):189-200

Oren A (2000) In The Prokaryotes: An Evolving Electronic Resource for the Microbiological Community Springer-Verlag. New York

Oren A (2006) The order halobacteriales. The Prokaryotes: Volume 3: Archaea Bacteria: Firmicutes, Actinomycetes:113-164

Oren A (2012) Salts and Brines. In: Whitton BA (ed) Ecology of Cyanobacteria II: Their Diversity in Space and Time. Springer Science & Business Media, Netherlands, Dordrecht, pp 401-426

Oren A (2015) Halophilic microbial communities and their environments. Current opinion in biotechnology 33:119-124

Overbeek R, Olson R, Pusch GD, Olsen GJ, Davis JJ, Disz T, Edwards RA, Gerdes S, Parrello B, Shukla M, Vonstein V, Wattam AR, Xia F, Stevens R (2014) The SEED and the Rapid Annotation of microbial genomes using Subsystems Technology (RAST). Nucleic Acids Res 42 (Database issue): 206-214

Paduch R, Trytek M, Król SK, Kud J, Frant M, Kandefer-Szerszeń M, Fiedurek J (2016) Biological activity of terpene compounds produced by biotechnological methods. Pharmaceutical Biology 54 (6):1096-1107

Palmer RJ, Jr., Friedmann EI (1990) Water relations and photosynthesis in the cryptoendolithic microbial habitat of hot and cold deserts. Microbial ecology 19:111-118

Parks DH, Imelfort M, Skennerton CT, Hugenholtz P, Tyson GW (2015) CheckM: assessing the quality of microbial genomes recovered from isolates, single cells, and metagenomes. Genome research 25 (7):1043-1055

Parro V, De Diego-Castilla G, Moreno-Paz M, Blanco Y, Cruz-Gil P, Rodríguez-Manfredi JA, Fernández-Remolar D, Gómez F, Gómez MJ, Rivas LA, Demergasso C, Echeverría A, Urtuvia VN, Ruiz-Bermejo M, García-

Villadangos M, Postigo M, Sánchez-Román M, Chong-Díaz G, Gómez-Elvira J (2011) A microbial oasis in the hypersaline atacama subsurface discovered by a life detector chip: Implications for the search for life on mars. Astrobiology 11 (10):969-996

Patel S (2017) A critical review on serine protease: key immune manipulator and pathology mediator. Allergologia et immunopathologia 45 (6):579-591

Patzelt DJ, Hodač L, Friedl T, Pietrasiak N, Johansen JR (2014) Biodiversity of soil cyanobacteria in the hyper-arid Atacama Desert, Chile. Journal of Phycology 50 (4):698-710.

Pierce J, Omata T (1988) Uptake and utilization of inorganic carbon by cyanobacteria. In: Govindjee (ed) Molecular Biology of Photosynthesis. Springer Science & Business Media Netherlands, Dordrecht, pp 593-606.

Pikuta EV, Hoover RB, Tang J (2007) Microbial Extremophiles at the Limits of Life. Critical Reviews in Microbiology 33 (3):183-209

Pitt J (1975) Xerophilic fungi and the spoilage of foods of plant origin.Water Relations of Foods. Academic Press, London pp:273-307

Pointing SB, Belnap J (2012) Microbial colonization and controls in dryland systems. Nature reviews Microbiology 10 (8):551-562

Pointing SB, Chan Y, Lacap DC, Lau MCY, Jurgens JA, Farrell RL (2009) Highly specialized microbial diversity in hyper-arid polar desert. Proceedings of the National Academy of Sciences 106 (47):19964-19969

Postgate JR (1967) Viability measurements and the survival of microbes under minimum stress. In: Advances in microbial physiology, vol 1. Elsevier, pp 1-23

Potts M (1994) Desiccation tolerance of prokaryotes. Microbiol Mol Biol Rev 58 (4):755-805

Priya B, Premanandh J, Dhanalakshmi RT, Seethalakshmi T, Uma L, Prabaharan D, Subramanian G (2007) Comparative analysis of cyanobacterial superoxide dismutases to discriminate canonical forms. BMC genomics 8 (1):435-445

Proteau P, Gerwick W, Garcia-Pichel F, Castenholz R (1993) The structure of scytonemin, an ultraviolet sunscreen pigment from the sheaths of cyanobacteria. Experientia 49 (9):825-829

Pueyo JJ, Chong G, Jensen A (2002) Neogene evaporites in desert volcanic environments: Atacama Desert, Northern Chile. Sedimentology 48:1411-1431x

Qu E, Omelon C, Oren A, Meslier V, Cowan DA, Maggs-Kölling G, DiRuggiero J (2019) Trophic Selective Pressures Organize the Composition of Endolithic Microbial Communities from Global Deserts. bioRxiv:761262

Quesada A, Mouget JL, Vincent WF (1995) Growth of Antarctic cyanobacteria under ultraviolet radiation: UVA counteracts UVB inhibition. Journal of Phycology 31 (2):242-248.

Quesada A, Vincent W (1997) Strategies of adaptation by Antarctic cyanobacteria to ultraviolet radiation. European Journal of Phycology 32 (4):335-342

Rabot E, Wiesmeier M, Schlüter S, Vogel H-J (2018) Soil structure as an indicator of soil functions: a review. Geoderma 314:122-137

Rahman MA, Sinha S, Sachan S, Kumar G, Singh SK, Sundaram S (2014) Analysis of proteins involved in the production of MAA′s in two Cyanobacteria *Synechocystis* PCC 6803 and *Anabaena cylindrica*. Bioinformation 10 (7):449-453

Rajneesh, Pathak J, Richa, Häder DP, Sinha RP (2019) Impacts of ultraviolet radiation on certain physiological and biochemical processes in cyanobacteria inhabiting diverse habitats. Environmental and Experimental Botany 161:375-387.

Rastogi G, Sani RK (2011) Molecular Techniques to Assess Microbial Community Structure, Function, and Dynamics in the Environment. In: Ahmad I, Ahmad F, Pichtel J (eds) Microbes and Microbial Technology: Agricultural and Environmental Applications. Springer New York, New York, NY, pp 29-57

Rastogi R (2015) UV-Induced Oxidative Stress in Cyanobacteria: How Life is able to Survive? Biochemistry & Analytical Biochemistry, ISSN: 2161-1009

Rastogi R, Madamwar D, Incharoensakdi A (2015) Sun-screening bioactive compounds mycosporine-like amino acids in naturally occurring cyanobacterial biofilms: role in photoprotection. Journal of applied microbiology 119 (3):753-762

Rastogi R, Sinha R, Moh SH, Lee T-K, Kottuparambil S, Kim Y-J, Rhee J-S, Choi E-M, Brown M, Häder D, Han T (2014) Ultraviolet radiation and cyanobacteria. Journal of Photochemistry and Photobiology B Biology 141:154-169

Rastogi RP, Incharoensakdi A (2014) Characterization of UV-screening compounds, mycosporine-like amino acids, and scytonemin in the cyanobacterium *Lyngbya* sp. CU2555. FEMS microbiology ecology 87 (1):244-256

Rastogi RP, Kumar A, Tyagi MB, Sinha RP (2010a) Molecular mechanisms of ultraviolet radiation-induced DNA damage and repair. Journal of nucleic acids 2010 (592980): 1-32

Rastogi RP, Singh SP, Häder D-P, Sinha RP (2010b) Detection of reactive oxygen species (ROS) by the oxidant-sensing probe 2′, 7′-dichlorodihydrofluorescein diacetate in the cyanobacterium *Anabaena variabilis* PCC 7937. Biochemical and biophysical research communications 397 (3):603-607

Rastogi RP, Singh SP, Häder D-P, Sinha RP (2010c) Mycosporine-like amino acids profile and their activity under PAR and UVR in a hot-spring cyanobacterium *Scytonema* sp. HKAR-3. Australian Journal of Botany 58 (4):286-293

Rastogi RP, Sinha RP (2009) Biotechnological and industrial significance of cyanobacterial secondary metabolites. Biotechnology advances 27 (4):521-539

Rateb ME, Ebel R, Jaspars M (2018) Natural product diversity of actinobacteria in the Atacama Desert. Antonie van Leeuwenhoek 111 (8):1467-1477

Rateb ME, Houssen WE, Arnold M, Abdelrahman MH, Deng H, Harrison WT, Okoro CK, Asenjo JA, Andrews BA, Ferguson G (2011) Chaxamycins A–D, bioactive ansamycins from a hyper-arid desert *Streptomyces* sp. Journal of Natural products 74 (6):1491-1499

Raven JA (2012) Carbon. In: Whitton BA (ed) Ecology of Cyanobacteria II: Their Diversity in Space and Time. Springer Science & Business Media, Netherlands, Dordrecht, pp 443-460

Reynolds CS, Oliver RL, Walsby AE (1987) Cyanobacterial dominance: the role of buoyancy regulation in dynamic lake environments. New Zealand journal of marine and freshwater research 21 (3):379-390

Rippka R, Deruelles J, Waterbury JB, Herdman M, Stanier RY (1979) Generic assignments, strain histories and properties of pure cultures of cyanobacteria. Microbiology 111 (1):1-61

Robinson CK, Wierzchos J, Black C, Crits-Christoph A, Ma B, Ravel J, Ascaso C, Artieda O, Valea S, Roldán M, Gómez-Silva B, Diruggiero J (2015) Microbial diversity and the presence of algae in halite endolithic communities are correlated to atmospheric moisture in the hyper-arid zone of the Atacama Desert. Environmental Microbiology 17 (2):299-315.

Roca I, Akova M, Baquero F, Carlet J, Cavaleri M, Coenen S, Cohen J, Findlay D, Gyssens I, Heure O (2015) The global threat of antimicrobial resistance: science for intervention. New microbes and new infections 6:22-29

Roldán M, Ascaso C, Wierzchos J (2014) Fluorescent fingerprints of endolithic phototrophic cyanobacteria living within halite rocks in the atacama desert. Applied and Environmental Microbiology 80 (10):2998-3006

Rondanelli R, Molina A, Falvey M (2015) The Atacama Surface Solar Maximum, vol 96. 406-418

Roszak D, Colwell R (1987) Survival strategies of bacteria in the natural environment. Microbiological reviews 51 (3):365-379

Rothschild LJ, Giver LJ, White MR, Mancinelli RL (1994) Metabolic activity of microorganisms in evaporites. Journal of phycology 30 (3):431-438

Rothschild LJ, Mancinelli RL (2001) Life in extreme environments. Nature 409 (6823):1092-1101

Rouhiainen L, Jokela J, Fewer DP, Urmann M, Sivonen K (2010) Two alternative starter modules for the non-ribosomal biosynthesis of specific anabaenopeptin variants in *Anabaena* (Cyanobacteria). Chemistry & biology 17 (3):265-273

Ruamps LS, Nunan N, Chenu C (2011) Microbial biogeography at the soil pore scale. Soil Biology and Biochemistry 43 (2):280-286

Sandonato BB, Santos VG, Luizete MF, Bronzel Jr JL, Eberlin MN, Milagre H (2017) MALDI imaging mass spectrometry of fresh water cyanobacteria: spatial distribution of toxins and other metabolites. Journal of the Brazilian Chemical Society 28 (4):521-528

Sapio MR, Fricker LD (2014) Carboxypeptidases in disease: insights from peptidomic studies. PROTEOMICS–Clinical Applications 8 (5-6):327-337

Sayed AM, Hassan MHA, Alhadrami HA, Hassan HM, Goodfellow M, Rateb ME (2019) Extreme environments: microbiology leading to specialized metabolites. J Appl Microbiol.

Schallenberg M, Kalff J, Rasmussen JB (1989) Solutions to Problems in Enumerating Sediment Bacteria by Direct Counts. Applied and Environmental Microbiology 55 (5):1214-1219

Schopf JW (1974) The development and diversification of Precambrian life. Origins of life 5 (1):119-135.

Schulz D, Beese P, Ohlendorf B, Erhard A, Zinecker H, Dorador C, Imhoff JF (2011) Abenquines A–D: Aminoquinone derivatives produced by *Streptomyces* sp. strain DB634. The Journal of antibiotics 64 (12):763-768

Sedmak B, Carmeli S, Eleršek T (2008) "Non-toxic" cyclic peptides induce lysis of cyanobacteria—an effective cell population density control mechanism in cyanobacterial blooms. Microbial ecology 56 (2):201-209

She W, Bai Y, Zhang Y, Qin S, Feng W, Sun Y, Zheng J, Wu B (2018) Resource Availability Drives Responses of Soil Microbial Communities to Short-term Precipitation and Nitrogen Addition in a Desert Shrubland. Frontiers in Microbiology 9 (186)1-14

Siebert J, Hirsch P (1988) Characterization of 15 selected coccal bacteria isolated from antarctic rock and soil samples from the McMurdo-Dry Valleys (South-Victoria Land). Polar Biology 9 (1):37-44

Silva-Stenico ME, Silva CSP, Lorenzi AS, Shishido TK, Etchegaray A, Lira SP, Moraes LAB, Fiore MF (2011) Non-ribosomal peptides produced by Brazilian

cyanobacterial isolates with antimicrobial activity. Microbiological Research 166 (3):161-175.

Singh G, Babele PK, Sinha RP, Tyagi MB, Kumar A (2013) Enzymatic and non-enzymatic defense mechanisms against ultraviolet-B radiation in two *Anabaena* species. Process Biochemistry 48 (5):796-802

Singh RK, Tiwari SP, Rai AK, Mohapatra TM (2011) Cyanobacteria: an emerging source for drug discovery. The Journal of antibiotics 64 (6):401-412

Singh S, Kate BN, Banerjee U (2005) Bioactive compounds from cyanobacteria and microalgae: an overview. Critical reviews in biotechnology 25 (3):73-95

Sinha R, Lebert M, Kumar A, Kumar H, Häder D (1995) Disintegration of phycobilisomes in a rice field cyanobacterium *Nostoc* sp. following UV irradiation. Biochemistry and molecular biology international 37 (4):697-706

Sinha RP, Häder D-P (2008) UV-protectants in cyanobacteria. Plant Science 174 (3):278-289

Sinha RP, Singh N, Kumar A, Kumar HD, Häder D-P (1997) Impacts of ultraviolet-B irradiation on nitrogen-fixing cyanobacteria of rice paddy fields. Journal of Plant Physiology 150 (1-2):188-193

Smith HD, Baqué M, Duncan AG, Lloyd CR, McKay CP, Billi D (2014) Comparative analysis of cyanobacteria inhabiting rocks with different light transmittance in the Mojave Desert: A Mars terrestrial analogue. International Journal of Astrobiology International Journal of Astrobiology, 13(3), 271-277.

Sønstebø JH, Rohrlack T (2011) Possible implications of chytrid parasitism for population subdivision in freshwater cyanobacteria of the genus *Planktothrix*. Appl Environ Microbiol 77 (4):1344-1351

Stacy A, McNally L, Darch SE, Brown SP, Whiteley M (2016) The biogeography of polymicrobial infection. Nature Reviews Microbiology 14 (2):93-105

Stan-Lotter H, Fendrihan S (2017) Adaption of microbial life to environmental extremes: Novel research results and application, second edition. Adaption of Microbial Life to Environmental Extremes: Novel Research Results and Application, Second Edition.

Stevenson A, Cray JA, Williams JP, Santos R, Sahay R, Neuenkirchen N, McClure CD, Grant IR, Houghton JDR, Quinn JP, Timson DJ, Patil SV, Singhal RS, Antón J, Dijksterhuis J, Hocking AD, Lievens B, Rangel DEN, Voytek MA, Gunde-Cimerman N, Oren A, Timmis KN, McGenity TJ, Hallsworth JE (2015) Is there a common water-activity limit for the three domains of life? The ISME journal 9 (6):1333-1351

Stivaletta N, Barbieri R, Billi D (2012) Microbial Colonization of the Salt Deposits in the Driest Place of the Atacama Desert (Chile). Origins of Life and Evolution of Biospheres 42 (2):187-200.

Stratmann K, Burgoyne DL, Moore RE, Patterson GM, Smith CD (1994) Hapalosin, a cyanobacterial cyclic depsipeptide with multidrug-resistance reversing activity. The Journal of Organic Chemistry 59 (24):7219-7226

Szubert K, Wiglusz M, Mazur-Marzec H (2018) Bioactive metabolites produced by *Spirulina subsalsa* from the Baltic Sea. Oceanologia 60 (3):245-255

Tashyreva D, Elster J, Billi D (2013) A novel staining protocol for multiparameter assessment of cell heterogeneity in *Phormidium* populations (cyanobacteria) employing fluorescent dyes. PLoS One 8 (2):e55283

Tecon R, Or D (2017) Biophysical processes supporting the diversity of microbial life in soil. FEMS microbiology reviews 41 (5):599-623

Thompson JD, Higgins DG, Gibson TJ (1994) CLUSTAL W: improving the sensitivity of progressive multiple sequence alignment through sequence weighting, position-specific gap penalties and weight matrix choice. Nucleic Acids Res 22 (22):4673-4680.

Tofalo R, Perpetuini G, Schirone M, Fasoli G, Aguzzi I, Corsetti A, Suzzi G (2013) Biogeographical characterization of *Saccharomyces cerevisiae* wine yeast by molecular methods. Frontiers in microbiology 4 (166): 1-13

Tooming-Klunderud A, Rohrlack T, Shalchian-Tabrizi K, Kristensen T, Jakobsen K (2007) Structural analysis of a non-ribosomal halogenated cyclic peptide and its putative operon from *Microcystis*: Implications for evolution of cyanopeptolins. Microbiology (Reading, England) 153:1382-1393

Tosca NJ, Knoll AH, McLennan SM (2008) Water activity and the challenge for life on early Mars. Science 320 (5880):1204-1207

Tsukamoto S, Painuly P, Young KA, Yang X, Shimizu Y, Cornell L (1993) Microcystilide A: a novel cell-differentiation-promoting depsipeptide from *Microcystis aeruginosa* NO-15-1840. Journal of the American Chemical Society 115 (23):11046-11047

Undabarrena A, Beltrametti F, Claverías FP, González M, Moore ER, Seeger M, Cámara B (2016) Exploring the diversity and antimicrobial potential of marine actinobacteria from the comau fjord in Northern Patagonia, Chile. Frontiers in microbiology 7 (1135): 1-16

Uritskiy G, Getsin S, Munn A, Gómez-Silva B, Davila A, Glass B, Taylor J, DiRuggiero J (2019) Halophilic microbial community compositional shift after a rare rainfall in the Atacama Desert. The ISME journal

Uritskiy GV, DiRuggiero J, Taylor J (2018) MetaWRAP—a flexible pipeline for genome-resolved metagenomic data analysis. Microbiome 6 (1):158-171

van der Gast CJ (2015) Microbial biogeography: the end of the ubiquitous dispersal hypothesis? Environmental Microbiology 17 (3):544-546

Verseux C, Baqué M, Cifariello R, Fagliarone C, Raguse M, Moeller R, Billi D (2017) Evaluation of the resistance of *Chroococcidiopsi*s spp. To sparsely and densely ionizing irradiation. Astrobiology 17 (2):118-125

Vishwakarma R, Rai AK (2014) Microcystin congeners contribute to toxicity in the halophilic cyanobacterium *Aphanothece halophytica*. Arch Biol Sci 66:1441-1446

Vítek P, Ascaso C, Artieda O, Casero MC, Wierzchos J (2017) Discovery of carotenoid red-shift in endolithic cyanobacteria from the Atacama Desert. Scientific Reports 7 (11116):1-10

Vítek P, Ascaso C, Artieda O, Wierzchos J (2016) Raman imaging in geomicrobiology: endolithic phototrophic microorganisms in gypsum from the extreme sun irradiation area in the Atacama Desert. Analytical and Bioanalytical Chemistry 408 (15):4083-4092.

Vítek P, Cámara-Gallego B, Edwards HGM, Jehlička J, Ascaso C, Wierzchos J (2013) Phototrophic Community in Gypsum Crust from the Atacama Desert Studied by Raman Spectroscopy and Microscopic Imaging. Geomicrobiology Journal 30 (5):399-410.

Vítek P, Edwards HGM, Jehlička J, Ascaso C, De Los Ríos A, Valea S, Jorge-Villar SE, Davila AF, Wierzchos J (2010) Microbial colonization of halite from the hyper-arid atacama desert studied by Raman spectroscopy. Philosophical Transactions of the Royal Society A: Mathematical, Physical and Engineering Sciences 368 (1922):3205-3221.

Vítek P, Jehlička J, Ascaso C, Mašek V, Gómez-Silva B, Olivares H, Wierzchos J (2014a) Distribution of scytonemin in endolithic microbial communities from halite crusts in the hyperarid zone of the Atacama Desert, Chile. FEMS Microbiology Ecology 90 (2):351-366.

Vítek P, Jehlicka J, Edwards HGM, Hutchinson I, Ascaso C, Wierzchos J (2014b) Miniaturized Raman instrumentation detects carotenoids in Mars-analogue rocks from the Mojave and Atacama deserts. Philosophical Transactions of the Royal Society A: Mathematical, Physical and Engineering Sciences 372 (2030)

Vos M, Wolf AB, Jennings SJ, Kowalchuk GA (2013) Micro-scale determinants of bacterial diversity in soil. FEMS microbiology reviews 37 (6):936-954

Walker JJ, Pace NR (2007) Endolithic microbial ecosystems. Annual Review of Microbiology, vol 61. 331-347

Warren-Rhodes KA, Rhodes KL, Pointing SB, Ewing SA, Lacap DC, Gómez-Silva B, Amundson R, Friedmann EI, McKay CP (2006) Hypolithic cyanobacteria, dry limit of photosynthesis, and microbial ecology in the hyperarid Atacama Desert. Microbial Ecology 52 (3):389-398.

Welker M, Brunke M, Preussel K, Lippert I, von Döhren H (2004) Diversity and distribution of *Microcystis* (Cyanobacteria) oligopeptide chemotypes from natural communities studied by single-colony mass spectrometry. Microbiology 150 (6):1785-1796

Welker M, Von Döhren H (2006) Cyanobacterial peptides—nature's own combinatorial biosynthesis. FEMS microbiology reviews 30 (4):530-563

Whitton B (1992) Diversity, Ecology, and Taxonomy of the Cyanobacteria. In. pp 1-51.

Whitton B, Potts M (2000) Introduction to the cyanobacteria, in the Ecology of Cyanobacteria: Their Diversity in Time and Space (Eds B. A- Whitton, M. Potts.) Springer. 1-11

Whitton BA (Ed.) (2012) Ecology of cyanobacteria II: Their diversity in space and time. Springer Science & Business Media.

Wierzchos J, Ascaso C (1994) Application of back-scattered electron imaging to the study of the lichen-rock interface. Journal of Microscopy 175 (1):54-59

Wierzchos J, Ascaso C (2001) Life, decay and fossilisation of endolithic microorganisms from the Ross Desert, Antarctica, vol 24 (11): 863-868

Wierzchos J, Ascaso C, McKay CP (2006) Endolithic cyanobacteria in halite rocks from the hyperarid core of the Atacama Desert. Astrobiology 6 (3):415-422.

Wierzchos J, Cámara B, De los ríos A, Davila AF, Sánchez Almazo IM, Artieda O, Wierzchos K, Gómez-silva B, McKay C, Ascaso C (2011) Microbial colonization of Ca-sulfate crusts in the hyperarid core of the Atacama Desert: Implications for the search for life on Mars. Geobiology 9 (1):44-60

Wierzchos J, Casero MC, Artieda O, Ascaso C (2018) Endolithic microbial habitats as refuges for life in polyextreme environment of the Atacama Desert. Current Opinion in Microbiology 43:124-131

Wierzchos J, Davila AF, Artieda O, Cámara-Gallego B, de los Ríos A, Nealson KH, Valea S, Teresa García-González M, Ascaso C (2013) Ignimbrite as a substrate for endolithic life in the hyper-arid Atacama Desert: Implications for the search for life on Mars. Icarus 224 (2):334-346

Wierzchos J, Davila AF, Sánchez-Almazo IM, Hajnos M, Swieboda R, Ascaso C (2012a) Novel water source for endolithic life in the hyperarid core of the Atacama Desert. Biogeosciences 9 (6):2275-2286

Wierzchos J, de los Ríos A, Ascaso C (2012b) Microorganisms in desert rocks: The edge of life on Earth. International Microbiology 15 (4):173-183

Wierzchos J, DiRuggiero J, Vítek P, Artieda O, Souza-Egipsy V, Škaloud P, Tisza MJ, Davila AF, Vílchez C, Garbayo I, Ascaso C (2015) Adaptation strategies of endolithic chlorophototrophs to survive the hyperarid and extreme solar radiation environment of the Atacama Desert. Frontiers in Microbiology 6 (934).

Williams JP, Hallsworth JE (2009) Limits of life in hostile environments: no barriers to biosphere function? Environmental microbiology 11 (12):3292-3308.

Winston PW, Bates DH (1960) Saturated solutions for the control of humidity in biological research. Ecology 41 (1):232-237

World Health Organization (2014) Antimicrobial resistance: global report on surveillance. World Health Organization.

Wright DJ, C Smith S, Joardar V, Scherer S, Jervis J, Warren A, Helm R, Potts M (2006) UV Irradiation and Desiccation Modulate the Three-dimensional Extracellular Matrix of *Nostoc commune* (Cyanobacteria), Journal of Biological Chemistry, 280 (48), 40271-40281.

Wu H, Gao K, Villafañe VE, Watanabe T, Helbling EW (2005) Effects of solar UV radiation on morphology and photosynthesis of filamentous cyanobacterium *Arthrospira platensis*. Appl Environ Microbiol 71 (9):5004-5013

Xiao L, Wang J, Dang Y, Cheng Z, Huang T, Zhao J, Xu Y, Huang J, Xiao Z, Komatsu G (2017) A new terrestrial analogue site for Mars research: The Qaidam Basin, Tibetan Plateau (NW China). Earth-Science Reviews 164:84-101

Yadav S, Rai S, Rai R, Shankar A, Singh S, Rai L (2017) Cyanobacteria: Role in Agriculture, Environmental Sustainability, Biotechnological Potential and Agroecological Impact. In: Plant-Microbe Interactions in Agro-Ecological Perspectives. Springer Science & Business Media, pp 257-277

Yan F, Auerbach D, Chai Y, Keller L, Tu Q, Hüttel S, Glemser A, Grab HA, Bach T, Zhang Y (2018) Biosynthesis and Heterologous Production of Vioprolides: Rational Biosynthetic Engineering and Unprecedented 4-Methylazetidinecarboxylic Acid Formation. Angewandte Chemie International Edition 57 (28):8754-8759

Yang SC, Lin CH, Sung CT, Fang JY (2014) Antibacterial activities of bacteriocins: application in foods and pharmaceuticals. Frontiers in microbiology 5:241

Yogabaanu U, Weber J-FF, Convey P, Rizman-Idid M, Alias SA (2017) Antimicrobial properties and the influence of temperature on secondary metabolite production in cold environment soil fungi. Polar Science 14:60-67

Zeeshan M, Prasad S (2009) Differential response of growth, photosynthesis, antioxidant enzymes and lipid peroxidation to UV-B radiation in three cyanobacteria. South African Journal of Botany 75 (3):466-474

Ziolkowski LA, Wierzchos J, Davila AF, Slater GF (2013) Radiocarbon evidence of active endolithic microbial communities in the hyperarid core of the atacama desert. Astrobiology 13 (7):607-616

Acknowledgements / Agradecimientos

Esta tesis muestra tan solo la cara científica de lo que todo el trabajo, idas y venidas, satisfacciones y quebraderos de cabeza, han supuesto durante estos últimos años. Que el balance haya sido absolutamente positivo, pese a todo lo que implica, se debe a la presencia de muchas personas en las distintas etapas de este periodo y a distintos niveles. Todos vosotros tenéis en vuestras manos una parte muy importante de este proyecto.

En primer lugar, me gustaría dar las gracias a mis directores, el Dr. Jacek Wierzchos y el Dr. Antonio Quesada. Gracias por la confianza y la libertad que me habéis dado desde el primer minuto hasta hoy. Jacek, me has permitido conocer de primera mano lo "poliextrema" que es la investigación, las maravillas que guarda el desierto de Atacama y cómo disfrutar de ellas con los propios ojos. Gracias por trabajar codo con codo y transmitirme tu pasión por este trabajo. Antonio, gracias porque me diste la primera oportunidad para conocer la investigación hace ya siete años y siempre me has hecho sentir valorada. Gracias por tener siempre las puertas abiertas y haberme apoyado tanto especialmente en esta última etapa, corrigiendo lo cuestionable y animándome a no tener miedo a mojarme, ¡gracias! Por otro lado, agradecer a los revisores internacionales por el tiempo y esfuerzo dedicados a evaluar esta tesis en tan poco tiempo.

Esta tesis ha sido posible también gracias al grupo de investigación de EcoGeo en el MNCN. La eterna paciencia y consejos de Carmen, y el permanente apoyo recibido de Asun, Virginia, Isaac han sido claves para que haya llegado de una pieza a este momento. También gracias a ti Miguel Ángel, mi primer compañero con quien sigo disfrutando de compartir ciencia. Esta tesis también lleva el sello de Octavio, quien me ha hecho reencontrarme con la geología y sus maravillas ocultas, gracias por tu paciencia y por hacerme los días más fáciles bajo el sol y

el frío de Atacama, ¡al tiro! Gracias también a Carlos, a los Servicios de Microscopía y Cromatografía del MNCN y a Elisa por su ayuda y asesoramiento. No puedo dejar de mencionar a todas las personas de nuestro edificio compartido (ICA+MNCN) de ayer y hoy, compañeros de batallas. Mikel, gracias por transmitirme tu pasión, por ser un equipo, por escuchar mis lamentos y celebrar cada pequeña victoria, gracias. Viki, mi compi de principio a fin pasando por USA y vuelta, Elena, gracias por comprenderme siempre, y por supuesto, Carol y tu sonrisa que por fin regresó, Leti, por ser ejemplo de trabajo y buen ánimo ante todo y Jorge, por compartir parte de este camino. Gracias chicos, por cada día.

Es imposible no dar gracias por todo el apoyo recibido en mi segunda casa, la UAM. Gracias en general al pasillo de Fisio Vegetal por soportar mis idas y venidas, por poner a mi disposición instalaciones y material, a pesar de que en ocasiones puede que no haya sido su mejor "aliada" (perdón, French press…). En primer lugar, necesito dar las gracias a todos los "charcas-limnopolar" pasados y presentes, a tiempo completo y media jornada, ¡gracias por haber despertado en mí la chispa por entrar en este mundo de locos! Samu, gracias por estar al principio y haber sido mi hermano mayor, acompañándome a cada paso, ayudándome a lidiar con la ciencia y sus daños colaterales, gracias por cada consejo y por tu apoyo, por ser algo a lo que aspirar, gracias de corazón. A David, por enseñarme a ser productiva y ser mi Pepito Grillo evitando que me duerma en los laureles con tus "¡escribe!" y "¡termina ya la tesis!", gracias por ser referencia. A Ramsy, por haber sido ejemplo, por los favores express desde lejos, gracias. A Mar y Laura, por ser grandes compañeras al inicio de esta carrera de fondo. MA, un agradecimiento especial para ti, por los viajes, por transmitir tanta pasión, por ser una compañera en el pasado y el presente pese a no haber coincidido físicamente apenas, gracias. A Miguel, Pablo y Pedro, por vuestro apoyo y compañerismo, por los mil y un favores aceptados de buena gana, gracias. Gracias a todos los compañeros del pasillo de Fisio Vegetal, haciéndome

siempre sentir una más. Gracias Maiki, por toda la ciencia compartida, por cada discusión y cada palabra de ánimo, por todos y cada uno de los favores de última hora, por la confianza y la amistad, gracias. Gracias Jara, por ser mi compañera desde hace seis años y estar tan cerca en los momentos de máxima presión, gracias también a ti Dani, por responder a cada una de mis millones de dudas. Gracias Ger, por tu ayuda y tu ejemplo (aun te debo una tableta de chocolate). Gracias Kei, por cada palabra amable, cada sonrisa y cada día que no has dudado en echar un cable. Por supuesto, también quiero dar las gracias a Mabel, no sé qué habríamos hecho sin tu lámpara calibrada. Gracias Sonia, por cuidar de mis niñas en mis estancias. Gracias a todo el pasillo, profesores y estudiantes, por la acogida y el cariño de todos estos años.

Ahora permitidme que cambie a inglés. I would like to thank Dr. Jocelyne DiRuggiero from the Johns Hopkins University and Prof. Hanna Mazur-Marzec from University of Gdansk and their entire research groups for doing of my stays in their labs pleasant, productive and memorable experiences. Both of you made me feel at home and as a part of your teams with no differences during my stays. I would especially like to thank Diego, Jeremiah, Victoria and Gherman for sharing their enormous knowledge, patience and crazy scientific ideas. You have been very present all these years. Thanks also to Anna, Karolina, Justyna and the rest of the girls, I learnt a whole new world working with you during those two months from your incredible all-women research group.

And now I need to switch again to Spanish to continue these acknowledgements. También quisiera acordarme en este momento de las personas de distintos centros con los que he tenido la suerte de colaborar y que no han dudado en tenderme la mano. Gracias a los compañeros de CIDERTA, Carlos, por la acogida y la confianza, Zaida, por hacerme sentir en casa y no dudar en compartir cada cosa que estaba en tu mano. Gracias al grupo de Víctor Parro del Centro de Astrobiología, por la acogida y la generosidad, Yolanda por tu tiempo y tu infinita

paciencia (y a los dos MAs, que han salido a mi encuentro en varios puntos de este largo camino). Gracias Ernesto por salvarme con la French press del CIB, no sé qué habría hecho sin vuestra ayuda.

Gracias a todos los buenos amigos de la familia SaFa. A los de la Urba, en especial a Miky, Anita y Eto, no os habéis perdido un minuto de este camino, gracias. A los y las de los Olmos, por vuestro cariño y paciencia.

Y por último necesito dar las gracias a mis cuatro patas, los que desde la sombra han hecho posible que haya llegado aquí. Gracias a mis Fratelos, por vuestra comprensión, paciencia, seguimiento y apoyo, por ser hogar al que regresar, gracias. Gracias a ti, Patis, por todos estos años de camino, por traerme con tu locura la cordura necesaria para no perder el norte cuando todo se tuerce. Gracias familia, Mamá, Papá, Coru, Emilio y Petros. Por cuidarme, aconsejarme y aguantarme incluso cuando lo merezco poco. Por hacer que lo imposible pueda ser y que esté donde estoy hoy. Por regalarme una vida en la que poder construir estos sueños locos sin miedo. Gracias, en especial a ti Petros, por luchar con mis preposiciones erróneas y mis incontables “also”. Y gracias a ti, Marcos, bien sabes que esta tesis existe por todo lo que has dejado a un lado para “estar” y ser mi compañero. Esta tesis es, ante todo, vuestra.

Appendix: Scientific Divulgation

Casero, M.C. (2017). Con la muerte en los talones: los microorganismos salen adelante en el desierto de Atacama. NaturalMente 16, 27-31 (MNCN, CSIC). http://revista.mncn.csic.es/nm16/27/

Casero, M.C. (2019). Nuevo método para identificar cianobacterias tóxicas en embalses. NotiWeb, Madri+D
http://www.madrimasd.org/notiweb/noticias/nuevo-metodo-identificar-cianobacterias-toxicas-en-embalses